A Survey of Axonal Transport Function and Motor Behaviour in *Drosophila* Models of Amyotrophic Lateral Sclerosis

Thesis submitted in fulfilment of the degree of Doctor of Philosophy at the University of Sheffield

by

Katie Baldwin

Department of Biomedical Science
University of Sheffield

September 2015

Contents

Chapter 1: Introduction

Chapter 2: Materials and Methods

Chapter 3: TDP-43

Chapter 4: FUS

Chapter 5: C9orf72

Chapter 6: Discussion

Glossary of Abbreviations

ALS-Amyotrophic lateral sclerosis
ALS-Bi-Amyotrophic lateral sclerosis - behavioural impairment
ALS-Ci-Amyotrophic lateral sclerosis - cognitive impairment
ALS-FTD-Amyotrophic lateral sclerosis – frontotemporal dementia
ANOVA-Analysis of variance
APP-Amyloid precursor protein
bvFTD-Behavioural variant frontotemporal dementia
C9orf72-Chromosome 9 open reading frame 72
Caz-Cabeza
CCAP-Crustacean cardioactive peptide
CMT2-Charcot Marie Tooth disease type 2
CNS-Central nervous system
DDR-DNA damage repair
DENN-Differentially Expressed in Normal and Neoplasia
DNA-Deoxyribonucleic acid
DPR-Dipeptide repeat protein
DRP1-Dynamin-related protein 1
DSB-Double strand break
ELAV-Embryonic lethal abnormal vision
ELF-EMF-Extremely low frequency electromagnetic fields
EMG –Electromyography
EWS- Ewing RNA-binding protein
FA-Flail arm
fALS-Familial amyotrophic lateral sclerosis
FF-Fast fatigable
FL-Flail leg
FR-Fast resistant
fFTD- Familial frontotemporal dementia
FTD-Frontotemporal dementia
FTD-MND-Frontotemporal dementia- motor neuron disease
FTLD-Frontotemporal lobar degeneration
FUS-Fused in Sarcoma
Fzo-Fuzzy onions
G37R-Glycine-37 to Arginine
G85R-Glycine-85 to Arginine
G93A-Glycine-93 to Alanine
GAL4-Galactose-responsive factor 4
GFP-Green fluorescent protein
GP-Glycine Proline
GR-Glycine Arginine
GSK3β-Glycogen synthase kinase 3 β
HSP-Hereditary spastic paraplegia
IM-Inner membrane
KIF-Kinesin family
KLC-Kinesin light chain
LMN-Lower motor neuron
M337V-Methionine-337 to Valine
Marf-Mitochondrial assembly regulatory factor
MBO-Membrane bound organelle

MN-Motor neuron
MND-Motor neuron disease
mRNA-Messenger ribonucleic acid
mSOD1-Mutant superoxide dismutase 1
NEFL-Neurofilament light chain
NES-Nuclear export signal
NLS-Nuclear localisation signal
NMD-Nonsense mediated decay
NMJ-Neuromuscular junction
NPY-Neuropeptide-Y
NTD-N-terminal domain
OM-Outer membrane
OPA1-Optic atrophy 1
P398L-Proline-398 to Leucine
P525L-Proline-525 to Leucine
PA-Proline Alanine
PLS-Primary lateral sclerosis
PMA-Primary muscular atrophy
PNFA-Progressive non-fluent aphasia
PR-Proline Arginine GA-Glycine Alanine
RAN-Repeat Associated Non-ATG
RGG-Arginine Glycine Glycine
RNA-Ribonucleic acid
RNP-Ribonucleoprotein
RO-RNA only
RRM-RNA recognition motif
S-Slow
sALS-Sporadic amyotrophic lateral sclerosis
SCA8-Spinocerbellar ataxia 8
SD-Semantic dementia
sFTD- Sporadic frontotemporal dementia
SG-Stress granule
SMA-Spinal muscular atrophy
SOD1-Superoxide dismutase 1
SQSTM1/p62-Sequestosome 1
TAF15-TATA-binding protein associated factor 2N
TBPH -TAR DNA binding protein homolog
TDP-43 -TAR DNA binding protein 43 kDa
TRAK1-Trafficking kinesin protein 1
TSC-Terminal Schwann cell
UAS-Upstream activator sequence
UBQLN2-Ubiqullin 2
UMN-Upper motor neuron
VCP-Valosin containing protein
VEGF-Vascular endothelial growth factor
WT-Wild type
ZnF-Zinc Finger

Index of Figures and Tables

Figures

Results

Mitochondrial Transport

Vesicle Transport

Mitochondrial Length

Mitochondrial Number at the NMJ

Tables

Abstract

Amyotrophic Lateral Sclerosis (ALS) is a neurodegenerative disorder that is primarily characterised by the loss of the upper and lower motor neurons and which manifests as a progressive and fatal paralysis. The related proteins TDP-43 and FUS and the recently identified expansion within the *C9orf72* locus are of major importance within this disorder. Evidence suggests ALS occurs as a distal axonopathy and axonal transport of cellular components is a process vital for the functioning of neuronal terminals and the survival of the neuron. SOD1-related ALS models have indicated axonal transport is an early pathology that precedes cell loss and clinical symptoms. Here, a survey of axonal transport of mitochondria and vesicles was conducted in *Drosophila* models of TDP-43, FUS and C9orf72. Axonal transport was found to be affected in some way in all models and thus represents pathology common to ALS-linked genes. However, the exact nature of the dysfunction varied between genes and conditions. Loss of dTDP-43 (TBPH) caused a decrease in mitochondrial but not vesicle transport, whereas the opposite was true for gain of the wild type and ALS-linked mutant proteins. However, loss and gain of dFUS (Caz) affected both forms of transport, although ectopic expression of the human protein only affected vesicle transport. Both forms of transport were affected as a result of C9orf72 expansion, which is attributable to dipeptide repeat production and not RNA toxicity. Furthermore, in all models axonal transport dysfunction is correlated with the symptoms of neuromuscular dysfunction via the assessment of motor behaviours, suggesting it may be a contributory factor to the decline in motor functioning in these models of ALS.

CHAPTER 1: Introduction

1.1: Amyotrophic Lateral Sclerosis

Amyotrophic lateral sclerosis (ALS) is typically an adult onset progressive neurodegenerative disorder and the most common form of motor neuron disease (MND) first described in the 1860s by the 'father of neurology' Jean-Martin Charcot (Kumar et al., 2011). It is characterised by the loss of both the upper motor neurons (UMN), a type of pyramidal cell known as Betz cells and the lower motor neurons (LMN), representing a catastrophic loss of motor nervous system functioning. 90% of ALS cases are of a sporadic origin (sALS) with the remaining 10% familial (fALS). The latter are predominantly caused by autosomal dominant mutations, but there are also a minority of cases showing autosomal recessive and X-linked inheritance (Robberecht and Philips, 2013). A large array of genes have been linked to ALS (see section 1.2.1) including *SOD1*, *TDP-43*, *FUS* and *C9orf72* (Renton et al., 2014). The prevalence of ALS in America has been defined as an average of 3.9 per 100,000 (Mehta et al., 2014). Similarly in Europe the average is 2.16 per 100,000 (Logroscino et al., 2010). The condition is fatal, usually due to respiratory failure, with average life expectancy being 3-5 years from diagnosis (Robberecht and Philips, 2013).

1.1.1: Motor System Architecture

ALS preferentially, but not exclusively (see sections 1.2.4 and 1.2.5), affects the motor nervous system, the main cell type of which are the motor neurons. The UMN cell bodies reside in the primary motor cortex within the precentral gyrus of the frontal lobe. Their axons project downwards through the midbrain, the middle pons and middle medulla and are organised into two tracts collectively known as the pyramidal tracts. All the axons initially form the corticospinal tract but at the levels of both the pons and medulla some of the axons are routed to form the corticobulbar

tract to synapse with LMNs within the cranial nuclei, which go on to innervate the facial muscles. The remaining axons undergo a cross over known as the pyramidal dessication from ventral to lateral at the level of the caudal medulla to form the lateral corticospinal tract. This tract extends into the spinal cord where the UMN axons synapse with the spinal LMNs in the ventral horn. From here, the LMN axons project out of the ventral root to innervate the muscles of the body (Purves et al., 2001).

1.1.2 Signs, Symptoms, Diagnosis and Treatment

As is the case with many neurodegenerative disorders, ALS is a severely debilitating and fatal medical condition. In the United States it is known as 'Lou Gherig's disease' after the famous New York Yankee's baseball player who's promising career and life were claimed by the disease in 1941. As demonstrated by Gherig, the principal presenting symptoms of LMN degeneration in ALS are progressive muscle weakness, which leads to difficulties with physical movement such as walking, fasciculation (involuntary contraction and relaxation of muscles), loss of strength and power, such as batting a baseball, and hyporeflexia. These issues become relentlessly worse until physical movements become impossible and the patient is robbed of all strength and power. The affected body muscles correspondingly suffer from atrophy leading to the visible appearance of wasting (Gordon, 2013). Indicative of UMN dysfunction are hyperreflexia, spasticity (increased muscle tightness) and the abnormal regaining of Babinski's reflex (upwards curling of the big toes upon stroking of the sole, a reflex that desists between 1-2 years of age) (Van Gijn, 1995). There is also the presence of Hoffman's reflex which involves flicking the nail of the middle finger, which in positive cases, elicits a pathologic flexing of the thumb. The presence of these two reflexes is not exclusive to ALS, but is useful for diagnosis in conjunction with other signs. Patients may also demonstrate slurring of speech (dysarthria) and difficulty swallowing (dysphagia), the former of which can exacerbate emotional feelings of

frustration, while the latter can lead to malnutrition. The presence of the spilt-hand sign is considered to be a specific indicator of ALS (Kuwabara et al., 2008). It arises from the preferential atrophy of the thenar muscles. Why these muscles are targeted specifically is unknown (Benny and Shetty, 2012). Interestingly, some form of cognitive dysfunction is now recognised to be present in as many as half of patients to varying degrees of severity, with a subset (15%) meeting the criteria for frontotemporal dementia (FTD) (see section 1.2.4). Ultimately, the condition drives towards paralysis, and death occurs generally due to failure of the respiratory muscles (Gordon, 2013).

It is considered to be somewhat challenging to give a definitive ALS diagnosis due to the current lack of biomarkers, although a number of these are on the horizon. For example, a low corticospinal fluid (CSF) ratio between phosphorylated tau and total tau is being put forward as a possible biomarker (Grossman et al., 2014). Despite these historic challenges, diagnosis is found to have a 95% accuracy (Gordon, 2013). Presently, a clinical diagnosis of ALS is a process of elimination to exclude an array of similarly-presenting disorders of the motor system. These include spinal muscular atrophy and multiple sclerosis. Compounded by the variable age at onset of symptoms between patients, the diagnosis process is often long, over a year in many cases (Nzwalo et al., 2014). ALS has been defined for the purpose of clinical trials on the basis of the revised El Escorial criteria, which involves a battery of electrophysiological tests including electromyography and nerve conduction velocity, performed to ascertain the level of LMN and UMN involvement and the number of areas affected, which provides a sliding scale of probability ranging from ‘definite’ to ‘suspected’ (Brooks, 1994; Miller et al., 1999). New revisions were made in 2006, termed the Awaji algorithm, which declared the equivalence of clinical and electromyogram (EMG) tests for the diagnosis and this has been demonstrated to be more useful and is now favoured (Carvalho and Swash, 2009).

There is no cure for ALS and treatment options are poor. Currently there is only one drug approved for use, Riluzole, which targets the excitotoxicity pathology of ALS (see section 1.4) and has been shown to decrease the release of glutamate neurotransmitter (Jehle et al., 2000). The effect of treatment with Riluzole however is small, with gains in lifespan of only an average of three months (Miller et al., 2012).

The remaining options of care are restricted to the aim of increasing patient comfort for as long as possible. The dysphagia (difficulty swallowing), muscle weakness and atrophy all conspire to make malnutrition a severe threat to patients and it has been shown that those whose weight loss is greater at the time of diagnosis have reduced survival times (Limousin et al., 2010). Tube feeding becomes an option as patients decline as does the use of ventilation support when patients' enter the stage of respiratory muscle incapacity. The majority of patients die from respiratory failure (Gordon, 2013).

1.1.3: Histopathology

ALS patient tissue at autopsy is characterised by a loss of the UMNs from the cortex. Within the ventral horns of the spinal cord, a loss of LMN cell bodies is observed. Cellular proteinaceous inclusions in MNs, glia and neurons in other brain regions are clearly visible upon immunostaining and are subdivided into multiple categories, the first of these is characterised as staining positive for ubiquitin, the protein that acts as a tag for the process of protein degradation via the proteasome. Ubiquitin-positive inclusions are characterised as being skein-like (stringy) or round. The round inclusions have been suggested to resemble the Lewy bodies that characterise Parkinson's disease, however they are devoid of α-synuclein and tau. These inclusions are positive for a number of proteins such as TDP-43, UBQLN2, and SQTSM1/p62 (see section 1.3 and 1.4) ALS is also specifically characterised by the presence of Bunina

bodies. These are eosinophilic inclusions positive for the proteins cystatin C and transferrin, although it's likely other proteins are also included but these again exclude α-synuclein and tau and also amyloid precursor protein among others (Okamoto et al., 2008). A third type of inclusion observed in ALS are neurofilament inclusions, which contain aggregates of neurofilaments and are more commonly seen in familial cases (Wijesekera et al., 2009).

1.2: The Variability of ALS

ALS is by no means a simple disorder, with broad variation observed for multiple clinical measures. The underlying reasons for much of the variability remain unknown and are the subject of intense research as we increase our understanding regarding what this variation can tell us about the disease and our efforts to treat it.

1.2.1 Location of Onset

The region(s) of the body where symptoms first arise is subject to variability; spinal onset is the most common, occurring asymmetrically within the limbs. Bulbar onset ALS, as the name suggests has presenting symptoms arising from pathogenic involvement of the bulbar muscles in the face and throat. Many patients suffer early from tongue fasciculation, which is a useful clinical measure of bulbar onset ALS, and have pronounced dysarthria and dysphagia. These patients also go on to develop limb and respiratory muscle involvement (Gordon, 2013). The rarest form of ALS onset is that of the respiratory muscles which in a retrospective study of incidence at a large ALS clinic, made up only 2.7 % of cases (Shoesmith et al., 2007).

1.2.2 LMN vs. UMN Involvement

ALS can also present with much variation in the degree of LMN vs UMN involvement. 'Flail arm syndrome' (FA) and 'Flail leg syndrome' (FL) are both caused primarily by LMN dysfunction. In the case of FA the upper limbs and back are affected, with weakness and wasting and in FL these symptoms are present in either leg, with usually one affected at onset. Both are classified as being a variant of ALS, as there are some pathologic UMN signs, but these are much less apparent. In both, other body regions become affected towards the end of disease course, which is longer than classic spinal ALS (Wijesekera et al., 2009). Pyramidal phenotype ALS in contrast is characterised by primary UMN involvement with moderate LMN signs, the main symptoms are extreme spasticity and hyperreflexia (Chiò et al., 2011).

Also undergoing consideration in the field is the classifications of the motor neuron disorders primary lateral sclerosis (PLS) and primary muscular atrophy (PMA) as specific disorders. They have been characterised as having pure UMN and pure LMN involvement, respectively and therefore as being distinct from any variant of ALS, which requires at least some involvement from both LMNs and UMNs (Brooks, 1994). However this distinction has become difficult; in a recent study on autopsy samples, Riku and colleagues found 84.6% of the samples classified during life as PMA showed evidence of UMN degeneration (Riku et al., 2014). Similarly, a longitudinal study examining PLS category patients found 40% eventually develop electromyography signs of LMN degeneration and in their review of published autopsy studies, discovered only 2 out of 10 showed no histological changes consistent with LMN degeneration (D'Amico et al., 2012). Thus, these disorders are not definitively separate and should be described as an ALS spectrum from LMN to UMN dominance (Swinnen and Robberecht, 2014).

1.2.3 Differential Sex Effects, Age of Onset and Survival Time

It is clear from epidemiological studies that men have a higher risk than women for ALS. In the United States there is a sex comparison of 4.8 men to 3 women per 100,000 per year diagnosed (Mehta et al., 2014). In Europe men again have a higher representation with a sex comparison of 3.0 men to 2.4 women per 100,000 per year (Logroscino et al., 2010). However, studies that focus on familial cases, have reported no difference in incidence between genders (McCombe and Henderson, 2010). In terms of location of onset, women are more likely to have a bulbar onset., whereas spinal onset occurs more often among men (Haverkamp et al., 1995; Traxinger et al., 2013) and respiratory onset patients in a large case study were 76% male (Shoesmith et al., 2007). In terms of level of presenting LMN and UMN involvement, both flail arm and flail leg variants also show a male prevalence (Chiò et al., 2011). These sex differences are also seen with the age of onset measure, with men more likely to have an earlier onset than women, possibly because women tend to make up a greater proportion of bulbar onset cases, which has a higher age of onset (Traxinger et al., 2013). No clear reasons for these sex differences have currently been elucidated, but have been postulated to include differences in exposure to environmental risk factors. It is an important area of research to understand how disease pathogenesis may be influenced by this factor (McCombe and Henderson, 2010).

Aside from being influenced by sex, age of onset is influenced by several other factors. There is a high-risk age window around middle age for ALS, between 40 and 60 for familial and 58 and 63 for sporadic (Ingre et al., 2015). However, whilst ALS is quoted as an adult onset neurodegenerative disorder, there are many documented cases of juvenile onset and early adult onset ALS. Juvenile and early adult onset are considered separate variations of ALS, with the juvenile form usually familial and interestingly, different mutations within the same disease-linked gene are associated

with different ages of onset (see section 1.3) (Gouveia and de Carvalho, 2007). Age of onset also varies with other factors, bulbar cases are much more likely in older people (Turner et al., 2010), whereas preferential UMN involvement most often strikes juvenile and early adult onset cases (Sabatelli et al., 2008).

Survival time is influenced by many of the above factors. An older age of onset is negatively associated with survival (Jordan et al., 2015), while young onset before 55 is characterised by greatly extended survival time (Magnus et al., 2002). Unsurprisingly, in most cases of respiratory muscle onset survival does not extend beyond 18 months (Shoesmith et al., 2007). Bulbar onset is also associated with decreased survival times of 33 months on average (Turner et al., 2010). There is currently no consensus upon whether sex *per se* influences survival time (McCoombe and Henderson, 2010).

1.2.4 The ALS-FTD Spectrum

Since the time it was defined as a distinct disease by Charcot in the 1860s until recently, it was thought that it was a 'pure' disease affecting only the motor function with no effect on cognition, something that was used as a silver-lining to console the newly diagnosed (Bennion Callister and Pickering-Brown, 2014), and it is often cited how fortunate it was that Stephen Hawking's brain was not going to be touched by the disease. However, it has become apparent, largely from advances in clinical evaluation and continued assessment practices that there is a cognitive element to an estimated 50% of suffers. 15% of these are diagnosed with frontotemporal dementia (FTD). The converse is also true, with 15% of FTD patients meeting an ALS diagnosis with a further 35% exhibiting some signs of motor system dysfunction (Bennion Callister and Pickering-Brown, 2014).

FTD is an umbrella term for a group of disorders characterised by degeneration in the frontal and temporal lobes of the brain resulting in behavioural and cognitive deficits, including in speech and language. Onset is typically in late middle age before the age of 65, with a prevalence of 15-22 per 100,000 (Onyike and Diehl-Schmid, 2013). There are also a number of variants: the majority of sufferers are diagnosed with the behavioural form (bvFTD); the remainder present more clearly with speech or language difficulties, and are classified respectively as either progressive non-fluent aphasia (PNFA), or semantic dementia (SD) (Bennion Callister and Pickering-Brown, 2014). Patients who exhibit ALS with some cognitive or behavioural impairment are classified as ALS-Ci or ALS-Bi respectively. Patients who meet the criteria for both ALS and FTD are referred to as being ALS-FTD. From the other end of the spectrum, those with FTD and some degree of measured motor dysfunction are known as FTD-MND (Robberecht and Philips, 2013).

Patients with FTD may be positive for TDP-43 containing ubiquitinated inclusions, which are a hallmark of ALS histopathology, and thus have a histopathological classification (termed frontotemporal lobar degeneration or FTLD) of FTLD-TDP. It has also been seen that ALS patients with dementia have TDP-43 positive ubiquitinated inclusions in their frontal and temporal lobes. These discoveries further demonstrated the connection between ALS and FTD (Forman et al., 2007). It is therefore now recognised that ALS and FTD represent the extreme poles of a disease continuum termed the ALS-FTD spectrum (Figure 1.1) (Robberecht and Philips, 2013).

Figure 1.1: The ALS-FTD spectrum showing the placement of key genes along the spectrum based on the disease manifestation of patients associated with mutations in each gene. Adapted from Ling et al., (2013).

1.2.5 Reclassification as a Multisystem Disease

Further to the understanding of ALS as one of the extreme phenotypes of a spectrum disorder, ALS classification has now evolved to the awareness that ALS should be recognised as a multisystem disease. This is the understanding that ALS pathology is observed outside of the motor system, as discussed above. It was noted that pathology is seen in a number of cases in the frontal and temporal lobes, but also to other nervous system subdivisions, indeed it has been known for several decades that motor neuron diseases were associated with Parkinsonism, dementia and other system involvement (Hudson, 1981). For example, ALS-Parkinsonism is a clinically recognised condition wherein signs and symptoms associated with Parkinson's disease are also present. A case study involving three sporadic ALS cases that showed no cognitive impairment were seen to have neurodegeneration occurring in their substantia nigra and accompanying Parkinson's associated symptoms including reduced body movement or hypokinesia (Desai and Swash, 1999). Many genes recently discovered to be associated with the ALS-FTD spectrum give rise to additional pathologies in brain regions, such as the cerebellum in the case of C9orf72 and in muscle and bone in the case of VCP (Renton et al., 2014).

1.3: Etiology

90% of ALS cases are sporadic in origin and 10% exhibit a familial inheritance. Like many diseases, ALS is classified as a multifactorial disease and the contributions of disease causing loci and the role of the environment on the disease initiation and progression are all-important areas of research in understanding the complex causes of this disease.

1.3.1 Environmental Risk Factors

As a multifactorial disease, the influence of the environment and gene-environment interactions on causation and progression of ALS has been examined in depth. A number of factors have been assessed through epidemiology studies for a possible link to the development of ALS, such as sports injuries, herbicides/heavy metals and electromagnetic fields, to lifestyle factors like smoking.

Sports injury has been associated with ALS in recent times. An increased incidence of ALS among Italian male professional football players had been noted at the turn of the millennium and was subjected to a retrospective study by Chiò and colleagues, who examined Italian-born, Italian-based professional players between 1970 and 2002. They found a strong relationship between playing professional football and ALS in this population. Interestingly there was an increased incidence of the bulbar onset form among this population and a predilection for midfielders. This risk was also positively associated with career length with an increase incidence among those with the longest careers. The age of onset in these cases was also significantly lower than in the general population. Reasoning for this effect include engagement in high levels of physical activity in general, football-specific physical trauma, such as heading the ball (a logical hypothesis for the higher incidence of the bulbar onset

form), use of illegal toxic performance-enhancing substances and increased exposure to possibly toxic chemicals used on pitches (Chiò et al., 2005). In 2009 they conducted a further study on the same population and included two further professional athlete groups, basketball players and road cyclists. Follow up of the footballers revealed three new ALS cases and confirmed the increased risk previously observed. However, no elevated risk was found for either of the other groups, suggesting that this risk may be a football-specific effect and not related to high rates of aerobic activity or use of drugs, as both these measures were noted to be higher in road cyclists or to general physical trauma, which was higher in basketball players. This narrowed the proposed environmental explanations to football related injury and the use of toxic chemicals including herbicides and pesticides on pitches. The higher incidence among midfielders was considered to be likely an effect of their genetic predisposition to physical endurance combined with football-specific environmental factor(s) (Chiò et al., 2009).

Aside from professional football and its associated risks, there is evidence for other occupational hazards in developing ALS. Notably, it has been proposed that the increased incidence of ALS among those who work closely with electricity, such as electricians and electric machine operators (Deapen and Henderson, 1986), may be explained by a high exposure to extremely low frequency electromagnetic fields (ELF-EMF), which are those in the range of 3-3,000Hz. A meta-analysis on the available data by Zhou and colleagues sought to clarify the results from a myriad of conflicting reports and came to the conclusion that there was a moderate increase in risk to be found in those with electrical based occupations, but conceded this effect may be mediated by other factors such as increased frequency of electric shocks in these occupations instead of ELF-EMF itself. More work needs to be done to fully untangle these factors and to elucidate the true level of risk (Zhou et al., 2012).

There is strong evidence to suggest that pesticides confer a high risk of ALS, particularly in males (Ingre et al., 2015). A number of heavy metals and non-metals found in industry and in the wider environment have also been examined as risk factors, including cadmium, mercury, lead and the non-metal selenium (Trojsi et al., 2013). For example, drinking water with high levels of selenium was established to have a causal link to a set of ALS cases in Italy (Vinceti et al., 1996) and this was found to be positively correlated with the length of selenium exposure (Vinceti et al., 2010). A possible explanation has arisen from the fact high exposure has been shown to increase SOD1 (see section 1.3.2.1) localisation within mitochondria in culture, in a manner mimicking the effects of SOD1 mutation, which provides one explanation as to how wild type SOD1 is implicated in sALS (Maraldi et al. 2011). Overall, epidemiology studies are still conflicted over the role of exposure to the heavy metals in ALS risk, but a general consensus for selenium as a risk factor appears to have emerged (Vinceti et al., 2012).

ALS has been put forward as yet another disease in which smoking is a risk factor, with smokers having a reported 2-fold incidence over never-smoked controls in a large European cohort. Number of years smoked also had an effect on developing ALS, as did number of years since giving up smoking (Gallo et al., 2009). However, there is not total agreement in the literature as no smoking association was observed in a recent Michigan case-control study (Yu et al., 2014), or in one conducted in Philadelphia (Malek et al., 2014).

There are also some interesting biological environmental hazards; in particular, ingesting cyanobacteria is strongly evidenced to increase ALS risk and was discovered as the cause of ALS-like disease observed in Guam (Bradley et al., 2013). These bacteria produce a neurotoxin, β-N-methylamino-l-alanine, which in an *in vivo* study in rats, led to increased levels of active GSK3β and TDP-43, which are both associated with ALS

Table 1.1: Genes associated with ALS-FTD spectrum disease. Adapted from Marangi and Traynor, (2015).

Confirmed Causative Genes		
Name	**Type**	**Other Disease Associations**
SOD1	AD, AR	
FUS	AD, AR	
TARDBP	AD	FTD
OPTN	AD, AR	POAG
VCP	AD	FTD, PDB, IBM
UBQLN2	XL	FTD
SIGMAR1	AR	
CHMP2B	AD	FTD
PFN1	AD	
C9orf72	AD	FTD
MATR3	AD	
CHCHD10	AD	FTD, cerebellar ataxia, myopathy
SQSTM1	AD	FTD, PDB, IBM
HNRNPA1	AD	FTD, PDB, IBM
HNRNPA2B1	AD	
ERLIN2	AR	HSP
SS18L1	AD	
Putative Causative Genes		
ALS2	AR	HSP
SETX	AR	SCA
SPG11	AR	HSP
VAPB	AD	SMA
ANG	AD	
FIG4	AD, AR	CMT4J, Yunis-Varon syndrome
TAF15	AD	
EWSR1	AD	
SPAST	AD	HSP
PRPH	AD	
DCTN1	AD	Perry syndrome
DAO	AD	
PNPLA6	AR	HSP, BNHS, GHS
Confirmed Susceptibility Genes		
ATXN2		SCA
VEGF		
HFE		Hemochromatosis
CHRNA4		NFLE
UNC13A		
ZNF512B		
GRN		
SMN1		SMA
MAPT		FTD
TREM2		AD
Putative Susceptibility Genes		
NEFH		
PON 1,2,3		
CHRNA3		
DPP6		Ventricular fibrillation
ELP3		
ITPR2		
FGGY		
CHGB		
DPYSL3		
Confirmed Modifier Genes		
UNC13A		
ZNF512B		
GRN		
KIFAP3		
EPHA4		
PPARGC1A		
APOE		AD
MAOB		
CX3CR1		
Putative Modifier Genes		
ANG		

(de Munck et al., 2013). Aside from cyanobacteria, infection with retroviruses is implicated in raising risk level for ALS (Alfahad and Nath, 2013).

1.3.2 Genes associated with the ALS-FTD spectrum

The genetic study of this disease has been a field of exciting and rapid advances for over twenty-five years. In this time a large array of genetic loci have been linked to the disease (Table 1.1.). Genes associated with ALS-FTD spectrum causality are found on nearly every chromosome and almost all of them act in an autosomal dominant manner.

1.3.2.1 SOD1

The first genetic locus to be definitively linked to ALS was that of Superoxide dismutase 1 or *SOD1* (Rosen et al., 1993) after a concerted hunt of the long arm of chromosome 21 via linkage analysis (Siddique et al., 1989; Siddique et al., 1991). The gene is located at 21q22.11 and to date, more than 170 mutations have been found within the gene (Ajroud-Driss and Siddique, 2015). *SOD1* contains five exons all of which have been found to harbour ALS causative mutations, although the majority cluster in the last two exons. There are a few nonsense mutations caused by both deletions and insertions, however most are missense mutations caused by substitutions, the majority of which lead to autosomal dominant ALS (Finsterer, 2006). A notable exception is the D90A mutation, which can be both recessive and dominant (Anderson et al., 1995; Robberecht et al., 1996). The best studied mutations include A4V, which is the most frequent mutation in the United States, which arose from two founders approximately 500 years ago (Saeed et al., 2009) and G93A, a rare mutation but which was the first to be modelled in a transgenic mouse (Gurney et al., 1994). SOD1 mutations account for approximately 12% of

familial ALS cases (Scotter et al., 2015). In terms of sporadic cases, a frequency of 1-2% is generally reported (Pasinelli and Brown, 2006) though a smaller frequency of 0.7% for SOD1 mutations was seen by Chiò et al., (2008). There is great heterogeneity in the manifestation of these mutations. One of the most severe is the A4V mutation, which leads to a rapidly progressing ALS disease, with a maximum survival time of just 24 months (Juneja et al., 1997).

SOD1 encodes for Cu/Zn superoxide dismutase, which acts as a homodimer containing two copper and two zinc ions (Beckman, 1973). Both metal ions and a disulphide bond between cysteines 57 and 146 are required for the structural integrity of the protein (Foreman and Fridovich, 1973). It is ubiquitously expressed (Fridovich, 1995) and is largely localised to the cytoplasm, but is also found in the mitochondrial intramembrane space (Weisiger and Fridovich, 1973). It can also be secreted in the extracellular fluid (Mondola et al., 2003) where it has a role in signal transduction (Rotunno and Bosco, 2013). SOD1 operates primarily in a protective function against oxidative stress caused by the free radical superoxide by converting it in a dismutation reaction involving copper to oxygen and hydrogen peroxide (McCord and Fridovich, 1969). SOD1-associated ALS is characterised by inclusions of the protein in neurons and also glial cells, which are negative for TDP-43 and FUS.

1.3.2.2 TDP-43

In their seminal studies, Neumann et al., (2006) and Arai et al., (2006) discovered that the then little-studied, ubiquitously expressed DNA/RNA binding protein TDP-43 was a component of the round and skein-like ubiquitinated inclusions that are characteristic of ALS and FTD patients. Subsequently, it was uncovered that the gene encoding it, *TARDBP*, harboured mutations within its structure that were causative of ALS (Gitcho et al., 2008; Sreedharan et al., 2008; Kabashi et al., 2008).

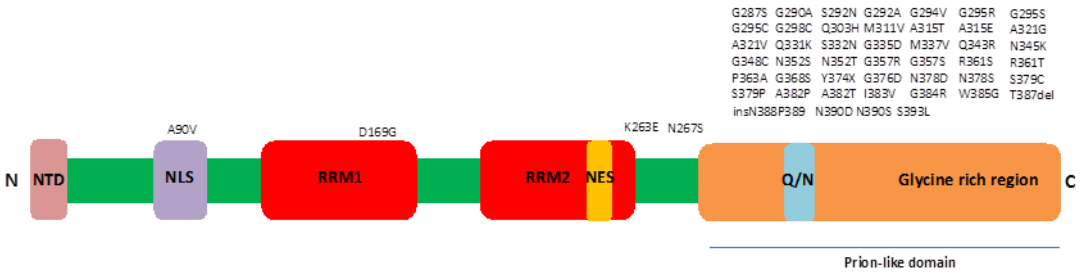

Figure 1.2: The structure of TDP-43. NTD= N-terminal domain – involved in homodimerisation, and aiding splicing. NLS = nuclear localisation signal – bipartite sequence allowing entry into nucleus. RRM1= RNA- recognition motif 1 – required for RNA binding, splicing activity, autoregulation, homodimerisation and incorporation into stress granules. RRM2- RNA-recognition motif 2 – Involved in DNA binding and homodimerisation. NES – nuclear export signal – required for shuttling into the cytoplasm. Glycine-rich region – Required for protein-protein interactions and incorporation into stress granules; also involved in RNA processing. This region shares homology with yeast prion proteins and is designated as prion-like owing to its aggregative propensity, it contains a Glutamine/Asparagine rich-region which is important for this behaviour. The majority of pathogenic mutations are situated in the Glycine-rich region and are almost all missense. Adapted from Janssens and Van Broeckhoven, (2013).

Currently there are over 40 known pathogenic mutations in *TARDBP*, which account for approximately 4% of fALS cases, 1% of sALS cases and <1% of sporadic FTD (sFTD) cases, giving it a position towards the ALS end of the ALS-FTD spectrum (Scotter et al., 2015).

TAR DNA Binding Protein of 43 kDa, TDP-43, was first described twenty years ago as a protein that bound to the TAR region, a regulatory element in the long terminal repeat of the DNA of the HIV-1 virus (Ou et al., 1995). Ubiquitously expressed and highly conserved through evolution, TDP-43 is composed of 414 amino acids and contains an N-terminal region (NTD), two RNA-recognition motifs (RRM), nuclear localisation (NLS) and nuclear export signals and a glycine rich C-terminal region (Figure 1.2). Most of the pathogenic mutations in TDP-43 are located within this glycine rich C-terminal domain, suggesting this domain is important in disease (Pesiridis et al., 2009).

The two RRMs can be subdivided into two components, the octomeric ribonucleoprotein 1 (RNP1) and hexameric ribonucleoprotein 2 (RNP2), appearing in the order of RNP2 – RNP1 (Maris et al., 2005; Kuo et al., 2009). The two RRMs of TDP-43 are situated in the middle of the protein with RRM1 comprising 90 amino acids from 101-191 and the slightly larger RRM2 comprising 93 amino acids, from 192-285 (Kuo et al., 2009). The NLS is situated between the NTD and RRM1 and is a bipartite sequence ranging from aa 82-98, whilst the NES is buried within RRM2 and is composed of the lecuine rich stretch from aa 239-250 (Winton et al., 2008). The C terminal of TDP-43 was noted as being glycine-rich and a mediator of protein-protein interactions. Indeed, TDP-43 requires its C-terminal region to mediate interactions with proteins such as hnRNP A/B (Buratti et al., 2005). Thus, based on this structure, TDP-43 is a member of the heterogeneous nuclear ribonucleoprotein family (Ou et al., 1995).

Functionally, TDP-43 operates as a homodimer (Kuo et al., 2009) to carry out a diverse array of cellular roles. The presence of the NLS and NES sequences indicated that TDP-43 was localised to both the nucleus and the cytoplasm and indeed the protein shuttles between these two compartments. However, there is a nuclear bias to its normal physiological distribution, with the majority localised to this compartment (Ayala et al., 2008), suggestive of its importance for nuclear function. Indeed, TDP-43 has nuclear roles in gene transcription and mRNA splicing regulation. In terms of transcription, TDP-43 has been shown to be a repressor of the promoter for the *acrv1* gene in mouse spermatids (Lalmansingh et al., 2011). However, its role in mRNA splicing has been extensively studied. TDP-43 binds preferentially to UG-rich sequences contained within single-stranded RNA, which was first described in regard to its behaviour in binding to the transcript of the *CFTR* gene to promote skipping of exon 9 (Buratti and Baralle, 2001). Subsequently, in view of the growing understanding of TDP-43 as a gene expression and splicing regulator, several studies (Tollervey et al., 2011; Polymenidou et al., 2011;

Xiao et al., 2011; Sephton et al., 2011; Colombrita et al., 2012) sought to define its RNA targets and the nature of its splicing regulatory role. These studies utilised crosslinking, immunoprecipitation and high-throughput sequencing (CLIP-Seq) techniques to reveal that TDP-43 binds to and regulates thousands of RNA targets. Results from the studies formed a strong consensus that TDP-43 binds preferentially to long stretches of UG repeats and to intronic sites significantly distant from exon-intron boundaries and functions to conduct alternative splicing and control of transcript levels. In the study by Polymenidou and colleagues, knockdown of TDP-43 in mouse brain revealed the majority of transcripts downregulated were those pre-mRNAs with long introns and were enriched for roles at the synapse. They also included those transcripts for neurodegeneration-associated proteins, including the ALS associated Fused in Sarcoma (*Fus)* and neurofilament light chain (*Nefl).* These findings were corroborated in the study of FTLD-TDP cortical tissue by Tollervey et al., (2011). These studies also showed TDP-43 binds within the 3'UTR to a number of transcripts, with such binding enriched within the cytoplasmic fraction of human brain tissue and SH-SY5Y cells in the study on by Tollervey et al., (2011). TDP-43 can also reduce the levels of its own transcript through binding within the 3'UTR, which has been shown to lead to an alternative splicing event, triggering nonsense-mediated decay (Polymenidou et al., 2011) or by promoting instability of the transcript without splicing activity (Ayala et al., 2011).

Within the nucleus, TDP-43 also localises with the Drosha complex (Gregory et al., 2004), where it is involved in the processing of pri-miRNAs, to which it has been shown to also bind, for the formation of pre-miRNAs. Among those miRNAs regulated by TDP-43 is miR-132-3p, which is involved in neuronal growth. TDP-43 knockdown decreases miR-132-3p expression and leads to concomitant disruption of neuronal outgrowth in cells, indicating miRNA control is an important function of TDP-43 (Kawahara and Mieda-Sato, 2012).

TDP-43 can shuttle between the nucleus and cytoplasm and the fraction that localises into the latter compartment serves a number of RNA-related functions. Several studies indicate that TDP-43 can translocate to the cytoplasm in response to cellular stress and stalling of translation initiation. TDP-43 is found, along with other RNA-binding proteins, within stress granules (Colombrita et al., 2009; Liu-Yesucevitz et al., 2010), which function to sequester those mRNAs that are not required for the cellular stress response in order to streamline translation towards necessary transcripts (Lindquist, 1981). These stress granules (SGs) can also associate with processing bodies (P- bodies), which serve as sites for RNA degradation and mRNAs can shuttle between the two, suggestive of a process of RNA triage (Anderson and Kerdersha, 2008). Incorporation of TDP-43 within stress granules requires its first RRM and the C-terminal domain (Bentmann et al., 2012), this domain contains a Q/N rich region, and shares homology with the yeast prion proteins, is designated as prion-like and thus as expected, is highly prone to aggregation (Johnson et al., 2009; (Fuentealba et al., 2010).

Aside from SGs and P-bodies, TDP-43 is a component of another class of RNA-binding protein (RNP) granules within the cytoplasm, those that are involved in the transport of mRNA. Such TDP-43 and mRNA-containing granules have been found within the dendrites of rat hippocampal neurons co-localising with mRNAs of CAMKIIα and β-actin and were increased upon neuronal stimulation with KCl. TDP-43 was shown to act as a repressor of translation in an *in vitro* assay (Wang et al., 2008). This study also showed TDP-43 co-localising with other RNPs, namely Staufen and FMRP, which was corroborated in the work by Fallini et al., (2012) in which TDP-43 was observed within granules translocating along live axons of primary cultured mouse motor neurons, where TDP-43 was postulated to have a regulatory role on the process of axonal outgrowth. Work by Alami et al., (2014) also demonstrated mRNA-containing granules translocating along mouse primary cortical neurons which co-localised

with TDP-43, thus TDP-43 appears to have an important role in mediating the spatial distribution and regulation of mRNAs within neurites and regulating local translation.

In ALS, TDP-43 is mislocalised from the nucleus to the cytoplasm, is cleaved to form C-terminal fragments and forms insoluble aggregates that are hyperphosphorylated and ubiquitinated (Arai et al., 2006; Neumann et al., 2006; Hasegawa et al., 2008). Mutations in TDP-43 associated with ALS also lead to these outcomes (Yokoseki et al., 2008). The implications and relevance of each of these phenotypes in disease pathogenesis has been a matter of great debate within the field (see section 1.4).

1.3.2.3 FUS

Originally discovered as forming part of a fusion protein in sarcoma cancers (Crozat et al., 1993; Rabbitts et al., 1993), Fused in Sarcoma (FUS), otherwise known as Translocated in Liposarcoma (TLS), (herein referred to as FUS) was the second DNA/RNA-binding protein to harbour mutations linked to ALS (Vance et al., 2009; Kwiatkowski et al., 2009). Similarly to *TDP-43*, *FUS* lies towards the ALS end of the disease spectrum, with mutations occurring in 4% of fALS and 1% of sALS and no familial FTD (fFTD) cases are attributed to mutation in *FUS*, along with <1% of sFTD (Scotter et al., 2015). Missense, deletion and insertion mutations are all represented within *FUS*, although the former is the most prevalent and the majority act in a dominant manner to cause disease (Lagier-Tourenne et al., 2010).

FUS is a member of the FET family, which also includes Ewing RNA-binding protein (EWS) and TATA-binding protein-associated factor 2N (TAF15), both themselves also implicated in ALS. Being a DNA/RNA-binding protein, FUS is structurally similar to TDP-43, although it is a larger protein of 526

amino acids owing to the presence of several additional domains (Figure 1.3). The first 165 amino acids form the QGSY rich region, this is immediately followed by the first of three Arg-Gly-Gly (RGG) motif-repeat regions from aa 165-267. The only RRM within FUS comprises aa 285-371 and harbours the nuclear exportation signal (NES). This lone RRM is followed by the second RGG motif region, a zinc finger domain (ZnF), the third RGG motif region and a non-classical nuclear localisation signal (NLS) (Iko et al., 2004). Over 50 mutations have been identified spread throughout the gene, but large clusters are found in all three RGG regions, the NLS and the QGSY rich region, however only a fraction of these have had their pathogenicity reliably proved to date (Deng et al., 2014).

As is the case for TDP-43, FUS shuttles between the nucleus and cytoplasm with the majority localised to the nucleus under normal conditions, where it serves a host of functions (Zinszner et al., 1997). Utilising its DNA binding ability, FUS has been shown to be involved in the maintenance of genomic stability as homozygous knockout led to an increased radiation sensitivity, disrupted B lymphocyte development, chromosomal instability and perinatal death in mice (Kuroda et al., 2000; Hicks et al., 2000). FUS is a component of the DNA-damage response (DDR); it is recruited via PARP-1 to DNA damaged through oxidative stress (Rulten et al., 2014) and is recruited to sites of double-strand breaks (DSBs) in neurons, where it is postulated to be involved in signalling the presence of the YH2AX marker of DSBs. DDR also requires FUS to interact with the repair protein HDAC1, with which it is postulated to form a complex (Wang et al., 2013b).

FUS is heavily involved in transcriptional regulation, associating with TFIID and RNA polymerase II, as well as an array of nuclear hormone receptors and other specific factors. Through this activity FUS has a role in control

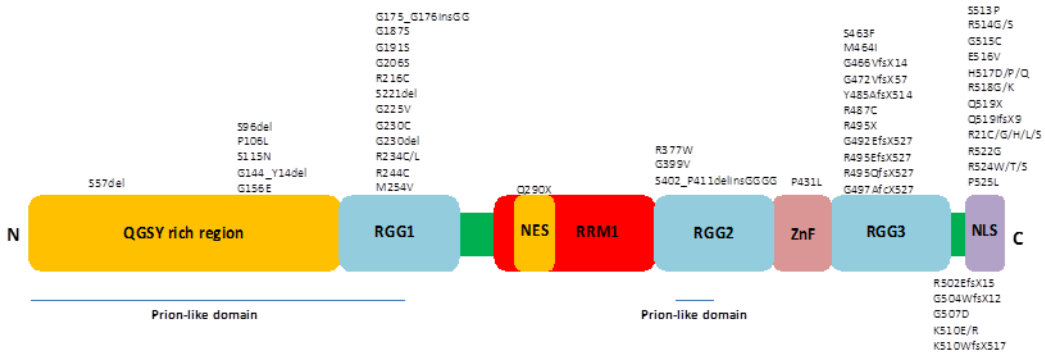

Figure 1.3: The structure of FUS. QGSY rich region= Glutamine/Glycine/Serine/Tyrosine - region, has homology with the prion like domain, important in FUS self-assembly. Three RGG motifs=Arginine-Glycine-Glycine motif-rich domains, involved in RNA-binding, the second of which harbours an additional small prion-like domain. RRM = RNA-recognition motif, involved in RNA binding, ZnF = Zinc finger domain, involved in RNA binding, NES = nuclear export signal, required for shuttling from nucleus to cytoplasm, NLS = Nuclear localisation signal, required for shuttling from cytoplasm to nucleus. Mutations encompassing missense, deletions, insertions and frameshifts are located throughout the protein but cluster with high frequency within the RGG domains and the NLS. Not all of these mutations have had their pathogenicity proven beyond a reasonable doubt at this time. Adapted from Deng et al., (2014).

of the cell cycle by repressing transcription of cyclinD1, the end result of a cascade of events stemming from DNA damage (Wang et al., 2008).

Like, TDP-43, FUS is known to regulate RNA processing. It is found within the spliceosome (Zhou et al., 2002) and interacts with a number of splicing factors including the serine-arginine repeat domain containing (SR) family (Meissner et al., 2003). FUS binds RNA, which seems to be specified by a GUGGU motif (Lerga et al., 2001; Lagier-Tourenne et al., 2012) and also RNA structure, likely AU-rich stem loops (Hoell et al., 2011). The RNA targets of FUS number in the thousands, with over 5000 targets: 650 and 350 RNA levels and splicing events are changed respectively, upon depletion of this protein in mouse striatum and human-derived neurons (Lagier-Tourenne et al., 2012).

FUS binds at multiple sites along its targets and maintains its binding until the completion of splicing, giving what has been dubbed a ‘saw-tooth’ appearance, which is postulated to function in transcriptional elongation

(Rogelj et al., 2012; Lagier-Tourenne et al., 2012; Ishigaki et al., 2012). Some of the transcripts bound by FUS are associated with ALS, such as *SOD1* and *UBQLN1* and *2* (Lagier-Tourenne et al., 2012). FUS also autoregulates its own expression levels by binding to exon 7 to promote its skipping; this creates a frame shift and a stop codon, thus subjecting the transcript to nonsense-mediated decay (Zhou et al., 2013).

There appears to be only limited overlap in the RNA targets of TDP-43 and FUS (Lagier-Tourenne et al., 2012; Colombrita et al., 2012; Honda et al., 2014). Indeed TDP-43 and FUS have a greater commonality in targets whose expression levels they control as opposed to those whose splicing they control (Honda et al., 2014). Targets that overlapped and were downregulated in mouse brain and human-derived neurons upon TDP-43 or FUS depletion are enriched for long introns, which are overrepresented in neurons and function in neuronal processes such as synaptic transmission (Lagier-Tourenne et al., 2012). The functions of distinct TDP-43 and FUS targets are also enriched for commonality, suggesting loss of TDP-43 or FUS could lead to common pathogenic outcomes (Honda et al., 2014).

FUS was also found with TDP-43 in the Drosha complex for the processing of a set of pri-miRNAs, which it specifically binds, that function in neuronal and synaptic development. FUS also binds specifically to Drosha and aids its localisation to chromatin in a co-transcriptional manner (Morlando et al., 2012).

Within the cytoplasm, an additional role for FUS as a transporter of mRNA to dendritic spines for the regulation of the actin cytoskeleton dynamics has been proposed (Fujii et al., 2005). Here, mRNA for Nd1-L, an actin stabilisation protein involved in maintaining dendritic spine morphology, was demonstrated to bind FUS via its 3'UTR and display significantly

enhanced spine localisation upon mGluR activation, which was disrupted with FUS knockout.

FUS-positive inclusions containing full length and protein fragments of FUS are observed in patients with *FUS* mutation-linked ALS who exhibit FUS mislocalisation to the cytoplasm (Mackenzie et al., 2010). The exact features of the inclusion morphology vary with mutation, for example the P525L mutation gives rise to FUS-positive, cytoplasmic, round inclusions and basophilic inclusions, but these were skein-like in patient tissue with the R521C mutation (Mackenzie et al., 2011; Deng et al., 2014) Interestingly, these FUS-positive inclusions are negative for TDP-43, a trait shared with inclusions deriving from *SOD1* patients. Unlike TDP-43 within inclusions, FUS does not appear to be abnormally phosphorylated or ubiquitinated (Mackenzie et al., 2010). FUS inclusion pathology, also known as FUS proteinopathy, is also a feature in the frontotemporal brain regions in a subsection of FTD patients with ubiquitinated inclusions, which are also negative for TDP-43, designated as FTLD-FUS (Mackenzie et al., 2008; Neumann et al., 2009). However, these patients do not harbour *FUS* mutations (Snowden et al, 2011) and show different features such as colocalisation with transportin 1 (Troakes et al., 2013) and hypomethylation of arginine residues, which may interfere with functioning of the NLS (Dormann et al., 2012). The inclusions also differ in localisation, being nuclear and generally skein-like in appearance (Neumann et al., 2009). In addition, FUS inclusion pathology is observed in other similar neurodegenerative conditions, such as Neuronal intermediate filament disease where the inclusions are cytoplasmic (Mackenzie et al., 2010) and in polyglutamine diseases, manifesting primarily as neuronal nuclear inclusions (Doi et al., 2008).

1.3.2.4 C9orf72

In 2011, the locus on chromosome 9 that had for some time been linked to ALS-FTD spectrum was uncovered as that of *C9orf72*. Patients can manifest ALS, FTD or both, providing a clear indication that these disorders are related as part of a spectrum (Renton et al., 2011; DeJesus-Hernandez et al., 2011). This locus has been linked to a world average of 7% sSALS, 39% fFALS, 6% sFTD and 25% fFTD cases (Scotter et al., 2015).

C9orf72 contains 12 exons and can give rise to three transcriptional variants due to alternative splicing termed variants 1-3. Two protein isoforms can arise from these variants, the long isoform (or A) from variants 1 and 3, and the short isoform (or B) from variant 2 (Figure 1.4).

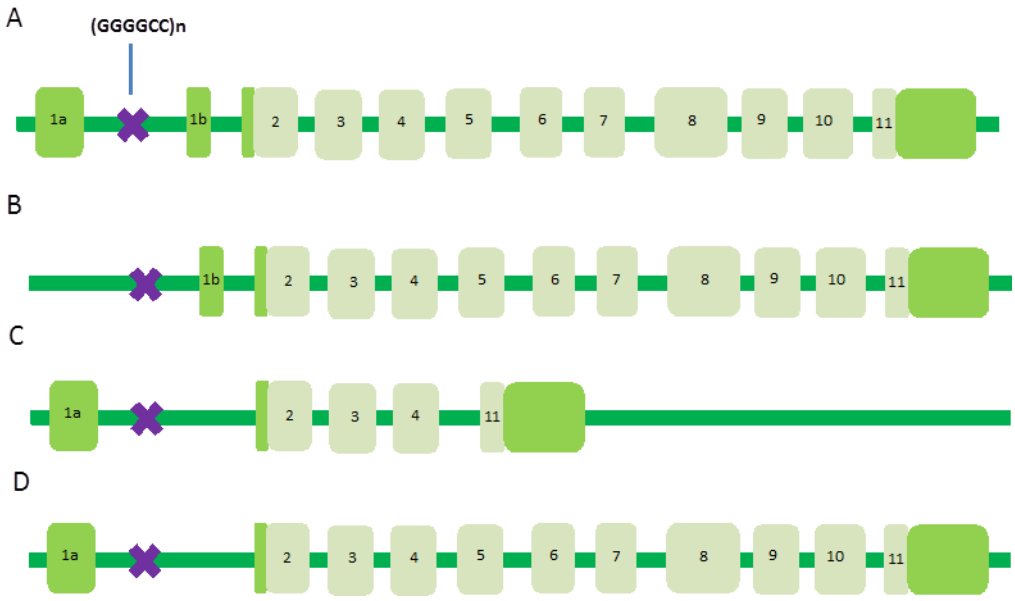

Figure 1.4: The structure of *C9orf72* and its transcript variants. (A) The *C9orf72* gene is comprised of 12 coding exons, two of which are non-coding (1a and 1b). Within the first intron which separates these exons, is a hexanucleotide repeat sequence (GGGGCC)n. Expansion of this repeat is causative of ALS and FTD. There are three possible transcription variants due to alternative splicing. (B) Variant 1 is spliced to retain only exon 1b. (C) Variant 2 skips exon 1b and exon 5 to 10. (D) Variant 3 skips exon 1b but retains all other exons. Adapted from Rohrer et al., (2015).

Pathogenicity related to *C9orf72* does not arise from point mutations or indels, but rather the expansion of a hexanucleotide repeat (GGGGCC) situated within the first intron or in the promoter region depending on the transcript variant (Renton et al., 2011; DeJesus-Hernandez et al., 2011). Wild-type alleles contain usually less than ten repeats with three common alleles of 2, 5 or 8 repeats (Suh et al., 2015).

There is debate over what should be defined as the minimum repeats length required for pathogenic risk. A figure as low as 30 is the current consensus and there exists an intermediate level of expansion between 30-500 that is shared among patients and controls, which is of unresolved consequence (Fratta et al., 2015). However patient alleles are frequently in the realm of several thousand repeats, representing a massive expansion (DeJesus-Hernandez et al., 2011; Beck et al., 2013). The expansion is also highly unstable and varies between tissues within the same person (Rohrer et al., 2015).

The functions of the protein C9orf72 are in the early stages of being elucidated. Sequence analysis revealed it to be related to the Differentially Expressed in Normal and Neoplasia (DENN) proteins, which function as Rab-GEFs for the activation of Rab GTPases involved in membrane trafficking dynamics. As such, functions for C9orf72 are arising in the autophagy and endocytic pathways (Levine et al., 2013).

Expanded *C9orf72* can be transcribed in the sense direction leading to hairpin and four-stranded G quadruplex formation (Fratta et al., 2012). It is also transcribed in the anti-sense direction generating GGGGCC and CCCCGG containing pre-mRNAs. These have been observed to form into nuclear RNA foci within the brains of these patients, which serve to sequester RNA binding proteins (DeJesus-Hernandez et al., 2011). The repeat-containing RNA, both sense and anti-sense is also subject to an unusual form of translation termed repeat associated non-ATG (RAN)

translation, which does not require an upstream start codon. This phenomenon was first described in relation to the CAG repeat expansion in the SCA8 gene resultant in Spinocerebellar ataxia type 8 and has subsequently been found to be common amongst repeat expansion disorders (Ash et al., 2013; Zu et al., 2011). All six reading frames of *C9orf72* RNAs can be translated in this way, resulting in the generation of a series of dipeptide repeat proteins (DPRs), which in the sense direction are GA, GP, GR and in the antisense direction are GP, PA and PR (Gendron et al., 2013; Mori et al., 2013b). However, GP and PR can also be generated by classical translation (Zu et al., 2011), which is interesting given a start codon is present in the reading frame that generates PR and that, at least in HEK293 cells, the presence of an AUG in this frame leads to increased PR abundance (Zu et al., 2013; Stepto et al., 2014).

These DPRs have a high propensity to aggregate and are observed forming inclusions within *C9orf72*-associated patient brains and spinal cords. Such inclusions are positive for ubiquitin and contain the important protein degradation pathway proteins p62 and Ubiquilin 2 (UBQLN2), whilst being free of TDP-43 (DeJesus-Hernandez et al., 2011; Al-Sarraj et al., 2011; Brettschneider et al., 2012). These inclusions join the RNA foci as specific pathologies of *C9orf72* expansion mediated ALS-FTD disease. However, TDP-43-positive inclusions are also present and are pervasive throughout the brain, although not in the cerebellum or hippocampus, in cases manifesting as FTD and additionally in the spinal cord of those with accompanying ALS (Rohrer et al., 2015). It is not understood why some patients with *C9orf72* expansion present with ALS and some with FTD, although it is known this can be influenced by genetic modifiers such as *ATXN2*, which reportedly increases the likelihood of an ALS phenotype (van Blitterswijk et al., 2014).

1.4: Mechanisms of Pathogenesis

The etiology of ALS is clearly varied. The 90% rate of sporadic cases and 10% of familial cases demonstrate the importance of both environmental and genetic factors. Yet sporadic and familial ALS are also clinically indistinguishable and despite the myriad of associated genes, the majority of cases share a common clinical pathology. This pathology is also shared in many patients with FTD in the cases of FTLD-TDP-43 and, as has been described, ALS and FTD are now recognised to form part of a spectrum. It appears the common denominator is TDP-43 inclusions and disorders in which this takes place are termed TDP-43 proteinopathies. Exceptions comprise cases arising from SOD1 and FUS, which nevertheless share varying degrees of relatedness that will be discussed below.

1.4.1 TDP-43-Mediated ALS

The majority of sporadic and familial ALS cases display TDP-43 proteinopathy, with both wild-type and mutant TDP-43 observed to undergo mislocalisation to the cytoplasm, C-terminal fragmentation, aggregation of both fragments and full length protein, ubiquitination and hyperphosphorylation (Arai et al., 2006; Neumann et al., 2006; Hasegawa et al., 2008; Yokoseki et al., 2008). The pathogenicity of these observations has been the subject of intense research: are they a cause or a consequence and is disease caused by TDP-43 loss of function or a gain?

Genetic knockout and overexpression studies have strived to answer these questions. Complete loss of TDP-43 homologs leads to an early lethality in animal model including mice (Sephton et al., 2010; Kraemer et al., 2010; Wu et al., 2010) and *Drosophila* (Feiguin et al., 2009; Fiesel et al., 2010; Diaper et al., 2013). However, depletion in a tissue and time-manipulated manner has revealed that TDP-43 loss can lead to the development of age-related progressive ALS phenotypes in these models

(Wu et al., 2012; Iguchi et al., 2013; Feiguin et al., 2009; Diaper et al., 2013). However, studies overexpressing wild-type TDP-43 have also returned results demonstrating ALS-like disease phenotypes (Wils et al., 2010; Guo et al., 2011; Hanson et al., 2010; Ritson et al., 2010; Voigt et al., 2010; Li et al., 2010; Miguel et al., 2011; Lin et al., 2011; Estes et al., 2011; Diaper et al., 2013). Hence, both loss and gain of TDP-43 appear able to cause pathogenesis.

But what are the mechanisms of this pathogenesis? In human disease, TDP-43 is cleared from the nucleus and accumulates in the cytoplasm (Neumann et al., 2006). There is thus a concomitant lack of it in the nucleus, a compartment where 70% is normally to be found (Barmada et al., 2010). The loss of TDP-43 from the nucleus compromises its array of nuclear functions in RNA processing, including RNA stability and splicing regulation. As described above, depletion of TDP-43 leads to many splicing changes and transcript up and down-regulations, the latter of which include micro-RNAs (Tollervey et al., 2011; Polymenidou et al., 2011a; Xiao et al., 2011; Sephton et al., 2011). Thus, mislocalisation to the cytoplasm serves to create a loss of function in nuclear RNA processing (Scotter et al., 2015). Although TDP-43 is cleared from the nucleus in human disease, some models do not recapitulate this, such as Diaper et al., (2013), who found no mislocalisation of wild type *Drosophila* TDP-43 with loss or overexpression. This suggested TDP-43 doesn't have to be removed from the nucleus to cause pathogenicity. This, they postulate, is caused through disruption of the stoichiometry of components within the ribonucleoprotein complexes in which TDP-43 functions. This suggested what seems to be important is the levels of TDP-43 within the nucleus.

Cytoplasmic TDP-43 can be cleaved into several species of C-terminal fragments of around 25 kDa (Neumann et al., 2006; Igaz et al., 2008). These fragment species all share the C-terminal domain and are highly prone to misfold and aggregation. They can therefore also form into aggregates that can sequester full length TDP-43 and other proteins and

become ubiquitinated and hyperphosphorylated, as seen in the patient tissue (Neumann et al., 2006; Igaz et al., 2008). Intriguing, recent evidence by Woerner et al., (2016) has suggested aggregates of cytoplasmic C-terminal fragments may be toxic through a mechanism disrupting nucleocytoplasmic transport of mRNA caused by altered distribution of nuclear pore complex components. However, whether these fragments represent a toxic species is debatable since the RRM1 with its RNA-binding activity has been suggested to be necessary for toxicity (Voigt et al., 2010), a domain that is missing from most of the C-terminal fragments. In addition, the clearance of TDP-43 is thought to be promoted by fragmentation, which reduces cellular toxicity (Li et al., 2015).

In addition to failure in RNA processing, protein degradation via the ubiquitin-proteasome system and autophagy is also considered to be defective in ALS (Thomas et al., 2013). The Ubiquitin-Proteasome System (UPS) and autophagy pathways degrade TDP-43 (Scotter et al., 2014). However, efficiency of protein degradation declines with age (Shringarpure et al., 2002; Cuervo, 2008) and may leave a cell susceptible to the consequences of cellular stress, which can be induced in myriad ways, such as oxidative and endoplasmic reticulum stress (Colombrita et al., 2009; McDonald et al., 2011), which may provide some explanation as to the age of onset of disease. These consequences are namely the mislocalisation, cleavage and misfolding of wild-type TDP-43 or mutant TDP-43, which has an increased propensity for those outcomes. The importance of proper protein degradation functioning in ALS is further evidenced by the fact ALS causative mutations are found in VCP, p62, UBQLN2 and OPTN, which are all components of these systems and that TDP-43 positive aggregates are a hallmark of ALS associated with mutation in all of these proteins (Scotter et al., 2015).

As stated above, environmental cellular stress is known to be able to trigger the cytoplasmic mislocalisation of TDP-43. This can occur normally

in physiological conditions as part of the stress response, leading to its incorporation into stress granules (Liu-Yescucevitz et al., 2010). However the disease state likely represents a dramatic mislocalisation, as a consequence of continuous cellular stress. These stress granules are characterised as temporary structures assembling in stress and disassembling when the stress is removed. However, if the cellular stressors remain, it is postulated that these stress granules persist (Parker et al., 2012). Such cytoplasmic mislocalisation and stress granule persistence is also demonstrated with many mutations, occurring as they do in the aggregation prone, prion-like C-terminal domain of TDP-43 (Dewey et al., 2011), which itself is required for aggregation and stress granule recruitment (Bentmann et al.,2012). As a consequence, it has been suggested that persistent stress granules 'seed' the development of protein aggregates. In support of this, the core stress granule protein TIA-1 has been found to be present in the TDP-43-positive inclusions in patients' spinal cords (Liu-Yesucevitz et al., 2010).

These aggregates are subject to hyperphosphorylation and ubiquitination (Neumann et al., 2006), with hyperphosphorylation achieved via casein kinases 1 and 2 (Hasegawa et al., 2008; Kametani et al., 2009). However, it is not clear what the precise outcome of phosphorylation is in regard to toxicity (Scotter et al., 2015). This is also the case with ubiquitination of TDP-43, which can be achieved by several ubiquitin ligases, including Parkin (Hebron et al., 2013); clearly more work needs to be done to resolve this uncertainty (Scotter et al., 2015).

Whether aggregates themselves are toxic is also a matter of debate: Cellular toxicity in the absence of aggregate formation has been seen, suggesting that it is cytoplasmic mislocalisation and not aggregates themselves that is toxic (Barmada et al., 2010; Arnold et al., 2013). However it is conceivable that this toxicity of cytoplasmic accumulation is occurring via smaller aggregates, such as oligomers that are hard to

detect, and that these may be contributing to toxicity in a dominant negative manner by sequestering wild-type TDP-43, other RNA binding proteins and proteins with which TDP-43 is known to bind as well as RNA (Barmada et al., 2010; Scotter et al., 2015).There is also the prospect that they disrupt nucleocytoplasmic transport of mRNA out of the nucleus by altering localisation of nuclear pore complex proteins (Woerner et al., 2016).

Some further evidence in support of a toxic role for aggregates of some kind, even if not 'mature' aggregates, stems from the fact that activating autophagy leads to the clearance of aggregates and reduces TDP-43 toxicity (Barmada et al., 2014; Maniecka and Polymenidou, 2015). Further consideration comes from the fact that ALS is observed to spread from location to location within the bodies of patients. This is highly reminiscent of prion like spread and aided the conception of the prion-like theory of ALS progression and spread, similar theories have also been proposed in other neurodegenerative disorders such as Alzheimer's disease (Polymenidou and Cleveland, 2011). This theory suggests that protein aggregates containing misfolded proteins highly prone to aggregation, such as TDP-43, can self-template their own assembly in a process by which they convert wild type, normally folded protein into a pathological misfolded form (Maniecka and Polymenidou, 2015). As was alluded to above for TDP-43, it has been suggested that the seeding of these self-templating aggregates may be via stress granules, which become pathologically persistent and act as high protein concentration clusters. This situation may be further exacerbated by the function of TDP-43 to auto-regulate the levels of its own transcript, generating a 'feed-forward' loop in which auto-regulation is impaired by the cytoplasmic mislocalisation of the protein, leading to greater retention of TDP-43 transcripts, increasing the concentration of the protein available for incorporation into the aggregates and pathologic conversion

(Polymenidou et al., 2011; Ayala et al., 2011; Maniecka and Polymenidou, 2015).

1.4.2 FUS-Mediated ALS

Like TDP-43, FUS appears to be important in development as knockout animal models display reduced viability. Knockout of *Fus* in mice produces perinatal lethality, a developmental abnormality in B-lymphocytes, chromosome instability and male sterility (Hicks et al., 2000). In *Drosophila*, knockout of the *FUS* homolog, *caz*, leads to a sub-viability phenotype, wherein only rare escapers make it to adulthood. These escapers are short-lived and exhibit locomotor defects and morphological abnormalities in wings, eyes and genitals (Wang et al., 2011). They have also been characterised with disrupted neuromuscular junctions (NMJs) (Sasayama et al., 2012; Xia et al., 2012), though this phenotype was not present in other models (Wang et al., 2011; Shahidullah et al., 2013).

Wild-type and mutant FUS overexpression studies also demonstrate neurodegenerative phenotypes. In *Drosophila*, a rough eye phenotype is observed with overexpression of the human gene in this tissue, indicating loss of photoreceptor neurons (Chen et al., 2011). It also leads to an increase in the number of synaptic boutons in *Drosophila,* though for wild type only (Wang et al., 2011) and a reduction in the number of presynaptic active zones and impairment in synaptic transmission (Machamer et al., 2014). Motor neuron cell bodies also appear to contain swellings and demonstrate axonal loss (Chen et al., 2011). In terms of viability and locomotor phenotypes, some studies have found no adult climbing defects at young adult stages (Wang et al., 2011), however others using different strains observed reduced viability and locomotion (Xia et al., 2012; Chen et al., 2011; Machamer et al., 2014). ALS-linked FUS mutants are variable in their ability to rescue knockout phenotypes. They appear able

to rescue viability but not locomotion (Wang et al., 2011), suggesting a loss of this function at least of the P525L and R522G mutations.

The pathogenesis of FUS-mediated disease share many similarities with TDP-43 although with the absence of TDP-43 proteinopathy. Many mutations in FUS lead to cytoplasmic mislocalisation of the protein. Such an event serves to sequester FUS from the nucleus leading to the loss of its RNA processing functions, resulting in mass changes in RNA transcript levels and splicing; some of these RNA targets are shared with TDP-43. This has given rise to the concept that TDP-43 and FUS converge on a common pathway to pathogenesis and further recognises RNA processing in ALS disease formation (Lagier-Tourenne et al., 2012; Honda et al., 2014). In further support of this, it is known that TDP-43 and FUS interact within complexes in an RNA-binding dependent way and that they operate in a pathway in which FUS is downstream of TDP-43, which was demonstrated by the fact *caz* can rescue locomotor phenotypes caused by knockout of the Drosophila *TARDBP* homolog, *TBPH* (Wang et al., 2011).

Additionally, as for TDP-43, wild-type FUS can incorporate into stress granules in response to cellular stress (Anderson et al., 2008) and this tendency is increased by mutations, likely via increased cytoplasmic localisation (Bosco et al., 2010). These stress granules also show persistence after the removal of stress. Such stress granule recruitment has also been proposed to seed the formation of aggregates and drive the prion-like spread of disease, acting as concentration points for the recruitment of further FUS protein and pathogenic conversion (Vance et al., 2013; Maniecka and Polymenidou, 2015). In support of this, FUS contains several prion-like domains, which render it extremely aggregate-prone, being able to do so spontaneously in solution, (Sun et al., 2011) and these are required for FUS incorporation into stress granules (Bentmann et al., 2012). FUS also auto-regulates and loss of this function through cytoplasmic sequestration is thought to lead to the progression of these

insoluble prion-like aggregates, as it does in the case of TDP-43 (Zhou et al., 2013; Maniecka and Polymenidou, 2015). The recent evidence by Woerner et al., (2016) also hints at the possibility FUS aggregates, as TDP-43 aggregates, cause disruption to nucleocytoplasmic transport, which likely contributes to toxicity.

1.4.3 C9orf72-Mediated Disease

As a more recently linked locus, *C9orf72* pathogenesis is in the early stages of being elucidated; nevertheless an intensive study regime is rapidly shedding light on the potential disease mechanisms.

Haploinsufficiency has been proposed, wherein levels of the transcript and of C9orf72 protein are decreased below what is physiological sufficient for function. In support of this, a 5' CpG island of the expanded allele has been reported to be hypermethylated (Xi et al., 2013; Liu et al., 2014), a sign of gene silencing, and reductions in *C9orf72* transcript expression are noted in the affected central nervous system (CNS) regions in these patients (DeJesus-Hernandez et al., 2011). To this end, there is also a reported trimethylation of lysine residues of histones H3 and 4 (Belzil et al., 2013). However, reduction of C9orf72 levels in patient-derived motor neurons actually served to ameliorate the observed transcriptional changes and even be protective (Sareen et al., 2013; Liu et al., 2014). Furthermore, *in vivo* modelling of C9orf72 knockdown in mice indicates that reduced expression is not causative of pathogenesis. Reduction via antisense oligonucleotides did not lead to overt phenotypes in one study (Lagier-Tourenne et al., 2013) and this has been corroborated recently in another, which employed neuronal and glial conditional knockout, discovering no evidence of neurodegenerative phenotypes (Koppers et al., 2015).

C9orf72 repeat expansion is transcribed in both sense and antisense directions and both can form into RNA foci within the nucleus. Such foci are an established hallmark of C9orf72 disease (DeJesus-Hernandez et al., 2011). In multiple models their presence correlates with toxicity, for example in several non-neuronal cell lines as well as SH-SY5Y cells, expression of 38 and 72 repeats led to RNA foci formation within the nucleus, which were twice as numerous for the longer repeat indicating a relationship between repeat length and foci burden. No RNA foci were observed when a repeat length of 8 was expressed, which is within the normal range. Furthermore the RNA foci-containing SH-SY5Y cell population, but not controls, were subject to apoptotic machinery activation and concomitant increases in cell death. These results were corroborated *in vivo* with Zebrafish embryos (Lee et al., 2013).

A well-known gain of function consequence of RNA foci in other diseases is the binding and sequestration of RNA binding proteins. Many such proteins have been found within these foci including hnRNP A1 and Purα in iPSC derived motor neurons and Neuro-2a cells (Sareen et al., 2013; Xu et al., 2013) In motor neurons of *C9orf72* expansion ALS patients the RNA foci sequester SRSF2, hnRNP H1/F, ALYREF, with the addition of hnRNP A1 in the cerebellum (Cooper-Knock et al., 2014), and in another study the cerebellar p62 positive and TDP-43-negative inclusions in patient tissue were positive for hnRNP A3 (Mori et al., 2013b). The sequestration of these RNA-binding proteins was linked to toxicity through serving to prevent their functions in RNA metabolism and evidence supports this. Pathogenic repeat length containing Neuro2a cells which sequester Purα into RNA foci, had toxicity alleviated by the additional overexpression of Purα itself, which was also seen *in vivo* in the *Drosophila* photoreceptors (Xu et al., 2013). In addition, the binding and sequestration of hnRNP H reduces the inclusion of exon 7 within *TARBP2* transcripts (Lee et al., 2013). Thus, the sequestration of multiple RNA-binding proteins within repeat expansion induced RNA foci is very likely an underpinning of

toxicity in *C9orf72*-mediated disease. This concept has further implications given that *C9orf72* expansion disease is technically a TDP-43 proteinopathy, since such TDP-43 positive inclusions are present. No evidence suggests TDP-43 is a binding partner of the hexanucleotide repeats. Rather, it is hypothesised that the sequestration of hnRNPs, which are TDP-43 interactors, may lead to TDP-43 dysfunction (Stepto et al., 2014). Further, a set of studies has proposed that a dysfunction in nucleo-cytoplasmic shuttling caused by toxic gain of function of the expanded RNA. A screen in *Drosophila* revealed genes with products involved in nucleocytoplasmic transport, to be modifiers of toxicity (Freibaum et al., 2015). Additionally, overexpression of the important nucleocytoplasmic transport protein RanGAP, which is a binding partner of the expanded RNA, prevented toxicity in cell and *Drosophila* models (Zhang et al., 2015).

However, as previously described, *C9orf72* expansion RNA is translated in both sense and antisense directions via RAN translation to form dipeptide repeat proteins. Aggregates containing all of these were detected within the hippocampus of patient tissue and evaluation of the pro-arg (PR) species revealed their presence led to an increase in cell death compared to controls, indicating that they are toxic (Zu et al., 2013). This work on the PR species is interesting given further recent evidence that it is arginine-containing DRPs that causes toxicity. Mizielinska and colleagues generated flies expressing expanded *C9orf72* repeats engineered so that in each only one species of DPR was produced. In the proline-arginine 'PR only' and glycine-arginine 'GR only flies', neurodegeneration was observed via the measures of egg to adult viability, lifespan and rough eye phenotype. None of these measures were affected in control or 'GA only' and 'PA only' flies (Mizielinska et al., 2014). This is supported by the report that the GA species pathology is not correlated with neurodegeneration and the suggestion this might even be neuroprotective (Mackenzie et al., 2013). The study by Mizielinska et al., (2014) also sought to seperately

consider RNA- and DPR-mediated toxicity by generating 'RNA only' constructs with stop codons in each reading frame to prevent DPR formation. Flies expressing these did not display any of the aforementioned neurodegenerative phenotypes in any of the range of repeat lengths or temperatures examined. Therefore, neurodegenerative toxicity can arise solely from DPR expression. A mechanism for this is also proposed through acting to block the functioning of nuclear pores and prevent nucleo-cytoplasmic shuttling. In a yeast model, PR dipeptides alone were observed to be capable of causing toxicity, which could be ameliorated by increasing nucleocytoplasmic transport towards control levels by overexpressing various genes connected to this function (Jovičić et al., 2015). However, given the evidence also in favour of RNA mediated toxicity, a strong case for both RNA and DPR toxicity is apparent for the likely causes of toxicity in human disease.

1.4.4 SOD1-Mediated ALS

SOD1 mediated disease is considered to occur via different mechanisms than other forms of ALS, given that it does not lead to TDP-43 proteinopathy.

It became apparent with the arrival of the first mouse models soon after its discovery as a fALS locus that mutant SOD1 (mSOD1) did not operate via a loss of function mechanism. For example, Reaume and colleagues generated a knockout mouse that did not demonstrate definitive ALS phenotypes (Reaume et al., 1996), but these were apparent in the G93A overexpressing model generated by Gurney et al., (1994). Thus, the consensus view is that mSOD1 acts via a toxic gain of function.

To this end, it is known that mutations in SOD1 cause misfolding of the protein, which is subsequently ubiquitinated to target it to the proteasome for degradation. This clearance mechanism is perturbed

however by the capacity of mSOD1 to block the ubiquitin-proteasome system (Urushitani et al., 2002; Cheroni et al, 2009). Thus mSOD1 prevents its own degradation and persists in the cell, forming aggregates. mSOD1 also leads to dysfunction in endoplasmic reticulum-associated degradation (ERAD), due to its presence within the ER, which further exacerbates misfolded protein persistence (Kikuchi et al., 2006). Another organelle affected by mSOD1 is the mitochondria. A small amount of SOD1 is normally localised to the mitochondrial intermembrane space (IMS), where it carries out its dismutase reaction. mSOD1 is localised on the outer membrane and (OM), and within the latter its misfolded state disrupts mitochondrial function including alterations in redox potentials (Ferri et al., 2006). Glutamate excitotoxicity was one of the first pathogenic mechanisms proposed for mSOD1. It occurs via extracellular glutamate clearance failure and concomitant excessive calcium influx that is beyond the neurons' storage capacity, which is thought to be mediated by reductions in astroglial glutamate transporter EAAT2 (Rothstein et al., 1996).

This last point illustrates the important relationship between the surrounding glia and motor neurons for disease; models suggest that mSOD1 drives non-cell autonomous progression. Indeed, astrocyctes expressing mSOD1 cause toxicity to and increased death of motor neurons (Nagai et al., 2007; Di Giorgio et al., 2007). mSOD1 is secreted from both neurons and glial, which activates the microglial. Such activated microglia from mSOD1 mice cause toxicity to motor neurons in culture, which appears to be due to aberrant prostaglandin signalling (de Boer et al., 2014).

In common with TDP-43 and FUS, there is evidence to suggest that misfolded SOD1 propagates via prion-like spread. Wild-type SOD1 is not aggregation prone and is inherently stable, yet as stated above mutant SOD1 is misfolded and aggregates and has been shown to be able to seed

misfolding of wild-type SOD1 (Chia et al., 2010). Interestingly, it has also been suggested that oxidation of wild-type SOD1 can cause it to misfold, mimicking the actions of SOD1 mutation (Ezzi et al., 2007), a finding that has implications for sALS.

1.5: ALS: Distal Axonopathy

In patients, the pathogenesis described above ultimately drives neuronal destruction and loss and a noticeable absence of motor neurons from patient tissue upon examination. However, the question of precisely where within nervous system physiology ALS begins is a matter of some contention, and, like all studies seeking to elucidate information about disease onset, has been greatly hindered by the fact relevant patient tissue is usually gathered from those who died from the disease and thus represents the end-stages. However, clinical evidence from earlier disease time points demonstrates that there is a temporal disconnect between the manifestation of functional deficits at the NMJ, the onset of disease symptoms and the observed loss of the cell bodies.

1.5.1 The Dying-Back Hypothesis

One theory has been gaining a significant degree of support to explain this phenomenon. The 'dying-back' hypothesis states that ALS is a distal axonopathy in which pathological alterations occur within axonal terminals long before the manifestation of observable symptoms and death of the cell bodies themselves and that this distal dysfunction progresses backwards from the terminal, proximally towards the soma. Many neurodegenerative diseases have been classified as distal axonopathies such as Alzheimer's disease, Hereditary Spastic Paraplegia and Charcot Marie Tooth disease Type 2 (Millecamps and Julien, 2013).

For ALS, a considerable amount of support for this hypothesis has been accumulating for a number of years from both human patients and animal models. In a compelling study, Fischer and colleagues made use of the premature death of an ALS patient from non-related factors early in disease course to examine the relationship between clinical symptoms and motor neuron loss. The man had been demonstrating physical weakness and atrophy and had electrophysiological changes indicating nervous dysfunction. However the autopsy showed no degeneration of the corticospinal tract, motor cortex or ventral roots and interestingly there was also no evidence of activated astrocytes or microglia, but rather a grouped atrophy of muscle fibres (Fischer et al., 2004). In a functional context, studies examining the state of axonal excitability in ALS have shown that the dysfunction observed in the potassium channels in patients is more severe in the distal region of the axon (Nakata et al., 2006).

Multiple animal studies have also provided data that such neuromuscular function alterations occur at the earliest points of disease and have made extensive use of the G93A SOD1 mouse model. It had been noted by Chiu and colleagues that at P90, when the physical symptoms began, there was an extensive loss of the lower motor neurons and denervation of the limb muscles (Chiu et al., 1995). Subsequently this denervation was shown to be underway as early as P50, long before symptom onset (Frey et al., 2000). Based on these findings, Fischer and colleagues also used the G93A mouse model to test the dying back hypothesis. Denervation of motor end plates had begun by P47 in the mice, which did not display symptom onset until P80, after which motor neuron cell bodies began being lost from the spinal cord. This was a clear indication of distal to proximal progression (Fischer et al., 2004).

Although most extensively studied for SOD1, such findings are also forthcoming for models of TDP-43 and FUS associated ALS. In their study

of wild-type TDP-43, Diaper et al., (2013) found synaptic transmission defects in larvae experimentally determined to be the result of pre-synaptic dysfunction, and that these defects occurred before neuronal cell death. With regard to FUS, recent evidence using a *Drosophila* model has demonstrated that overexpression too leads to defects in synaptic functioning with reductions in NMJ active zone number and reduced quantal size and content leading to synaptic transmission defects already apparent at the larval stage (Machamer et al., 2014).

Many factors are implicated in this distal axonal degeneration and loss of the NMJs that centre on destruction of cytoskeletal integrity and NMJ stability, evidence of which is mostly gathered from the mSOD1 mouse. These include neuronal intrinsic and extrinsic factors involving muscles and the supporting terminal Schwann cells (TSC). For example, in these an aberrant increase in the levels of the repellent axon guidance proteins Sema-3a and Nogo-A have been recorded in TSCs and muscle cells, respectively. This leads to a scenario in which the nerve terminals are actively repelled from the NMJ (Krakora et al., 2012). The presence of neurotrophic factors is also critical and it has been shown that muscle specific expression of such factors like vascular endothelial growth factor (VEGF) can increase the number of NMJs and motor neurons maintained through disease (Keifer et al., 2014).

1.5.2 Selective Vulnerability

The motor system is noted as being particularly vulnerable to the development of ALS. The precise reasons for this are not completely understood, but likely arise from a combination of many factors, such as a relative fragility in view of excitotoxicity (Van Den Bosch et al., 2006). An element of selectivity is also apparent within the population of motor neurons. Many studies have demonstrated that muscles are not uniformly affected in ALS and that this depends on the properties of the different

motor units, which is the collective name for all the muscle fibres innervated by one motor neuron. There are three types of motor unit. Motor units in which the neuron innervates Type IIb/x muscle fibres are designated as fast-fatigable (FF), Type IIa muscle fibres characterise fast-resistant (FR) motor units and the third group, the slow (S) motor units, consist of Type I muscle fibres. A particular muscle's motor neuron innervation or motor pool is determined by a mix of these motor units and can be highly variable in number (Burke et al., 1973).

The decisions of the order of which motor units are recruited are laid down in Henneman's size principle, which states that the smallest motor units are recruited first and the largest last. The size of a motor unit depends on the size of the motor neuron, as smaller motor neurons have fewer terminal branches. These smallest motor neurons have the lowest current requirements to reach threshold and so small motor units are most easily recruited (Henneman., 1957). The small motor units are Type S and contain the muscle fibres that have the most extended contraction times and lowest force generating capacity. Type FF motor units have the largest motor neurons and are the largest motor units and therefore, the recruitment of motor units in general proceeds from the slow, lowest force producing, least fatigable units to the fast, highest force producing and most fatigable units, from Type S to Type FF (Heckman and Enoka, 2004).

Thus, not all motor neurons are created equal. This has implications for ALS as examined in the G93A SOD1 mouse by Frey et al., (2000), Pun et al., (2006) and by Hegedus et al., (2007) who saw that the denervation occurring before symptom onset involved the Type FF motor units and represents a preferential denervation of these units. A further interesting phenomenon is that denervated IIb/x muscle fibres change to I and IIa and are innervated by the remaining motor neurons (Hegedus et al., 2008). This sprouting ability is lacking in Type FF motor units and is greatest in

Type S which are the last to be touched. It appears that loss of Type FF units leads to weakening but progression of symptoms becomes apparent when compensatory sprouting begins to fail in the Type S units later in disease (Frey et al., 2000; Pun et al., 2006; Hegedus et al., 2008; Maloney et al., 2014).

It was suggested by Pun et al., (2006) and Hegedus et al., (2007) that a possible reason contributing to why Type FF units are preferentially lost earliest in disease might be due to the fact that they possess the largest motor neurons and was coupled with the fact that such neurons have the greatest metabolic requirements. Thus the importance of axonal transport in these neurons is apparent. Such transport is required for the delivery of components such as proteins and mRNA to the distal compartments and for the delivery of organelles such as mitochondria to provide the energy necessary for distal functioning. Conversely, it is also necessary for the removal of waste products out of the periphery and for the delivery of neurotrophic factors received at distal synapses to the cell soma. The importance of axonal transport integrity is further highlighted by the fact distal axonopathy can occur as a direct result of disruption to retrograde transport through excessive levels of a molecular motor subunit, Dynamitin (LaMonte et al., 2002). The importance of axonal transport might also contribute to the explanation as to why it is motor neurons are a preferentially affected cell type in ALS (Dadon-Nachum et al., 2011). Motor neurons are one group of neurons noted for their exceedingly long axons, which can grow up to a metre in length and it can be easily envisaged that disruption to this in such axons has negative consequences for its prolonged survival.

1.5.3 Mechanisms of Axonal Transport

The main form of intracellular transport takes place via microtubules, which are the largest of the cytoskeleton filaments. Microtubules are built

up sequentially from subunits, which themselves are a heterodimer of α and β tubulin, into protofilaments and thirteen of these coalesce together to form a hollow cylindrical filament. Each end of the microtubule has a distinct polarity owing to the differential exposure of either an α or β tubulin. Exposure of the former designates that end as the 'minus' end and exposure of latter designates the end as 'plus'. Within the axons, the microtubules exist in parallel arrays that make use of the difference between the two microtubule ends to provide a sense of directionality. They are oriented so that their plus ends point distally and the minus ends point towards the soma. Thus, microtubules act as the roads or tracks upon which axonal transport takes place (Conde and Caceres, 2009).

Cargoes are taken along the microtubules by motor proteins. Transport towards the plus end, that is, towards the distal axon, which is termed anterograde transport, is achieved by members of the kinesin family. Kinesin 1, known as the conventional kinesin, is composed of two heavy chains (KHC), which each have a globular head domain in which the motor activity is situated, and the two heavy chains wind around each via their middle sections. Kinesins have a level of inherent variability in terms of their heavy chains, in humans Kinesin 1 has three types termed KIF5A, B, and C. Kinesins bind to microtubules via their head domains and use the energy from ATP hydrolysis to literally 'walk' along the microtubules, detaching and reattaching their head domains like feet. Retrograde transport, towards the cell soma, is achieved by cytoplasmic Dynein, which is a large protein complex containing two heavy chains, which again possess the motor activity and a number of intermediate, light intermediate and light chains. The head domains attach to the microtubule via a stalk that projects from this domain and similarly to Kinesins, Dynein utilises ATP hydrolysis to walk along the microtubules. Kinesins attach to cargo via the aid of kinesin light chain (KLC) or via a plethora of other adaptor proteins, which can be specific for individual

types of cargo. Dynein requires the aid of Dynactin, another large protein complex, in order to bind to cargo with this connection being performed by the smaller subunits of Dynactin which bind to the large subunit $p150^{glued}$ that also binds to Dynein and the microtubule, thus forming a connection between the cargo, the motor and the microtubule (Figure 1.5). Transported cargoes move at varying speeds, characterised as either fast or slow. Mitochondria, lysosomes, vesicles and mRNA move via fast axonal transport (FAT) and many proteins such as neurofilaments are moved via slow axonal transport (SAT) (Millecamps and Julien, 2013). Both are however mediated by the same molecular motors; the difference in speed is thought to arise from the number and length of pauses (Brown, 2003).

1.5.4 Axonal Transport in Neurodegenerative Diseases

It is known that axonal transport is required for the proper functioning and survival of neurons, as mutations within proteins involved in it can cause neurodegeneration.

Mutations in the kinesin motor protein KIF5A can underpin Hereditary Spastic Paraplegia (HSP) and cause axonal transport disruption and HSP too demonstrates distal axonopathy (Reid et al., 2002). HSP can also be caused by mutations in *SPAST* that codes for the protein spastin, which is a microtubule severing protein important for microtubule homeostasis. Knockout in mice causes development of axon blockages containing mitochondria and a motor phenotype (Tarrade et al., 2006). Another HSP gene locus, *SPG7* encoding Paraplegin, a mitochondrial ATPase, causes retrograde transport defects when knocked out in mice, and gives rise to enlarged mitochondria and axonal swellings (Ferreirinha et al., 2004).

Charco-Marie Tooth Disease Type 2 (CMT2) causes distal sensorimotor dysfunction and is also a distal axonopathy with axonal transport defects.

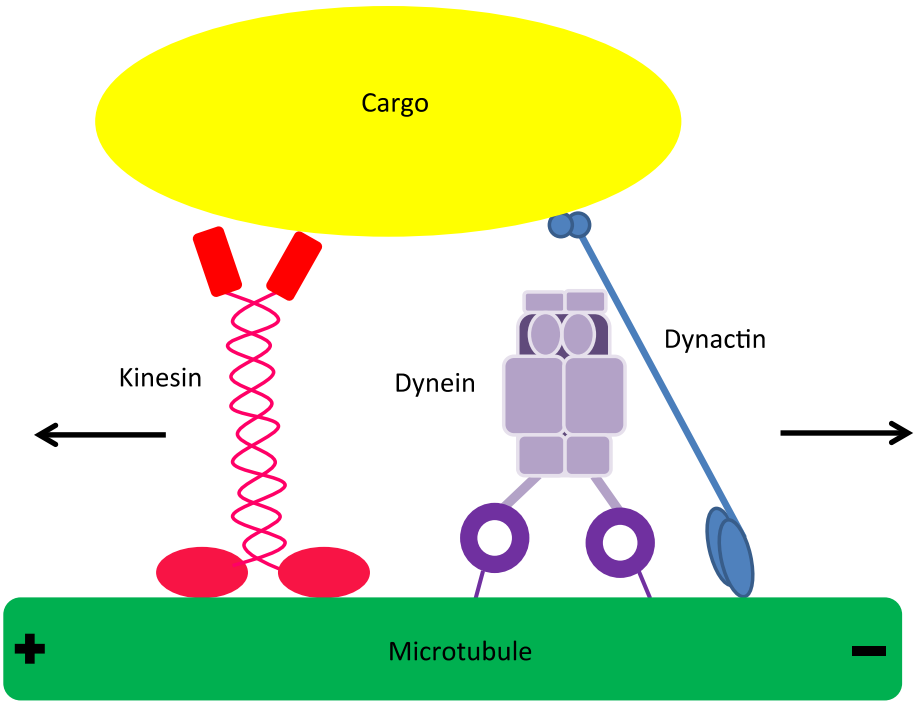

Figure 1.5: Molecular motors involved in axonal transport. Microtubules act as tracks upon which transport takes place; the two ends of the microtubule are different with the 'plus' end exposing β tubulin and the 'minus' end exposing α tubulin. Microtubules in axons are oriented as parallel arrays with the plus ends pointing distally. Cargoes are transported with aid of molecular motor proteins. Kinesins are responsible for plus end directed transport. Kinesin 1 consists of two heavy chains with globular head domains that possess the motor ability, which bind to and walk along microtubules. It uses a light chain (KLC) or other adaptor proteins to bind cargo. Dynein is a large protein complex that mediates minus end directed transport. It binds to microtubules via stalks arising from its two head domains, which themselves possess the motor activity to allowing walking along the microtubule. Dynein requires the aid of another protein complex, Dynactin, to bind cargo. Diagram not to scale. Adapted from Millecamps and Julien., (2013).

There are multiple subtypes and each possesses its own transport dysfunction phenotype. CMT2A is characterised by mutations in *MFN2* encoding Mitofusin2, a mitochondrial outer membrane protein required for mitochondrial fusion. When expressed in mice, these mutations lead to long arrays of fused mitochondria, which accumulate through axons. These mice develop motor axon loss and weakness in muscles leading to hindlimb gait defects (Detmer et al., 2008). Organelle retrograde transport is affected following mutation in the GTPase Rab7, which are

associated with CMT2B (Deinhardt et al., 2006). Axonal transport disruption caused by neurofilament aggregation underpins CMT2E and CMT2F, caused by mutations in neurofilament light chain and Heat shock protein B1 respectively, which in culture leads to progressive degeneration of neurites (Zhai, 2007). By contrast, mutations in cytoplasmic Dynein heavy chain 1 have been associated with CMT2O and Spinal muscular atrophy (SMA) characterised by severe retrograde defects (Weedon et al., 2011; Hafezparast et al., 2003; Millecamps and Julien, 2013).

1.5.5 Axonal Transport as a Contributory Factor to ALS Dying-Back

In terms of ALS there is also evidence implicating dysfunctional axonal transport within the disease. Histopathological investigations showed abnormal enlargements composed of organelles and neurofilaments within the proximal axons of motor neurons (Carpenter, 1968; Okamoto et al., 1990; Saskai et al., 1990; Millecamps and Julien, 2013). The involvement of neurofilaments is interesting given that the major ALS spectrum-linked protein TDP-43, is intimately tied to this cytoskeletal component, being involved in transcriptional regulation of Neurofilament light chain (*NEFL)* mRNA and with its transport along axons in mRNA containing RNP (mRNP) granules. Furthermore, it is known that mutations in TDP-43 disrupt the axonal transport of mRNPs containing *NEFL* mRNA (Alami et al., 2014). Indeed, mouse models of mutant TDP-43 have revealed an overexpression of Peripherin and a decrease in Neurofilament light chain resulting in neurofilament organisation abnormalities and proximal axonal aggregates of the same (Swarup et al., 2011). This study did not examine axonal transport but it had been previously discovered in cultured primary neurons that neurofilament transport can be reduced by phosphorylation through the aberrant activation of several kinases, such as p38, which was shown to occur in

response to glutamate and thus implicates excitotoxicity as an axonal transport disrupter (Ackerley et al., 2000).

With further regard to the ALS-linked proteins, TDP-43, FUS and C9orf72, the pathology attributed to them in being sequestered and sequestering away other proteins, is suggested to be linked to axonal transport dysfunction. Indeed, it has already been seen that mutant TDP-43 can disrupt axonal transport of mRNA-containing granules (Alami et al., 2014), which is projected to have consequences for the functioning of the NMJ, that is, as stated above, known to be disrupted early in disease.

However, within ALS, axonal transport has been most well studied for SOD1 models largely using the G93A mutation. In this model, axonal transport defects are considered to be one of the earliest defects arising and are pervasive, occurring in multiple types of cargo (Williamson and Cleveland, 1999; De Vos et al., 2007; Bilsland et al., 2010). In a modified G93A mouse model that had reduced expression of the transgene to elicit a milder phenotype, slow axonal transport was examined and found to be defective in the anterograde direction at P200, most likely due to the aggregations of neurofilaments, that occur in the proximal axons. Transport was impaired for neurofilaments but also other cytoskeletal components such as tubulin. Furthermore, fast axonal transport of proteins was also reduced (Zhang et al., 1997). In the G37R and G85R models this defect to slow axonal transport was an early event in pathogenesis and in fact has been reported as the earliest observable event in the G85R mouse (Williamson and Cleveland, 1999). However, in these models fast axonal transport of proteins was not impaired, suggesting some mutation specific effects. The neurofilaments in SOD1-mediated ALS are also phosphorylated (Krieger et al., 2003), a result that as described above can be the work of glutamate excitotoxicity, however, mSOD1 has also been demonstrated to lead to neurofilament phosphorylation via p38 activation (Morfini et al., 2013).

Further examinations of fast axonal transport of membrane bound organelles (MBOs) containing APP protein, showed this is reduced in both directions in the G93A mouse derived neurons (De Vos., 2007), although MBOs as a measure of fast axonal transport were only inhibited in the anterograde direction in squid axoplasm (Morfini et al., 2013). This study went further to elucidate a mechanism implicating kinase activation in which the activation of p38 by mSOD1, causes phosphorylation of Kinesin-1 to prevent Kinesin moving along microtubules and revealed that this was active in G93A mice.

The transport of mitochondria has also been studied for SOD1-mediated disease in which it was severely reduced in the anterograde direction, leading to a net loss of mitochondria at the distal axon. This could potentially have an effect on transport in general and the functioning of the NMJ due to reductions in available ATP (De Vos et al., 2007; De Vos et al., 2008). This may be caused by the pathological associations of mutant SOD1 with the mitochondrial outer membrane (Miller and Sheetz, 2004; Vande Velde et al., 2011).

However, a study attempting to rescue motor deficits by reducing Syntaphilin, a protein involved in anchoring mitochondria to prevent transport, was not able to do so (Zhu et al., 2011). There is also an interesting delay between the axonal transport dysfunction and axonal degeneration in several mSOD1 models. It has also been noted that in $SOD1^{WT}$ overexpression models axonal transport defects develop without distal axonal destruction until the advanced stage of disease (Marinković et al., 2012; Millecamps and Julien, 2013). Thus, the authors surmise this indicates that axonal transport dysfunction at least of mitochondria is not a prerequisite for axonal degeneration initiation at least in the SOD1 model (Marinković et al., 2012). However, they suggested this does not preclude such dysfunction, when it arises, from being a contributory factor for the progression of the disease. Although another group argues

that the G85R model has an atypical presentation and suggested their findings of mSOD1 mitochondrial dysfunction is consistent with a pathogenic role (Magrané et al., 2014).

In regards to TDP-43, initial experiments in mouse primary neurons and *in vivo* within the sciatic nerve indicate that overexpression of the wild type and several pathogenic mutant proteins leads to early onset mitochondrial transport dysfunction (Wang et al., 2013a; Magrané et al., 2014); however this was not observed in another study (Alami et al., 2014). Further work remains to be done to elucidate the relationship between mitochondrial and other cargo axonal transport and degeneration in this and other ALS models (Figure 1.6).

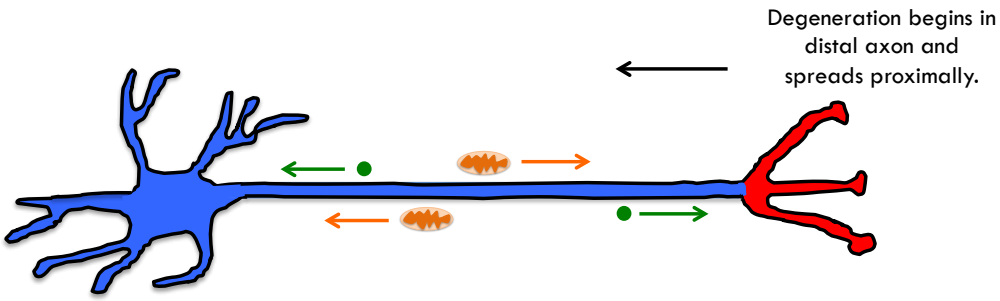

Figure 1.6: ALS is postulated to occur as a distal axonopathy whereby functional deficits at the distal axon or terminals occur in the initial stages of the disease before symptom onset and proceed backwards towards the cell body culminating in the loss of the cell body later in disease course. Defective Axonal transport is postulated to be a contributory factor to this process. Orange = mitochondria, green = vesicles. Adapted from Coleman., (2005).

1.6: Model Organism: *Drosophila melanogaster*

The fruit fly, *Drosophila melanogaster* is one of the most widely used organisms in biological research today. This owes much to its easy care and quick generation time. However, its enduring appeal as the model organism of choice for many researchers owes most to its genome, which

has been completely sequenced and is separated into only four chromosomes. Despite the gulf of evolutionary time, many of the genes have been highly conserved and functional homologs for many human disease associated genes are present in the *Drosophila* genome.

Arguably the most useful tool developed for use in *Drosophila* is the UAS-GAL4 system (Brand and Perrimon, 1993). This is a two-part system comprised of the yeast transcriptional activator Galactose responsive factor 4 (GAL4) and its upstream activating sequence (UAS) to which it binds with specificity. Genes of interest are engineered to contain this sequence upstream of their start sites. When co-expressed, the GAL4 protein will bind to the upstream activator sequences and induce expression of the gene of interest (Figure 1.7). The GAL4 protein can be placed under a range of promoters known as 'drivers' that can confer spatial and temporal selectivity. Some frequently used drivers include that of the daughterless gene which encodes a transcription factor (Cronmiller and Cummings, 1993) that is ubiquitously expressed and D42, which is specifically expressed in motor neurons. The GAL4-UAS system allows for numerous genetic manipulations from overexpression, to rescue when combined with a gene knockout line.

Drosophila has proved an extremely useful organism for the study of neurodegeneration. Their nervous system and its development is well defined and easily accessed. Many functional assays have been developed to evaluate perturbations to the nervous system, such as the adult climbing test and larval crawling assay. The nervous system itself is simple to reach and to keep intact through dissection. It is also easy to visualise, which has made it a very attractive organism for the modelling of axonal transport.

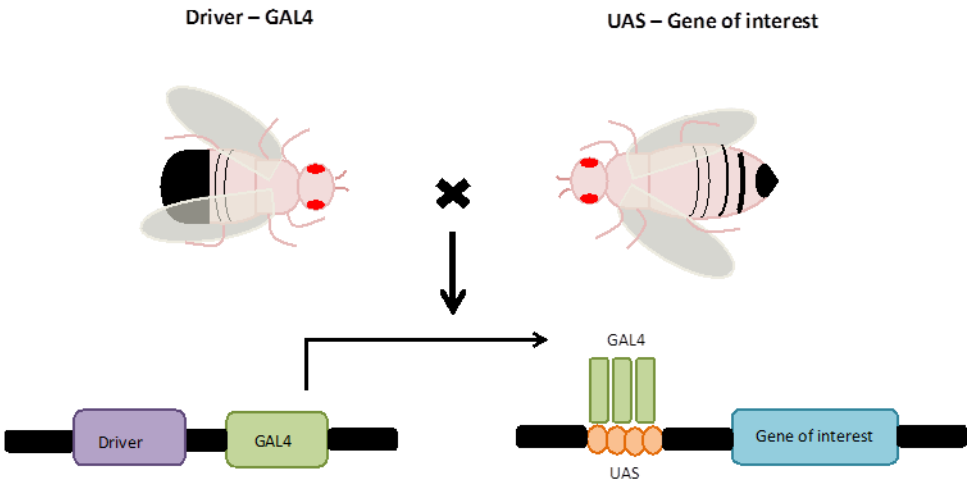

Figure 1.7: The two part GAL4 – UAS system. A fly line is engineered to contain the yeast transcription activator GAL4 downstream of a tissue-specific driver. This fly must be crossed to another containing the GAL4-specific upstream activator sequences (UAS) that have been placed upstream of a gene of interest. In the offspring containing these two elements, expression of GAL4 is driven in a tissue-specific manner, whereupon it binds to the UAS allowing for transcription of the gene of interest in that tissue. Adapted from St Johnston., (2002).

1.7: Project Aims

The primary aim of this project was to examine the state of fast axonal transport by live imaging fluorescently-tagged cargo within motor neuron axons of 3rd instar larvae in *Drosophila* models of *TARDBP (TDP-43)*, *FUS* and *C9orf72*-linked ALS. Furthermore, the motor activities of these models were assessed through the means of behavioural assays such as larval crawling and young and aged-adult climbing. In this manner it was possible to correlate them with potential defects in axonal transport.

Specifically, in regard to *TARDBP* and *FUS*, loss of the endogenous protein was examined as were the effects of overexpressing both the fly and human wild-type genes and pathogenic variants. This was to elucidate whether any defects arising operate via a loss or gain-of-function

mechanism. In regard to *C9orf72*, possible toxicity of hexanucleotide repeats number was examined and the contributions of two potential mechanisms, RNA gain of toxic function and DPR protein generation, dissected.

The hypotheses to be tested are as follows:

1. The disruption to TDP-43 functioning through knockout, overexpression or pathogenic mutation interferes with axonal transport and contributes to the dying back pattern of degeneration characteristic of a distal axonopathy.

2. The disruption to FUS functioning through knockout, overexpression or pathogenic mutation interferes with axonal transport and contributes to the dying back pattern of degeneration characteristic of a distal axonopathy.

3. The expression of a pathogenic number of GGGGCC (G4C2) repeats interferes with axonal transport and contributes to the dying back pattern of degeneration characteristic of a distal axonopathy.

CHAPTER 2: Materials and Methods

2.1: *Drosophila* Stocks

2.1.1 *Drosophila* Husbandry

Drosophila stocks were kept in standard vials and fed standard cornmeal media cooked by the fly facility with the addition of baker's yeast. The stocks were kept in replicates of three, each at a different stage in the life cycle to allow for a continuous supply of new flies. The stocks were kept at 18°C as at this temperature the *Drosophila* lifecycle extends for an average of 40 days and thus stocks required to be flipped into fresh vials once every 3 weeks. Some lines were kept at 25°C if it became clear that they struggled to reproduce adequately at 18°C, since 25°C is the optimum temperature for this organism. If stocks were required in high volume for crosses, they were grown in plastic bottles containing the same media.

Experimental crosses were grown at this optimum temperature of 25°C unless otherwise stated for individual experiments. At this temperature, the lifecycle is an average of 10 days, with third instar larvae appearing on the 5^{th} day. It was aimed that each fly cross would contain a minimum of 4 males and 7 virgin females. The crosses were flipped every two days to generate multiple replicates in case they were needed.

Flies were selected for crosses and experiments on pads extruding CO_2 to anesthetise them, thus making them amenable to being 'pushed' around with a paintbrush or forceps. The lowest CO_2 exposure for anaesthesia was used within the shortest timeframe possible to minimise any possible effects of this gassing on the flies.

2.1.2 *Drosophila* Stock Lines

The *Drosophila* stock lines used are listed below.

Table 2.1 Mutant Lines

BDSC = Bloomington Stock Centre

Genotype	Name	Source
w; TBPH[delta23]/CyO.GFP	$TBPH^{\Delta 23}$	Feiguin et al., 2009
w; TBPH[null]/CyO.GFP	$TBPH^{null}$	Fiesel et al., 2010
w; TBPH[DD96]CyO.GFP	$TBPH^{DD96}$	Diaper et al., 2013
w; TBPH[DD100]CyO.GFP	$TBPH^{DD100}$	Diaper et al., 2013
w; caz[1]/FM7.GFP	caz^{1}	Wang et al., 2011
w; Opa1[s3475]/CyO.GFP	$Opa1^{-}$	BDSC 12188 (Spradling et al., 1999)
y w Marf[B]FM7c,Kr>GFP; stat/TM6B	$Marf^{-}$	BDSC 57097 (Sandoval et al., 2014)

Table 2.2 Overexpression Lines

Genotype	Name	Source
w; P{w+, UAS-lacZ}	UAS-lacZ	BDSC 1777 (Brand and Perrimon, 1993)
w; P{UAS-TBPH}attP2	$UAS\text{-}TBPH^{WT}$	Wang et al., 2011
w; P{UAS-TDP-43 WT}attP2	$UAS\text{-}TDP\text{-}43^{WT}$	Wang et al., 2011
w; P{UAS-TDP-43 M337V}attP2	$UAS\text{-}TDP\text{-}43^{M337V}$	Wang et al., 2011
w; P{UAS-Flag-cazWT}attP2	UAS-cazWT	Wang et al., 2011
w; P{UAS-Flag-cazP398L}attP2	UAS-cazP398L	Wang et al., 2011
w; P{UAS-Flag-FUSWT}attP2	UAS-FUSWT	Wang et al., 2011
w; P{UAS-Flag-FUSP525L}attP2	UAS-FUSP525L	Wang et al., 2011
w; P{UAS-Pure(GGGGCC)3}attP40	UAS-Pure 3	Mizielinksa et al., 2014
w; P{UAS-Pure(GGGGCC)36}attP40	UAS-Pure 36	Mizielinksa et al., 2014
w; P{UAS-RO.36}attP40	UAS-RO.36	Mizielinksa et al., 2014
w; P{UAS-PR.36}attP40	UAS-PR.36	Mizielinksa et al., 2014
w; P{UAS-HA-mito.GFP}e	UAS-mito.GFP	BDSC 8443 (Pilling et al., 2006)
w; P{UAS-NPY.GFP}	UAS-NPY.GFP	Mudher et al., 2004

Table 2.3 Driver Lines

Genotype	Name	Source
w; P{da-GAL4}	da-GAL4	BDSC 8641 (Wodarz et al., 1995)
w; P{elav-GAL4}C155	elav-GAL4	BDSC 458 (Lin and Goodman, 1994)
w; P{D42-GAL4}	D42-GAL4	BDSC 8816 (Yeh et al., 1995)
y w; P{CCAP-GAL4}16	CCAP-GAL4	BDSC 2565 (Park et al., 2003)

A number of genotypes were created from these stocks for this study. For example, for the rescue experiments, each *TBPH* knockout line was

crossed into each of the overexpression transgene backgrounds. Also, in this study it was necessary to generate flies containing two genetic manipulations on the same chromosome, for example, for the study of the axonal transport of mitochondria. Here, recombinants *TBPH⁻, CCAP-GAL4* on chromosome II were required so that these may be crossed with *TBPH⁻/CyO.GFP; UAS-mito.GFP/TM6B* flies to produce homozygous *TBPH* knockout larvae expressing mito.GFP in the CCAP expression pattern:

TBPH⁻,CCAP-GAL4 / TBPH⁻ ; UAS-mito.GFP/+

To achieve this, *TBPH⁻/CyO.GFP* flies were crossed with *CCAP-GAL4/CyO* flies to produce *TBPH⁻/CCAP-GAL4* progeny. Recombination only occurs in female flies and thus female progeny were selected and crossed with *Gla/CyO* males to generate potential *TBPH⁻,CCAP-GAL4 /CyO*. To test for recombination, male progeny from this cross were individually mated with *TBPH⁻/CyO.GFP* flies. The straight-winged and thus potential homozygous *TBPH⁻* progeny were assessed for the presence of *CCAP-GAL4* by the observation of the yellow eye colour phenotype caused by the presence of the mini-w+ marker in the *CCAP-GAL4* construct. As an additional test, these flies were crossed with *UAS-mito.GFP* line and the larvae were dissected to assess for presence of fluorescent cargo expressed in the *CCAP-GAL4* pattern. To test that *TBPH⁻* had recombined *with CCAP-GAL4*, the straight-winged yellow-eyed flies locomotor ability was observed. Those flies exhibiting the characteristic extreme motor defect as described by Feiguin et al., (2009) represented recombinants. Progeny from this cross was then established as a stock. Similarly, the *TBPH⁻*, *UAS-mito.GFP* recombinants were also generated and tested for the presence of the *UAS* transgene in the potential recombinant progeny through crossing with *CCAP-GAL4* and the larvae dissected and assessed for the presence of fluorescent cargo.

2.2: Statistical Analysis

The type of statistical test to be carried out depends on whether the data are normally distributed. To assess this all data sets were subjected to the D'Agostino-Pearson normality test, which tests the extent to which the distributions of the data are different from the normal 'Gaussian' distribution. This test allows for ties between data points unlike some others. All data sets except those of the climbing assays passed the normality test.

A parametric test can be used when data is normally distributed. For such data sets with only two independent groups (Figures 3.5, 3.8, 3.10), an unpaired two-tailed *t* test was carried out. This compares the difference between the means in consideration of the variability of the data. The null hypothesis is: $H_{0=}\mu_1=\mu_2$. A significant result, that is, the acceptance of the alternative hypothesis (H_A), states that the means are significantly different.

For all data sets (except for the climbing assay and those discussed above), which involve more than two groups, One-way analysis of variance (ANOVA) was conducted. This is a standard robust test on data with more than two independent groups. It functions to compare the means between the groups and indicates whether any of those means are significantly different. To do this it tests the null hypothesis (H_0) which is: $H_0=\mu_1=\mu_2=\mu_3=\mu_{k.}$ A significant result states that two or more means are significantly different.

However, in order to discover which of the group means are significantly different from each other a post-hoc test must be carried out. These tests function to control for the increase in the experiment-wise error rate that is, they prevent the increased chance of a type 1 error (false rejection of H_0), which occurs as an effect of conducting multiple

comparisons, keeping this to 5% as standard. There are many post-hoc tests to choose from, the choice of which is dependent on the type of comparisons to be carried out. The Tukey post-hoc test for example is used for the purposes of comparing every mean with all other means in the data set, however if it is necessary, as in this project, only to compare a specific set of means, then the Bonferroni or Sidak is required. The Sidak is described as a modification of the Bonferroni that is slightly less strict (conservative) and thus has more power. Whilst the Bonferroni is an appropriate test, it has been criticised as too conservative particularly with a large number of comparisons, thus the Sidak was chosen for this project.

The Kruskal-Wallis test was used for the climbing assay analysis (Figures 3.13, 3.14D, 3.16, 4.16, 4.17B, 4.19, 4.20, 5.5) as these data sets failed the normality test. This test is the non-parametric equivalent of the ANOVA and thus can be used when the distribution assumptions required for the ANOVA have not been met. It also allows for more than two groups to be compared, which the data in this study required to be compared, unlike the similar Mann-Whitney U test. The data are ranked from lowest to highest and assessed for the differences in the rank sums. It tests the null hypothesis that the differences in rank sums are a product of random sampling. The post-hoc test is the Dunn's multiple comparisons test, which allows for selected pairs of columns. Here, the sum of ranks between a pair and the value of the expected average difference is compared.

Each figure shows the mean with the error bars corresponding to the standard error of the mean (SEM) as it was desired to show an indicator of the accuracy of the mean values.

2.3: Live Imaging Axonal Transport

For the assessment of axonal transport of mitochondria and vesicles, a live imaging approach was employed using the intact axons of motor neurons from *Drosophila* wandering third instar larvae. The following technique is adapted from that of Kuznicki and Gunawardena, (2010). In order to study live transport of mitochondria in *Drosophila*, this study utilised the *UAS-mito.HA-GFP* fly line (herein referred to as UAS-mito.GFP) (Pilling et al., 2006), which was created using the fusion protein generated by Rizzuto et al., (1995). This protein is comprised of the mitochondrial-targeting signal of the Complex IV subunit VIII with the N terminal of the S65T GFP variant. To study vesicle transport, the *UAS-NPY-GFP* fly line (Mudher et al., 2004) was used, which encodes a transport vesicle marking human Neuropeptide Y-GFP fusion protein.

Table 2.4:Live imaging dissection solution from Kuznicki and Gunawardena, (2010):

Stock Solution	Working Solution	10ml
1 M NaCl (Fisher Scientific 10326390)	128 mM NaCl	1.28 ml
0.1 M EGTA (amnesco 0732)	1 mM EGTA	0.1 ml
1 M $MgCl_2$ (BDH 101494V)	4 mM $MgCl_2$	0.04 ml
1 M KCl (BDH 101984L)	2 mM KCl	0.02 ml
0.5 M HEPES (Sigma 1001889450)	5 mM HEPES	0.1 ml
0.5 M Sucrose (Sigma 101285288)	36 mM Sucrose	0.72 ml

The solution was made fresh for each microscope session and adjusted to pH 7.2.

2.3.1 Fillet Preparation

Third instar larvae of the correct genotype were recovered from the vial with forceps and washed in dissection solution to clean off any food attached to them. Each larva was placed onto the Sylgard (Sigma761028)

slide and arranged so that it was straight and horizontal, dorsal side up. A dissection pin (Fine Science Tools 26002-10) was inserted within the tail and inserted into the plate. The mouth hook was pierced by a pin and pulled back so that the larva was stretched longitudinally as far as possible. This pin was then inserted into the plate. The lava was then immersed in a 1 ml bubble of dissection solution. Using the microdissection scissors (Fine Science Tools 15000-00), an incision was made at the tail end and using this as a starting point, the larva was cut open along its length from posterior to anterior. The guts, salivary glands and tracheal system within the larva were removed using forceps gently so as not to disturb the ventral ganglion or the motor nerves. The larva cuticle was then pinned back at the top and bottom on each side. A pin was inserted into the top of the ventral ganglion and pulled backwards so that the attached motor nerves are pulled taut in one focal plane. To prevent possible microscope lens damage, all the pins were pushed as far as possible into the Sylgard slide to avoid contact with the lens. More dissection solution was added slowly to the preparation in order to produce a large bubble of solution on the slide.

2.3.2. Microscopy

The Olympus FV1000 Fluoview confocal microscope (Olympus corporation) was used for all axonal transport experiments. The details of the setting parameters for mitochondria and vesicle microscopy were as follows:

Table 2.5: Microscope parameters

Parameter	Mitochondria	Vesicles
Objective	60x Water NA 0.90 Olympus LUMPLFL	60x Water NA 0.90 Olympus LUMPLFL
Laser line	488	488
Laser power	20%	60%

The prepared fillet was mounted into the microscope stage. The ventral ganglion was then located, this can be done via fluorescence for *CCAP-GAL4>mito-GFP* larvae, however the signal from the *CCAP-GAL4>NPY-GFP* larvae was not sufficient to allow this and thus brightfield was used to locate the ventral ganglion in this instance. Once located, the slide was adjusted so that the ventral ganglion was just outside of the field of view. Locations for the movies were selected from the fluorescing motor axons within this field of view. Once selected, a region of interest (ROI) was defined that covered 75% of the computer screen. The mitochondria or vesicles within this ROI must all be clearly visible within the focal plane to allow clear kymograph production. Movies were taken at 1 frame per 5 s for 100 frames for mitochondria and 1 frame per 0.5 s for 100 frames for vesicles. Mitochondria movies therefore took a total of 500 s to record, whereas vesicle movies took 50 s. One movie per larva was taken for mitochondrial movies and up to 2 per larva for vesicle movies due to the reduced time required to take the movies.

It must be noted that the results for some genotypes differ slightly between experiments, such as the *TBPH* knockout fly in Figure 3.1 and 4.6. This highlights that there is a level of inherent variability within the transport assay system that may result from difficult to control variables such as the temperature of the assay environment, which is noted to affect this transport (Godena, personal communication). However these differences do not affect the overall conclusions to be drawn for the data.

2.3.3 Data Analysis

2.3.3.1 Kymograph Production

Movies were analysed using the ImageJ software. They were changed into grey scale and subjected to the 'stackreg' plugin, which removes shaking or 'drift' from the images. A defined ROI was used to crop the movie; for

this the ROI was taken for the area providing the most mitochondria or vesicle coverage. The 'straighten' plugin was then used to create a straight line of mitochondria or vesicles and then the 'reslice' and 'Z projection' tools were used to create a kymograph, which is a visual representation of the directional movement of an object through time (Figure 2.1).

2.3.3.2 Kymograph Scoring

Each trace on a kymograph represents one mitochondria or vesicle (cargo). Traces moving from left to right are cargo moving in the anterograde direction towards the synapse, those moving oppositely from right to left are moving in the retrograde direction towards the cell body. Vertical traces represent cargoes that have not moved during the time the movie was taken. Thus, cargos were scored into three categories, anterograde, retrograde and stationary.

However, due to the bidirectional nature and stop-start behaviour of this axonal transport, many of the traces do not follow a perfect path. Some traces represent cargo that displayed motion in one direction followed by a stationary period or a sudden reversal. In addition, some cargo moved into or out of the movie region during the time period of the movie and thus do not extend from top to bottom. Therefore, a scoring system was developed to deal with this possible ambiguity (see section 2.3.3.3). The kymographs were coded to allow for blinded scoring. Furthermore, the manual nature of the scoring introduced a level of subjectivity and thus, to counteract this, the kymographs were scored blind by an additional researcher and the scores compared, any discordant results that could not be resolved were discarded.

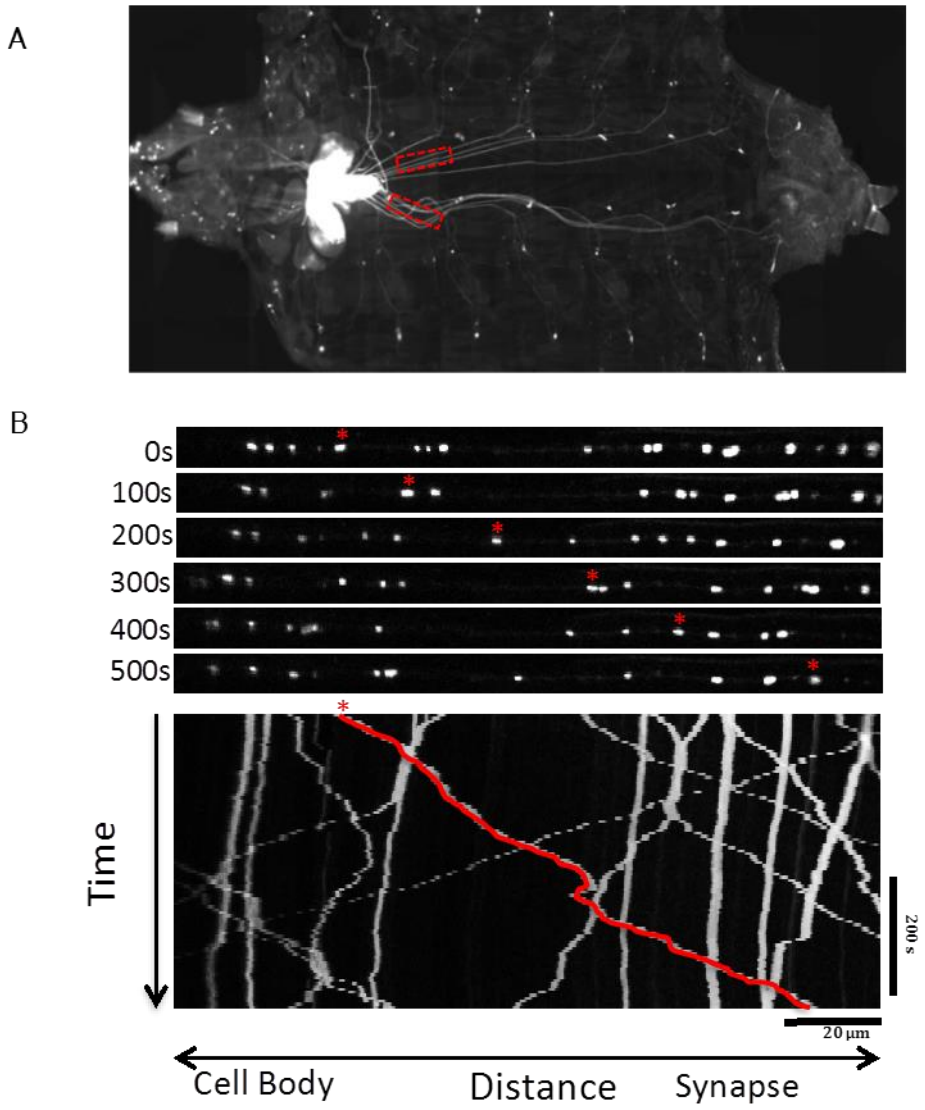

Figure 2.1: Live Imaging of axonal transport in third instar larvae. (A) Larvae were fillet dissected and movies were taken from axons within the field of view just distal to the ventral ganglion (red boxes). (B) Kymographs were generated of the resultant movies, which display distance travelled through time. Shown are frames from a movie of mitochondrial transport taken at intervals of 100 s and the kymograph of this movie. The movement of one mitochondrion is followed through time (red asterix) as seen on the frames and the resultant line interpretation on the kymograph.

2.3.3.3 Example Kymograph Scoring

Movement must be over 60% for cargo to be designated as either anterograde or retrograde. Likewise non-movement must total at least 60% to be considered as stationary. Anything between these such as 50% movement and 50% non-movement is classed as 'indeterminate' and is excluded from the analysis. An example of a scored mitochondrial transport kymograph is illustrated in Figure 2.2A. Mitochondria 1,3,5,6,7 and 10 are all very clearly straight vertical traces and are comfortably assigned as 'stationary'. Similarly, 2 uniformly extends from left to right and is assigned as 'anterograde'. However, mitochondrion 4 demonstrates a brief stationary period as it intersects with 6, but this is sufficiently short to allow this trace to fall into the anterograde category. In the same vein, mitochondrion 9 begins with a short stationary period but the majority of movement (measured by eye) is from right to left and thus is assigned as 'retrograde'. Mitochondria 8 and 11 do not start at the top or end at the bottom of the kymograph, respectively. These represent mitochondria that travelled outside the region of axon being examined or which entered it after the movie had begun. In these instances, they are included for scoring if they are present for at least 50% of the movie time. For 8 this is measured by the pale red line on the right side of the kymograph in Figure 2.2A and is just over 50%. Thus 8 is admitted to be scored as anterograde. The pale green line measures 11 and this too passes this test and is admitted to be assigned as retrograde.

The scoring of vesicle transport kymographs was also undertaken according to these criteria (Figure 2.2B), but is more difficult owing to the smaller size of the vesicles and fainter fluorescent signal. In this example, vesicles 1 and 2 are not present for sufficient time and are excluded. Vesicles 3 and 4 pass this test and are included and assigned as anterograde. Vesicles 5,6 and 7 are all clearly anterograde whereas 9 and 10 are clearly stationary and 11 has a stationary period but as per the rules described above is assigned as retrograde. Vesicles 8, 12 and 1

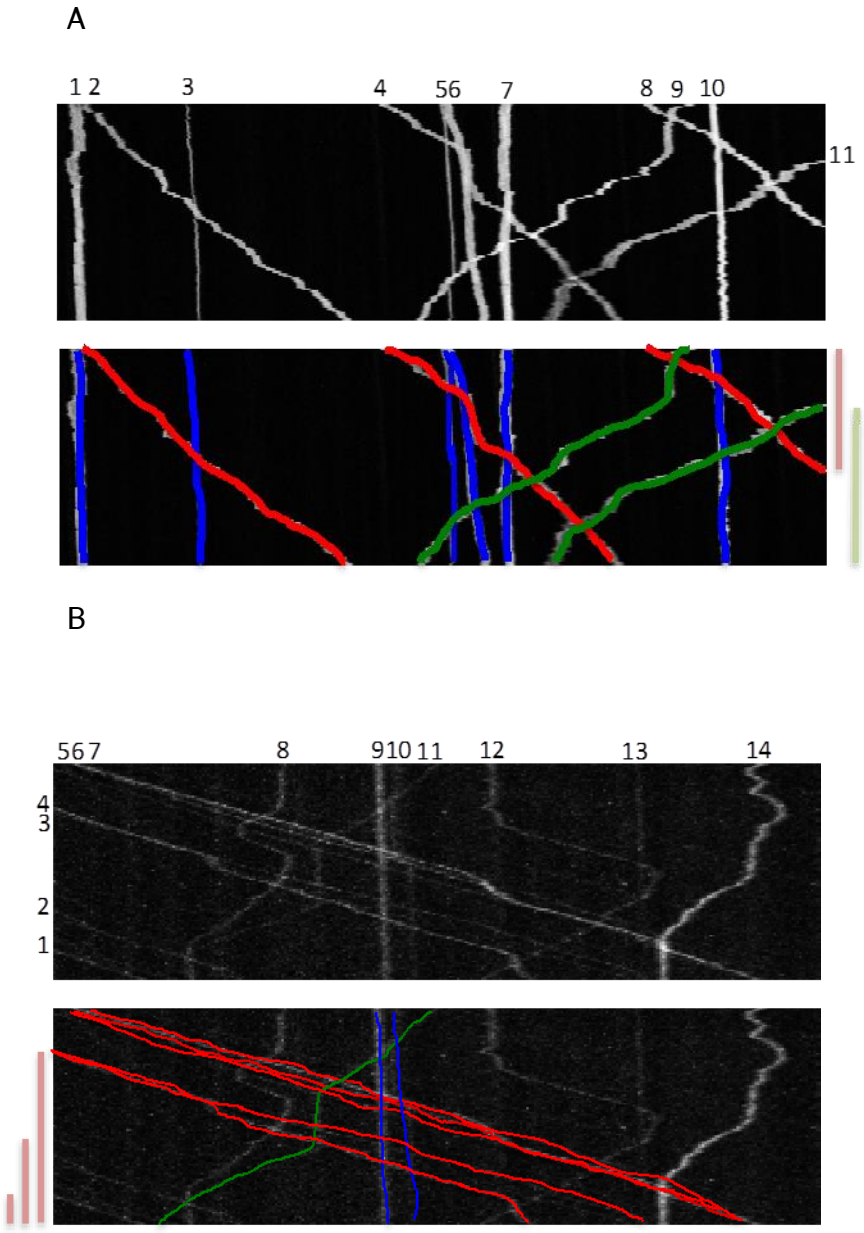

Figure 2.2: Examples of scored kymographs of axonal transport for (A) mitochondria and (B) vesicles. Each cargo is numbered and assessed according to a set of criteria. Red = accepted anterograde cargo. Green = accepted retrograde cargo. Blue = accepted stationary cargo. Unmarked traces are not scored (see text for details).

demonstrate considerable variability in direction that is not deemed to total at least 60% in any one way, thus these vesicles are excluded from the score. Vesicle 13 appears stationary but it cannot be accurately followed all the way through the kymograph and is excluded on that basis.

2.3.3.4 Statistics

For each movie the cargo in each category were multiplied by 100 and then divided by the total number of cargo in that movie to find the percentage of the total cargo within that category. These numbers for each movie were then statistically analysed by the GraphPad Prism software 6.0. One-Way ANOVA was carried out for each category with the Sidak multiple comparison test on selected genotypes to allow pairwise comparisons. These pairs were control versus each experimental genotype and also between experimental genotypes as necessary.

2.3.4 Mitochondrial Length Analysis

The movies of the selected genotypes were subject to the kymograph production protocol up to the formation of the straight-line stacked movie. From this, single images of frames 1, 50 and 100 were taken and each was colour inverted. Images were then resliced from the top and stacked via the Z projection tool to create an image in which the mitochondria were uniformly 1 pixel high. The image was then made binary according to the default threshold to remove any background noise and the length of each mitochondrion was calculated using the 'analyse particle' tool. This gave the length in pixels which was then converted to μm (1 pixel = 4.831μm based on microscope calculations). These scores were then statistically analysed by the GraphPad Prism software 6.0 using the student's unpaired two-tailed *t*-test. At least 7 animals and 70 mitochondria were analysed for each genotype.

2.4: Behavioural Assays

To test the functional capacity of the neuromuscular system, a number of behavioural assays on both larvae and adult flies were carried out that give a readout of the effects of neurodegeneration within the nervous system on key locomotor phenotypes.

2.4.1 Eclosion

Pupae were picked gently from the vial and placed in a new vial at a maximum number of 25. The number of adult flies that emerged from the pupal case was assessed as a proportion of the total in each vial. A minimum of three biological replicates was used per genotypes. The scores from each replicate for each genotype were analysed by the Graphpad Prism software 6.0 using One-Way ANOVA with Sidak multiple comparison test.

2.4.2 Larval Crawling and Turning

2.4.2.1 Crawling

Control and experimental crosses were established at 25 °C and flipped every two days. On the 5th day, the vials containing wandering third instar larvae were coded by an independent researcher, placed in the behavioural assay room at 23 °C and left to acclimatise for 2 hours. One larva at a time was recovered from its vial by forceps and washed gently in a dish of distilled water to remove any residual food from its body that may interfere with its crawling ability. The agarose (Bioline 41025) surface was then placed under the viewing microscope (Zeiss Stemi 1000) and the lamp was turned on. The washed larva was then placed using forceps on the starting centre dot and left to acclimatise for 5 seconds. The timer

was then started and the number of peristaltic wave movements in a 2 minute period was counted with the aid of the viewing microscope and recorded with a clicker counter (Figure 2.3B). When undergoing the crawling assay, larvae were placed at the centre of the plate. They typically crawled in a straight direction to reach the edge of the plate and then proceeded to crawl around the edge for the remainder of the assay. If a larva crawled up the side of the plate to the top and over, the experiment was stopped and that result was not counted.

2.4.2.2 Turning

After the crawling count, the larva was turned over to ventral side up gently with the aid of a paintbrush. The time the larva took to corkscrew its body back to dorsal side up was recorded as the larval turning count (Figure 2.3C). The larval locomotion assays were adapted from Feiguin et al., (2009) and Estes et al., (2011).

2.4.2.3 Data Analysis

For both crawling and turning, 5 larvae were counted per session over 4 sessions to provide a total of 20 larvae per group. The experimental set-up is as detailed in Figure 2.2. The scores from each replicate for each genotype were analysed by the GraphPad Prism software 6.0 using One-Way ANOVA with Sidak multiple comparison test.

2.4.3 Young Adult Climbing

Young male flies between 0 and 3 days post-eclosion were placed in the behavioural assay room set at 23 °C to acclimatise for 1 hour. The flies were then transferred to the climbing tubes at a maximum number of 25 per tube for a further 1 hour. The climbing tube containing the flies was inserted into position 1 of the countercurrent apparatus. The whole

apparatus was banged down gently onto the table surface to knock the flies to the bottom of the tube and the apparatus top section was slid across to allow the flies access to climb into the first of the top tubes. Concurrently to this motion, the timer was activated. Flies were given 10 seconds to climb after which time the top section of the apparatus is slid back across. The flies were then banged down and dropped into the bottom tube at position 2 and the climbing process proceeds again a further 4 times until the flies have had the possibility to make it into the bottom tube at position 6 (Figure 2.4).

2.4.3.1 Data Analysis

The number of flies within each of the bottom tubes was then counted. A climbing index score was generated based on the number of flies at each of the positions. The first position was given a score of 0 and position 6 given a score of 5. The scores for each experiment were combined and the numbers of flies at each position were ranked. These were then analysed by the GraphPad Prism software 6.0 using One-Way ANOVA with the Sidak multiple comparison test. At least 50 flies were used in this analysis. The climbing index of each of the genotypes within an experiment were normalised to the experiment control score to enable comparisons to be made more easily between experiments.

2.4.4 Aged Adult Climbing

For the longitudinal study of the effects of age-related neurodegeneration on climbing ability, male flies were aged in cohorts and the climbing assay was performed at set time points as indicated in figures. Between assays, the flies were flipped every two days into fresh vials with no more than 25 per vial.

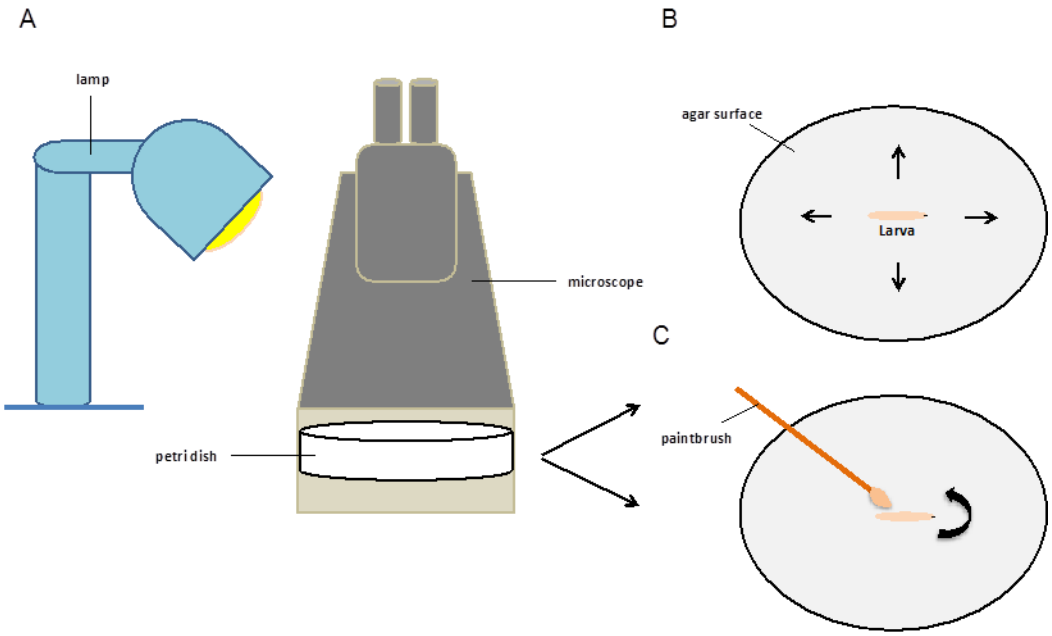

Figure 2.3: The experimental equipment set-up for the larval crawling and turning behavioural assays. (A) The agar surface plate is placed on the microscope stage. The microscope did not have its own light source and so a lamp was used for this purpose to aid viewing. (B) During the crawling assay, larvae begin in the centre and typically crawl towards the plate edge and around. The number of peristaltic wave movements is counted in a 2-minute period. (C) In the turning assay, larvae are carefully turned ventral side up with a paintbrush and the time taken to reorient is counted.

2.4.5 Comparison of Climbing with Males and Mated Females

The climbing assays conducted in this study used cohorts of male flies of both control and experimental groups, which we have found has yielded the most consistent results within our lab. An alternative approach is the use of mated females. To test this, an aged climbing assay was conducted using the FUS ectopic expression lines driven by *D42>GAL4*. The results (Figure 2.5) illustrate that the conditions of mated female only (Figure 2.5A) and male only (Figure 2.5C) gave comparable results. This is also true at day 30 (Figure 2.5B&D) with the mated female condition (Figure 2.5B) producing a mild increase in severity compared to the males (Figure

2.5D). It is concluded that the use of male flies only for this assay is an appropriate experimental design.

2.5 Immunohistochemistry

In this project, specific genotypes were subject to immunohistochemistry for analysis of mitochondrial number at the NMJ in abdominal segment II (A2) (Figure 2.6A). These genotypes all expressed *D42>mito.GFP* to provide a mitochondrial signal and were stained with horseradish peroxidase (HRP) to provide a signal for the pre-synaptic neuronal membrane, allowing visualisation of the NMJ structure.

Table 2.6: Antibodies:

Type	Name	Source	Code	Dilution	Host
Primary	HRP	Jackson Immunoresearch	323-005-021	1 in 250	Rabbit
Secondary	Alexa Fluor® 594 Anti-Rabbit	Life Technologies	A-21207	1 in 1000	Donkey

Table 2.7: NMJ Dissection solution from Kuznicki and Gunawardena, (2010):

Stock Solution	Working Solution	10ml
1 M NaCl	128 mM NaCl	1.28 ml
1 M $MgCl_2$	4 mM $MgCl_2$	0.04 ml
1 M KCl	2 mM KCl	0.02 ml
1 M $CaCl_2$ (Fisher Scientific 10158280)	0.1 mM $CaCl_2$	0.001 ml
0.5 M HEPES	5 mM HEPES	0.1 ml
0.5 Sucrose	36 mM Sucrose	0.720 ml

2.5.1 Sample Preparation

Wandering third instar larvae were washed in NMJ dissection solution and dissected open as defined in section 2.2.2. However in this case, the

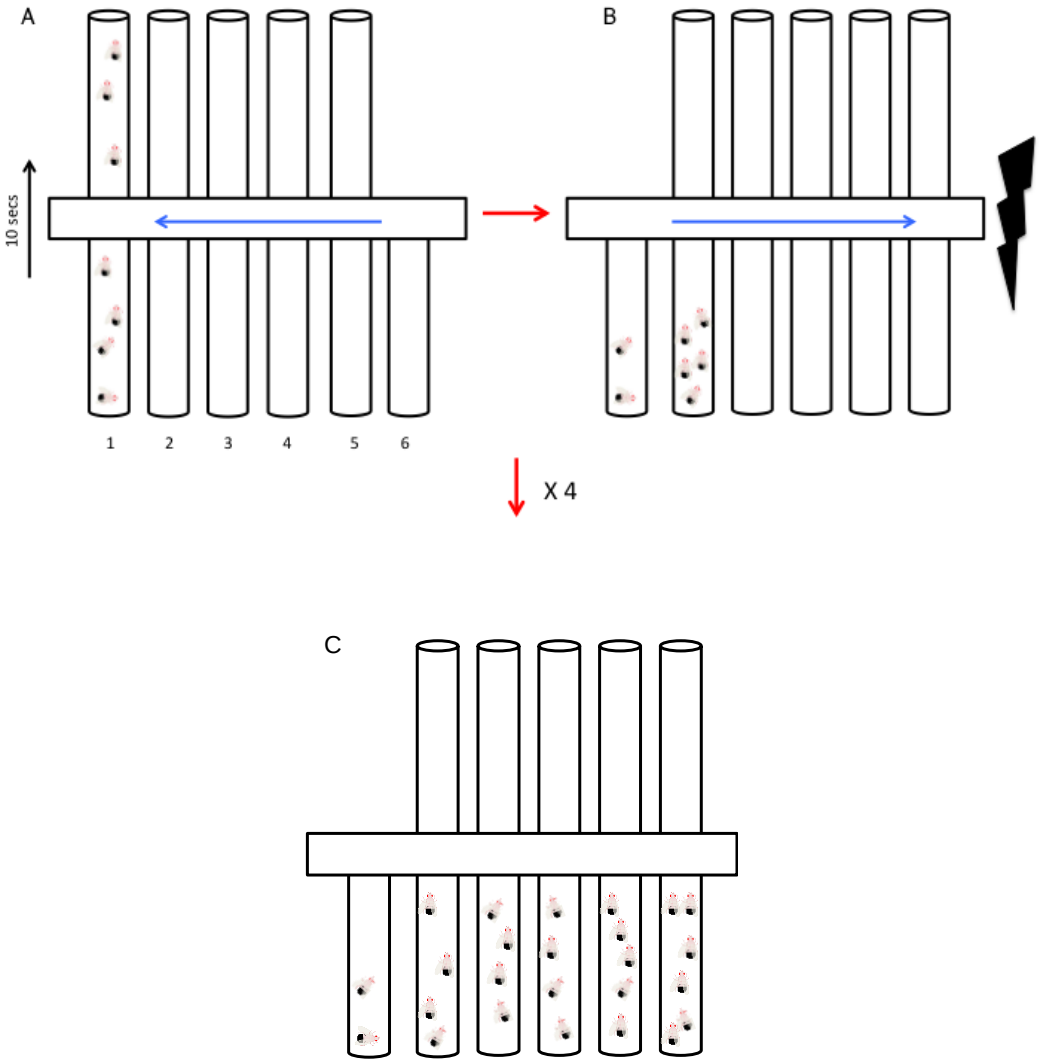

Figure 2.4: The climbing assay. (A) A climbing tube containing the flies is added to position 1 of the counter-current apparatus. The flies are banged to the bottom of the tube (not shown) and the top part of the apparatus is shifted across (blue arrow) allowing the flies to climb up into the 1st top tube. They are given 10 seconds to climb after which point (B) the top part of the apparatus is shifted back preventing further climbing of the flies still within the bottom tube. The apparatus is then banged down (black lightning bolt) forcing the flies to drop into the bottom tube at position 2. (C) This procedure is repeated 4 more times until the flies have had the chance to reach the last bottom tube.

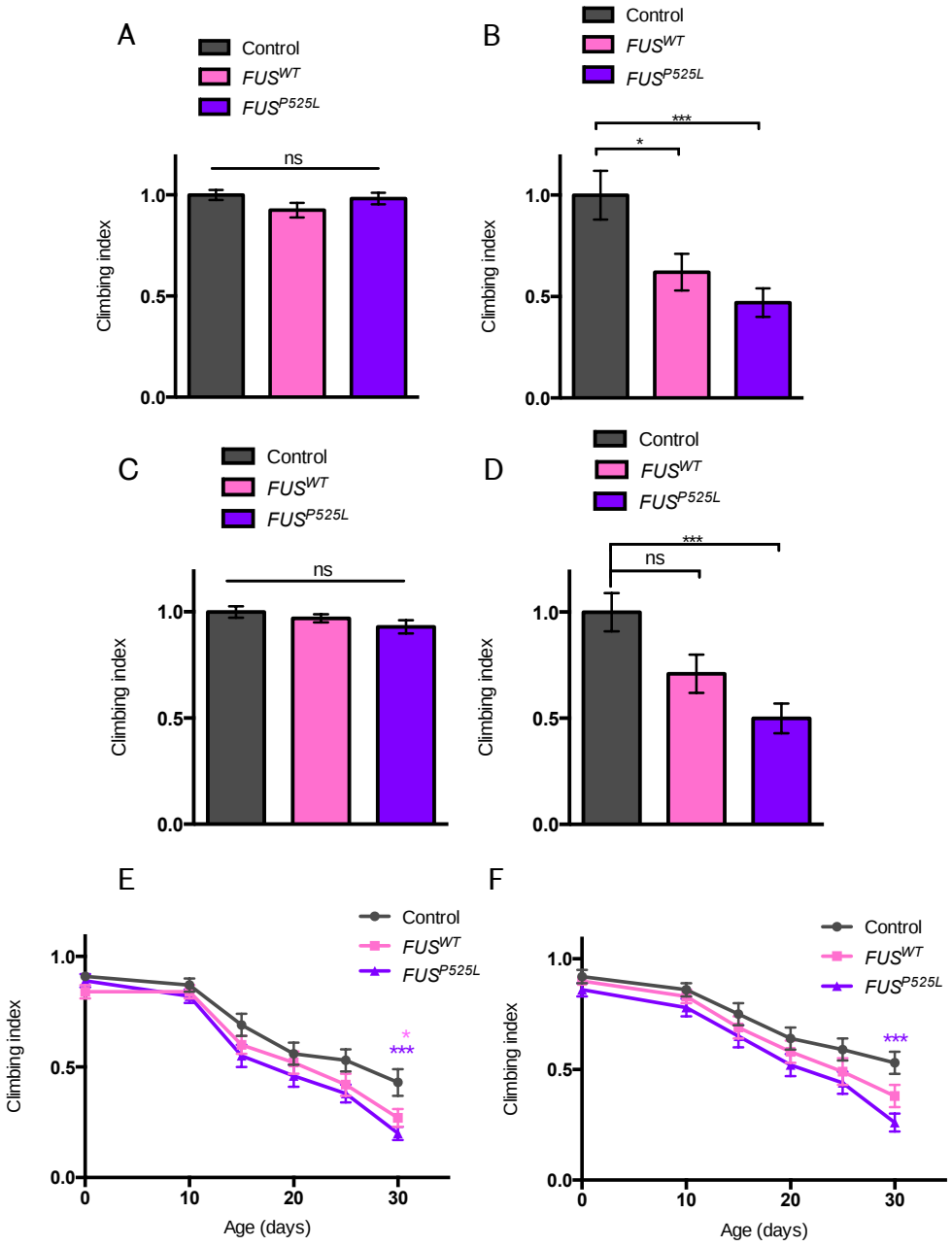

Figure 2.5: Aged climbing assay on FUS ectopic expression flies driven by *D42-GAL4*, using mated females at (A) day 0 and (B) day 30. Comparable results were shown when the same assay was conducted with males at (C) day 0 and (D) day 30. Climbing ability through time for (E) mated females and (F) males. A-D normalised to control. Control = D42> LacZ. Statistics calculated using Kruskal-Wallis with Dunn's multiple comparison test: * $p < 0.05$, *** $p < 0.001$.

ventral ganglion and the attached motor nerves were also removed. The dissection solution was then removed and the larvae were fixed with 4% paraformaldehyde (Agar Scientific AGR1026) for 20 minutes. The larvae were then washed 3 x 15 minutes in phosphate buffered saline with 0.1% Tween20 (Sigma P1379) (PBST) on a rocker at room temperature. The larvae were subject to a minimum of 1 hour blocking in 5% foetal bovine serum (FBS) (Sigma F4135) in 0.1% PBST on a rocker at room temperature. Anti-HRP was added to this solution at a dilution of 1 in 250 and placed at 4 °C overnight. Larvae were washed 3x 15 minutes in PBST on a rocker at room temperature. The larvae were then added to a 1 in 1000 dilution of anti-Rabbit Alexa Fluor® 594 in a solution of 5% FBS in 0.1% PBST, wrapped in foil and placed on a rocker at room temperature for 1 hour. Another round of washing 3x15 minutes in PBST followed.

Larvae were mounted onto slides (Thermo Scientific 10144633A) and dried of solution before Mowiol (Polysciences 17951-500) was added and a coverslip (BDH 406) placed down. This was sealed with nail varnish. Sample slides were stored in darkness at 4°C.

2.5.2 Microscopy

The Olympus FV1000 Fluoview confocal microscope (Olympus corporation) was used for all immunofluorescence experiments.

Table 2.8: Microscope parameters

Parameter	Mitochondria	NMJ
Objective	60x Oil Plan Apo NA 1.42 (Nikon)	60x Oil Plan Apo NA 1.42 (Nikon)
Laser line	488	543
Laser power	20%	50%

Z- stack images of 1 μm per slice were taken sequentially for 10-12 slices. Bright field images of muscles 6 and 7 were taken for each of the A2

segments used in the immunofluorescence microscopy. These images were taken using the Zeiss Axioskop MOT (Zeiss Corporation) using the 10x Plan-NEOFLUAR objective (Zeiss).

2.5.3 Data Analysis

2.5.3.1 Image Analysis

Images were analysed using the ImageJ software. Each image was split into its constituent colour channels and these were stacked. For the green channel (mitochondria), the rectangle selection tool was used to define a region of interest (ROI) encompassing only the NMJ area and the image was cropped for this region. This image was then made binary and the 'analyse particle' tool was employed to generate the number of mitochondria dots present in the image. For images of both mitochondria and NMJ staining, the channels were separated; both channels were stacked and then remerged.

2.5.3.2 Mitochondrial Count Analysis

The bright field muscle images of muscle 6/7 were used to measure the area of these muscles (Figure 2.6B). In ImageJ, the free-hand selection tool was used to draw around each muscle individually and the area was calculated using the 'measure' function. The scores for the each muscle were added together to create the muscle surface area (MSA) score.

The MSA of the experimental larvae were normalised to the MSA of the control larvae to produce a normalised muscle surface area (NMSA) score; this is to remove the variable of different MSAs that could account for differences in mitochondrial number as larger muscles have larger NMJs.

The mitochondrial count of the experimental genotypes and the control (MC) was then normalised to the respective NMSA to give the normalised mitochondrial count (NMC). This was then normalised to the control NMC to provide the mitochondrial score (MS). These scores were then statistically analysed by the Graphpad Prism software 6.0 using either students unpaired two tailed *t*-test or One-Way ANOVA depending on the number of experimental groups with the Sidak multiple comparison test.

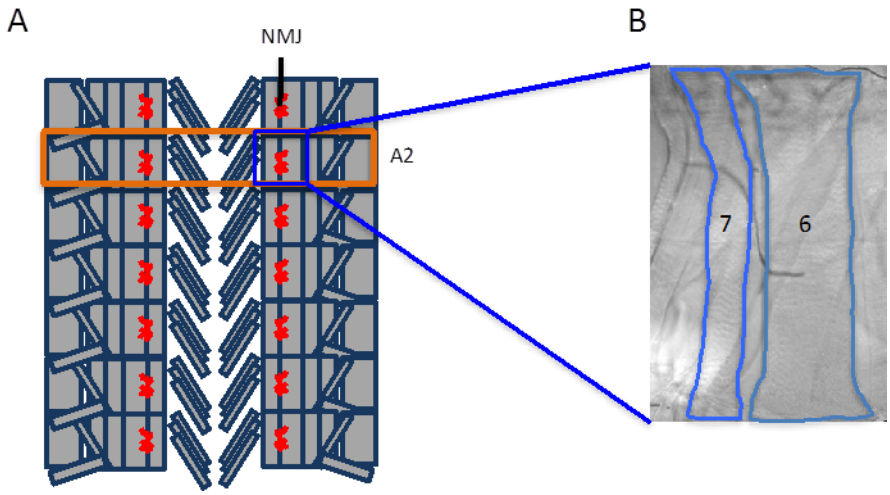

Figure 2.6: Mitochondrial number at the NMJ analysis. (A) The *Drosophila* third instar larva has a distinct abdominal repeating muscle architecture arranged into segments. The analysis was undertaken at the second segment termed 'A2'. Within this segment, the NMJ on muscles 6 and 7 was analysed by fluorescence and (B) bright field images were taken for the calculation of muscle surface area for the mitochondrial count analysis.

Chapter 3: TDP-43

3.1: Aims and Hypothesis

The primary aim of this project was to conduct a survey of axonal transport in terms of mitochondrial and vesicle cargoes, in three genetic models of ALS, and to examine whether this has any correlational effect on the behavioural motor functions of these models, tested through both larval and adult locomotor assays. The first to be assessed was TDP-43.

It was hypothesised that disruption to TDP-43 functioning through knockout, overexpression or pathogenic mutation interferes with axonal transport and contributes to the dying back pattern of degeneration characteristic of a distal axonopathy.

3.2: Considerations For Axonal Transport Studies

3.2.1 *Drosophila* as a Model Organism For Axonal Transport

Drosophila is an ideal model organism for testing a wide range of biological questions due to many factors pertaining to its simple husbandry and genome. However, in terms of axonal transport, the majority of initial studies had been conducted using other organisms. Isolated giant squid axoplasm has been used extensively, as have primary mouse neurons grown in culture. The main advantages here are the ease of visualisation and, for axoplasm, the removal of potentially confounding factors such as functions of the cell body including transcription (Morfini et al., 2013). However, *Drosophila* has been gaining favour as a useful *in vivo* model and has been used successfully to study axonal transport by among others Pilling et al., (2006) and Godena et al., (2014). In the same year Alami et al., (2014) reported use of *Drosophila* motor neuron live imaging in their assessment of TDP-43 granule axonal transport. Though an *in vivo* model, it is experimentally difficult to successfully visualise and

capture movies from whole larvae, although a protocol for this is available (Miller et al., 2005). In practice, however, this method in our hands caused a shaking effect on the movies referred to as 'drift' due to the inherent internal movement within the larva that cannot be satisfactorily counteracted (Godena, personal communication). Thus, the fillet dissection approach of Kuznicki and Gunawardena, (2010) was employed. This method allows for easy exposure of the *Drosophila* central nervous system whilst leaving the motor neuron axons intact *in situ* within a live animal.

3.3.2 CCAP as a Driver For Axonal Transport

The main challenge when designing experiments investigating axonal transport is the clear visualisation of that transport. As the archetype strong motor neuron driver, *D42-GAL4* (Yeh et al., 1995) is used in the majority of studies of behavioural motor function and is used in this study for those purposes. However, the use of it to study axonal transport (Pilling et al., 2006; Wang and Schwarz, 2009a) indicate that it is not best suited for this purpose. The segmental nerves projecting from the ventral ganglion contain between 60-80 motor and sensory axons, thus driving fluorescently tagged proteins involved in axonal transport with the all motor neuron driver *D42-GAL4* creates a crowded view of transport occurring within the whole motor axon complement of the nerve. This leads to a severe difficulty in accurately following individual cargo. For this reason *D42-GAL4* was not used in this study of axonal transport.

An alternative motor neuron driver that has been used successfully in axonal transport studies (Wang and Schwarz, 2009a; Godena et al., 2014) is crustacean cardioactive pepetide (CCAP), which is a neuropeptide with functions in regulating heart rate (Nichols et al., 1999) and the circadian regulation of ecdysis (Park et al., 2003). It is expressed by a specific set of neurons within the brain and ventral ganglion. In the latter, there is at

least one bilateral pair of CCAP expressing neurons within each neuromere, with two bilateral pairs present in thoracic (t) 3 and abdominal (a) 1-4, one pair in a5-7 and one pair in a8-9. One of the pairs within t3, a1-4 and a8-9 are efferent neurons each projecting an axon that leaves the ventral ganglion in the segmental nerves (Ewer and Truman, 1996). The *CCAP-GAL4* driver line accurately follows this pattern of expression (Park et al., 2003; Santos et al., 2007; Karsai et al., 2013). Thus, the *CCAP-GAL4* driver allows for the visualisation of fluorescently- tagged axonal transport cargo in one axon only of these segmental nerves and therefore allows accurate following and assessment of each cargo through its transport. For this reason it was chosen as the driver in this study.

3.3: Mitochondrial Axonal Transport

3.3.1 TBPH is the *Drosophila* Homologue of TDP-43

The gene encoding for TDP-43, *TARDBP*, has been highly conserved through evolution. The *Drosophila* homolog of TDP-43 is known as TAR DNA binding protein homolog (TBPH) and the gene is located on the right arm of chromosome 2 at position 60A4 to 60A5 of the cytogenetic map (FlyBase). TDP-43 and TBPH share great structural and sequence similarity demonstrating 59% identity and 77% similarity over the N-terminal and RNA recognition motifs, however, the C-terminal domain is not highly conserved and is markedly longer in TBPH, being comprised of 532 amino acids to 414 of TDP-43 (Ayala et al., 2005; Romano et al., 2012). Previous studies have indicated that TDP-43 and TBPH are also functionally conserved through evolution. Indeed, the phenotypes of TBPH knockout flies can be rescued by expression of TDP-43^{WT}. These include viability, lifespan, locomotor behaviours and NMJ morphology (Feiguin et al., 2009; Diaper et al., 2013).

TBPH also demonstrates conserved splicing functionality (Ayala et al., 2005), consistent with the fact both proteins share the preferential binding of UG or TG repeats of RNA or DNA, respectively (Ayala et al., 2005) and for the binding of other hnRNPs, such as hnRNP A1/A2 (D'Ambrogio et al., 2009; Romano et al., 2014). Thus *Drosophila* is an excellent *in vivo* model for the study of the effects of loss of TDP-43.

3.3.2 The Effect of Different Knockout Lines on Mitochondrial Axonal Transport

A number of *TBPH* knockout alleles have been generated to date. The initial phase of this study utilised two of these, $TBPH^{\Delta 23}$ (Feiguin et al., 2009) and $TBPH^{null}$ (also referred to as $TBPH^{1}$) (Fiesel et al., 2010). The former is a partial deletion of 1616 base pairs removing the 5' regulatory region and a part of the coding region. No TBPH protein was detected by western blot. The latter is a complete deletion of coding sequence and no mRNA was detected via RT-PCR.

To generate fly lines for this assay of mitochondrial axonal transport, these lines were recombined with *CCAP-GAL4* and balanced using *CyO.GFP*. The lines were also separately recombined with *UAS-mito.GFP* and these were crossed together to generate homozygous $TBPH^{null}$ and $TBPH^{\Delta 23}$ flies expressing mito.GFP driven by *CCAP-GAL4*. In addition, these recombinant lines were crossed with each other to produce $TBPH^{null/\Delta 23}$ trans-heterozygous knockout flies.

Mitochondrial transport was assessed as described in section 2.3. Both homozygous knockout lines and the trans-heterozygous knockout demonstrate a significant reduction in the motile fraction of axonal mitochondria (Figure 3.1), with a concomitant increase in the stationary fraction, which is indicated by the increase in the number of vertical lines on the kymographs (Figure 3.1B). This phenotype is most severe for the

TBPH^{null} homozygous knockout line. The trans knockout line shares this phenotype, but is slightly less severe than either homozygous line. This is likely due to a modifying effect of the chromosomal backgrounds of the two knockout mutants. For this reason, the trans-heterozygous knockout combination was chosen for all further experiments.

3.3.3 TBPH^{WT} Rescues the Knockout Mitochondrial Transport Deficit

To validate whether this phenotype is a specific consequence of the loss of TBPH, a rescue experiment was conducted wherein TBPH^{WT} was re-expressed in the trans-heterozygous knockout background. Here, mitochondrial transport was rescued to a comparable level with the control (Figure 3.2). Thus a reduction in the axonal transport of mitochondria is a direct consequence of the loss of TBPH. This rescue could also be achieved by the expression of TDP-43^{WT} and TDP-43^{M337V}.

3.3.4: The Effect of Ectopic Expression of TBPH, TDP-43 and a Human Pathogenic Variant on Mitochondrial Axonal Transport

Previous studies have demonstrated that the ectopic expression of TDP-43 also causes neurodegenerative phenotypes in a number of experimental systems including *Drosophila*. (Guo et al., 2011; Hanson et al., 2010; Ritson et al., 2010; Voigt et al., 2010; Li et al., 2010; Miguel et al., 2011; Lin et al., 2011; Estes et al., 2011; Diaper et al., 2013) Thus, overexpression of both the fly and human wild type protein was examined for mitochondrial axonal transport. In addition, the expression of a protein containing an ALS-linked C-terminal mutation, M337V was also assessed. This variant was first described in the study linking mutation in *TARDBP* with ALS pathogenesis (Sreedharan et al., 2008) and was associated with both

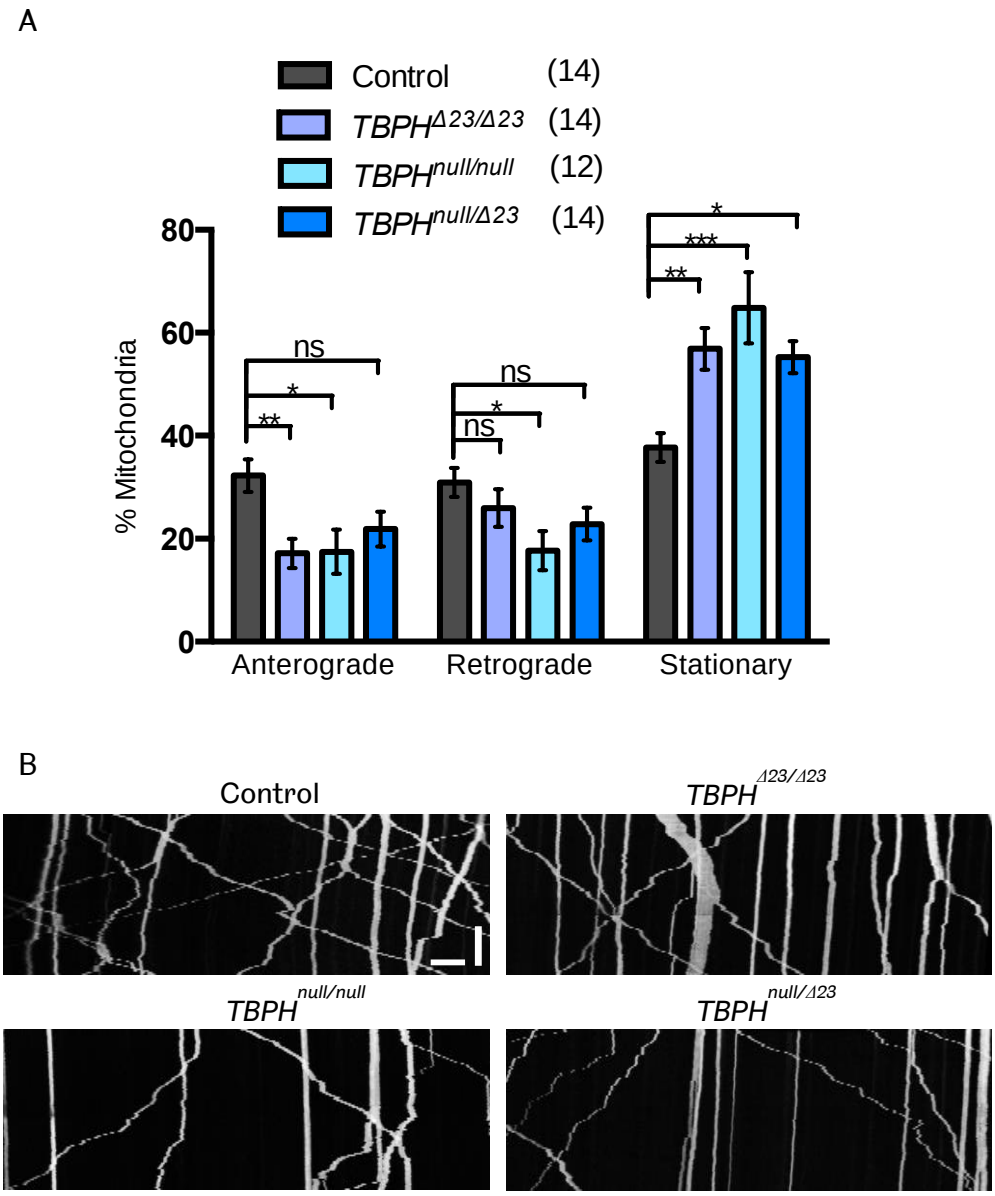

Figure 3.1: TBPH loss results in a mitochondrial transport deficit. The two knockout mutants give rise to a clear deficit in mitochondrial transport with a concomitant increase in the stationary fraction. This result is also shared by but is slightly less severe in the trans-heterozygous knockout line. (A) Quantification, the number in brackets indicates number of movies analysed. (B) Representative kymographs of the indicated genotypes. Scale bars: Horizontal (distance) =10 µm, Vertical (time) =125 s. Control = *CCAP-GAL4/+; UAS-mito.GFP/+*. Graph shows mean ± SEM. Statistics calculated using One-way ANOVA with Sidak's multiple comparison test: * $p < 0.05$, **$p< 0.01$, *** $p < 0.001$.

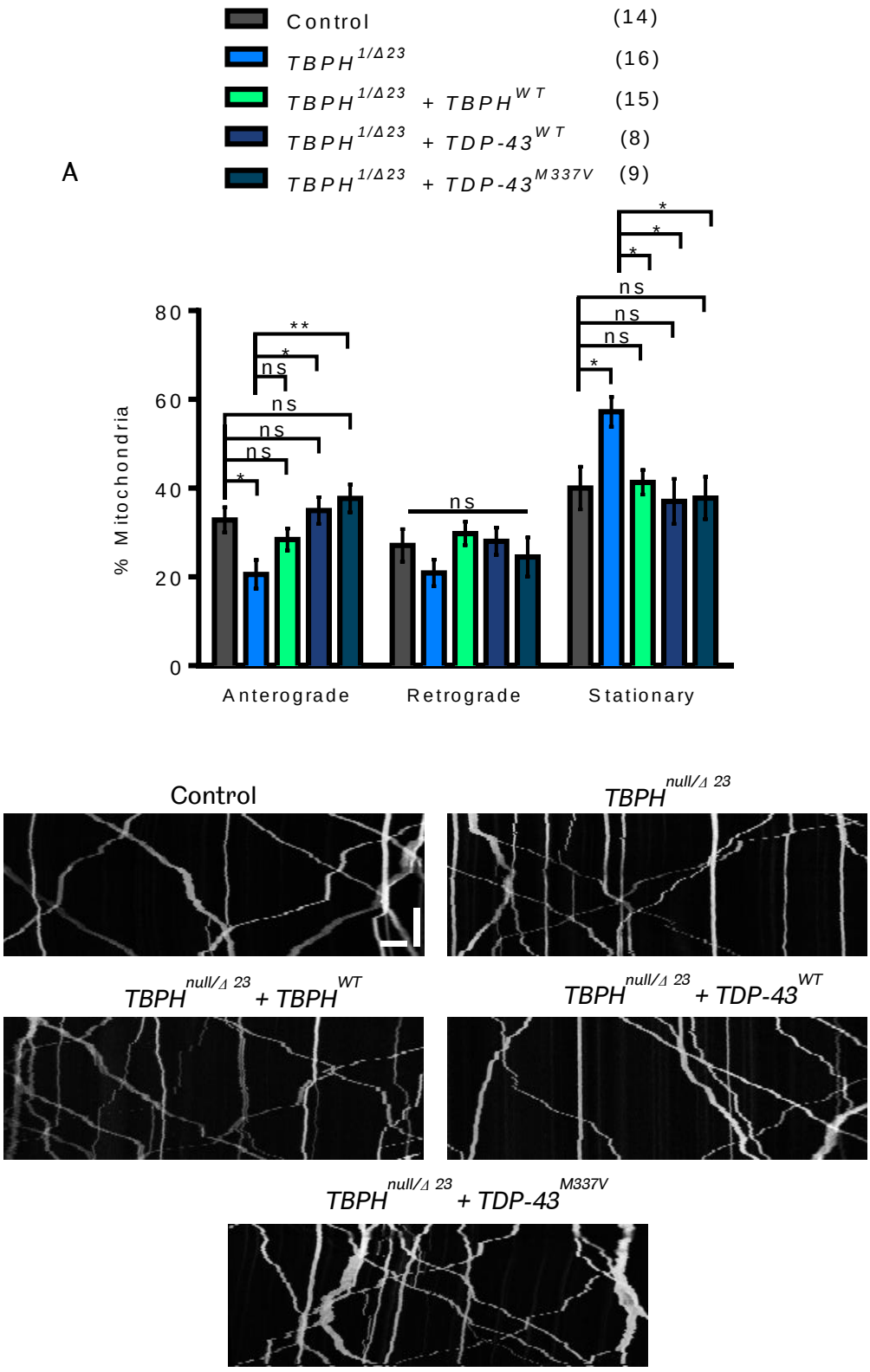

Figure 3.2: The mitochondrial transport defect observed in the trans-heterozygous *TBPH* knockout fly could be completely rescued by the expression of *TBPH*^{WT} / *TDP-43*^{WT} and *TDP-43*^{M337V} transgenes. (A) Quantification, the number in brackets indicates number of movies analysed. (B) Representative kymographs of the indicated genotypes. Scale bars: Horizontal (distance) =10 µm, Vertical (time) =125 s. Control = *CCAP-GAL4/+; UAS-mito.GFP/+*. Graph shows mean ± SEM. Statistics calculated using One-way ANOVA with Sidak's multiple comparison test: * $p < 0.05$, ** $p < 0.01$.

spinal and bulbar onset cases. These transgenes were created by Wang et al., (2011) and are targeted insertions expressing at the same level. For this study they were combined with the *CCAP-GAL4*; *UAS-mito.GFP*.

In contrast to the loss of TBPH, expression of either the fly or human protein (GOF) did not result in any alterations to the amount of mitochondrial transport. This was also the case for the human pathogenic variant, TDP-43^{M337V} (Figure 3.3).

3.4: Vesicle Axonal Transport

3.4.1 Vesicle Imaging Frame Rate Optimisation

Vesicle transport was assessed in terms of the movements of transport vesicles expressing a human Neuropeptide Y-GFP (NPY-GFP) fusion transgene (Mudher et al., 2004). These vesicles are continuously subject to axonal transport making them a good candidate for studies of axonal transport.

Unlike for the mitochondrial transport, optimisation of this vesicle transport movie parameters had not been carried out within our lab before the start of this project. Neuropeptide-filled vesicles move birectionally through the axon at a speed of a minimum four-fold greater than that achieved by the fastest moving mitochondria (Millecamps and Julien, 2013). Attempting to image this transport at the mitochondrial rate of 1 frame per 5 s proved to be far too slow to sufficiently capture the movement of individual vesicles and led to a severely crowded view of transport that cannot be analysed from the kymographs (Figure 3.4A). The frame rate at which the movies of this transport were taken at therefore required optimisation. Several different frame rates were examined: 3 s, 1 s, 0.5 s (Figure 3.4B-D). The results indicate that the rate of 1 frame per 3 s is still insufficiently fast to capture a view of transport

that can be analysed from the resultant kymographs. A frame rate of 1 per 1 s was a significant improvement however a rate of 1 frame per 0.5 s gave the clearest kymograph results and was therefore chosen as the frame rate for vesicle movie capture.

In similarity to the mitochondria imaging parameters, the vesicle movies were taken for 100 frames. The region of interest from which the movies were taken was also reduced due to the comparative difficulty in finding NPY-GFP expressing axons remaining in the focal plane for the necessary distance.

3.4.2 Vesicle Transport in TBPH Loss

To generate trans-heterozygous knockout fly lines for the examination of vesicle transport, the *TBPH*$^{\Delta 23}$*,CCAP-GAL4* recombinant fly line was crossed into the *UAS-NPY-GFP* background and was then mated with *TBPH*^{null}.

Vesicle transport was assessed as described in section 2.2. Here, there was no observable defect in the amount of vesicle movement, which remained comparable to the control (Figure 3.5).

3.4.3 The Effect of Overexpression of TBPH and Ectopic Expression of TDP-43 and a Human Pathogenic Variant on Vesicle Axonal Transport

The transgenes described previously were mated with the *CCAP-GAL4; UAS-NPY-GFP* line to generate larvae bearing one copy of the transgene.

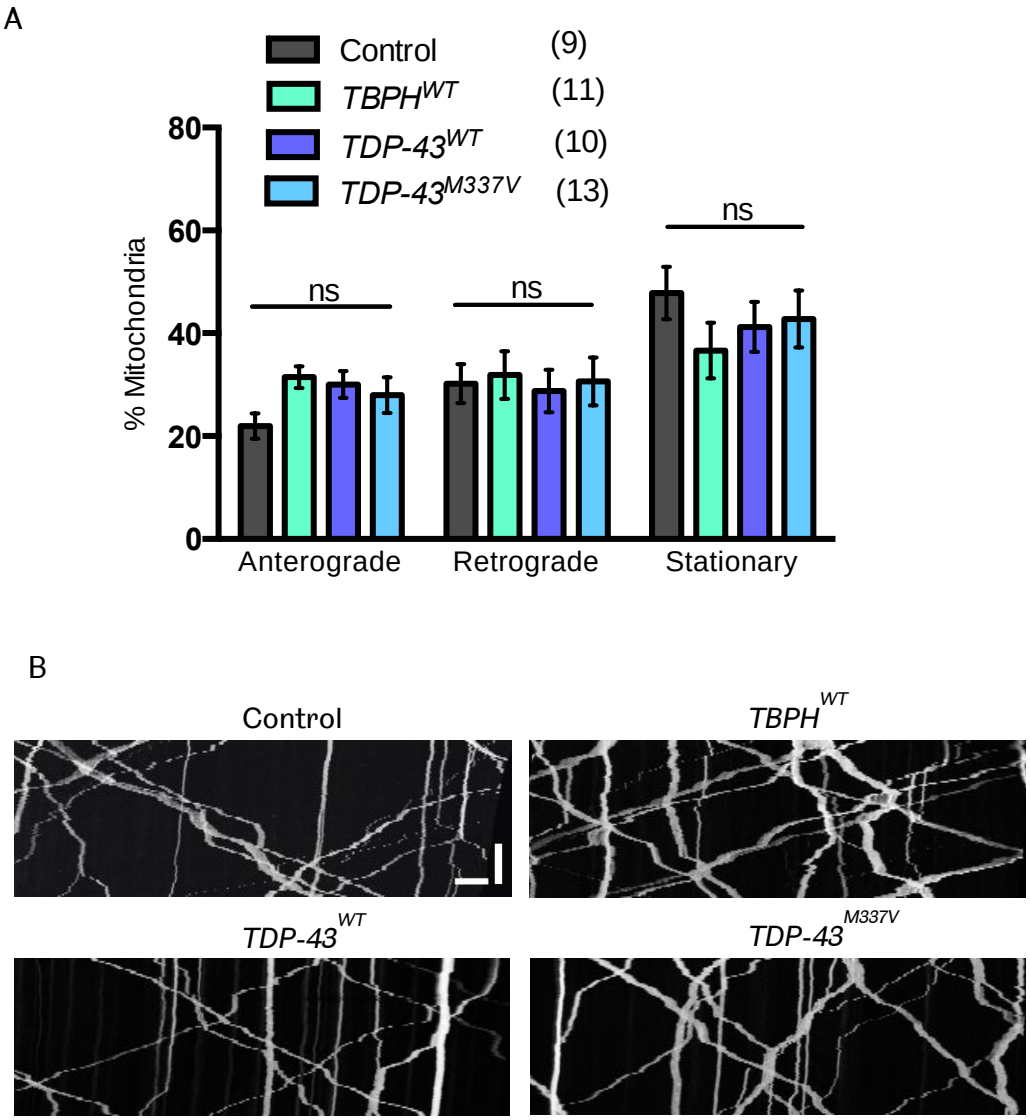

Figure 3.3: Gain of TDP-43 does not affect the level of mitochondrial transport. The overexpression of the fly wild type or ectopic expression of the human wild type protein and a human pathogenic variant TDP-43^{M337V} did not lead any alterations in the axonal transport of mitochondria. (A) Quantification, the number in brackets indicates number of movies analysed (B) Representative kymographs of the indicated genotypes. Scale bars: Horizontal (distance) =10 µm, Vertical (time) =125 s. Control = *CCAP-GAL4/+; UAS-mito.GFP/LacZ*. Graph shows mean ± SEM. Statistics calculated using One-way ANOVA with Sidak's multiple comparison test.

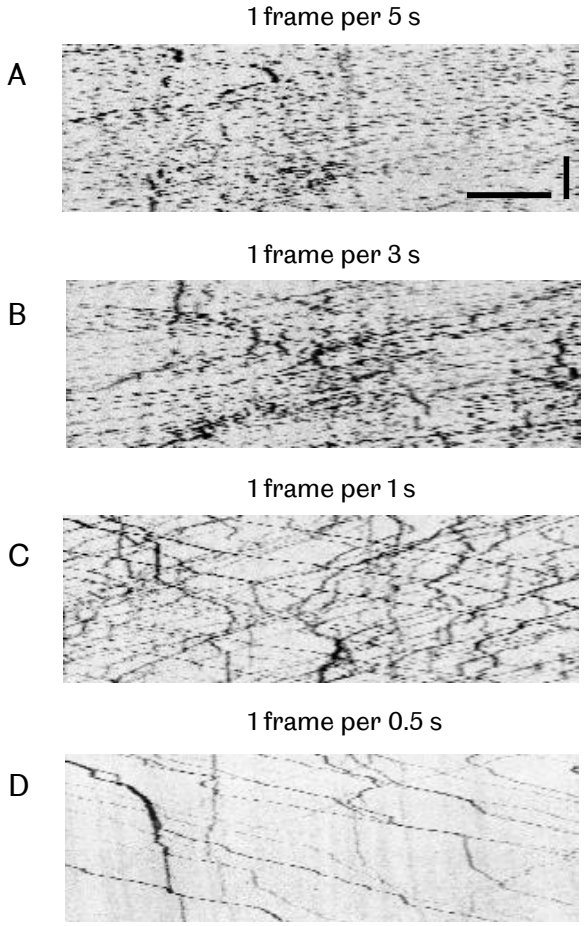

Figure 3.4: Frame rate optimisation for vesicle transport. (A) Imaging at a rate of 1 frame per 5 s provides a crowded view of transport that is impossible to analyse via kymographs. (B) This effect is only slightly improved reducing the frame rate to 1 per 3 s. (C) A further reduction to 1 per 1 s leads allows for the possibility to follow individual cargo however this is still difficult. (D) A frame rate of 1 per 0.5 provides a clear ability to follow cargo through transport and was chosen for the study. Scale bars: Horizontal (distance) =10 μm, Vertical (time) =12.5 s.

In contrast to the loss of TBPH, gain of this protein does cause a defect to the amount of vesicle transport as indicated by a significant increase in the stationary fraction (Figure 3.6). Neither the anterograde nor retrograde transport was reduced to the point of significance, however both were trending in that direction and the cumulative effect of this significantly increases the stationary fraction.

Expression of the pathogenic mutant M337V also causes an increase in the stationary fraction and here this is can be traced to a significant reduction in the retrograde direction of transport, whereas anterograde transport is not affected. However, unlike the fly protein, gain of the wild-type human homolog did not disrupt this transport to any significant degree, although it was trending in that direction.

3.5: The Effect of TBPH Gain on Mitochondrial Morphology

Whilst the gain of $TBPH^{WT}$ does not lead to any disruption to the amount of mitochondrial axonal transport, it was observed that the mitochondria appeared to be markedly increased in length compared to those of the control or $TDP\text{-}43^{WT}$ and $TDP\text{-}43^{M337V}$. This was quantified as described in section 2.3.4 and found to be significant throughout the course of the movies (Figure 3.7).

As a further validation of this observation, the lengths of mitochondria from the trans-heterozygous knockout (LOF) genotype were also assessed. Here, no significant difference in length was apparent during the movies (Figure 3.8). These mitochondria were not subjected to ultrastructural analysis and so it cannot be explicitly ruled out that the long lengths do not in fact represent a series of short clumped mitochondria. However, the fission/fusion genetic interaction studies described below render this unlikely.

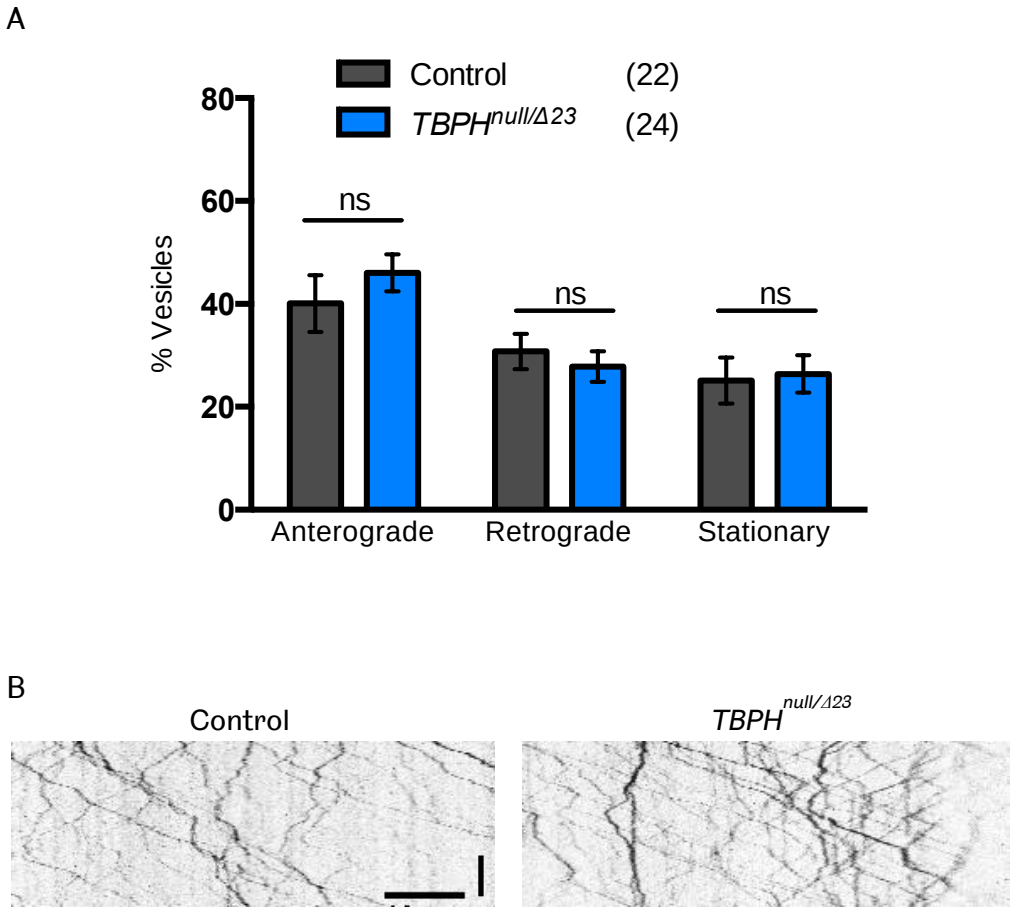

Figure 3.5: Loss of TBPH does not cause any alterations to the transport of vesicles. (A) Quantification, the number in brackets indicates number of movies analysed (B) Representative kymographs of the indicated genotype. Scale bars: Horizontal (distance) =10 µm, Vertical (time) =12.5 s. Control = *CCAP-GAL4/+; UAS-NPY-GFP/+*. Graph shows mean ± SEM. Statistics calculated using Student's *t*-test.

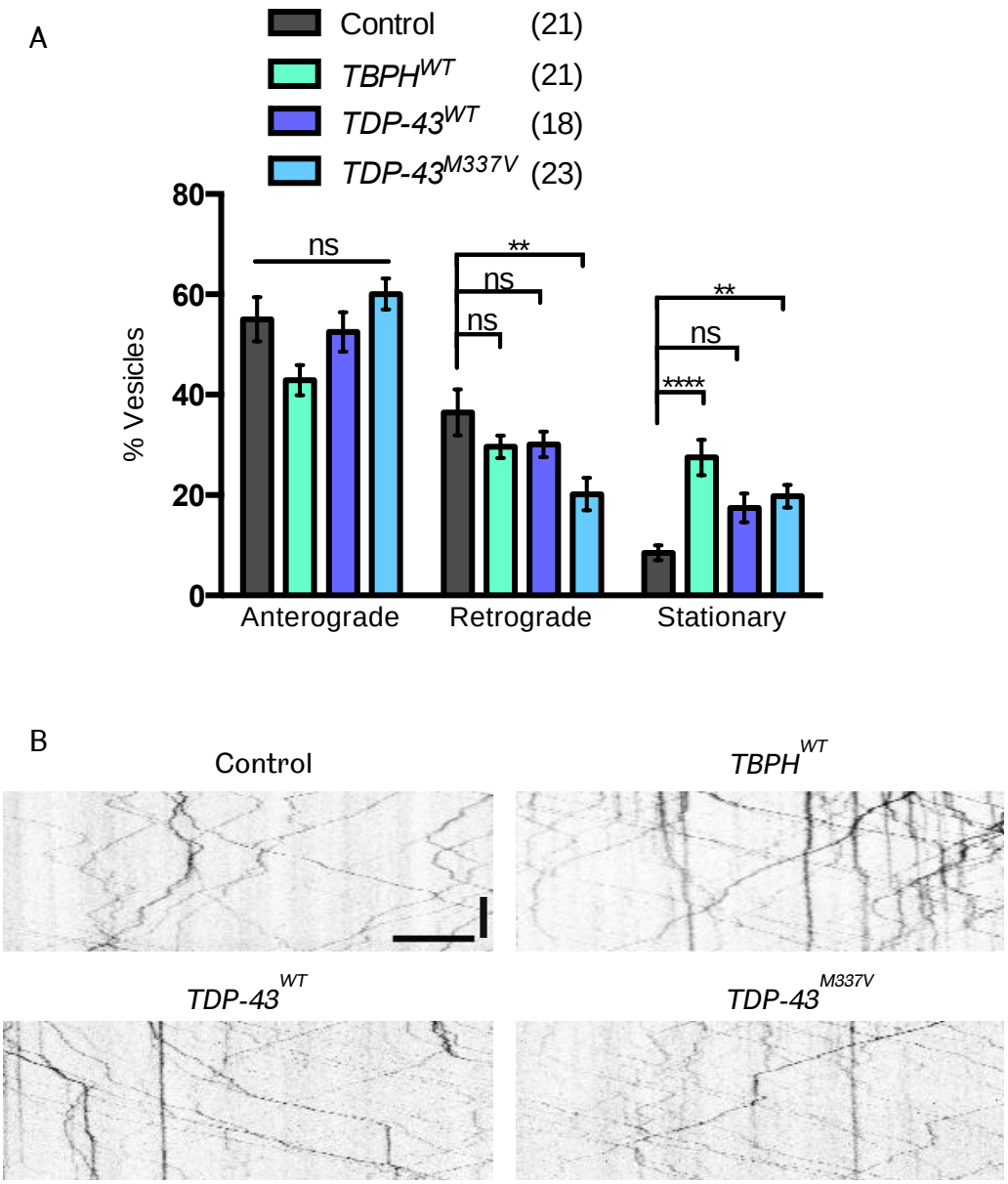

Figure 3.6: Overexpression of wild-type fly or human pathogenic variant M337V causes a defect in the axonal transport of vesicles with an increase in the stationary fraction of vesicles. This is caused by cumulative reductions in anterograde and retrograde transport, which is significant in the retrograde fraction for the pathogenic mutant. Overexpression of the human wild-type did not lead to any significant defect in this aspect of transport. (A) Quantification, the number in brackets indicates number of movies analysed. (B) Representative kymographs of the indicated genotypes. Scale bars: Horizontal (distance) =10 µm, Vertical (time) =125 s. Control = *CCAP-GAL4/+; UAS-NPY-GFP/LacZ*. Graph shows mean ± SEM. Statistics calculated using One-way ANOVA with Sidak's multiple comparison test: $^{**}p< 0.01$, $^{****}p<0.0001$.

3.5.1 Genetic Interaction of TBPH^{WT} with Mitochondrial Fission and Fusion Genes

Mitochondrial morphology is highly dynamic. Within cell bodies, they are commonly seen fused together to form long tubular networks. However, when travelling through axons, they do so as short, independent organelles. This fission and fusion of mitochondria is a property vital for their health and functioning and significant failure in these processes results in cell death and is a factor related to a number of diseases (van der Bliek et al., 2013).

A considerable amount has been elucidated regarding the molecular machinery governing these processes, specifically the role of Dynamin related GTPases. Fission is caused by Dynamin-related protein 1 (DRP1) that acts similarly to Dynamin in the final constriction of separating mitochondria (Smirnova et al., 2001). Mitochondrial fusion is more complex, requiring different proteins for the fusion of the inner and outer membranes. Inner membrane fusion is mediated by Optic atrophy 1 (OPA1), so named as mutations within it underpin Dominant Optic Atrophy (Delettre et al., 2000; Alexander et al., 2000). The GTPases Mitofusin 1 and 2 are the mediators of mitochondrial tethering and outer membrane fusion. Mutations in Mitofusin 2 are responsible for Charcot Marie Tooth Disease Type 2A (Zuchner et al., 2004), which is characterised as a distal axonopathy.

DRP1 and OPA1 have corresponding *Drosophila* homologs named Drp1 and Opa1 respectively. There are two *Drosophila* homologs of the mitofusins, Fuzzy onions (Fzo) of which expression is restricted to sperm, and Mitochondrial assembly regulatory factor (Marf), which is ubiquitously expressed (Hwa et al., 2002).

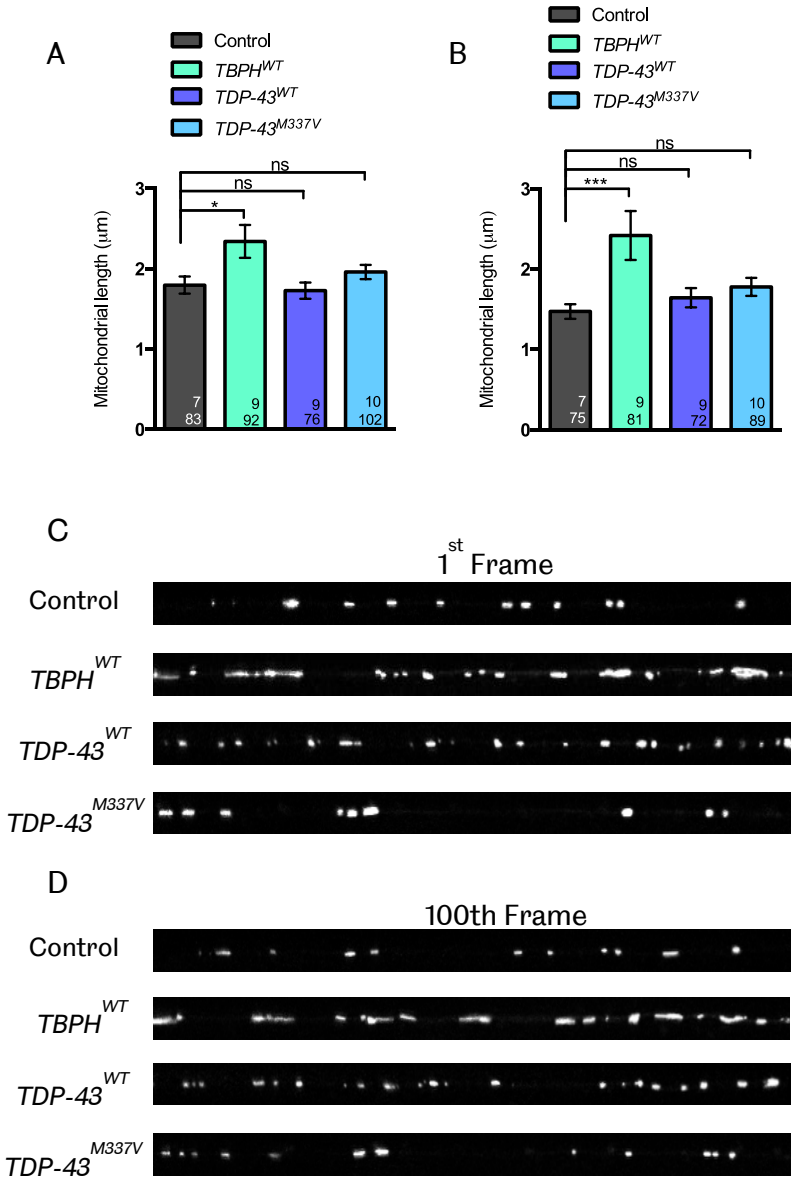

Figure 3.7: Mitochondria are on average significantly longer in the axons of TBPH^{WT} overexpressing larvae. (A) Quantification of 1st frame. (B) Quantification of 100th frame. (C) 1st frame representative kymographs. (D) 100th frame representative kymographs. Control = *CCAP-GAL4/+; UAS-mito.GFP/LacZ.* Numbers on bars: Top number = Number of animals quantified. Bottom number = Number of mitochondria quantified. Graph shows mean ± SEM. Statistics calculated using One-way ANOVA with Sidak's multiple comparison test: * $p < 0.05$, *** $p < 0.001$.

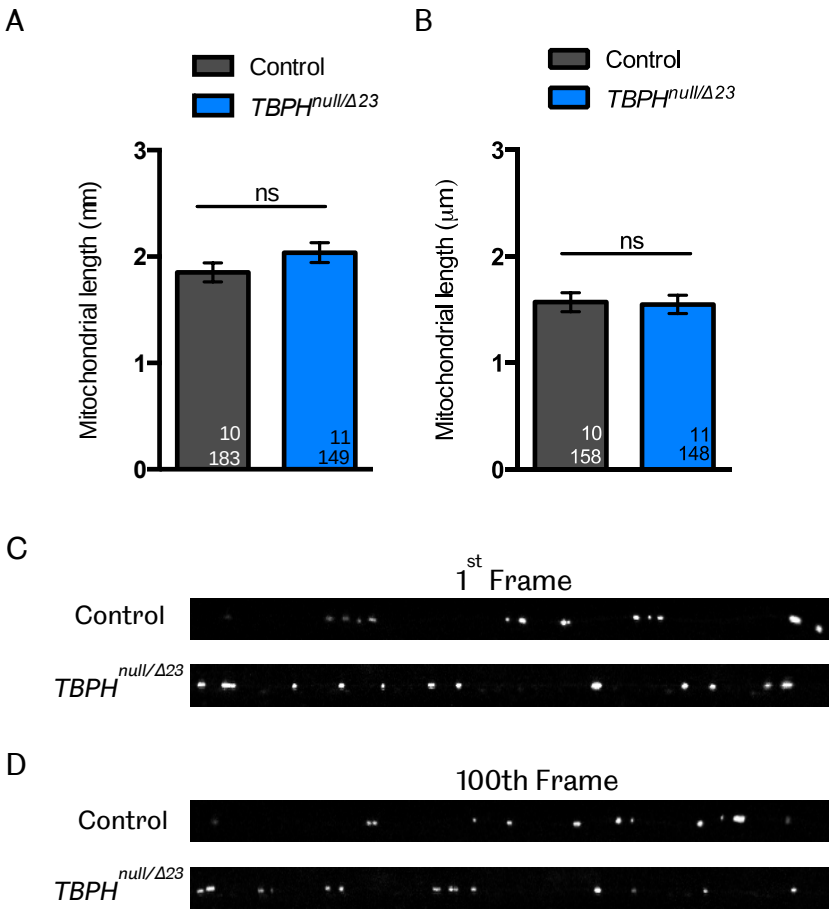

Figure 3.8: No alteration to mitochondrial length was observed in the trans heterozygous knockout condition quantified from the (A) 1st and (B) 100th frames. (C) 1st frame representative kymographs. (D) 100th frame representative kymographs. Control = *CCAP-GAL4/+; UAS-mito.GFP/+*. Numbers on bars: Top number = Number of animals quantified. Bottom number = Number of mitochondria quantified. Graph shows mean ± SEM. Statistics calculated using Student's t-test.

Genotypes for this analysis were created by combining each of these lines with the *UAS-TBPH*^{WT} fly and then with the *CCAP-GAL4; UAS-mito.GFP* line.

The Drp1 overexpression line by itself did not lead to any alterations in mitochondrial length, which is consistent with previous findings in HeLa cells (Chang et al., 2010). Further, overexpressing Drp1 together with TBPH did not lead to a rescue of the length phenotype, but did in fact exacerbate increases in mitochondrial length (Figure 3.9A-B).

The *Opa1*$^{-}$ heterozygote itself had no effect on mitochondrial length and did not cause a rescue of the TBPH overexpression effect. (Figure 3.9C-D).

However, while the *marf*$^{-}$ heterozygote also demonstrated a comparable mitochondrial length to the control, when introduced into the TBPH overexpression background, this resulted in a complete rescue of the mitochondrial length phenotype. This suggests an interaction, between TBPH and Marf in the regulation of mitochondrial length (Figure 3.9E-F).

3.6 Mitochondria At The NMJ in TBPH Loss

Due to the result that the loss of TBPH leads to a deficit in the axonal transport of mitochondria within motor axons, it was considered of interest to examine the possible effect of this on the number of mitochondria at the neuromuscular junction. Immunofluorescence was performed on fixed samples of third instar TBPH knockout larvae expressing *UAS-mito-GFP* driven by *D42-GAL4* (see section 2.4). Compared to the outcross control, there was a significant increase in the number of mitochondria at the NMJ of muscles 6 and 7. The fact that the

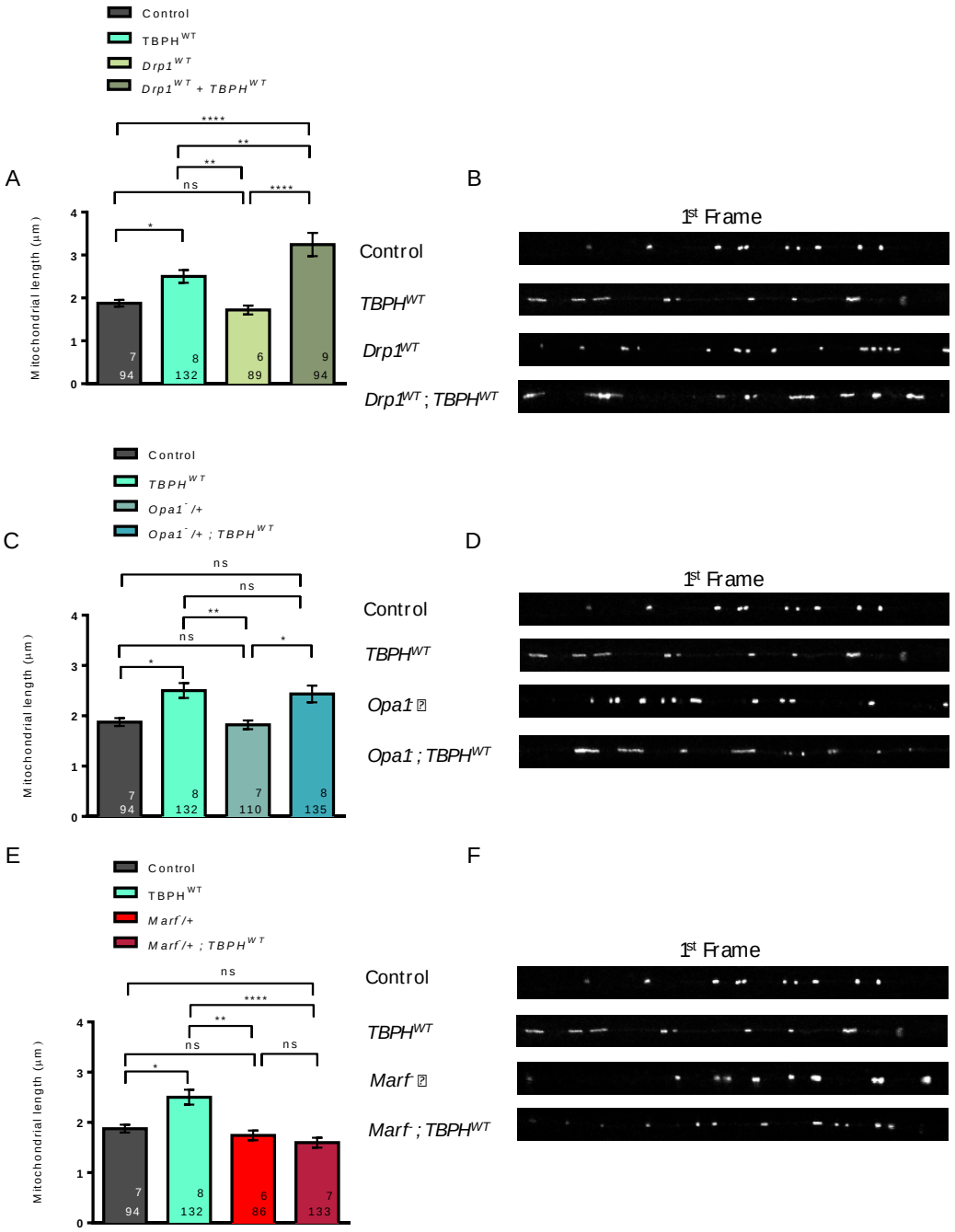

Figure 3.9: Genetic interaction of TBPH with mitochondrial fission and fusion genes to assess for rescue of the increased mitochondrial length phenotype seen with the overexpression of TBPH. (A-B) The overexpression of Drp1 (fission) results in a further increase in mitochondrial length. (C-D) The heterozygous loss of Opa1 does not alter this phenotype. (E-F) Heterozygous loss of Marf (OM fusion) fully rescues the length phenotype. Numbers on bars: Top number = Number of animals quantified. Bottom number = Number of mitochondria quantified. The same images are shown reiteratively for control and TBPH^{WT}. Control = *CCAP-GAL4/+; UAS-mito.GFP/LacZ.* Graph shows mean ± SEM. A/C/E analysed together due to shared control and TBPH^{WT} using One-way ANOVA with Sidak's multiple comparison test: * $p < 0.05$, **$p< 0.01$, ****$p<0.0001$.

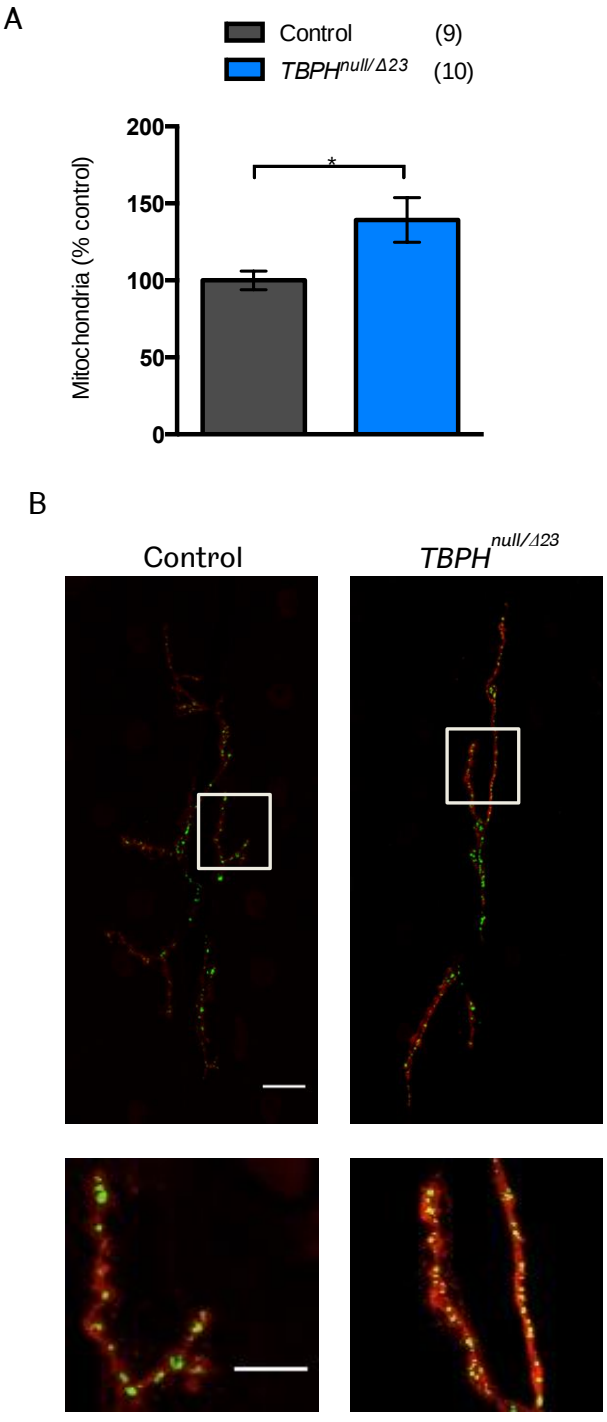

Figure 3.10: Loss of TBPH causes an increase in the number of mitochondria at the NMJ. (A) Quantification, the number in brackets indicates number of images analysed. (B) Representative images. Red = HRP, Green = mito.GFP. Scale bar = 20 μm (full image), 10 μm (crop). Control = *D42-GAL4> UAS-mito.GFP.* Graph shows mean ± SEM. Statistics calculated using Student's *t*-test (* $p < 0.05$).

number of mitochondria is increased was an interesting result that likely stems from consequences of the increased stationary behaviour of the mitochondria.

3.7: Behavioural Analysis of TBPH loss

3.7.1 Viability

In their original characterisation, the *TBPH*$^{\Delta 23}$ and *TBPH*^{null} lines were both assessed as having a severely reduced viability phenotype with only a few rare escapers eclosing in *TBPH*$^{\Delta 23}$ homozygotes with the majority dying at the L3 stage and a recorded lethality at the 2nd instar stage of *TBPH*^{null} homozygotes. However, the *TBPH*^{null} line in our hands was viable to the third instar stage and produced very rare escapers. Other modifying factors within the genome and interaction with our particular environment could potentially explain this discrepancy, in addition the results from the mitochondrial transport experiment, which demonstrated the likelihood of background modifier effects, formed the decision to use the trans-heterozygote combination of *TBPH*$^{null/\Delta 23.}$ Thus, for the purposes of this study, the viability of the trans-heterozygote was examined. In line with the milder phenotype observed for this fly compared to the two homozygotes, the level of eclosion was on average 18% that of the control. These adults however died within 5 days (Figure 3.11A).

Attempts were made to rescue this sub-viability phenotype with re-expression of TBPH^{WT} using several *GAL4* drivers. Use of the all-motor neuron driver *D42-GAL4* to express TBPH^{WT} resulted in an almost complete rescue of the eclosion defect (Figure 3.11A). Driving expression with the pan-neuronal driver, *elav-GAL4*, fully rescues eclosion to control (Figure 3.11B).

This rescue experiment was also carried out using human TDP-43 both wild type (Figure 3.11C) and M337V mutant (Figure 3.11D) using the *D42-GAL4* driver. Expression of both of these transgenes fully rescued the phenotype indicating this functional ability is conserved in the ALS-linked protein. In addition, it seems in terms of eclosion that, whilst expression exclusively within the motor system is sufficient to create a very significant rescue, the extra-motor neuronal role of this protein increases the efficiency of this rescue.

3.7.2 Larval Locomotion

Given the results of the mitochondrial axonal transport experiments, which demonstrate a clear deficit, the locomotor capacity of the larvae was assayed to examine whether there is any correlation between motor ability and axonal transport defects.

The larval crawling test was performed on these genotypes as described in section 2.4.2.1. Briefly, the larvae were set onto a smooth surface and the number of peristaltic wave crawling movements they performed in two minutes was recorded. The trans-heterozygous knockout larvae display a crawling ability 63% that of the control (Figure 3.12A). This was fully restored upon expression of wild-type and ALS mutant transgenes with *D42-GAL4* (Figure 3.12A/C/E). In the turning test (section 2.4.2.2), which involved turning the larvae ventral-side-up with a paintbrush and recording the time taken to self-right, these results were also true. Turning ability was drastically compromised in the knockout larvae and fully rescued by motor neuron expression of the wild-type or mutant transgenes indicating this functional ability is conserved in the ALS linked protein (Figure 3.12 B/D/F).

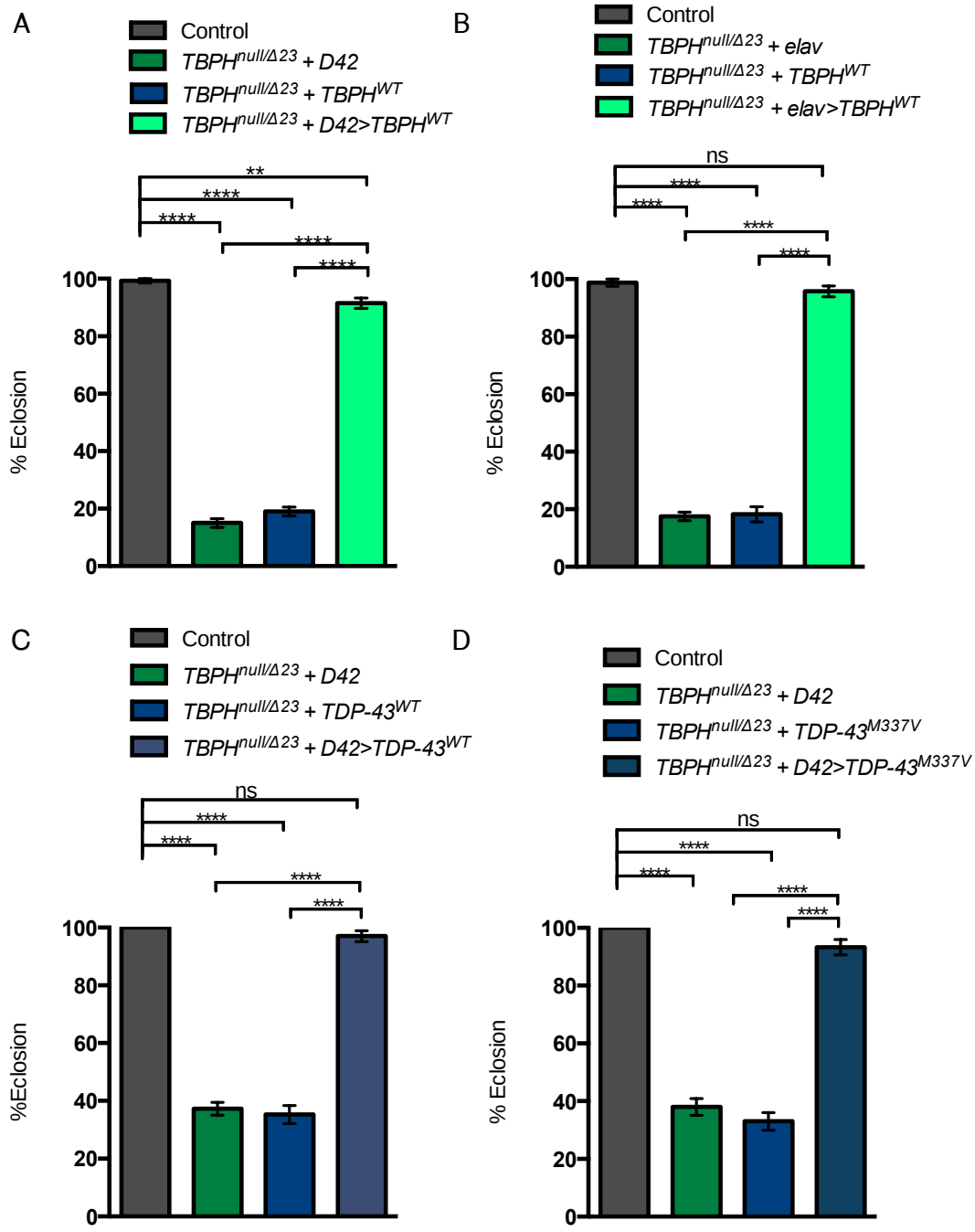

Figure 3.11: *TBPH* knockout flies have a severe eclosion defect that can (A) be almost completely rescued by TBPH^{WT} expression driven by *D42-GAL4* and (B) fully rescued when this is driven by *elav-GAL4.* (C-D) The phenotype can also be fully rescued by TDP-43^{WT} and TDP-43^{M337V} driven by *D42-GAL4.* N= 4. Total number of animals = 100. Control = *D42>LacZ* or *elav>LacZ.* Graph shows mean ± SEM. Statistics calculated using One-way ANOVA with Sidak's multiple comparison test: **p< 0.01, ****p<0.0001.

3.7.3 Adult Locomotion

The *TBPH*$^{null/\Delta 23}$ adults that eclose also exhibit severe locomotor dysfunction displaying no quantifiable capacity to climb on day 0. Unlike locomotion at the third instar larval stage, this phenotype could not be fully rescued by the motor neuronal expression of either wild type protein or TDP-43^{M337V}. Rather, only a modest partial rescue is achieved (Figure 3.13A-C). This result suggests that this motor neuronal expression of the transgenes is not sufficient to rescue the climbing phenotype. This is an interesting result, particularly in relation to the wild-type proteins, given the fact both viability and larval locomotion is rescued as well as the axonal transport defect. It's possible that within the adult, the expression levels of the proteins were not enough to rescue this form of locomotion. Another possibility is that extra-motor neuronal expression is required to rescue this phenotype.

3.7.4 Analysis of Alternative *TBPH* Knockout Alleles

The *TBPH*^{null} allele, may have additional effects on another gene, as in addition to being a complete deletion of the *TBPH* locus, also has a deletion of the 5'UTR of neighbouring gene *bgcn* (Voigt, personal communication). Therefore, to check that the *TBPH*$^{null/\Delta 23}$ trans-heterozygous fly represents an appropriate model to analyse the effect of TBPH loss, complementation analysis was performed with two additional mutant lines, *TBPH*^{DD96} and *TBPH*^{DD100} created by Diaper et al., (2013). The *TBPH*^{DD96} line is missing the promoter and the coding sequence up to and including that for the second RRM. The *TBPH*^{DD100} line is a smaller deletion of the promoter and start codon. Both these mutant flies have a maximum eclosion score of 20% and escaper lifespan of 7 days and exhibit severe deficits in larval crawling and adult walking behaviour and climbing behaviour (Diaper et al., 2013).

TBPH$^{null/DD96}$ and *TBPH*$^{null/DD100}$ trans-heterozygous knockout flies demonstrate non-complementation through a clear eclosion defect, which is similar in severity to that seen in the TBPH$^{null/\Delta 23}$ line. (Figure 3.14A). In addition this can also be almost completely rescued by motor neuronal expression of TBPH^{WT} (Figure 3.14A). In further similarity with the *TBPH*$^{null/\Delta 23}$ line, larval crawling was significantly reduced and turning time was increased four-fold (Figure 3.14B&C) and both these phenotypes could be fully rescued by expression of TBPH^{WT} within motor neurons. Unsurprisingly, adult locomotor ability was non-existent in either line and could only be partially rescued by motor neuronal expression of TBPH^{WT} (Figure 3.14D).

The level of similarity between these lines and the *TBPH*$^{null/\Delta 23}$ line indicate that the *TBPH*$^{null/\Delta 23}$ fly is likely to be an appropriate model for analysing the effect of TBPH loss.

3.8: Behavioural Analysis of TBPH Overexpression and Ectopic Expression of TDP-43

3.8.1 Viability and Larval Locomotion

Gain of TBPH and TDP-43 driven with *D42-GAL4* has no effect on the viability of the flies. The same is also true for expression of the M337V mutant protein (Figure 3.15A). Similarly, the gain of either wild-type protein does not alter the crawling and turning measures of larval locomotion. However, the D42>*TDP-43*^{M337V} line was characterised by a reduction in larval crawling to 88% of control and a 3.5 fold increase in turning time (Figure 3.15B-C). Thus, this suggests that in this model increasing the level of these wild- type proteins does not interfere with their development in terms of viability or motor function, but the ALS linked mutation causes a disruption to neuromuscular functioning at this early stage.

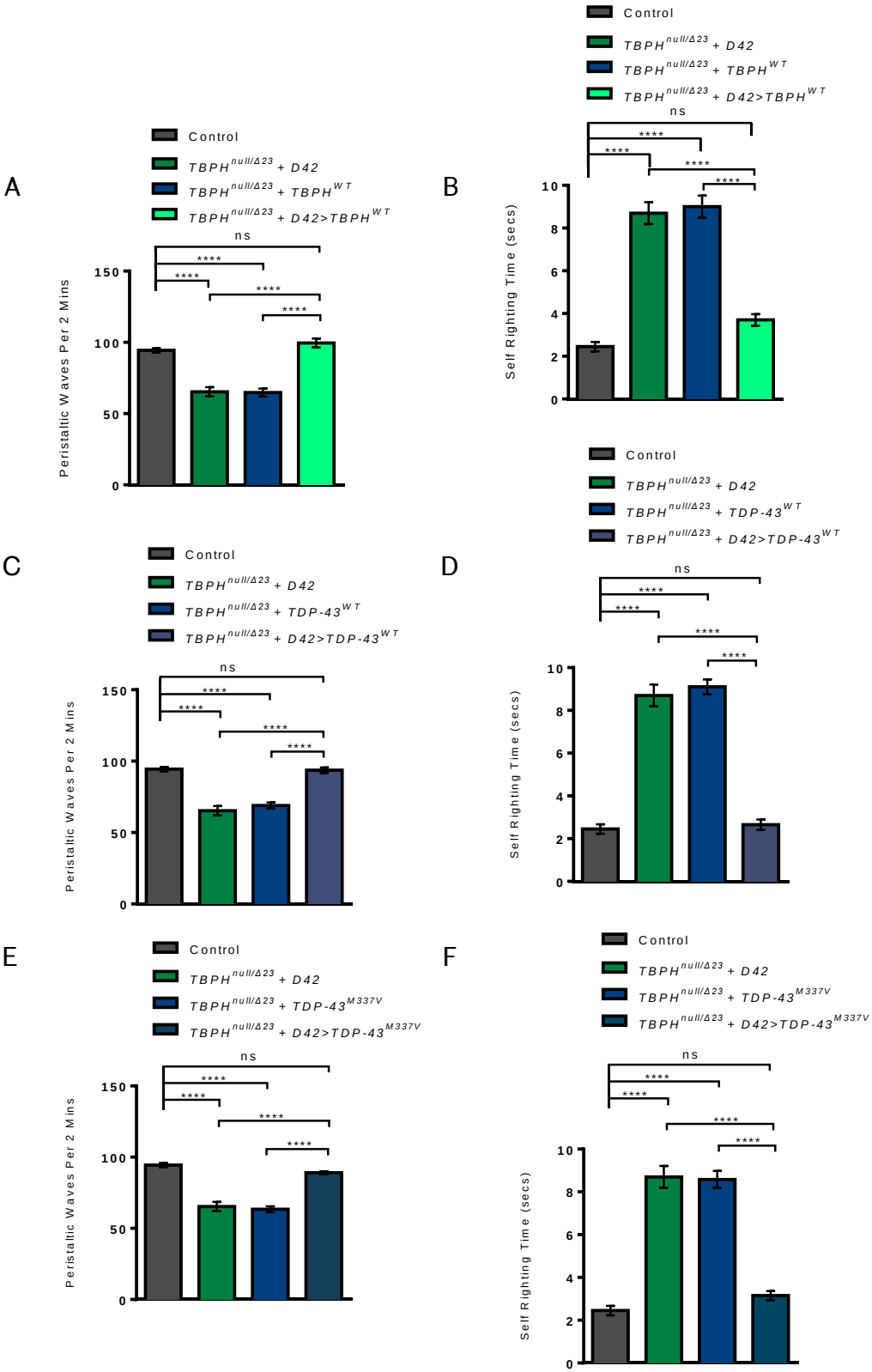

Figure 3.12: *TBPH* knockout larvae demonstrate a reduced locomotor capacity in terms of both crawling (A/C/E) and turning ability (B/D/F), which can be rescued by re-expression of (A-B) TBPH^{WT}, (C-D) TDP-43^{WT} and (E-F) TDP-43^{M337V} driven by *D42-GAL4*. N= 4. Total number of animals = 20. Control = *D42>LacZ*. Graph shows mean ± SEM. Statistics for A/C/E and B/D/F calculated together due to shared control using One-way ANOVA with Sidak's multiple comparison test: ****p<0.0001.

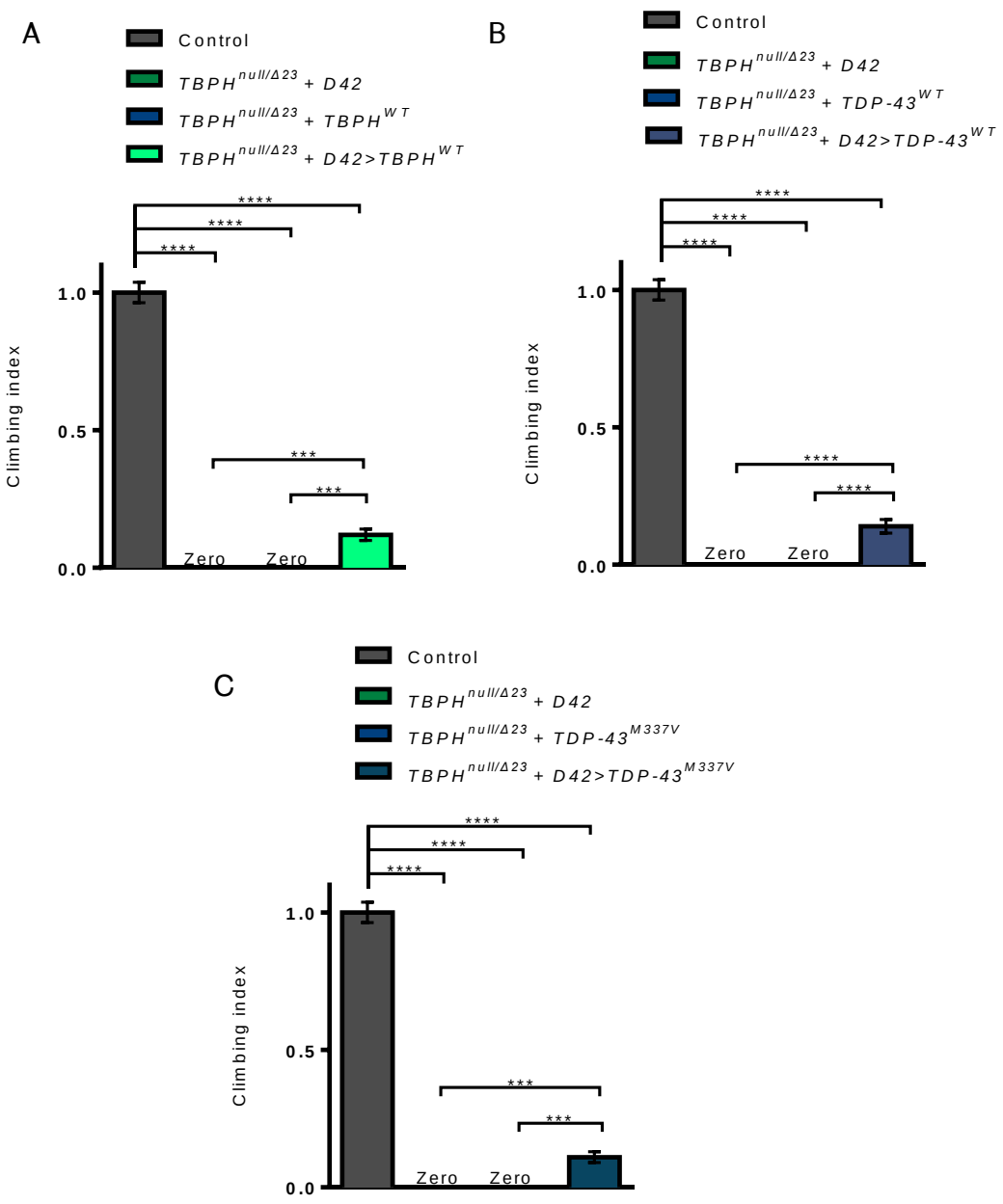

Figure 3.13: *TBPH* knockout adult flies display severely compromised motor function, which can only be partially rescued by re-expression of (A) TBPH^{WT}, (B) TDP-43^{WT} and (C) TDP-43^{M337V} driven by *D42-GAL4*. N= 3. Total number of animals = 50. Control = *D42>LacZ*. Graph shows mean ± SEM. A-C are normalised to control. Statistics (A-C) calculated together due to shared control using Kruskal-Wallis with Dunn's multiple comparison test : *** p<0.001, **** p<0.0001.

3.8.2 Adult Locomotion

The motor function of the adult flies mirrors that of the larvae when driven with *D42-GAL4*, with *D42>TDP-43^{M337V}* 0-3 day old flies exhibiting a reduction in this ability to 63% control level (Figure 3.16A). Since ALS is a age-related and progressive disorder, the flies were aged in cohorts and the climbing test was performed every five days until day 30. The *D42>TDP-43^{M337V}* flies continued to decline at a steady pace compared to the control, whereas the wild-type lines' climbing capacity decreased modestly until day 25, at which point they exhibited a sharp decline compared to control. By day 30 the climbing ability of both wild-type lines and the mutant were comparably poor at just 10% the level of the control (Figure 3.16B & E). Therefore, it seems the effect of the pathogenic mutant continues to affect locomotor capacity and neuromuscular functioning as was the case in the larvae; however overexpression of the wild type proteins also has detrimental effects on this system that develop over time through ageing, which is interesting given the fact ALS is an age-related neurodegenerative disease.

The picture of adult locomotor ability was more complex when these lines were driven by *elav-GAL4*. Unlike with *D42-GAL4*, the *elav>TDP-43^{M337V}* flies exhibited no climbing defect at day 0, as was the case with expression of the TBPH and TDP-43 wild type proteins at this time point (Figure 3.16C) in contrast to the lethality seen with other lines (Diaper et al., 2013). At day 20 *elav>TBPH^{WT}* and *elav>TDP-43^{M337V}* caused a significant reduction in climbing ability. Both these genotypes continued to decline until by day 30 they exhibited climbing capacity of just 18% and 53% respectively. By contrast, *elav>TDP-43^{WT}* did not lead to a climbing defect at any age examined (Figure 3.16D & F). The fact that *elav>TDP-43^{M337V}* led to no climbing deficit at day 0 is interesting given the result with *D42>GAL4* driver and suggests the strong expression of this protein within motor neurons is key to its early effect.

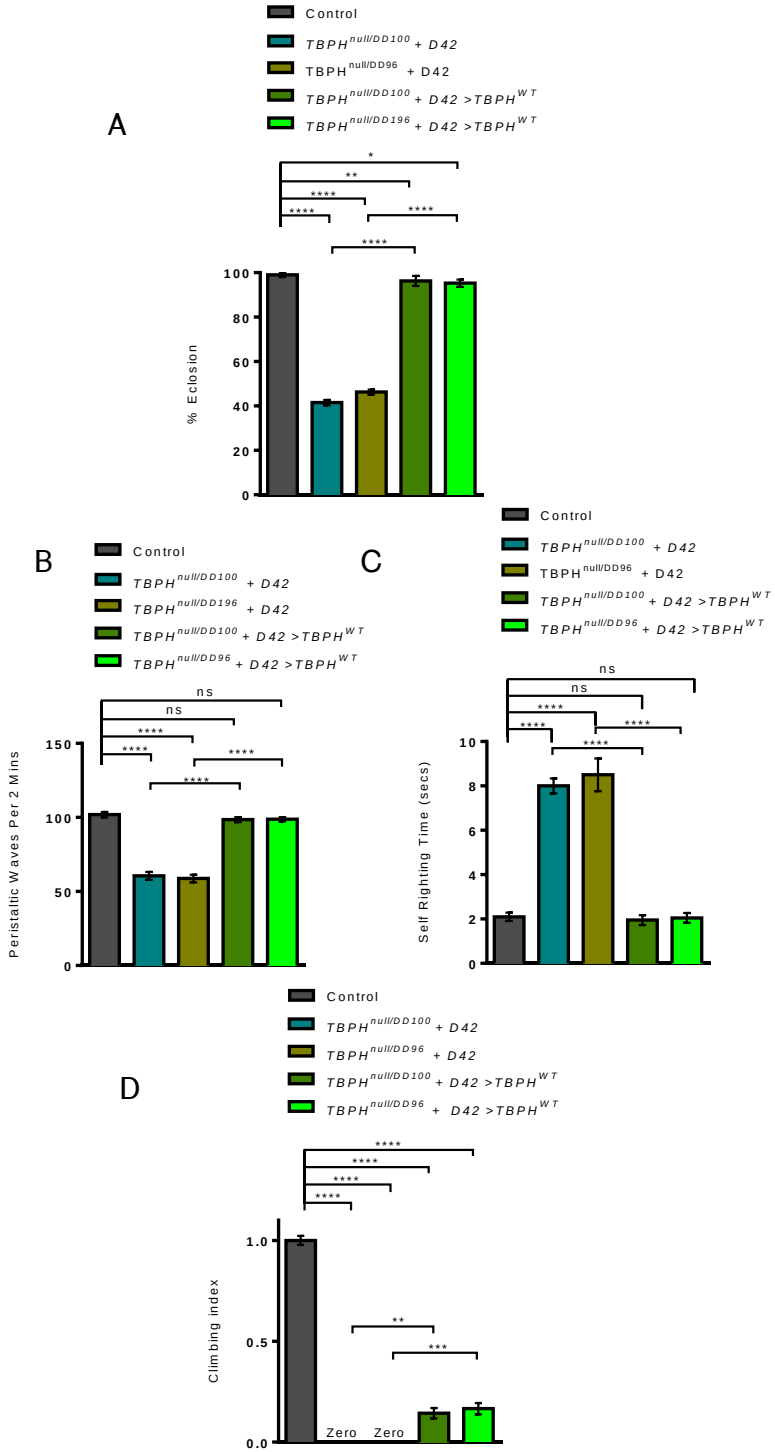

Figure 3.14: *TBPH*$^{null/DD96}$ and *TBPH*$^{null/DD100}$ trans-heterozygous knockout lines exhibit deficits in viability and motor behaviour. (A) *TBPH*$^{DD96/null}$ and *TBPH*$^{DD100/null}$ flies exhibit over a 50% reduction in eclosion. For both lines this can be almost completely rescued by re-expression of TBPH^{WT} with *D42-GAL4*. (B) Crawling and (C) turning behaviour is also reduced in both lines, which can be rescued by re-expression of TBPH^{WT} with *D42-GAL4*. (D) Adult climbing ability is non-existent in either knockout line and can only be partially rescued by motor neuronal re-expression of TBPH^{WT}. N= 4 (A), 4 (B/C), 3 (D). Total number of animals = 100 (A), 20 (B/C), 50 (D). Control = *D42>LacZ.* D is normalised to control. Graph shows mean ± SEM. Statistics (A-C) calculated using One-way ANOVA with Sidak's multiple comparison test, for D calculated using Kruskal-Wallis with Dunn's multiple comparison test : * $p < 0.05$, ** $p< 0.01$,*** $p<0.001$. ****$p<0.0001$.

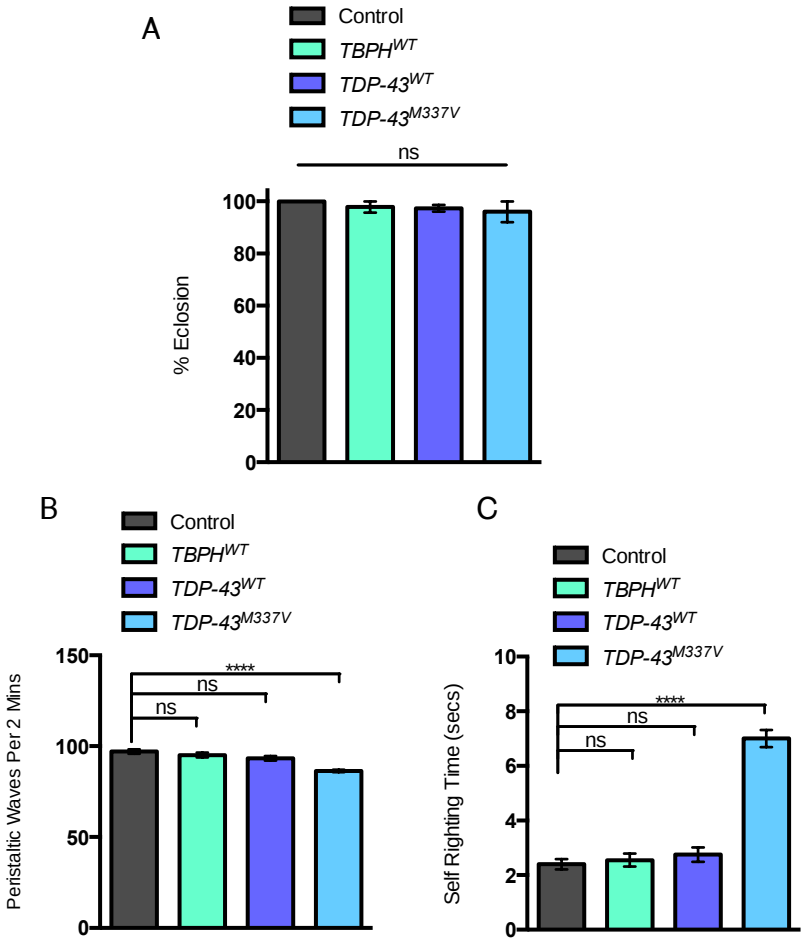

Figure 3.15: Ectopic expression of TDP-43^{M337V} driven by *D42-GAL4* causes viability and larval locomotor phenotypes. (A) No eclosion defect was observed with any of the three genotypes. (B) Only the human mutant has a significant larval crawling defect and (B) turning defect. N=4. Total number of animals = 100 (A), 20 (B/C). Control = *D42>LacZ*. Graph shows mean ± SEM. Statistics calculated using One-way ANOVA with Sidak's multiple comparison test: ****p<0.0001.

3.9: Summary

The results for all TDP-43 experiments are summarised in Table 3.1. The loss of TBPH leads to defective axonal transport of mitochondria in third instar larvae, which was found to be a specific effect of TBPH through the fact it can be completely rescued by expression of the wild-type protein. This transport phenotype however appears to be selective as the transport of vesicles was not altered. The disrupted transport of mitochondria may also lead to the observed increase in the number of mitochondria at the neuromuscular junction through downstream consequences of the increased stationary behaviour of the mitochondria, indicating possible functional consequences of this transport defect at this structure.

The disruption to axonal transport correlated with, and thus may contribute to, a severely reduced viability as measured by eclosion and in multiple measures of locomotion serving as readout of neuromuscular function. Specifically, TBPH loss results in significant reductions to crawling and turning ability of the third instar larvae and in adult climbing capacity, which is completely non-existent.

As was the case with rescue of the mitochondrial transport phenotype, these deficits could be rescued with the expression of the fly and human wild-type proteins and the human ALS mutant in motor neurons further supporting a relationship between these transport defects and motor abilities. An exception is documented with the climbing ability of the adults, which could only be partially rescued. This last result may stem from insufficient expression levels of the transgenes and/or the need for extra-motor neuronal involvement of TDP-43. If time allowed, it would have been interesting to attempt to raise these flies at the temperature of 29°C to increase the level of expression of the transgenes. In addition, attempting the rescue with the pan-neuronal driver *elav-GAL4* would

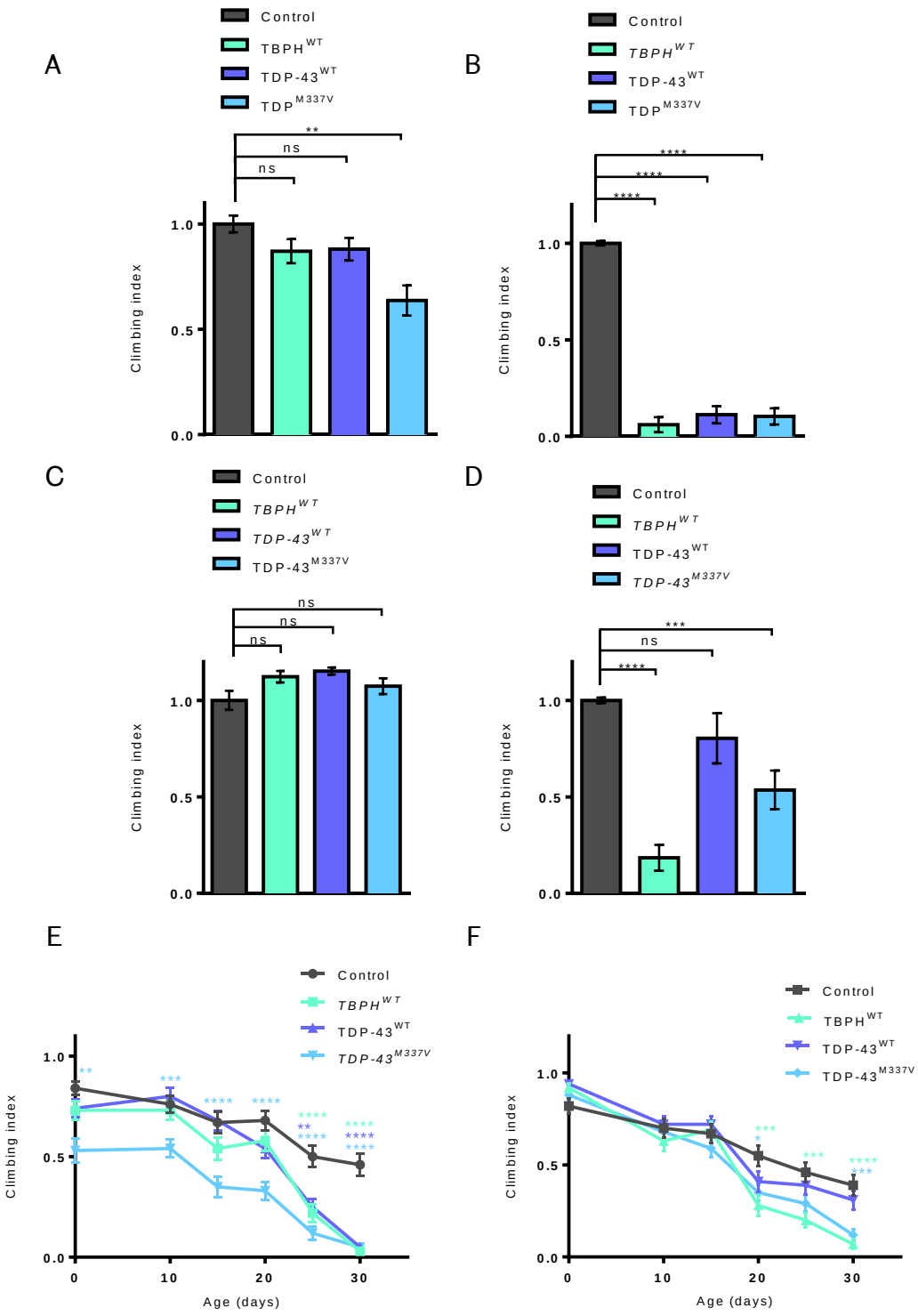

Figure 3.16: Climbing ability of TDP-43 overexpression flies declines with age. (A) *D42-GAL4* driven expression of the TDP-43^{M337V} causes a decrease in climbing ability. (B) However, in aged flies (30 days) expression of the wild-type proteins also caused a severe locomotion defect. (C) By contrast, expression with *elav-GAL4* causes no locomotor defect in young flies and (D) a severe reduction with *elav>TBPH*^{WT} and *elav>TDP-43*^{M337V} but *elav>TDP-43*^{WT} flies aged to 30 days. Climbing ability through time driven by (E) *D42-GAL4* and (F) *elav-GAL4*. N=3. Total number of animals = 50. Control = *D42>LacZ* (A/B/E), *elav>LacZ* (C/D/F). A-D are normalised to control. Graph shows mean ± SEM. Statistics calculated using Kruskal-Wallis with Dunn's multiple comparison test: * $p < 0.05$, ** $p < 0.01$, *** $p < 0.001$, **** $p < 0.0001$.

serve to elucidate whether other neuronal populations are necessary for this rescue.

The overexpression of TBPH^{WT} and the ectopic expression of TDP-43^{M337V}, but not TDP-43^{WT} also resulted in a defect to axonal transport, However, in contrast to what was found for TBPH loss, mitochondrial transport was unaffected but vesicle transport was decreased. Thus loss and gain of TBPH have differential effects on axonal transport.

Although the overexpression of TBPH does not lead to a defect in mitochondrial transport, it does appear to cause an increase in mitochondrial length. Genetic interaction experiments revealed that heterozygous loss of *marf*, the *Drosophila* homolog of Mitofusin 2, rescues this phenotype, indicating a relationship between Marf and TBPH.

However, the axonal vesicle transport defect is not correlated with an eclosion defect of these genotypes indicating that the disruption is not so severe as to compromise the organism's viability through development. Only the locomotor function in the motor neuronal expression of the pathogenic mutant larvae was affected. This was also true for young adults ability to climb. This climbing ability also displayed a progressive worsening with expression of all the proteins until day 30 when all three genotypes demonstrated just a fraction of the ability of the control. This mirrors the fact ALS in humans is generally an age-related disorder.

The climbing capacity was slightly different for the pan-neuronal expression of these transgenes, being unaffected in young flies and reduced to a lesser extent in aged flies and not significantly so in terms of the expression of the human wild-type protein. Therefore this may point to the idea that strong expression within motor neurons is an important factor and further highlights the specific vulnerability of these neurons in this disorder.

It also appears that expression of ALS linked mutant protein results in pathogenic outcomes for axonal transport that correlates with motor behaviour, which is affected at the third instar stage. Thus the ALS mutant protein seems to exert an effect on neuromuscular functioning at an early time-point, which may in part be contributed to by disruption to the axonal transport of these vesicles.

The finding that overexpression of wild-type protein, though causing vesicle transport disruption, doesn't lead to larval or young adult locomotor phenotypes may highlight the neurons' greater ability to cope with the effects of the increased amounts of the wild-type, as opposed to the mutant, protein. However, overexpression of wild type does lead, in a progressive, age-related manner, to locomotor dysfunction and the vesicle transport disruption highlighted here, could be a factor in this declining capacity to compensate.

The fact that disruption to TBPH/TDP-43 levels alters axonal transport and does so in different ways, is an interesting finding that correlates with neuromuscular dysfunction and may have consequences for ALS pathogenesis.

Table 3.1: Summary of experimental results for TDP-43. Arrows represent alterations to phenotype: Red = Reduction relative to control, yellow = increase, green = rescue and blue = no change. Thickness of arrow corresponds to strength of effect. Dashed line = Assay not undertaken.

	Mitochondrial Transport	Mitochondria at NMJ	Vesicle Transport	Eclosion	Larval Motor Ability	Adult Motor Ability (young)	Adult Motor Ability (Aged)
KNOCKOUT							
TBPH$^{null/\Delta 23}$	↓	↑	↔	↓	↓	↓	N/A
Rescue with TBPH	↑	------	N/A	↑	↑	↑	------
Rescue with TDP-43	↑	------	N/A	↑	↑	↑	------
Rescue with TDP-43^{M337V}	↑	------	N/A	↑	↑	↑	------
OVEREXPRESSION							
TBPH^{WT}	↔	------	↓	↔	↔	↔	↓
TDP-43^{WT}	↔	------	↔	↔	↔	↔	↓
TDP-43^{M337V}	↔	------	↓	↔	↓	↓	↓

Chapter 4: FUS

4.1: Aims and Hypothesis

The second genetic model of ALS to be assessed in this study was *FUS*. Here too, the aim was to survey the state of axonal transport of mitochondria and vesicles and to examine whether any defects have any correlational relationship with the flies' behavioural motor functions as assessed via larval and adult locomotor assays.

It was hypothesised that disruption to FUS functioning through knockout, overexpression or pathogenic mutation interferes with axonal transport and contributes to the dying back pattern of degeneration characteristic of a distal axonopathy.

4.2: Mitochondrial Axonal Transport

4.2.1: Caz is the *Drosophila* homolog of FUS

cabeza (*caz*) was identified as the *Drosophila* homolog of *FUS* (Stolow and Haynes, 1995). Within the fly genome *caz* is situated on the X chromosome at position 14B8 – 14B9 of the cytogenetic map (Flybase). It encodes a protein that is 53% identical to FUS. The general structure of both proteins is conserved with Caz also containing an N-terminal QGSY rich region followed by a glycine rich region, a single RRM harbouring the NES domain and a zinc finger domain sandwiched between two RGG rich regions. However, Caz is shorter than FUS at 399 amino acids compared to 526 (Stolow and Haynes, 1995).

Caz and FUS are also functionally conserved through evolution with the phenotypes of *caz* knockout flies rescued by the expression of FUS^{WT}; these include viability, locomotion and lifespan (Wang et al., 2011).

4.2.2 The Effect of Loss and Gain of Caz on Mitochondrial Axonal Transport

To study the loss of Caz, the *caz*^{1} knockout mutant was utilised. This represents a deletion of the promoter and 58% of the coding sequence. This mutant also included a deletion of the adjacent gene CG32576 for which a rescue construct was placed on this *caz* mutant chromosome (Wang et al., 2011). For the study of axonal transport of mitochondria, the *caz*^{1}*/FM7.GFP* line was combined with *CCAP-GAL4* and this new line was subsequently mated to UAS-*mito.GFP* flies. Since *caz* in located on the X chromosome, male wandering third instar larvae were selected for study.

The gain of Caz and FUS was also examined both in terms of the wild type protein and an ALS linked mutant protein. In humans, the P525L mutation situated within the N-terminal nuclear localisation domain, results in an aggressive juvenile/adult onset form (Sproviero et al., 2012). The P398L mutation of Caz is in the equivalent position to the P525L mutation ALS linked mutation of FUS. These transgenes were created by Wang et al., (2011) and are targeted insertions expressing at the same level. Expression analysis indicated FUS^{WT}, FUS^{P525L} and Caz^{WT} localised to the nucleus of motor neurons, whereas Caz^{P398L} localised to the cytoplasm. For the study of gain of Caz, these transgenes were crossed with the *CCAP-GAL4; UAS-mito.GFP* line.

The loss of Caz causes an increase in the stationary fraction of mitochondria within the axons. The same situation is apparent in the condition of Caz overexpression, although here the effect is marginally milder. The ectopic expression of the mutant protein Caz^{P398L} results in the most severe phenotype with 76% of mitochondria stationary. Thus it is clear that both loss and gain of Caz is sufficient to cause a disruption to the dynamics of this transport and this ability is retained within the mutant Caz^{P398L} protein (Figure 4.1).

4.2.3 Rescue of the *caz* Knockout Phenotype

In the same manner as was performed for TBPH loss, a rescue experiment was conducted with both Caz^{WT} and Caz^{P398L}. For this, the Caz overexpression transgenes were crossed into the *UAS-mito.GFP* background and then mated with *the* caz^{1}*/FM7.GFP; CCAP-GAL4/TM6B* line.

At the standard temperature of 25°C, expression of neither the wild type nor the ALS mutant rescued the phenotype (Figure 4.2). At least for the wild type this was an unexpected result given the ability of Caz^{WT} to rescue other *caz* knockout phenotypes. One possible explanation is the levels of Caz were not sufficient to rescue this phenotype. Thus, the rescue experiment was conducted again on wandering third instar larvae that had been grown at the higher temperature of 29°C, which is commonly used to increase expression levels. This resulted in the complete rescue of the *caz* knockout phenotype to a level comparable with the control for expression of both the wild-type protein and the ALS mutant (Figure 4.3). Thus, the *caz* knockout mitochondrial axonal transport phenotype is a direct consequence of the loss of *caz*. Furthermore, this analysis demonstrated that the ability to rescue this phenotype is not disrupted in the P398L mutation.

4.2.4 The Effect of FUS Ectopic Expression on Mitochondrial Axonal Transport

This analysis was repeated using the FUS containing fly lines *UAS-*FUS^{WT} and *UAS-*FUS^{P525L}. In contrast to the ectopic expression of the *Drosophila* equivalents that were inserted into the same attP site (attP40), the expression of neither of these proteins causes any disruption to the amount of axonal transport of mitochondria (Figure 4.4).

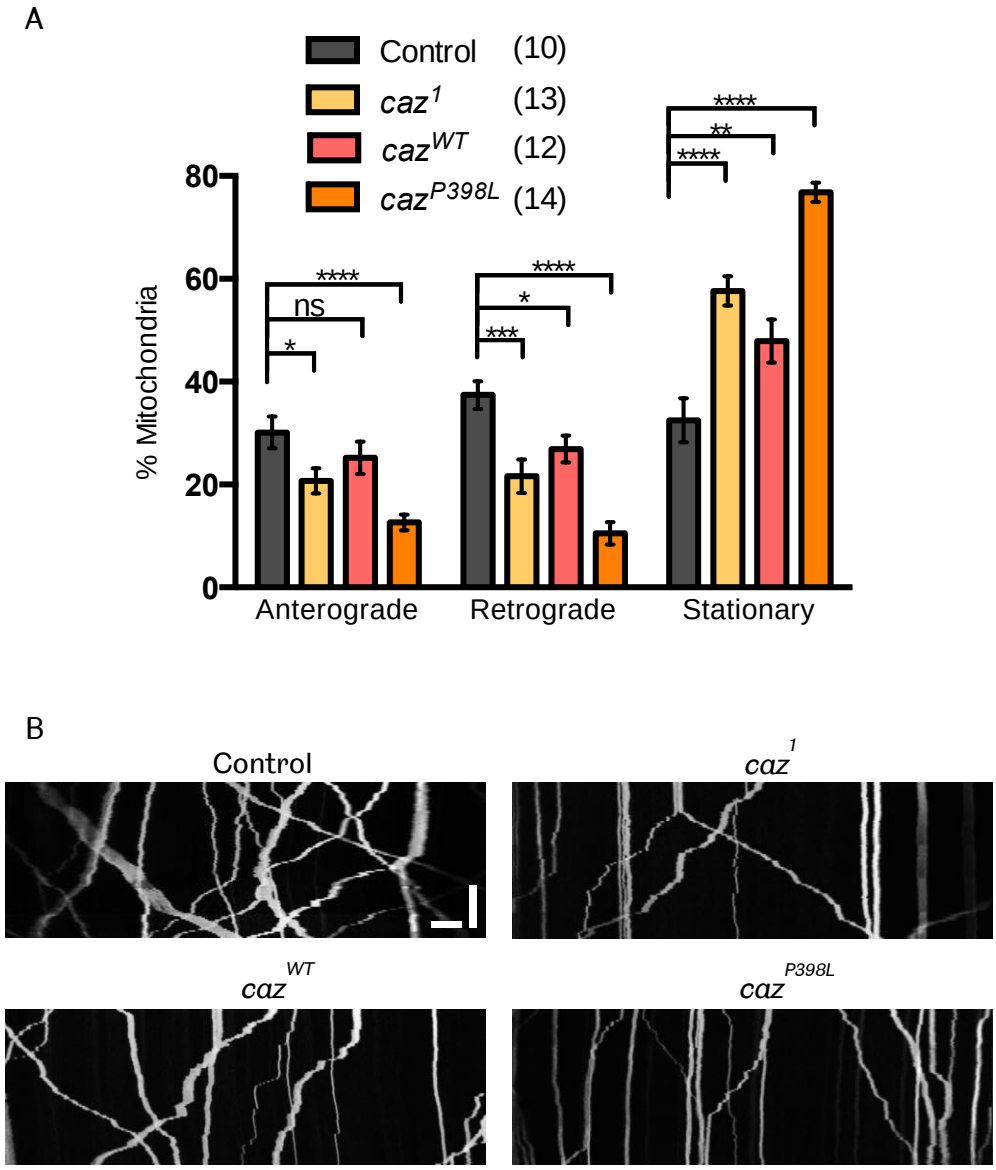

Figure 4.1: The loss of Caz results in severely defective mitochondrial transport, as does the overexpression of Caz^{WT} and Caz^{P398L}. (A) Quantification, the number in brackets indicates number of movies analysed. (B) Representative kymographs of the indicated genotypes. Scale bars: Horizontal (distance) =10 µm, Vertical (time) =125 s. Control = *CCAP-GAL4/+; UAS-mito.GFP/LacZ*. Graph shows mean ± SEM. Statistics calculated using One-way ANOVA with Sidak's multiple comparison test: * $p < 0.05$, ** $p < 0.01$, *** $p < 0.001$, **** $p < 0.0001$.

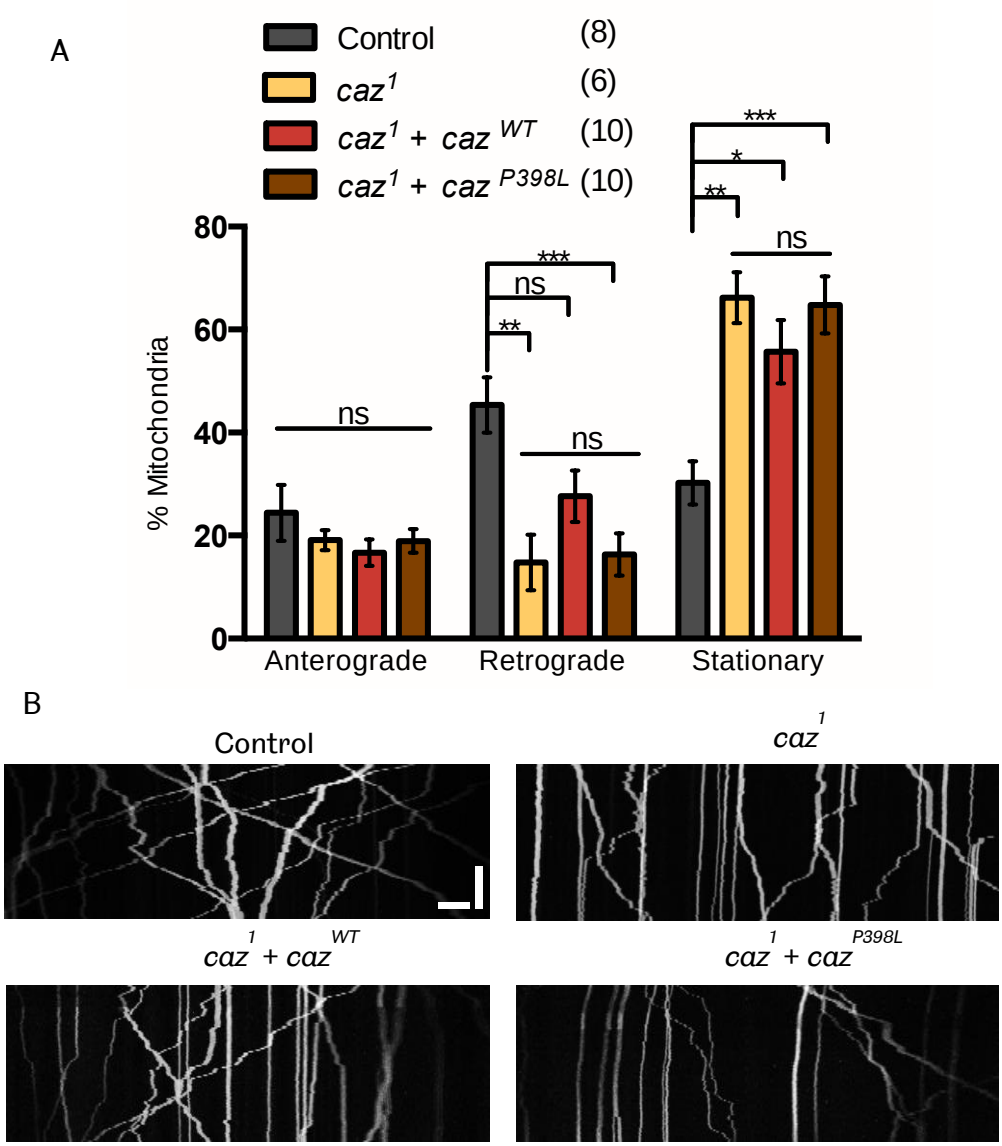

Figure 4.2: The loss of Caz phenotype cannot be rescued by wild type or mutant Caz at 25°C. (A) Quantification, the number in brackets indicates number of movies analysed. (B) Representative kymographs of the indicated genotypes. Scale bars: Horizontal (distance) =10 µm, Vertical (time) =125 s. Control = *CCAP-GAL4/+; UAS-mito.GFP/LacZ*. Graph shows mean ± SEM. Statistics calculated using One-way ANOVA with Sidak's multiple comparison test: * $p < 0.05$, ** $p < 0.01$, *** $p < 0.001$.

4.2.5 Rescue of *caz* Knockout Phenotype with *FUS*

Given that many of the phenotypes arising from the knockout of *caz* can be rescued by the expression of FUS^{WT}, an experiment was carried out to determine whether this was also true for this phenotype of mitochondrial axonal transport deficit. Similarly, the capacity of the ALS linked mutant protein FUS^{P525L} to rescue this phenotype was also examined. Fly lines for this analysis were made in the same manner as for the *Drosophila* homolog rescue experiment.

Larvae were raised at the standard temperature of 25°C. Here, ectopic expression of both of these proteins completely rescued the *caz* knockout phenotype to a level comparable with the control. Thus, in contrast to attempts to rescue with the expression of the Caz proteins at 25°C, this temperature allows for the rescue the *caz* knockout phenotype (Figure 4.5).

4.2.6 Rescue of *TBPH* Knockout Phenotype with *caz*

TDP-43 and FUS as well as their fly homologues have been shown to genetically and physically interact (Ling et al., 2010; Kim et al., 2010; Freibaum et al., 2010; Lanson et al., 2011; Wang et al., 2011), It was also shown by cross-rescue experiments that the viability and lifespan phenotypes of *TBPH* knockout flies could be completely rescued by expression of Caz in neurons and the locomotor phenotype partially rescued. However, the reciprocal cross-rescue attempts did not alter the caz^{1} phenotypes. The authors thus concluded that *caz* and *TBPH* genetically interact with *caz* downstream of *TBPH* (Wang et al., 2011).

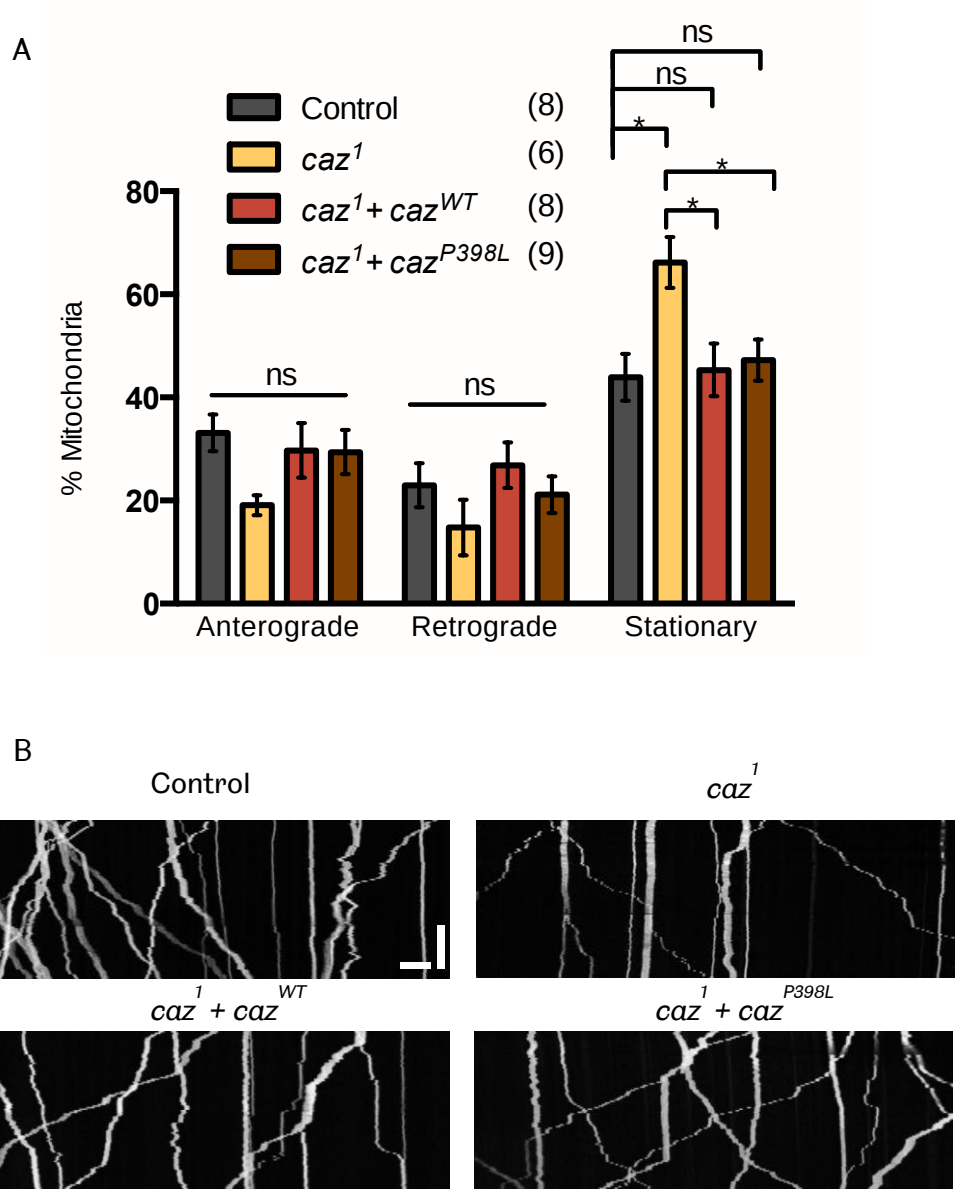

Figure 4.3: Expression of either Caz^{WT} or Caz^{P398L} rescues this transport back to control level at the higher temperature of 29°C. (A) Quantification, the number in brackets indicates number of movies analysed. (B) Representative kymographs of the indicated genotypes. Scale bars: Horizontal (distance) =10 µm, Vertical (time) =125 s. Control = *CCAP-GAL4/+; UAS-mito.GFP/LacZ*. Graph shows mean ± SEM. Statistics calculated using One-way ANOVA with Sidak's multiple comparison test: * $p < 0.05$.

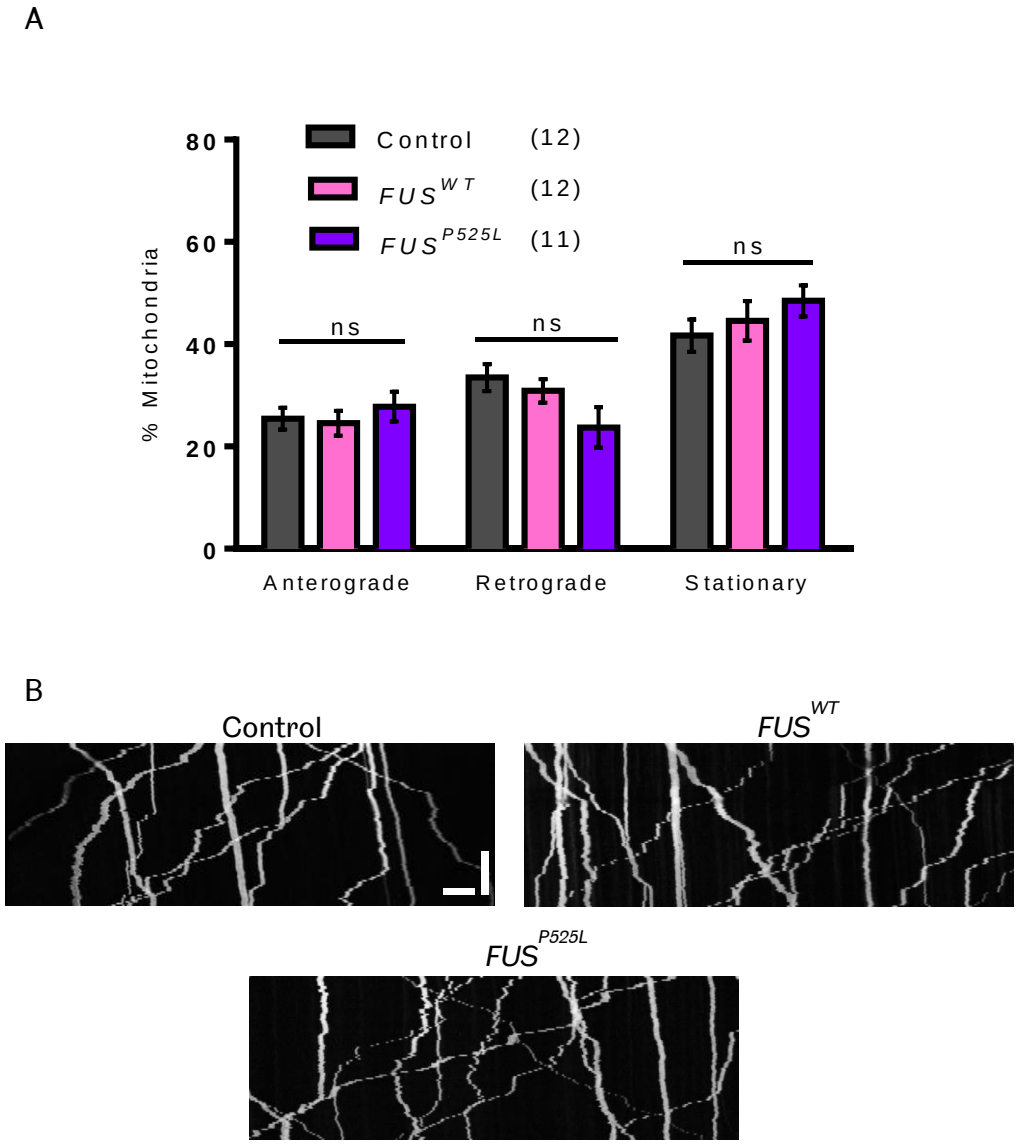

Figure 4.4: Expression of neither of FUS^{WT} or FUS^{P525L} had any effect on axonal transport of mitochondria. (A) Quantification, the number in brackets indicates number of movies analysed. (B) Representative kymographs of the indicated genotypes. Scale bars: Horizontal (distance) =10 µm, Vertical (time) =125 s. Control = *CCAP-GAL4/+; UAS-mito.GFP/LacZ*. Graph shows mean ± SEM. Statistics calculated using One-way ANOVA with Sidak's multiple comparison test.

Given this, an experiment was conducted to rescue the mitochondrial transport phenotype apparent in the *TBPH* knockout fly (see section 3.3.2) with overexpression of Caz^{WT} or Caz^{P398L} at 29°C. However, overexpression of neither was able to significantly rescue this defect, indicating that TBPH and Caz do not interact within a pathway to influence axonal transport of mitochondria (Figure 4.6).

4.3: Vesicle Axonal Transport

4.3.1 The Effect of Loss and Gain of Caz on Vesicle Axonal Transport

To generate *caz* knockout fly lines for the examination of vesicle transport, the *caz^{1}/FM7.GFP* line was crossed with *CCAP-GAL4*; *UAS-NPY-GFP*. To generate the overexpression lines, the *UAS-caz^{WT}* and *UAS-caz^{P398L}* lines were crossed with *CCAP-GAL4*; *UAS-NPY-GFP*.

Here, in a similar manner to the result gained for mitochondrial axonal transport, the loss of *caz* causes a marked increase in the stationary fraction of vesicles. This increase is attributed to a significant decrease in the number of vesicles specifically from the anterograde motile fraction. The ectopic expression of Caz^{WT} and Caz^{P398L} also resulted in significant increase in the stationary fraction of vesicles and a concomitant decrease in the number of vesicles in the anterograde fraction. In line with the assessment of the mitochondrial transport, this was considerably more severe than demonstrated in the knockout genotype (Figure 4.7).

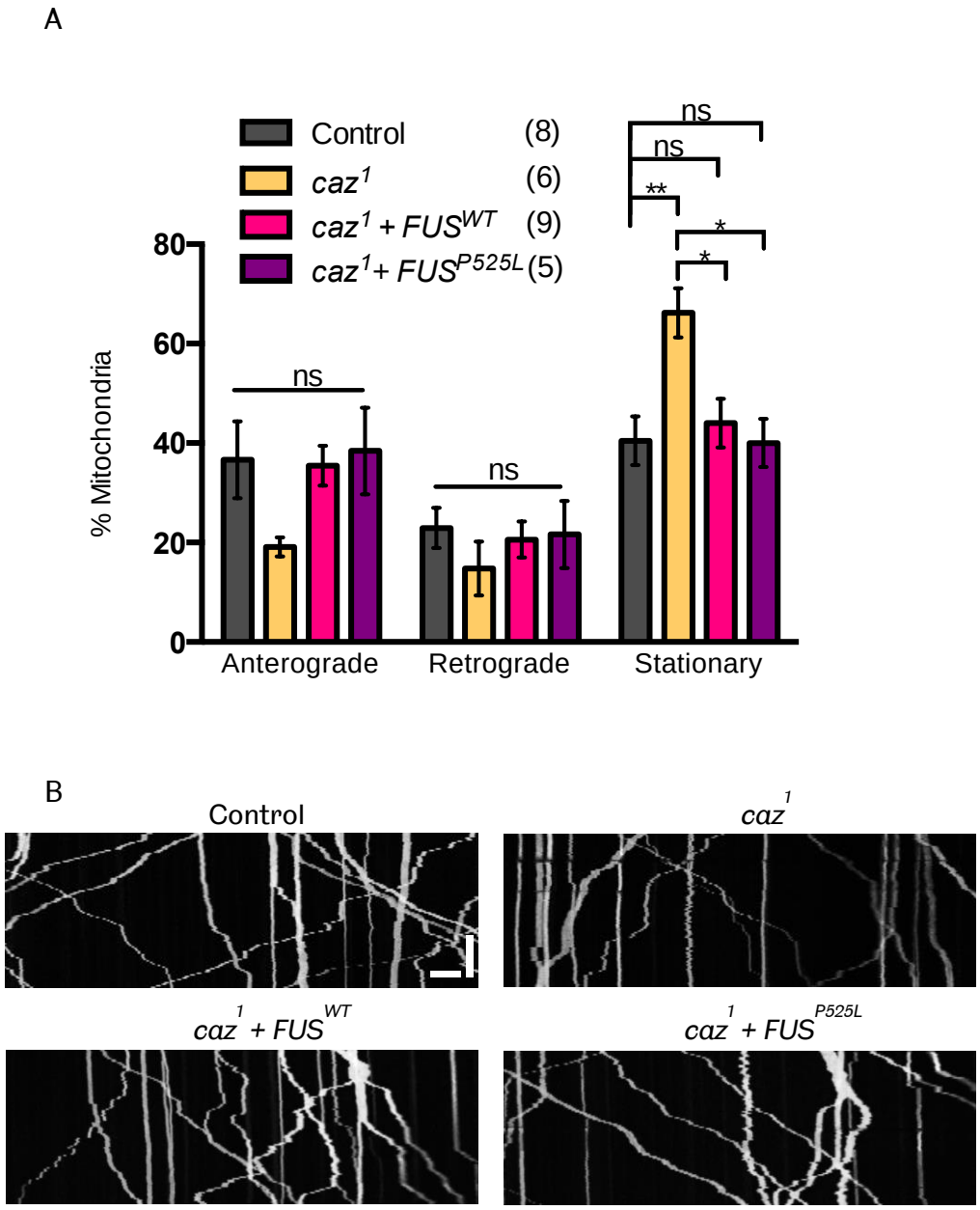

Figure 4.5: Expression of both of FUS^{WT} and FUS^{P525L} can rescue the *caz* knockout phenotype back to a comparable level with the control. (A) Quantification, the number in brackets indicates number of movies analysed. (B) Representative kymographs of the indicated genotypes. Scale bars: Horizontal (distance) =10 µm, Vertical (time) =125 s. Control = *CCAP-GAL4/+; UAS-mito.GFP/LacZ*. Graph shows mean ± SEM. Statistics calculated using One-way ANOVA with Sidak's multiple comparison test: * $p < 0.05$, ** $p < 0.01$.

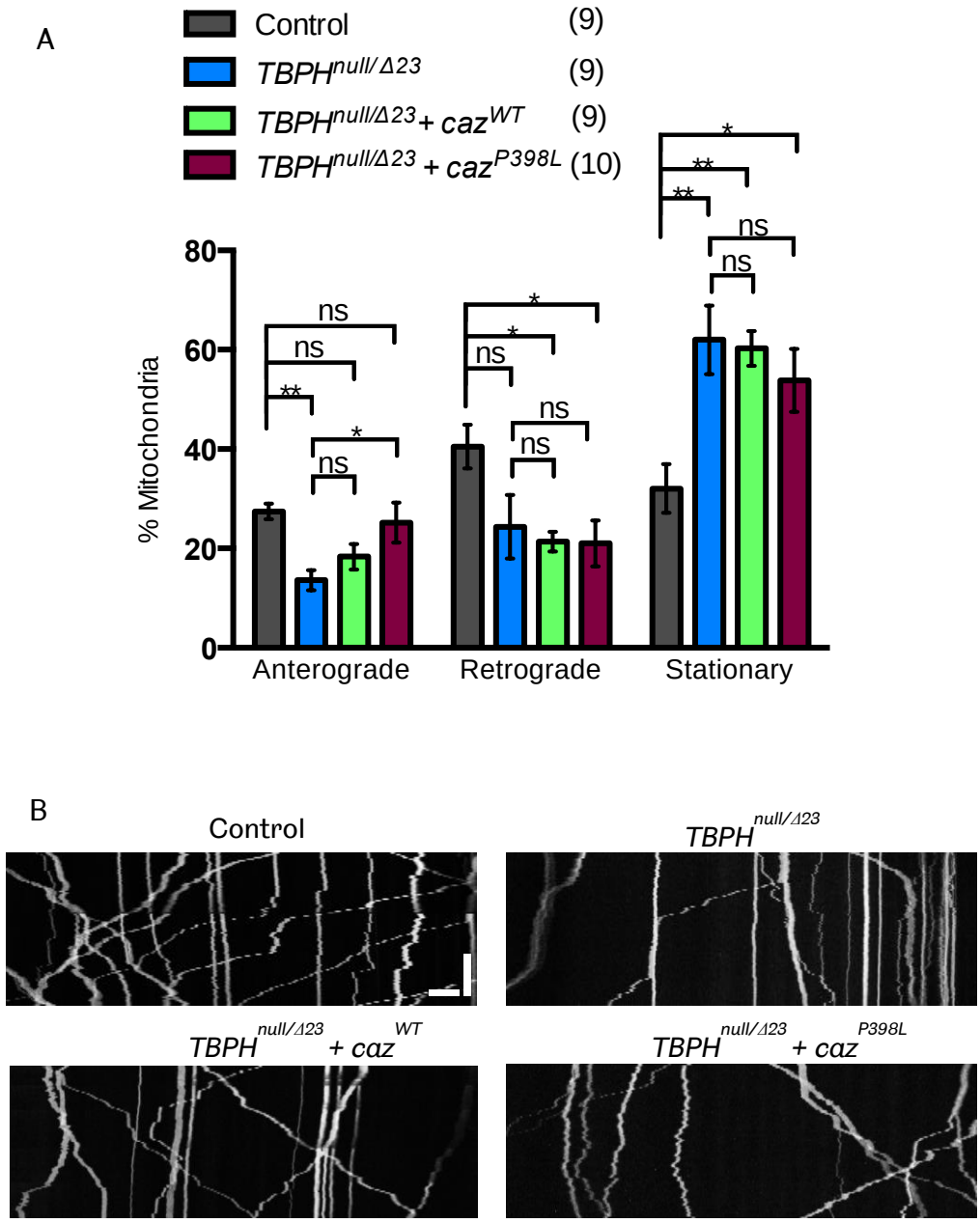

Figure 4.6: Expression of neither Caz^{WT} nor Caz^{P398L} can rescue the axonal transport phenotype arising from the loss of TBPH. (A) Quantification, the number in brackets indicates number of movies analysed. (B) Representative kymographs of the indicated genotypes. Scale bars: Horizontal (distance) =10 µm, Vertical (time) =125 s. Control = *CCAP-GAL4/+; UAS-mito.GFP/LacZ*. Graph shows mean ± SEM. Statistics calculated using One-way ANOVA with Sidak's multiple comparison test: * $p < 0.05$, ** $p < 0.01$.

4.3.2 The Effect of FUS Ectopic Expression on Vesicle Axonal Transport

The transgenes described previously were combined with the *CCAP-GAL4; UAS-NPY-GFP* line to generate larvae bearing one copy of the transgene.

Unlike mitochondrial transport, of which there was no defect in the amount of movement, the expression of both FUS^{WT} and FUS^{P525L} led to an increase in the stationary fraction of vesicles and a decrease in the anterograde moving vesicles (Figure 4.8). Thus, within this system, FUS ectopic expression has a selective negative effect on axonal transport that can be a product of both expression of the wild type protein and an ALS linked mutant, indicating the importance of correct levels of the protein.

4.3.3 Rescue of *caz* Knockout Vesicle Defect with *caz* and *FUS*

As was carried out for the mitochondrial transport disruption demonstrated in the *caz* knockout fly, experiments were also conducted to rescue the vesicle transport deficit. This was attempted with both the wild type and mutant proteins of both fly and human homologs. For this, one copy of each transgene were combined with *UAS-NPY.GFP* and then crossed with caz^{1}*/FM7.GFP; CCAP-GAL4/TM6B*.

The re-expression of Caz^{WT} at 25°C can rescue the stationary fraction of vesicles down to a comparable level with the control and can almost completely rescue the deficit observed in the anterograde fraction. However, the expression of Caz^{P398L} was not able to significantly rescue the increased number of stationary vesicle seen in the caz^{1} larvae, although it was able to partially rescue the level of anterograde moving vesicles to a level that was not significantly different from the control score but that was also not significantly different from caz^{1} (Figure 4.9). This could thus be considered a partial rescue.

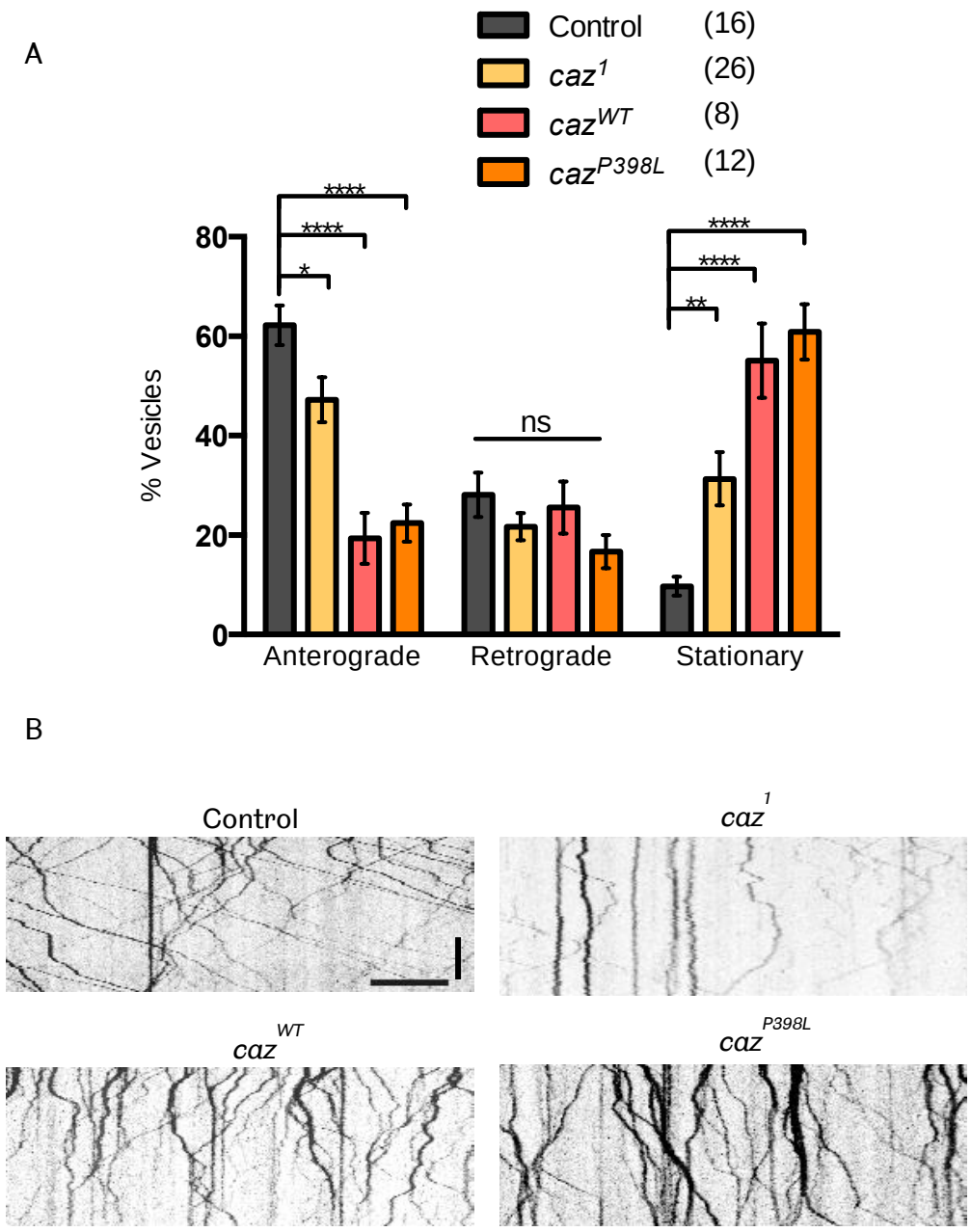

Figure 4.7: The loss of Caz results in a significantly increased percentage of stationary vesicles with the decrease in motility from the anterograde fraction. The result is similar with the expression of Caz^{WT} and Caz^{P398L} (A) Quantification, the number in brackets indicates number of movies analysed. (B) Representative kymographs of the indicated genotypes. Scale bars: Horizontal (distance) =10µm, Vertical (time) =12.5 s. Control = *CCAP-GAL4/+; UAS-NPY-GFP/LacZ*. Graph shows mean ± SEM. Statistics calculated using One-way ANOVA with Sidak's multiple comparison test: * $p < 0.05$, ** $p < 0.01$, **** $p < 0.0001$.

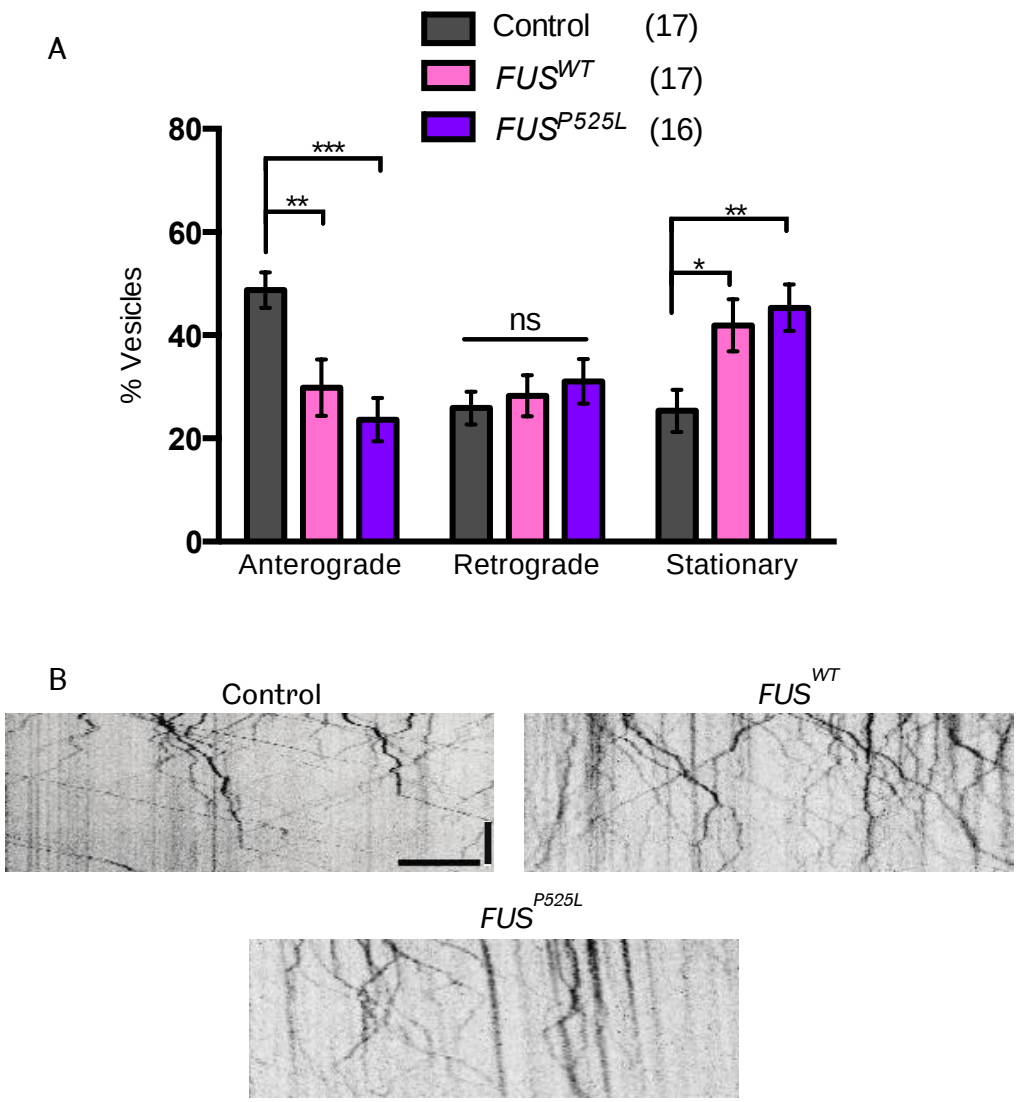

Figure 4.8: Expression of wild-type FUS or ALS mutant FUS^{P525L} causes an increase in the stationary fraction of vesicles with a decrease in the anterograde fraction of motile vesicles. (A) Quantification, the number in brackets indicates number of movies analysed. (B) Representative kymographs of the indicated genotypes. Scale bars: Horizontal (distance) =10µm, Vertical (time) =12.5 s. Control = *CCAP-GAL4/+ ; UAS-NPY-GFP/LacZ*. Graph shows mean ± SEM. Statistics calculated using One-way ANOVA with Sidak's multiple comparison test: * $p < 0.05$, ** $p < 0.01$, *** $p < 0.001$.

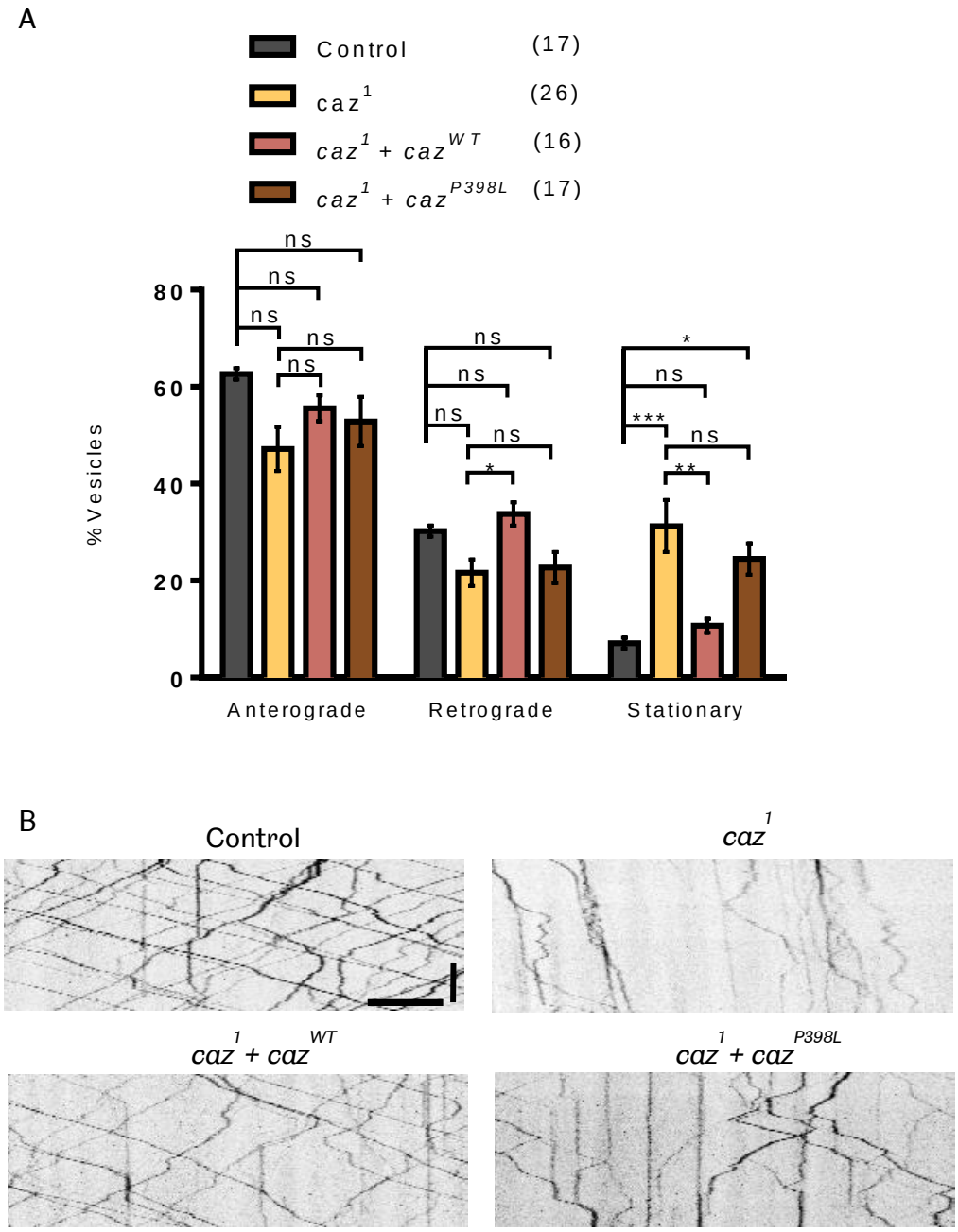

Figure 4.9: The vesicle transport phenotype arising from the loss of Caz can be rescued by the re-expression of Caz^{WT}; however, this is not the case when the rescue is attempted with Caz^{P398L}. (A) Quantification, the number in brackets indicates number of movies analysed. (B) Representative kymographs of the indicated genotypes. Scale bars: Horizontal (distance) =10µm, Vertical (time) =12.5 s. Control = *CCAP-GAL4/+; UAS-NPY-GFP/LacZ*. Graph shows mean ± SEM. Statistics calculated together with Fig 4.10 (shared control) using One-way ANOVA with Sidak's multiple comparison test: * $p < 0.05$, ** $p < 0.01$, *** $p < 0.001$.

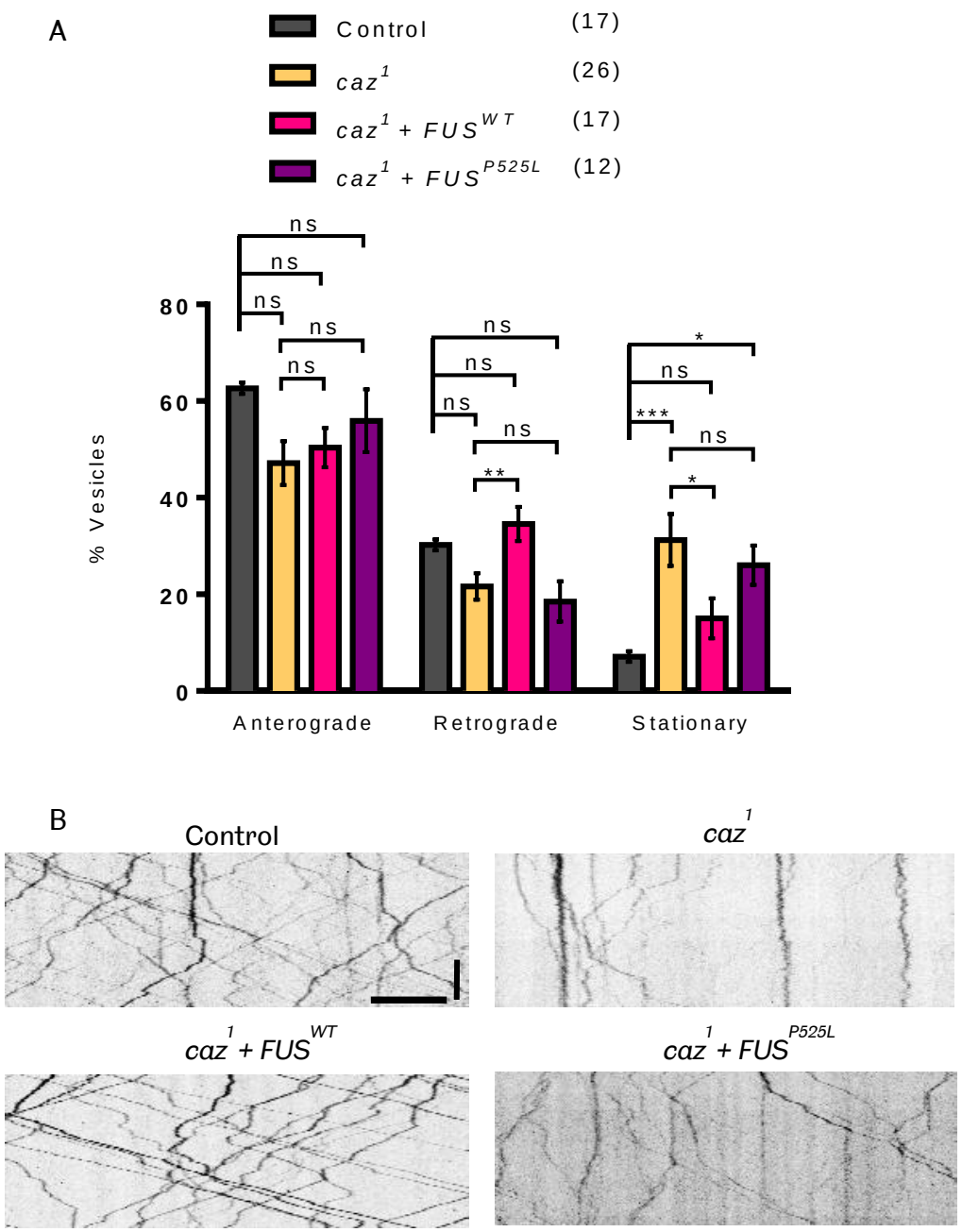

Figure 4.10: The vesicle transport phenotype arising from the loss of Caz can be rescued by the re-expression of FUS^{WT} but not with FUS^{P525L}. (A) Quantification, the number in brackets indicates number of movies analysed. (B) Representative kymographs of the indicated genotypes. Scale bars: Horizontal (distance) =10µm, Vertical (time) =12.5 s. Control = *CCAP-GAL4/+; UAS-NPY-GFP/LacZ*. Graph shows mean ± SEM. Statistics calculated together with Fig 4.9 (shared control) using One-way ANOVA with Sidak's multiple comparison test: * $p < 0.05$, ** $p < 0.01$, *** $p < 0.001$.

The results of the rescue experiments with the FUS transgenes follow this pattern with the wild type protein able to restore the stationary fraction to control level and increase the anterograde fraction to the point of being comparable to the control but not significantly different from *caz*^{1}. In the same way as the fly homolog, FUS^{P525L} was not able to rescue the increased amount of stationary vesicles but did increase the number of anterograde vesicles to a level comparable to the control but not significantly different to *caz*^{1} (Figure 4.10). This too, is characterised as a partial rescue.

4.4: Mitochondria At The NMJ

As with the model of TBPH loss, the number of mitochondria at the NMJ of muscles 6/7 was assessed within the *caz* knockout third instar larvae. Compared to the control, an increased number of mitochondria were apparent at this structure (Figure 4.11). This is likely as a result of the increased stationary amount of the mitochondria.

By comparison, the overexpression of Caz^{WT} and Caz^{P398L} resulted in no significant alteration to the number of mitochondria (Figure 4.12). This was a surprising finding given the effects upon mitochondrial axonal transport scores. Excess levels of Caz may therefore have a different effect on the processes leading on from the increased stationary behaviour of the mitochondria that results in a higher mitochondrial count at the NMJ. FUS^{WT} and FUS^{P525L} were not examined as neither had produced a mitochondrial transport phenotype.

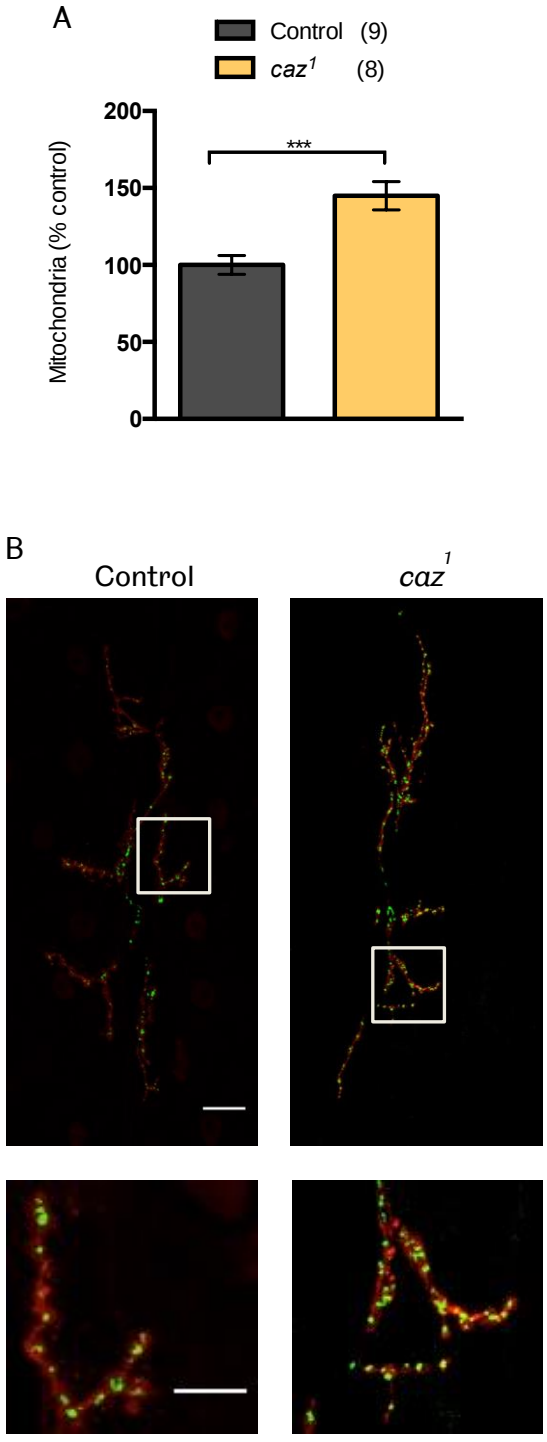

Figure 4.11: Loss of Caz causes an increase in the number of mitochondria at the NMJ. (A) Quantification, the number in brackets indicates number of images analysed. (B) Representative images. Red = HRP, Green = mito.GFP. Scale bar = 20 μm (full), 10 μm (crop). Control = *D42-GAL4>UAS-mito.GFP.* Graph shows mean ± SEM. Statistics calculated using Student's *t*-test (*** $p < 0.001$).

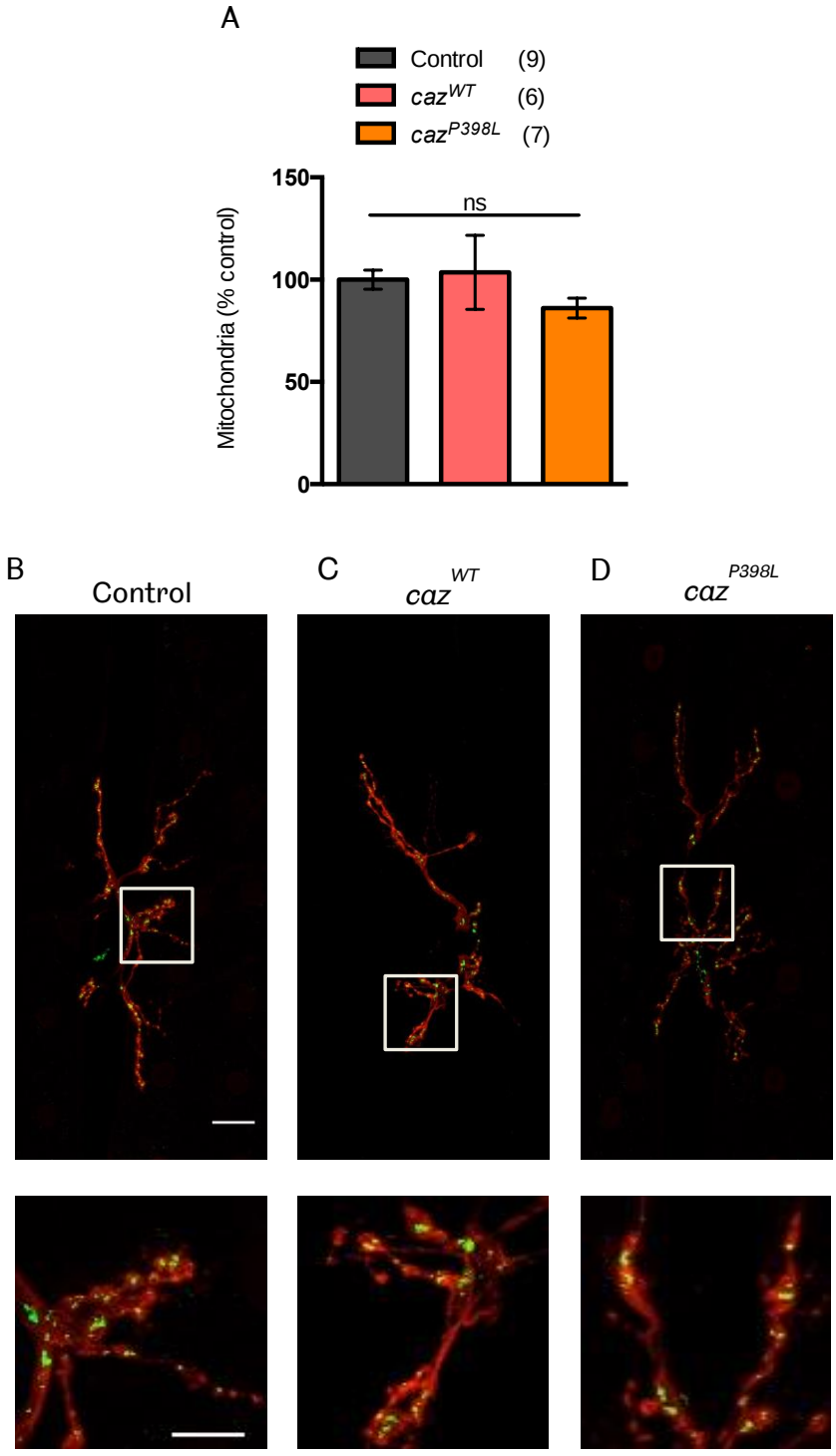

Figure 4.12: Overexpression of Caz^{WT} or Caz^{P398L} has no effect on the number of mitochondria at the NMJ. (A) Quantification, the number in brackets indicates number of images analysed. (B) Representative images. Red = HRP, Green = mito.GFP. Scale bar = 20 µm, 10 µm (crop). Control = *D42-GAL4> UAS-mito.GFP.* Graph shows mean ± SEM. Statistics calculated using One-way ANOVA with Sidak's multiple comparison test.

4.5: Behavioural Analysis of Caz Loss

4.5.1 Viability

In the original characterisation of the *caz*^{1} mutants, it was reported that only 14% successfully eclosed with the main lethal phase occurring between the third instar stage and late pupation (Wang et al., 2011). A comparable level of eclosion was demonstrated in this study with an average of 13% of mutant larvae eclosing (Figure 4.13).

Attempts were made to rescue this sub-viability phenotype by re-expressing the wild type protein with the motor neuron driver *D42-GAL4*. This resulted in an almost complete rescue of eclosion (Figure 4.13A). Performing the same rescue with the pan-neuronal driver *elav-GAL4* also resulted in an almost complete rescue with the wild type protein (Figure 4.13B), as was described previously (Wang et al., 2011). A similar outcome was also observed with the expression of the human homolog, although this reaches complete rescue (Figure 4.13C&D). Both of these drivers were also used to drive expression of caz^{P398L} and the FUS^{P525L}. Here, both resulted in an almost complete rescue of eclosion with both patterns of expression, demonstrating functional conservation between homologs and within the mutant protein.

4.5.2 Larval Locomotion

As in the study of TDP-43, the locomotor capacity of the *caz* genetic models were examined to determine if is a relationship exists between motor ability and axonal transport defects.

caz knockout third instar larvae demonstrate a severe larval crawling deficiency and over a 3–fold increase in time taken to self-right (Figure 4.14). These phenotypes are also directly linked to the loss of Caz as both

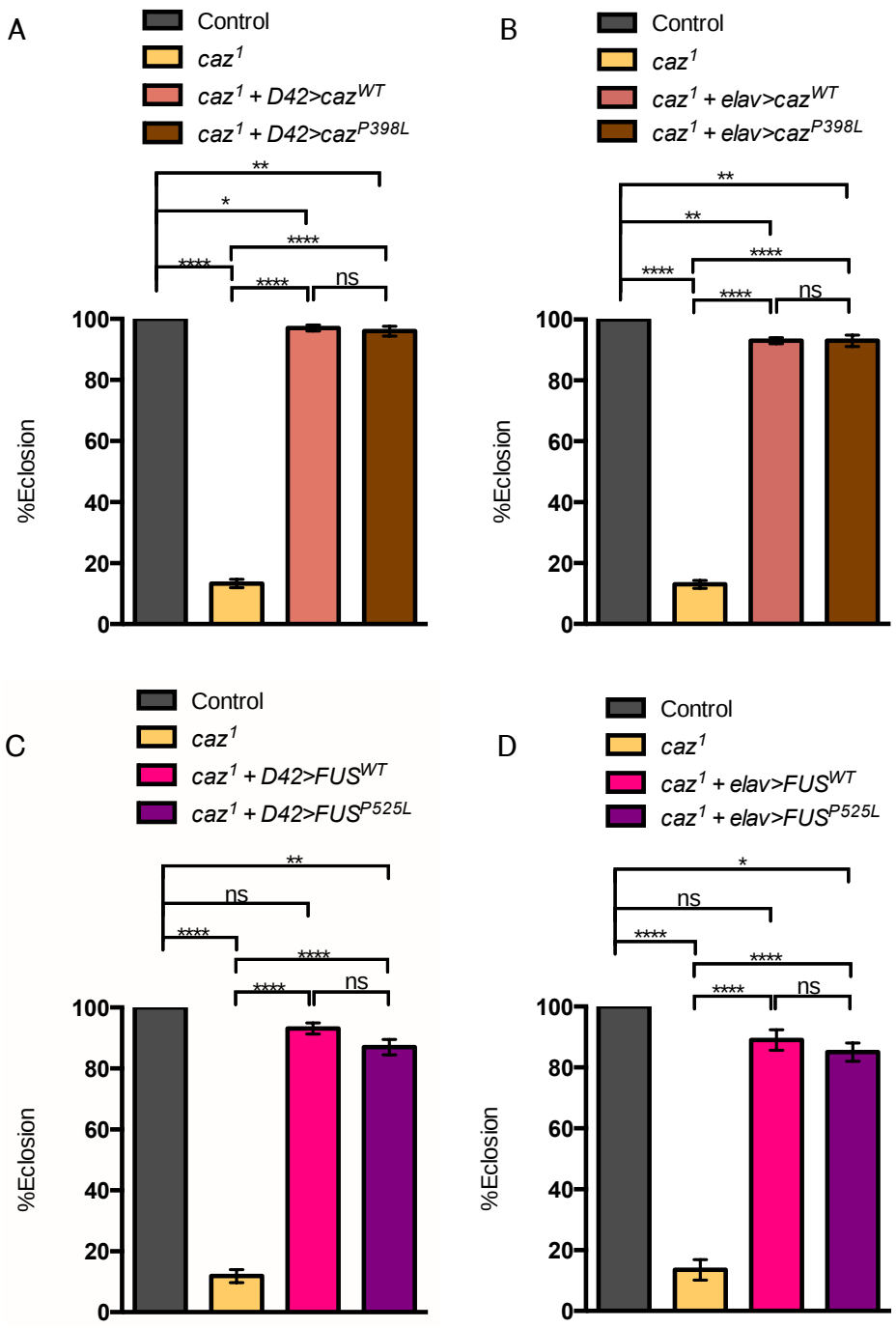

Figure 4.13: Loss of Caz causes a severe reduction in viability as measured by eclosion. This defect can be almost completely rescued by the expression of Caz^{WT} or Caz^{P398L} driven by either (A) *D42>GAL4* or (B) *elav>GAL4*. (C) *D42>GAL4* driven expression of FUS^{WT} but not FUS^{P525L} can completely rescue this phenotype, as can (D) expression of these proteins with *elav>GAL4*. N= 4. Total number of animals = 100. Control = *D42>LacZ* (A/C), *elav>LacZ* (B/D). Graph shows mean ± SEM. Statistics calculated using One-way ANOVA with Sidak's multiple comparison test: * $p < 0.05$, ** $p < 0.01$, **** $p < 0.0001$.

can be completely rescued by the re-expression of Caz^{WT} within motor neurons via the use of *D42-GAL4*. In addition both can also be completely rescued by the expression of Caz^{P398L} demonstrating this functional ability is conserved in the mutant protein (Figure 4.14A&B)

Rescue with *FUS* transgenes were also attempted for these larval locomotion phenotypes. Motor neuronal expression of FUS^{WT} resulted in an almost complete rescue of the phenotypes, as did this expression of ALS linked mutant FUS^{P525L} again suggesting conservation of this function not only within the human homolog but also within the human mutant protein (Figure 4.15A&B).

Both of these rescue experiments were also conducted using *elav-GAL4*. As expected, expression of both Caz proteins resulted in a complete rescue (Figure 4.14C&D), as did expressing of FUS^{WT} (Figure 4.15C&D). However, expression of the ALS mutant managed only an almost complete rescue that was marginally but significantly less than the wild type protein (Figure 4.15C&D). These data suggest for larval locomotion ability, a comparative difference exists between the fly and human homologs in their capacity to rescue and that the ALS linked protein is not as functionally effective in non-motor neurons.

4.5.3 Adult Locomotion

Rare escaper adult caz^{1} flies have severely compromised walking speed and frequency and climbing ability (Wang et al., 2011). The results in this study further corroborate this in terms of climbing ability, which was non-existent (Figure 4.16).

As was the case with larval locomotion, climbing capacity can be completely rescued by re-expression of the Caz^{WT} or Caz^{P398L} in motor

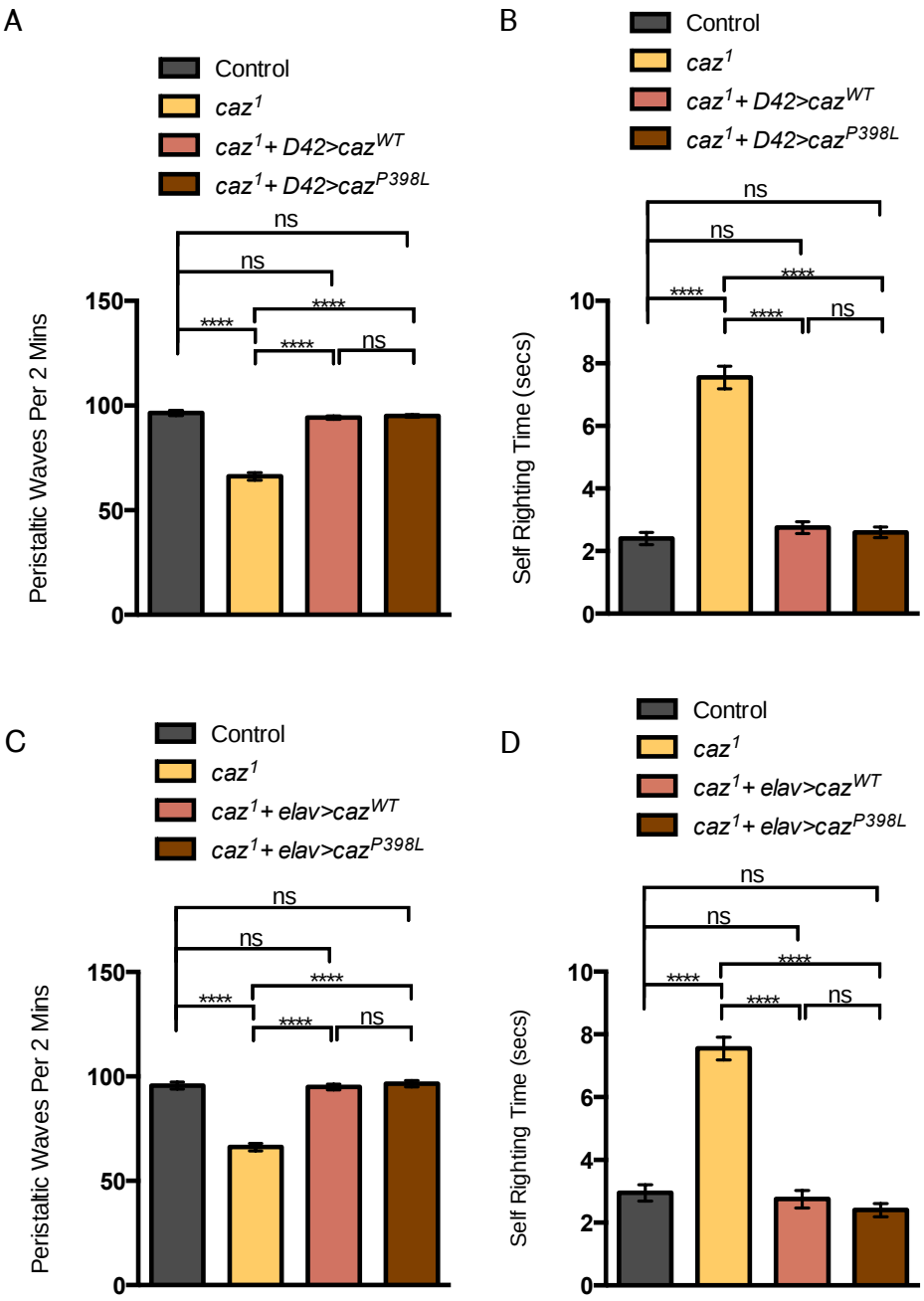

Figure 4.14: Loss of Caz results in severe deficits in larval crawling and turning, which can be completely rescued with (A/B) *D42-GAL4* or (C/D) *elav-GAL4* driven expression of Caz^{WT} or Caz^{P398L}. N= 4. Total number of animals = 20. Control = *D42>LacZ* (A/B), *elav>LacZ* (C/D). Graph shows mean ± SEM. Statistics calculated for (A & Fig 4.15A), (B & Fig4.15B), (C & Fig 4.15C), (D & Fig 4.15D) due to shared control, using One-way ANOVA with Sidak's multiple comparison test: ****p<0.0001.

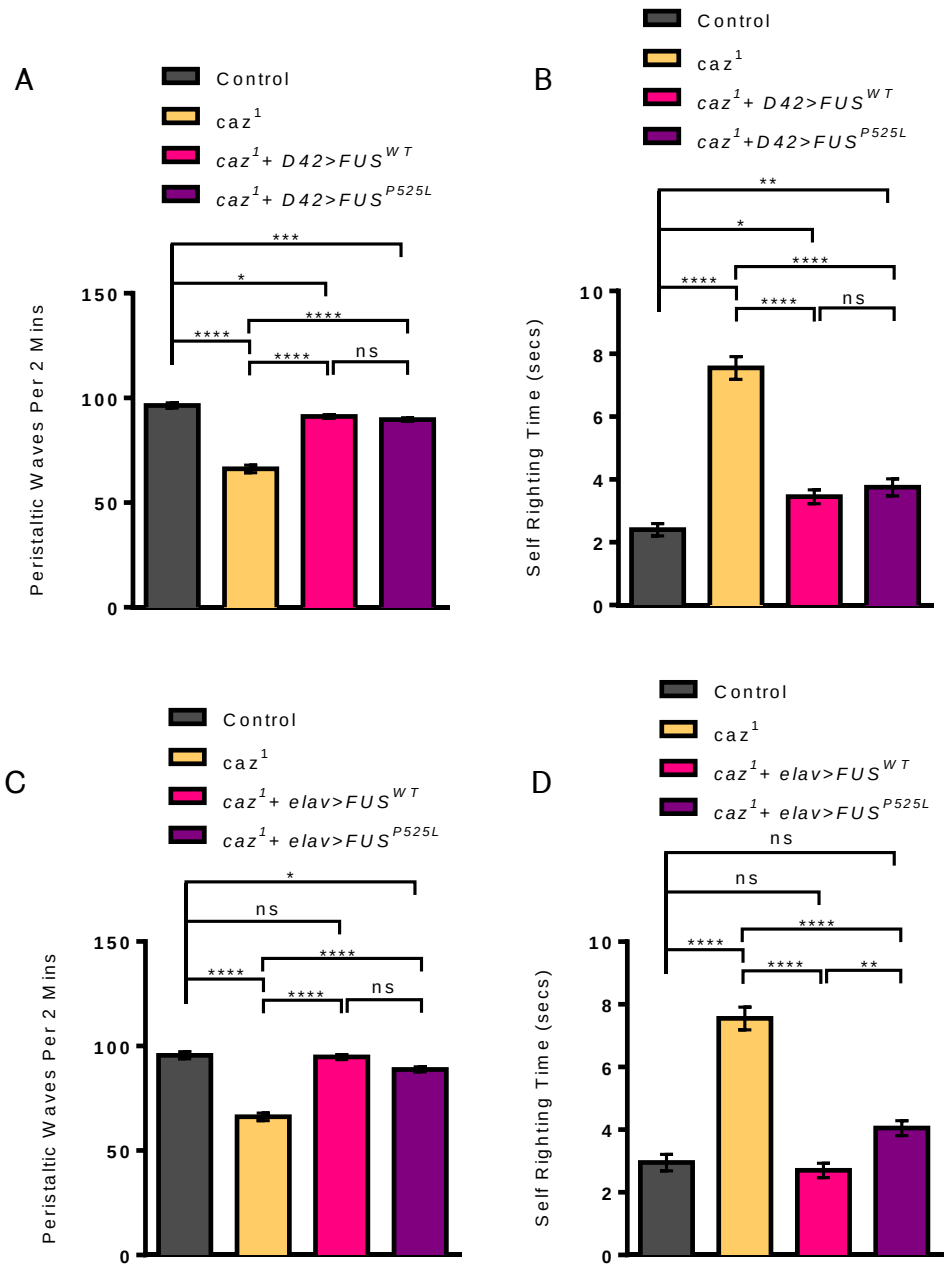

Figure 4.15: Loss of Caz results in severe deficits in larval crawling and turning, which can be almost completely rescued with (A/B) *D42-GAL4* driven expression of FUS^{WT} or FUS^{P525L}. However, when driven with elav>GAL4, expression of FUS^{WT} completely rescued these phenotypes whereas the expression of FUS^{P525L} provided an almost complete rescue. N= 4. Total number of animals = 20. Control = *D42>LacZ* (A/B), *elav>LacZ* (C/D). Graph shows mean ± SEM. Statistics calculated for (A & Fig 4.14A), (B & Fig 4.14B), (C and Fig 4.14C), (D & Fig 4.14D) due to shared control, using One-way ANOVA with Sidak's multiple comparison test: * $p < 0.05$, ** $p < 0.01$, **** $p<0.0001$.

neurons or in all neurons (Figure 4.16A&B). Similarly the human wild type was also capable of fully rescuing this phenotype when expressed in motor neurons or in all neurons (Figure 4.16C&D). However, in line with previous results for walking (Wang et al., 2011), the ALS-linked mutant, though significantly improved on the knockout was still considerably reduced compared to the control in both patterns of expression (Figure 4.16C&D). Therefore, the human mutant appears to have lost the functional ability necessary to fully mediate this motor skill.

4.6: Behavioural Analysis of TBPH Knockout Cross Rescue with Caz

As described previously, *TBPH* knockout phenotypes can be cross-rescued by Caz expression in neurons. To further corroborate this in view of the mitochondrial axonal transport result, eclosion and adult locomotion were assayed. Though here the assessment was made with motor neuronal expression of Caz^{WT} within the *TBPH* knockout background as opposed to pan-neuronally, the results are in agreement that Caz^{WT} can rescue viability (Figure 4.17A). The previous results of walking behaviour showed only a partial rescue, here in regard to climbing behaviour there was a full rescue (Figure 4.17B). Furthermore, both of these measures were also fully restored upon expression of Caz^{P398L} (Figure 4.17A&B).

4.7: Behavioural Analysis of Caz Overexpression and Ectopic Expression of FUS

4.7.1 Viability and Larval Locomotion

Gain of Caz, either wild type or mutant, caused no negative consequence

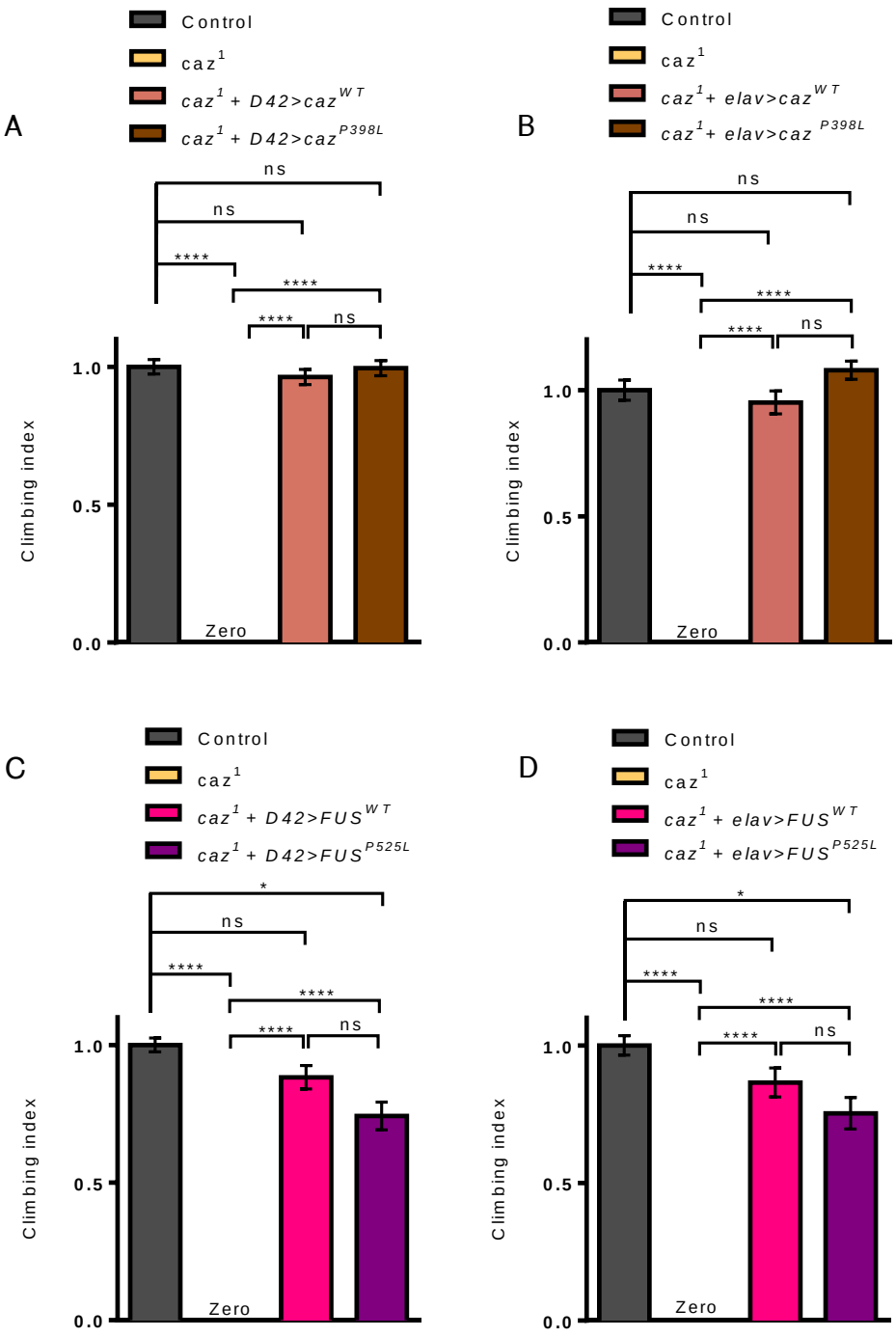

Figure 4.16: Loss of Caz causes a complete ablation of adult climbing ability at day 0, which can be completely rescued by the (A) *D42-GAL4* or (B) *elav-GAL4* driven expression of Caz^{WT} or Caz^{P398L}. Similarly, expression of FUS^{WT} with (C) *D42-GAL4* or (D) *elav-GAL4* can completely rescue this phenotype. Expression of FUS^{P525L} with either driver produced a reasonable level of rescue that was however, significantly lower than the control or the rescue produced with FUS^{WT}. N= 3. Total number of animals = 50. Control = *D42>LacZ* (A/C), *elav>LacZ* (B/D). A-D are normalised to control. Graph shows mean ± SEM. Statistics calculated using Kruskal-Wallis with Dunn's multiple comparison test: * $p < 0.05$, ****$p<0.0001$.

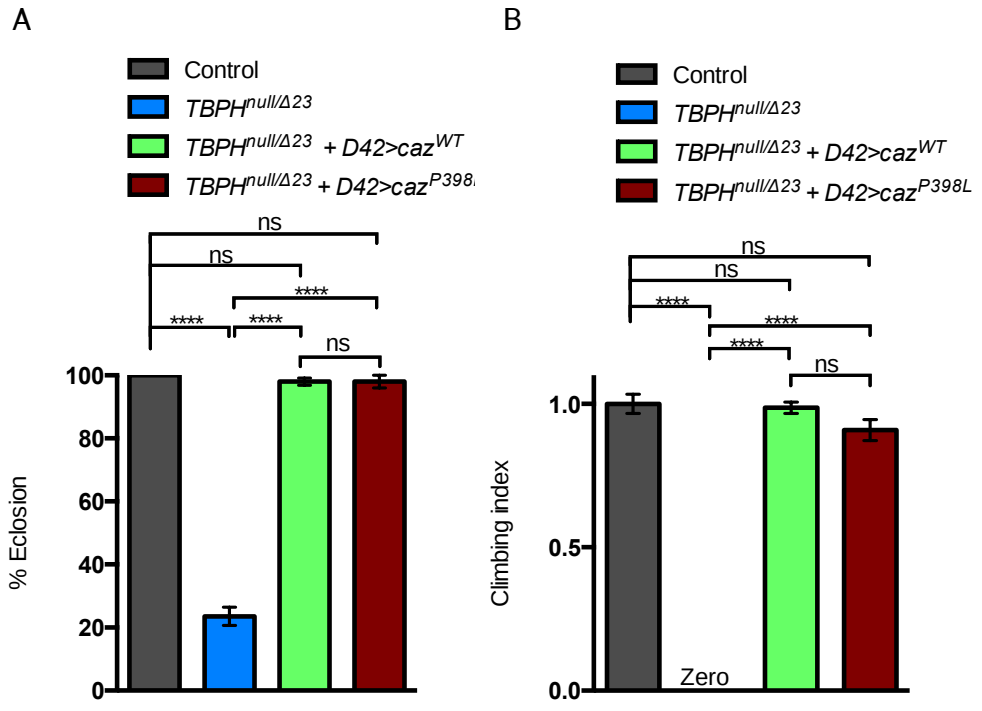

Figure 4.17: Loss of TBPH causes severe eclosion and climbing defects. (A) The eclosion phenotype can be completely rescued by *D42-GAL4* driven expression of either Caz^{WT} or Caz^{P398L}. (B) The non-existent climbing ability of the *TBPH* knockout adults can also completely be rescued by *D42-GAL4* expression of these proteins. N= 4 (A), 3 (B). Total number of animals = 100 (A), 50 (B). Control = *D42>LacZ*. B is normalised to control. Graph shows mean ± SEM. Statistics for A calculated using One-way ANOVA with Sidak's multiple comparison test, for B calculated using Kruskal-Wallis with Dunn's multiple comparison test : ****p<0.0001.

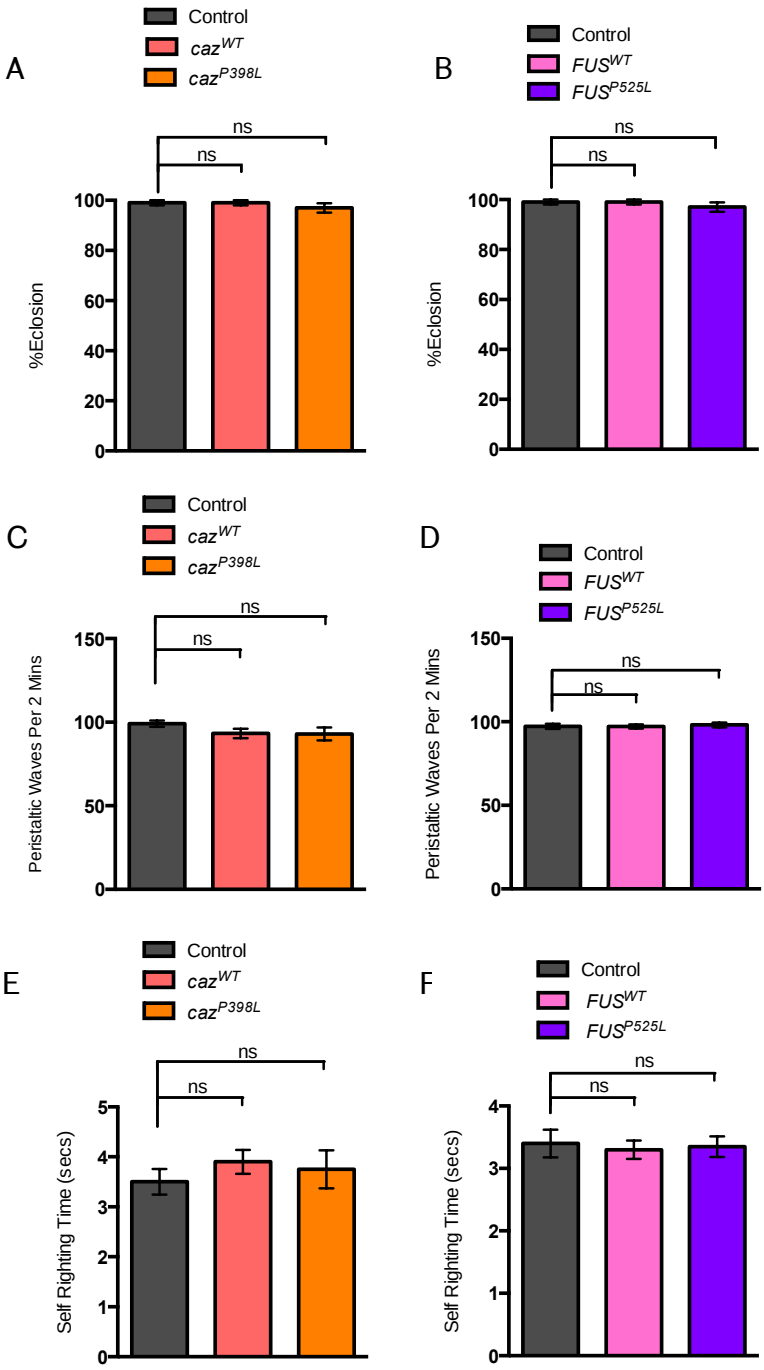

Figure 4.18: *D42-GAL4* driven overexpression of Caz proteins or ectopic expression of FUS proteins has no effect on (A&B) eclosion, (C&D) larval crawling and (E&F) larval turning. N= 4. Total number of animals = 100 (A&B), 20 (C-F). Control = *D42>LacZ* Graph shows mean ± SEM. Statistics calculated using One-way ANOVA with Sidak's multiple comparison test.

on the developmental viability of the flies, with no eclosion defect recorded (Figure 4.18A). This was also the case for ectopic expression of both wild type and mutant FUS (Figure 4.18B). Similarly, overexpression of the *Drosophila* or human proteins, both wild type and mutant, has no effect on larval locomotion phenotypes of crawling and turning (Figure 4.18C-F).

4.7.2 Adult Locomotion

Young adult flies expressing the Caz proteins were examined for climbing ability at age 0-3. Caz^{P398L} expressing flies exhibited no change in this locomotion, however a significant decrease was recorded for Caz^{WT} (Figure 4.19A). This represents an anomalous result and was not present when the flies were assayed again at day 10. These flies were aged through to 30 days at which point both *D42>caz*^{WT} and *D42>caz*^{P398L} flies had large reductions in climbing capacity, which had been progressively declining since significantly diverging from that of the control at day 20 (Figure 4.19B&E). By comparison, at day 0, pan neuronal expression of Caz^{WT} and Caz^{P398L} led to no alterations to climbing (Figure 4.19C), however again by day 30 this activity had reduced significantly (Figure 4.19D) although at a slightly later time point than when expressed in motor neurons alone (Figure 4.19F). These data suggest excessive levels of Caz exert an age-related and progressively detrimental effect to neuromuscular function.

In the same vein, the ectopic expression of FUS proteins was also assayed. In motor neurons, these proteins exerted no effect on climbing ability in young flies at day 0 (Figure 4.20A), however, at day 30 the *D42>FUS*^{P525L} flies were significantly impaired whereas those expressing the wild type protein were not (Figure 4.20B&F). Pan-neuronal expression also revealed that whilst neither FUS^{WT} nor FUS^{P525L} have any negative effect in young flies (Figure 4.20C), aged FUS^{P525L} expressing flies are significantly

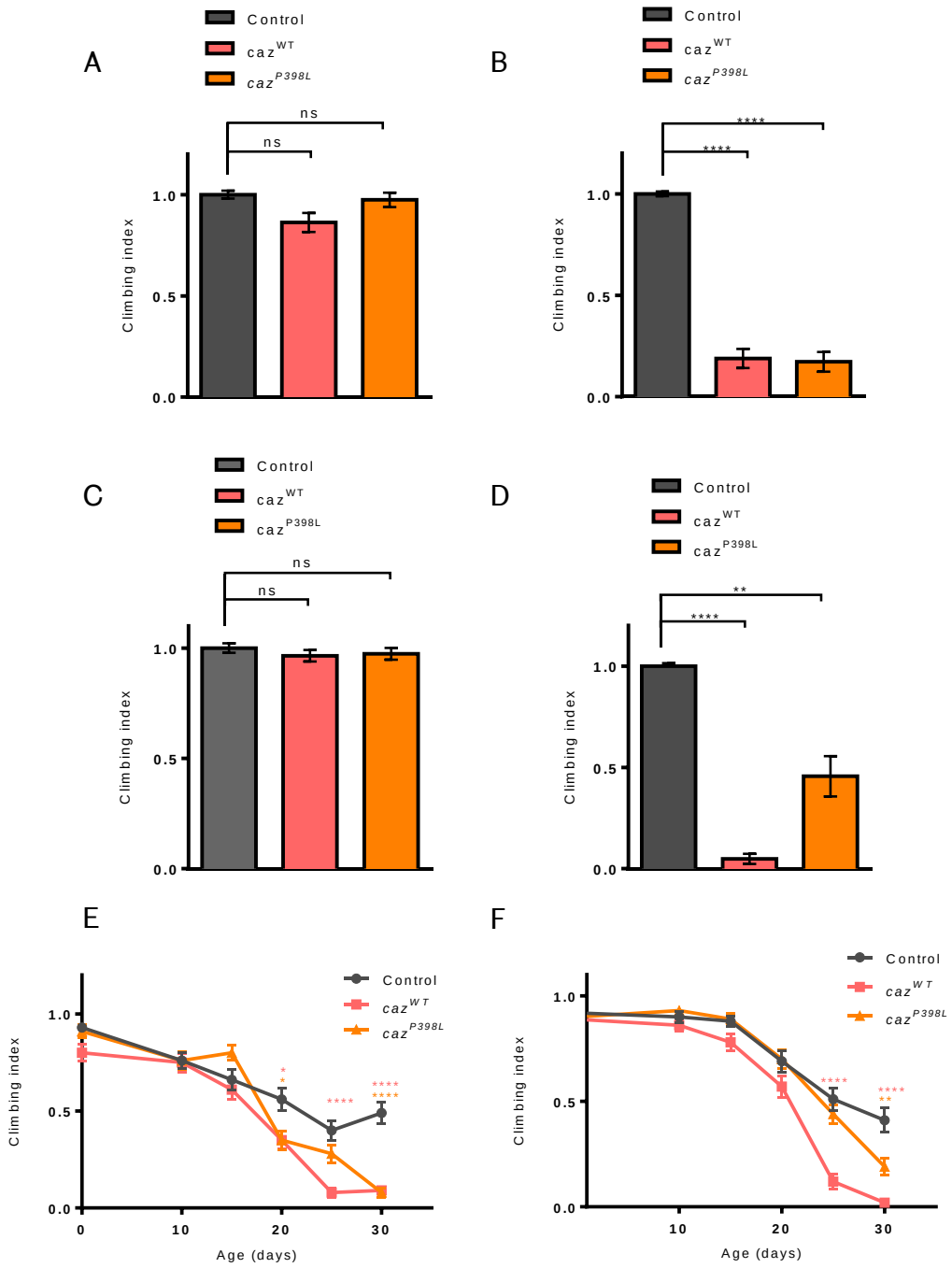

Figure 4.19: Climbing ability of Caz^{WT} and Caz^{P398L} expression flies declines with age. (A) *D42-GAL4* driven expression of Caz^{WT} leads to a moderate decrease in climbing capacity at day 0 that is not apparent at day 10. (B) However by day 30, both *D42>caz^{WT}* and *D42>caz^{P398L}* flies demonstrate decline in this locomotion. (C) Expression of neither protein with *elav-GAL4* causes a deficit in this activity at day 0, (D) however by day 30, a significant reduction in this is seen. Climbing ability through time driven by (E) *D42-GAL4* and (F) *elav-GAL4*. N= 3. Total number of animals = 50. Control = *D42>LacZ* (A/B/E), *elav>LacZ* (C/D/F). A-D are normalised to control. Graph shows mean ± SEM. Statistics calculated using Kruskal-Wallis with Dunn's multiple comparison test * $p < 0.05$, ***p*< 0.01, *****p*<0.0001.

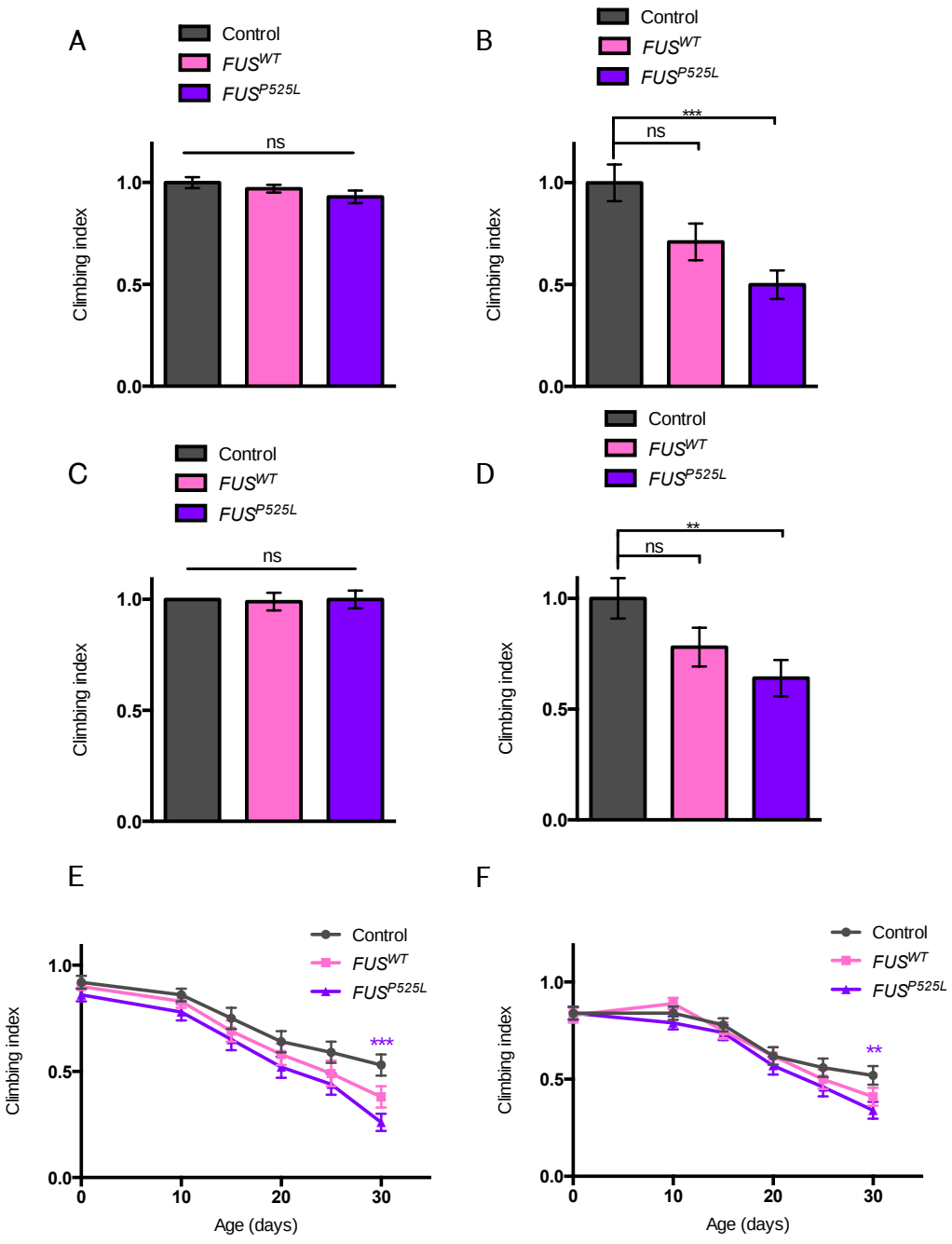

Figure 4.20: Climbing ability of FUS^{P525L} flies declines with age. (A) *D42-GAL4* driven expression of FUS^{WT} and FUS^{P525L} has no effect on climbing ability of young flies at day 0, (B) however in aged flies at day 30, flies expression FUS^{P525L} demonstrate a significant reduction in this ability. These results were mirrored in *elav>FUS^{WT}* and *elav>FUS^{P525L}* flies at (C) day 0 and (D) day 30. Climbing ability through time driven by (E) *D42-GAL4* and (F) *elav-GAL4*. N= 3. Total number of animals = 50. Control = *D42>LacZ* (A/B/E), *elav>LacZ* (C/D/F). A-D are normalised to control. Graph shows mean ± SEM. Statistics calculated using Kruskal-Wallis with Dunn's multiple comparison test: **p< 0.01, ***p<0.001.

impaired in their climbing ability (Figure 4.20D&F). Thus, in terms of the human proteins, excessive wild type levels within the central nervous system neurons exerts no negative effect at any time-point examined although this was trending towards significance whereas expression of the ALS-linked protein leads to an age-related and progressive detrimental effect to neuromuscular function.

4.8: Summary

The results for all the Caz and FUS experiments are summarised in Table 4.1. The loss of Caz causes a reduction in the amount of moving mitochondria within the axons of third instar larvae. This defect can be fully rescued by the re-expression of Caz^{WT}, however this does not occur at the standard temperature of 25°C but is apparent at the raised temperature of 29°C suggesting that the level of protein at 25°C was not sufficient for rescue of this phenotype and becomes so due to the higher temperature. The phenotype arising from the loss of Caz can also be completely rescued by the expression of Caz^{P398L} at 29°C, indicating that this mutant protein acts in a similar manner to the wild type protein in terms of this function.

This loss of Caz phenotype can also be completely rescued by both FUS^{WT} and ALS linked mutant FUS^{P525L} which unlike with the *Drosophila* homologs can be achieved at 25°C. These transgenes were subject to site-directed integration and were shown to be expressing at comparable levels (Wang et al., 2011) and thus it is unlikely that this difference represents a variable expression level and is most likely to result from an inherent functionality difference between the fly and human proteins.

caz knockout larvae also demonstrate an increase in the number of mitochondria at the neuromuscular junction, which may arise from the

resultant effects of the increased amount of stationary axonal mitochondria, which may have functional consequences for this structure.

The loss of Caz also results in a severe disruption to the axonal transport of vesicles demonstrating that the disruption to axonal transport attributable to Caz loss of function is not selective, regarding to these two types of cargoes and may represent a broad defect of axonal transport.

The axonal transport defects arising from the loss of Caz correlated with severe reduction in viability, as measured by eclosion, as well as several measures of larval and adult motor ability, and thus may be a contributory factor to these phenotypes.

The viability phenotype can be almost completely rescued by the expression of wild type and mutant Caz proteins in both motor neurons only and in all neurons highlighting the neuronal requirements for Caz expression for developmental viability and also the possibility that extra-neuronal expression is a factor as concluded previously by Wang et al., (2011). In addition, this study confirms these rescue results are also largely mirrored by ectopic expression of the human homologs and therefore show a functional conservation between fly and human and between wild type and mutant proteins in terms of mediating viability.

The reductions in larval crawling and turning can be completely rescued by both Caz proteins and when expressed in either motor neurons or all neurons. The wild type and mutant human homologs however were not as efficient, being able to provide an almost complete rescue in either expression pattern. This again suggests that neuronal expression of these proteins is almost sufficient for rescue of a knockout phenotype but that extra-neuronal expression may also be a factor. However, pan-neuronal expression of FUS^{WT} and FUS^{P525L} also revealed a significant difference in their ability to rescue this phenotype, which was slightly less efficient with

the mutant. Thus, it seems that expression of this protein in extra-motor neurons has a negative impact on the larvae that influences neuromuscular functioning.

The ablation of climbing ability in the *caz* knockout adult flies was also fully rescued by both Caz proteins and FUS^{WT} when expressed with *D42-GAL4* and *elav-GAL4*, however, this was not shared by the human ALS linked protein which gave only a mild rescue and thus represents a functional loss caused by this human ALS linked mutation.

In light of these rescue experiments, consideration of a correlational relationship between axonal transport defects and neuromuscular functioning, is complex. Mitochondrial transport is only rescued by *caz* transgenes at 29 °C whereas these viability and motor behaviour defects can be rescued at 25 °C. This would suggest there is no correlation between this transport defect and viability and locomotor behaviour, The vesicle transport defect however is fully rescued at 25 °C and this fact could be contributing to rescue of the motor behaviours, although this is only partially restored by the mutant protein. However it remains possible that at this young time point the flies demonstrate an ability to cope with the transport defects.

In terms of FUS proteins, mitochondrial transport is rescued at 25 °C with both proteins and vesicle transport is also rescued at 25 °C completely with the wild type and partially with the mutant. Thus, here, rescue of *caz* knockout transport defects correlates with and could contribute to rescue of larval motor behaviours. However, the partial vesicle transport rescue could be contributing to the inability of the human mutant to fully rescue all of these motor functions.

The cross rescue experiments between TBPH and Caz demonstrated that Caz overexpression cannot rescue the mitochondrial transport disruption that occurs as a result of the loss of TBPH. However, Caz variants can

rescue the eclosion and climbing defects observed. Therefore, it appears that TBPH and Caz act separately to influence axonal transport of mitochondria but act within a genetic pathway to influence viability and motor behaviours.

The overexpression of wild type and mutant protein of both fly and human homologs also results in severe disruption to the amount of axonal transport of vesicles. Thus, loss and gain of Caz result in similar effects on axonal transport of this cargo. However expression of neither FUS protein results in a mitochondrial transport phenotype in contrast to Caz and thus overexpression of fly and human homologs can exert differential effects on transport.

The overexpression of Caz proteins however does not cause an alteration to the number of mitochondria at the NMJ unlike with the loss of Caz, the mitochondria are decreased in number despite the similarity in the effect on mitochondrial transport between the conditions. Therefore, it appears that these conditions exert a differential effect on the processes that result from the increased amount of stationary mitochondria.

Interestingly, in this study the axonal transport phenotypes are not correlated with eclosion, larval locomotion or young adult climbing reduction indicating that within young flies, this compromised axonal transport is well tolerated. Aged adult flies expressing Caz proteins and the human ALS linked mutant on the other hand demonstrate a marked reduction in this activity and thus it is possible that the axonal transport phenotypes observed here are contributing in a progressive aged-related manner, to locomotor dysfunction. The situation is slightly different for the human homologs, where the wild type protein exerts no toxic effect on motor behaviours at any time point despite the axonal transport defects, this was however trending downwards and may after further ageing reach significance. The ALS-linked mutant became significantly

affected at a later point than the Caz equivalent and thus overexpression of the human proteins appears to have a slightly milder effect than the fly homologs.

Overall, both loss and gain of caz/FUS levels alters axonal transport of mitochondria and vesicles, which is an interesting finding that bares some correlational relationship with neuromuscular dysfunction and thus may have consequences for ALS pathogenesis.

Table 4.1: Summary of experimental results for FUS. Arrows represent alterations to phenotype: Red = Reduction relative to control, yellow = increase, green = rescue and blue = no change. Thickness of arrow corresponds to strength of effect. Dashed Line = Assay not undertaken. N/A= Assay not applicable.

	Mitochondrial Transport	Mitochondria at NMJ	Vesicle Transport	Eclosion	Larval Motor Ability	Adult Motor Ability (young)	Adult Motor Ability (Aged)
KNOCKOUT							
caz^{1}	↓	↑	↓	↓	↓	↓	N/A
caz^{1} rescue with Caz^{WT}	29C ↑	-----	↑	↑	↑	↑	-----
caz^{1} rescue with Caz^{P398L}	29C ↑	-----	↑	↑	↑	↑	-----
caz^{1} rescue with FUS^{WT}	↑	-----	↑	↑	↑	↑	-----
caz^{1} rescue with FUS^{P525L}	↑	-----	↑	↑	↑	↑	-----
TBPH rescue with caz transgenes	↔	-----	N/A	↑	-----	↑	-----
OVEREXPRESSION							
Caz^{WT}	↓	↔	↓	↔	↔	↔	↓
Caz^{P398L}	↓	↔	↓	↔	↔	↔	↓
FUS^{WT}	↔	-----	↓	↔	↔	↔	↔
FUS^{P525L}	↔	-----	↓	↔	↔	↔	↓

Chapter 5: C9orf72

5.1: Aims and Hypothesis

The third genetic model of ALS to be assessed in this study was *C9orf72*. Once again the aim was to survey the state of axonal transport of mitochondria and vesicles and to examine whether any defects have any correlational effect on the flies' behavioural motor functions as assessed via larval and adult locomotor assays.

It was hypothesised that the expression of a pathogenic number of GGGGCC (G4C2) repeats interferes with axonal transport and contributes to the dying back pattern of degeneration characteristic of a distal axonopathy.

5.2: The Effect of *C9orf72* Expanded G4C2 Repeats on Mitochondrial Transport

There is no *Drosophila* homologue of *C9orf72* and thus knockout studies cannot be carried out in this organism. A previous study carried out by Mizielinska et al., (2014) sought to examine the effect of *C9orf72* repeat expansions in *Drosophila*. To this end, they created pure repeat constructs of a non-pathogenic length of 3 repeats as well as various lengths within the pathogenic range such as 36 repeats. Although this is a low figure especially compared to the size of the expansions common in patients, it is considered within the currently defined pathogenic range. The authors carried out site directed insertion of these pure repeats to ensure comparable expression levels. With 36 repeats they found a moderate level of neurotoxicity in the fly eye when expressed with GMR-GAL4 which also led to severely reduced viability when raised above 27°C. Expression of 36 but not 3 pure repeats in the adults by way of *elav-GeneSwitch* driver also drastically reduces the flies' lifespan.

For the assessment of axonal transport of mitochondria within these models, they were combined with *CCAP-GAL4; UAS-mito.GFP*. As expected, the expression of 3 G4C2 repeats had no effect on mitochondrial transport, however, 36 repeats caused a significant increase in the stationary fraction of mitochondria (Figure 5.1).

The study by Mizielinska and colleagues also sought to separate the possible effects attributable to the expanded RNA and the DPR proteins. To this end, they created RNA only (RO) repeats of various lengths, which were made by inserting stop codons into each of the six reading frames thus inhibiting translation. In addition, they used alternative codons to produce protein only repeats. From their experiments of eye morphology, viability and lifespan they demonstrated that toxicity is attributable to the formation of DPR proteins given that they are absent in the RO flies even up to a repeat length of 288. Furthermore, they established that the neurotoxicity was specifically caused by those DPRs that contain arginine, namely PR (proline-arginine) and GR (glycine-arginine).

Thus, we also sought to understand whether the mitochondrial transport defect observed was an effect specific to the formation of arginine containing DPR proteins from the expanded repeat RNA. Here, expression of RO-36 had no effect on mitochondrial transport whereas PR-36 caused a very high increase in the stationary fraction and concomitant decrease in the motile fraction (Figure 5.1). Therefore it appears that expanded *C9orf72* G4C2 repeats disrupt the axonal transport of mitochondria and that this is attributable to a DPR protein species and is not a consequence of RNA toxicity in this model.

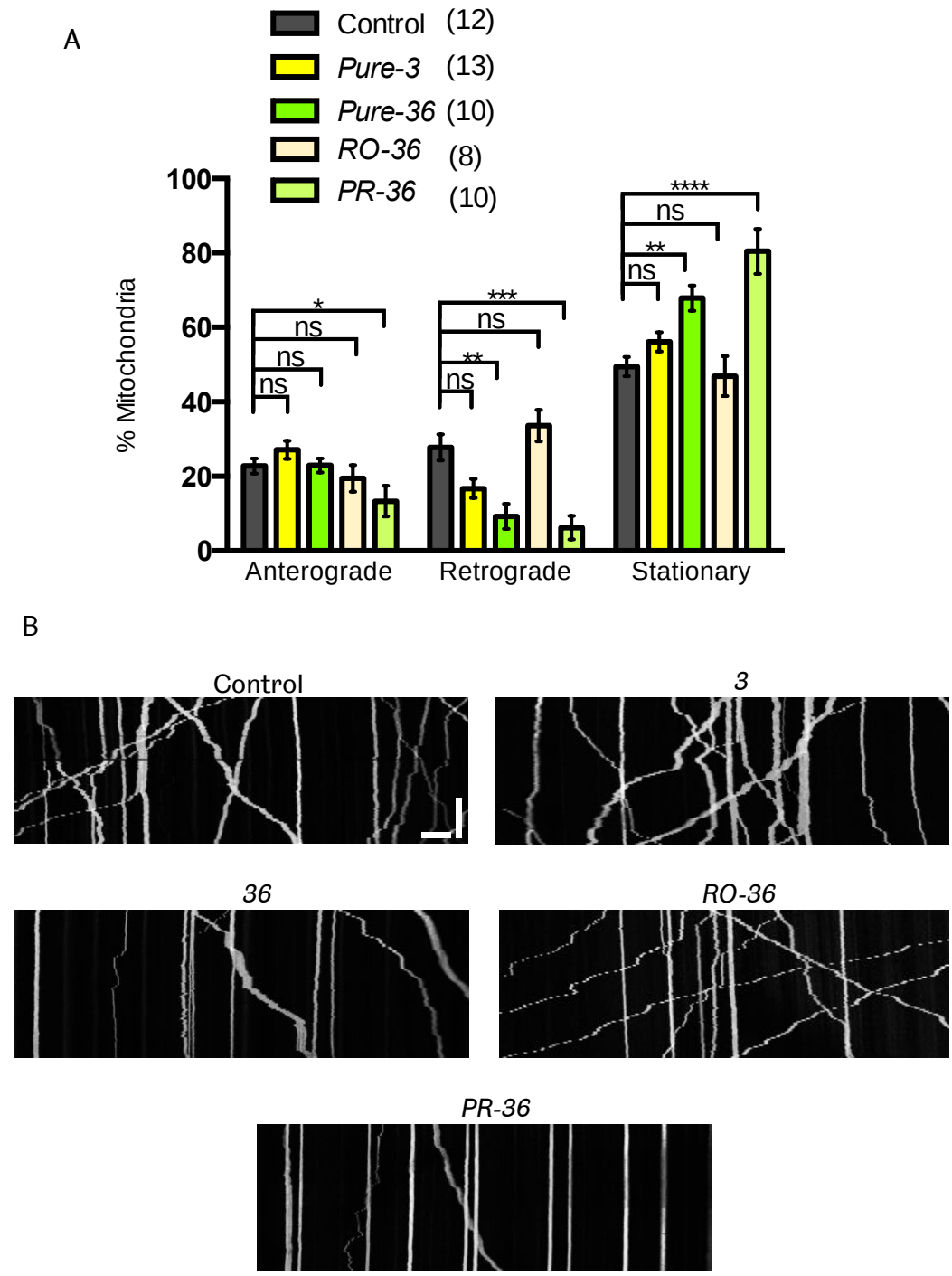

Figure 5.1: The expression of the 36 repeat construct and the PR-36 repeat construct cause a reduction on the level of motile mitochondria within axons. The phenotype is most severe in the PR-36 expressing larvae. By contrast there is no effect with the expression of the 3 repeat construct or the RO-36 construct. (A) Quantification, the number in brackets indicates number of movies analysed. (B) Representative kymographs of the indicated genotypes. Scale bars: Horizontal (distance) =10 µm, Vertical (time) =125 s. Control = *CCAP-GAL4/+; UAS-mito.GFP/LacZ*. Graph shows mean ± SEM. Statistics calculated using One-way ANOVA with Sidak's multiple comparison test: * $p < 0.05$, ** $p < 0.01$, *** $p < 0.001$, **** $p < 0.0001$.

5.3: The Effect of *C9orf72* Expanded G4C2 Repeats on Vesicle Transport

As with the TDP-43 and FUS models, transport of vesicles was also examined in the same manner as mitochondrial transport and each of these lines was combined with *CCAP-GAL4; UAS-NPY-GFP*. Rather unexpectedly, the expression of 3 repeats caused a mild disruption to this vesicle transport, which was only fractionally more severe in the 36 repeat larvae. However, there is no phenotype in the RO-36 condition as expected. Expression of PR-36 led to an extreme imbalance between stationary and motile vesicles (Figure 5.2).

Why a normal number of repeats would lead to this disruption is unknown (see chapter summary) but it is clear that vesicle transport is another function that is affected by an arginine containing DPR species and not by any toxic effect of the expanded RNA.

5.4: Mitochondria at the NMJ

As with the other models wherein mitochondrial transport disruption was recorded, the number of mitochondria at the NMJ of muscles 6/7 was examined. Here, compared to the control, the expression of 3 and 36 repeats was not significantly altered. In contrast, expression of both RO-36 and PR-36 led to a decrease in the number of mitochondria at this structure (Figure 5.3).

5.5: Behavioural Analysis of C9orf72 Expanded G4C2 Repeats

Viability was not formally quantified for these models due to time constraints, although no obvious defects at 25 °C were apparent through observation. However, the locomotor capacity of these models was

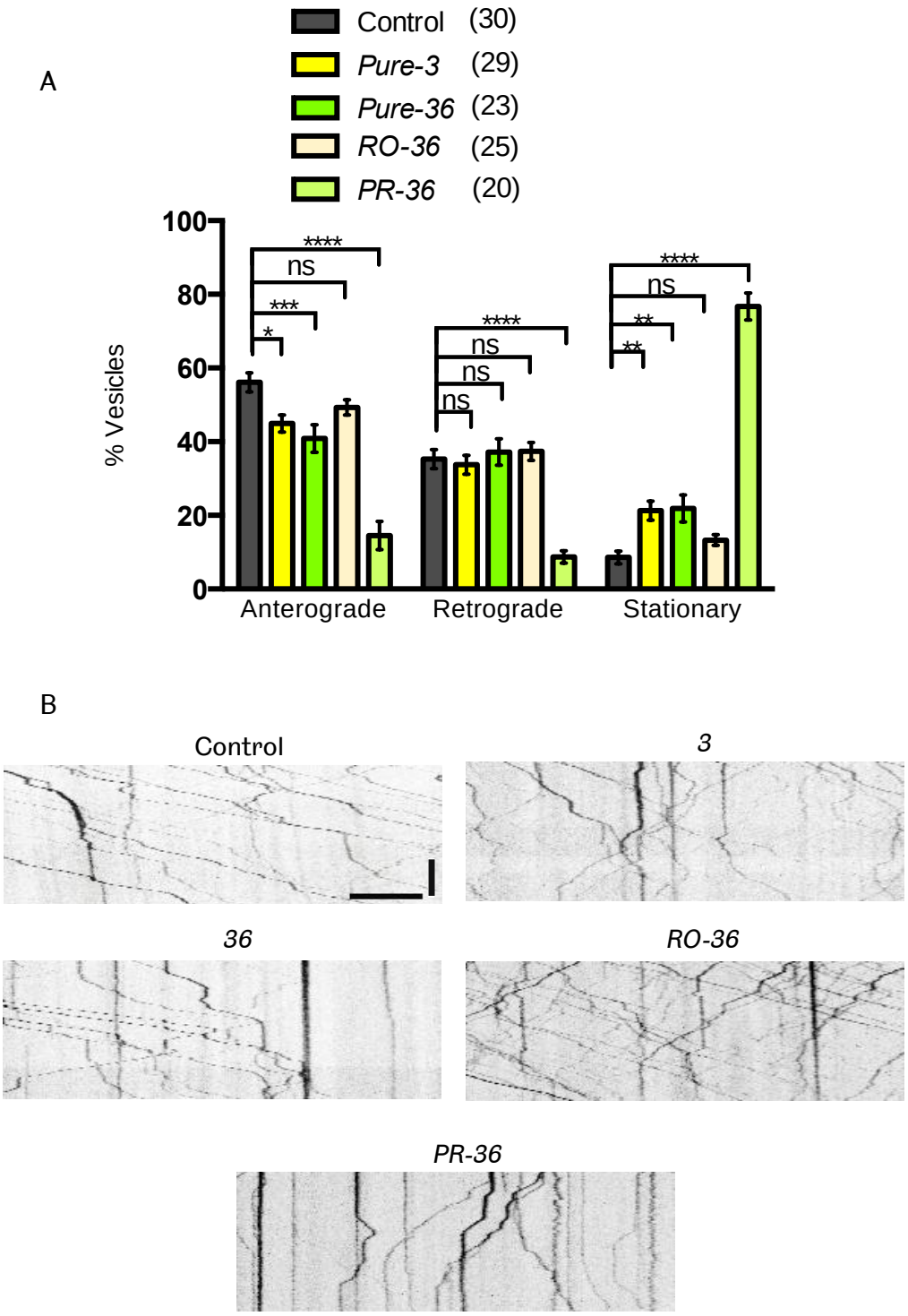

Figure 5.2: An increase in the stationary fraction of vesicles and a decrease in the motile fraction of vesicles is demonstrated in larvae with the expression of the 3, 36 and PR-36 repeat constructs and is not seen with expression of the RO-36 construct. PR-36 causes the most severe disruption. (A) Quantification, the number in brackets indicates number of movies analysed. (B) Representative kymographs of the indicated genotypes. Scale bars: Horizontal (distance) =10 µm, Vertical (time) =12.5 s. Control = *CCAP-GAL4/+; UAS-mito.GFP/LacZ*. Graph shows mean ± SEM. Statistics calculated using One-way ANOVA with Sidak's multiple comparison test: * $p < 0.05$, ** $p < 0.01$, **** $p < 0.0001$.

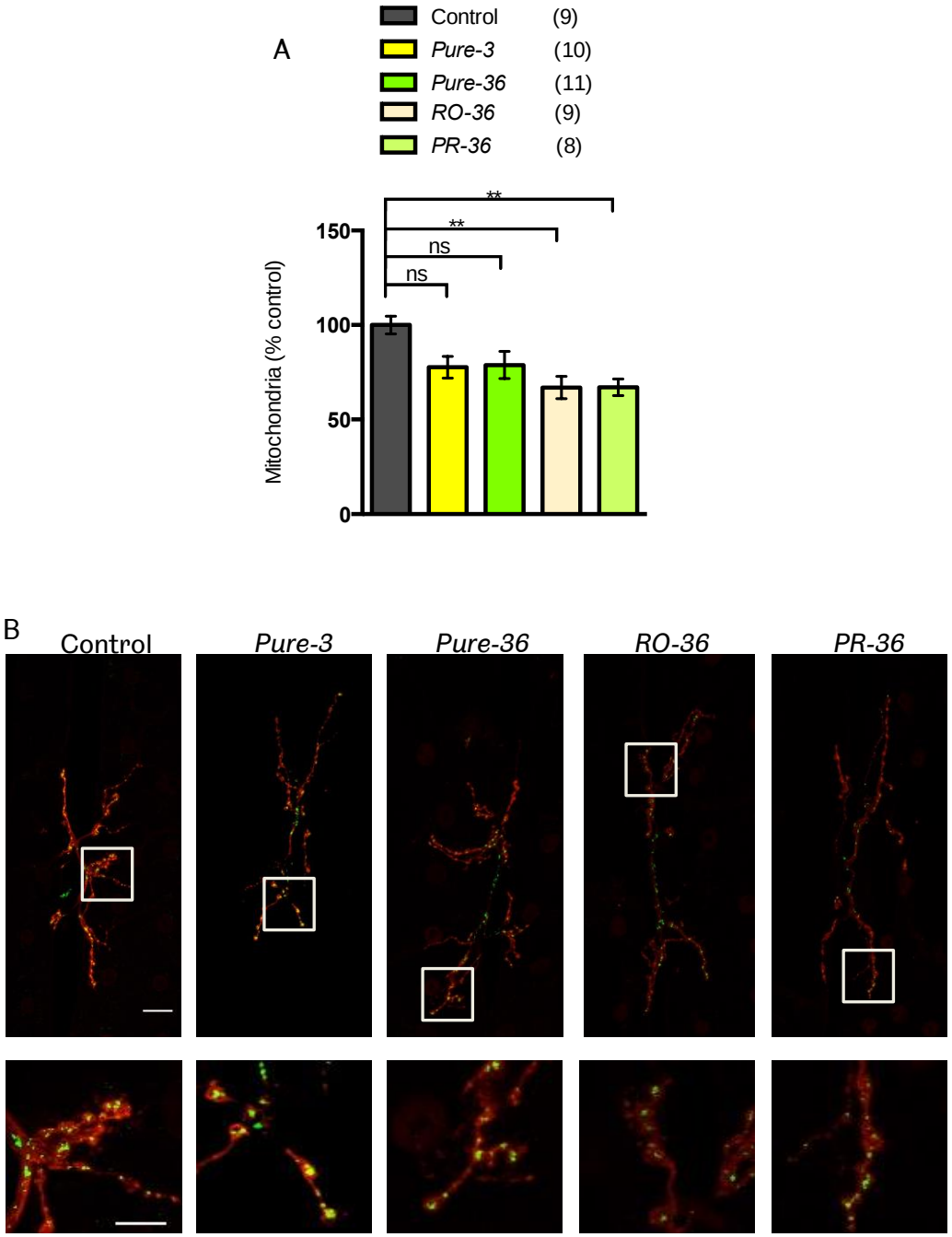

Figure 5.3: Expression of RO-36 or PR-36 results in a significant decrease in the number of mitochondria at the NMJ. (A) Quantification, the number in brackets indicates number of images analysed. (B) Representative images. Red = HRP, Green = mito.GFP. Scale bar = 20 µm (top) , 10 µm (bottom). Control = *D42-GAL4> UAS-mito.GFP.* Graph shows mean ± SEM. Statistics calculated using One-way ANOVA with Sidak's multiple comparison test: $^{**}p < 0.01$.

examined to determine if motor ability correlated with the axonal transport defects. Motor ability was not previously examined in the original study by Mizielinska and colleagues, however, here, in terms of the larval motor behaviour of crawling, only the PR-36 condition led to a significant reduction when expressed by either *D42-GAL4* (Figure 5.4A) or *elav-GAL4* (Figure 5.4B). However, a mild but significant turning defect was apparent in both Pure 36 and PR-36 conditions when expressed with *D42-GAL4*, although this was only seen in the PR-36 condition when expressed with *elav-GAL4.*

In terms of the locomotor ability of the adult flies, again it seems only the expression of PR-36 has any effect, producing a small yet significant reduction in this activity when expressed in motor neurons (Figure 5.5A) or all neurons (Figure 5.5B).

5.6: Summary

The results of all the C9orf72 experiments are summarised in Table 5.1. The expression of a pathogenic number of G4C2 repeats but not a wild type number results in a reduction in the amount of axonal transport of mitochondria. It was further identified that this is not a consequence of the expanded RNA transcript but is rather attributable to the formation of a DPR protein species. Vesicle transport in contrast appears to be affected by expression of both 3 and 36 repeats and may therefore be partly explained as an arbitrary consequence of the insertion of these transgenes within the fly. It is possible that expression of the pure 3 repeats interferes with RNA regulation through acting as short interfering RNAs (siRNAs) that target complementary mRNAs for cleavage and destruction. This possibility may explain the vesicle transport specific nature of the effect of the 3 repeats if those targeted mRNA sequences code for proteins that function specifically in vesicle transport. A question that could be answered with an examination of such mRNA levels.

However, it is clear that the expression of expanded RNA that cannot produce DPR proteins has no effect on this transport whereas the expression of the PR species of DPR protein led to an almost complete ablation of motile vesicles. These findings further demonstrate the phenotypic consequences of the expansion of *C9orf72* hexanucleotide repeats and argue in favour of a toxic role of DPR proteins and against that of a toxic gain of function of the expanded RNA itself.

However, despite the axonal transport phenotypes, neuromuscular functioning appears to be only mildly affected in both larvae and young adults and is confined to the expression of the DPR protein, with the exception of the measure of larval turning which is also significantly affected by the expression of the pure 36 repeat construct. The increased severity of the phenotypes arising from expression of the PR-36 construct is possibly a consequence of the likely relative increase in abundance of this DPR species over the level of toxic DPR species present in the pure 36 construct owing to the dedication of RAN translation to the PR species from the former.

Therefore, it seems that these disruptions to axonal transport are reasonably well tolerated in young flies. Had time allowed, it would have been pertinent to have aged the flies and assessed whether the compromised state of axonal transport bares any correlational relationship to a progressive aged-related decline in neuromuscular function, which would further support a pathogenic role for axonal transport defects.

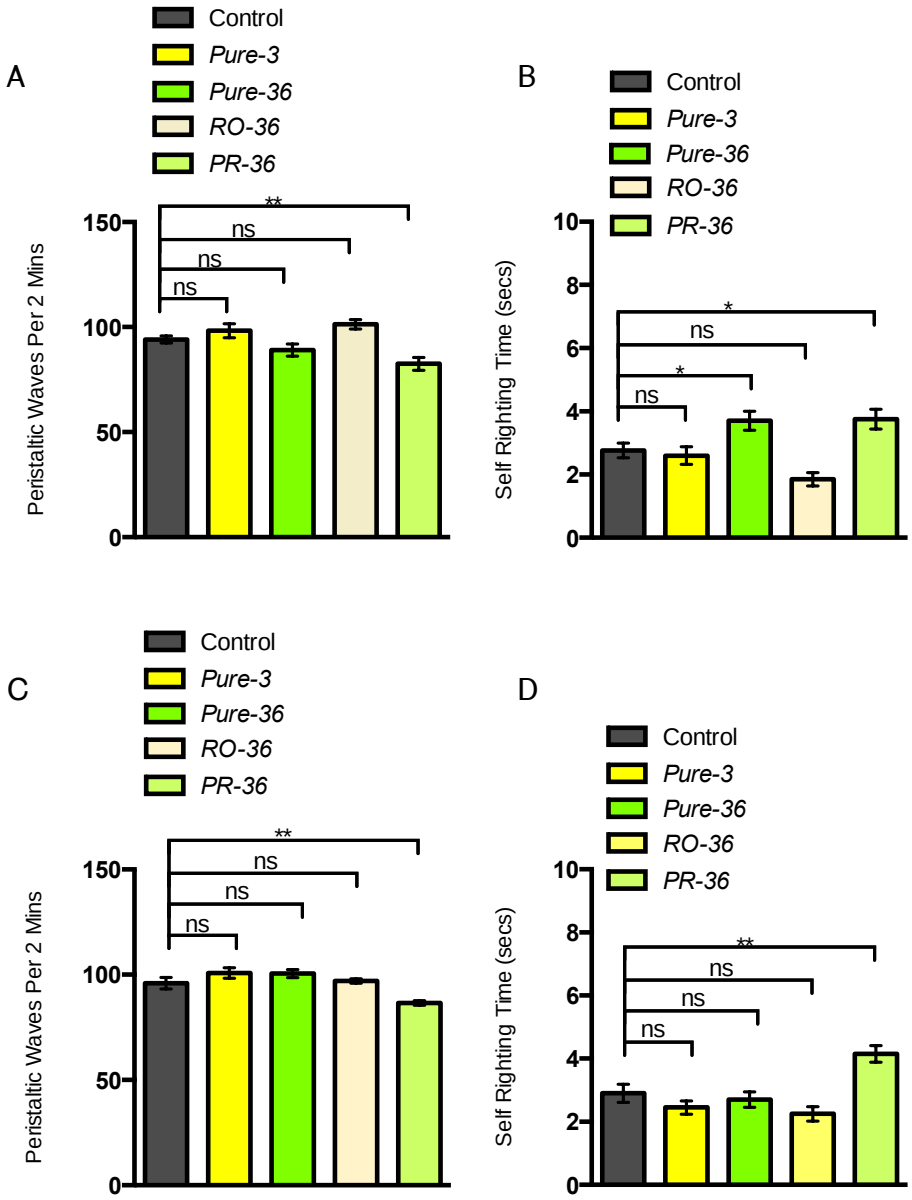

Figure 5.4: Expression of PR-36 causes a significant reduction in (A/C) larval crawling and (B/D) larval turning ability when expressed with either *D42-GAL4* (A/B) or *elav-GAL4* (C/D). N= 4. Total number of animals = 20. Control = *D42>LacZ* (A/B), *elav>LacZ* (C&D). Graph shows mean ± SEM. Statistics calculated using One-way ANOVA with Sidak's multiple comparison test: * $p < 0.05$, **$p<0.01$.

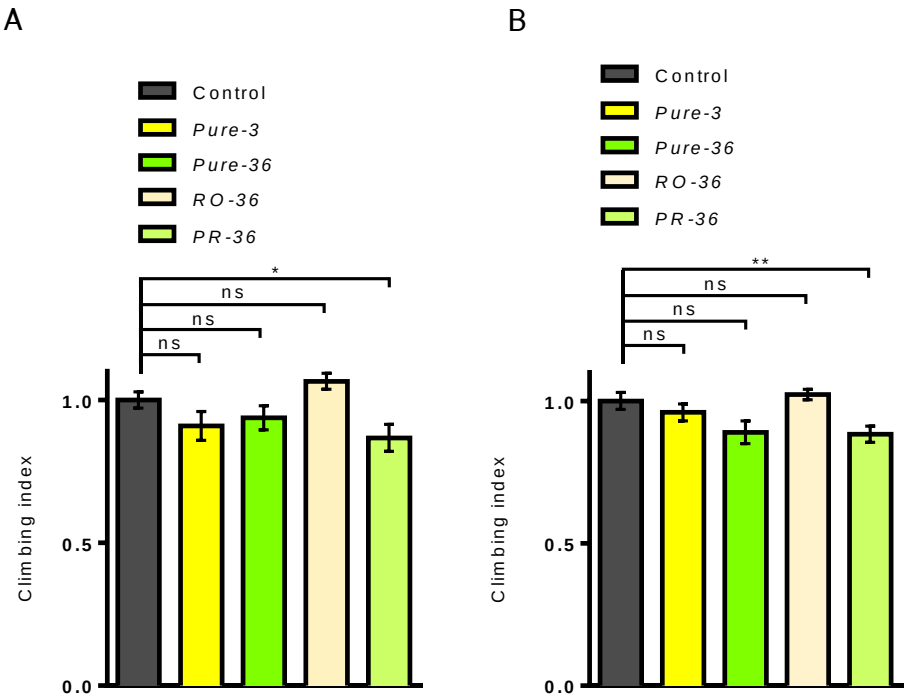

Figure 5.5: Climbing ability assayed at day 0 is significantly reduced by expression of PR-36 driven by (A) *D42-GAL4* or (B) *elav-GAL4*. N= 4. Total number of animals = 50. Control = *D42>LacZ* (A), *elav>LacZ* (B). A-B are normalised to control. Graph shows mean ± SEM. Statistics calculated using Kruskal-Wallis with Dunn's multiple comparison test: * $p < 0.05$, ** $p < 0.01$,

Table 5.1: Summary of experimental results for C9orf72. Arrows represent alterations to phenotype: Red = Reduction relative to control, yellow = increase, green = rescue and blue = no change. Thickness of arrow corresponds to strength of effect. Dashed line = assay not undertaken.

	Mitochondrial Transport	Mitochondria at NMJ	Vesicle Transport	Eclosion	Larval Motor Ability	Adult Motor Ability (young)	Adult Motor Ability (Aged)
Pure 3				-----			-----
Pure 36				-----			------
RO-36				-----			------
PR-36				-----			------

CHAPTER 6: Discussion

6.1: Summary

This study was concerned with examining axonal transport by way of two types of cargo, mitochondria and transport vesicles, in models of three of the major genes linked with ALS, *TARDBP* (TDP-43), *FUS* and *C9orf72*. The relationship between any such defects with viability and motor activity was carried out to determine whether axonal transport dysfunction is a possible contributory factor to neurodegeneration in ALS.

6.2 TDP-43

This study suggests that the loss of endogenous fly TDP-43 (TBPH) leads to a decrease in the transport of mitochondria and that this is a specific consequence of the loss of this protein. This dysfunction correlates with the severely reduced viability phenotype commonly seen in models of TDP-43 loss. The severity of the viability phenotype is striking with only a few rare escapers managing to eclose. It is certainly possible that the axonal transport disturbance in mitochondria within motor neurons is a factor in this lethality. This transport dysfunction also correlated with severe reductions in behavioural measures of neuromuscular function, that is, larval locomotion and adult climbing, and thus is also a possible contributory factor in this decline in locomotor capacity of the larvae and rare escaper adults. The neuromuscular junction is highly dependent on correct distribution and function of mitochondria and this reduced mitochondrial transport raises the possibility there may be an energy deficiency and calcium buffering abnormalities at the neuromuscular junction that impacts on its functioning.

All of the axonal transport and locomotor phenotypes with the exception of climbing behaviour could be rescued by the expression of the fly and human wild type proteins and the known ALS- linked mutant M337V in

motor neurons. This serves as a further indication of a relationship between axonal transport functioning and neuromuscular health. This result also suggests that this mutant acts similarly to the wild type protein in terms of effect on mitochondrial transport, which argues against this as a mechanism through which this mutation confers toxicity in human disease associated with this mutation. This result agrees with the assessment by Alami et al., (2014) made in mouse primary neurons. However, this is in contrast to the results recorded by Wang et al., (2013a) who saw a decrease in transport for this mutant and the wild type protein also in mouse primary neurons, which may be due to experimental differences such as in expression levels. Thus, this situation requires further study.

The lack of complete rescue by any of the transgenes of the adult climbing phenotype was a surprising finding in light of the results of the other behavioural assays. However, there was partial rescue, which was significantly improved on the knockout score. This suggests several possibilities, firstly, that the level of expression in the motor neurons may not be sufficient to give rise to a full rescue. Alternatively, this result may point to the possibility that since climbing is a complex behaviour, extra-motorneuronal expression is necessary to carry out this function at a level comparable to the control. Had time allowed it might have been useful to attempt this rescue with a broader expressing driver such as *elav-GAL4*.

The unaltered transport of vesicles in the condition of TBPH loss as measured in this study was a further intriguing finding. In view of the reduced mitochondrial transport result and the findings of both mitochondrial and vesicular disruption in SOD1 models of ALS (De Vos et al., 2007), it was considered likely that a similar dysfunction would be apparent, forming a hypothesis that loss of TBPH results in a general aberration to axonal transport. However, the lack of a phenotype as least as measured here in terms of motile and stationary fractions, rather

indicates that axonal transport dysfunction in this context is likely to be specific to mitochondria.

This study is limited to a descriptive analysis of axonal transport and has not entered into an examination of a mechanism to explain these findings. However, there are some possibilities to be raised in regards to this. It is clear that the loss of TBPH results in a widespread dysfunction to RNA processing; splicing alterations and up and down regulations of expression levels (Tollervey et al., 2011; Polymenidou et al., 2011), which may lead to a change in axonal transport component availability. RNA target studies (Table 6.1) have shown TDP-43 binds to those of several motor proteins such as KIF13, a kinesin 3 motor involved in vesicle transport (Colombrita et al., 2012) and important adaptor protein kinesin light chain 1 (KLC1) (Xiao et al., 2011).

In view of the mitochondrial specificity of TBPH knockout, it is interesting to note that TDP-43 is reported to bind to the mRNA of TRAK1 (Colombrita et al., 2012), which is the homologue of the *Drosophila* protein Milton. This is an adaptor protein that along with another, Miro, mediates the binding of mitochondria to the motor kinesin 1 (Glater et al., 2006). TDP-43 is also a reported binding partner of KIF1B, which is a kinesin 3 motor protein and also involved in the transport of mitochondria (Tollervey et al., 2011). A further interesting consideration is that TDP-43 has been reported through immunofluorescence and immunoblot analysis to be physically present within mitochondria in the axons of mouse primary motor neurons (Wang et al., 2013a), which is suggestive of a potential functional role through possible interactions with transport components. If this is true of TBPH, loss of such a function could impact on mitochondrial transport.

The analysis of mitochondrial number at the NMJ revealed that there is a greater number present upon the loss of TBPH. This was a surprising

finding given the transport phenotype. We expected that there would be a decrease at this structure as the overall reductions in the motile fraction result in more stationary mitochondria along the axon.

The dynamic nature of mitochondrial transport is important. Mitochondria have a limited functional lifespan and are constantly accumulating damage. It is important that those mitochondria at the NMJ are functioning optimally to meet the high-energy demands and allow for proper function of the NMJ. It is not entirely clear at this stage whether those mitochondria travelling in the retrograde direction are those that are less healthy and have decreased functioning compared to those moving anterograde (Miller and Sheetz, 2004; Verburg and Hollenbeck, 2008). Nevertheless, it remains possible that if axonal transport is becoming defective, more mitochondria remain at the NMJ and are not replaced nor are they sufficiently furnished with new components through fusing with incoming mitochondria (Schwarz, 2013), which leaves them vulnerable to accumulate damage. As a defence against this, mitochondria undergo fission to isolate such damage and to maximise the functionality of the healthy population. Such fission would result in an observed increase in the number of mitochondria. However, the functional state of these mitochondria at the NMJ was not examined in this analysis. It would be of interest to elucidate this information to gain a better understanding of whether the need to isolate dysfunction is causing the increase in mitochondria number at the NMJ.

In contrast to the results described above, the overexpression of TDP-43 proteins in this model did not produce any alteration to mitochondrial axonal transport. Rather, movement of transport vesicles is impaired, and mitochondrial transport is unaffected. Thus, it is clear that in this model, the loss and gain of TBPH exerts differential effects on axonal transport. It is well established that both loss and gain of TBPH results in neurodegenerative phenotypes and that correct levels of this protein are

of extreme importance. This work supports the concept that the stoichiometry of the proteins within the ribonucleoprotein complexes is a key factor and if altered through disturbed TDP-43 levels results in impaired functioning of these complexes (Diaper et al., 2013). Further, these changes to ribonucleoprotein complexes stoichiometry may result in differential effects of their functioning that may underpin the differences observed in the effect on axonal transport. Recent evidence has also suggested that cytoplasmic TDP-43 C-aggregates can block the export of mRNA out of the nucleus by causing altered distribution of nuclear pore complex components (Woerner et al., 2016), which again could lead to defects in axonal transport through the sequestration of those mRNAs coding for axonal transport related proteins. Ectopic expression of TDP-43^{WT} in *Drosophila* has been reported to cause aggregate induced axon swelling in motor neurons (Li et al., 2010), which could be envisaged to create a physical block of transport, although the selective effect of transport disruption would seem to argue against this, at least at this stage examined.

The level of vesicle transport dysfunction did not reach significance when the human wild type protein was expressed in the fly. However it was trending in that direction and may have reached significance if the number of samples in the analysis was to be increased. It is further anticipated that it may continue to decline and reach significance at a slightly later time point. This work also points to vesicle transport dysfunction as a consequence of the M337V mutation, which may have implications for the human disease.

The increase in mitochondrial length in the condition of TBPH overexpression was an intriguing finding. It is not clear why this would be an effect specific to only the fly wild type protein in this model, but likely points to a non-conserved difference between them. The fact that this phenotype can be rescued by a reduction in Marf, the fly homolog of

Mitofusin 2, the key protein involved in mitochondrial outer membrane fusion, indicates a relationship between TBPH and Marf in the regulation of mitochondrial length. It further suggests that excessive TBPH may interfere with the dynamics of fission and fusion through promoting fusion. This result is in contrast to that previously seen in mouse primary neurons (Wang et al., 2013b), wherein TDP-43 overexpression causes reduction in mitochondrial length with overexpression of Mitofusin2 ameliorating this phenotype. It is unclear why these differences are apparent but perhaps may represent differences inherent to the model systems or conditions.

In regards to the neuromuscular functioning in these overexpression models, no phenotype was observed in eclosion suggesting no effect on viability through development, which is consistent with the original characterisation of these fly lines (Wang et al., 2011), although this differs from some models (Estes et al., 2011; Diaper et al., 2013) as does the timing of motor deficits, although this was seen to be age dependent in severity in some models (Li et al., 2010; Voigt et al., 2010; Hanson et al., 2010; Lin et al., 2011; Estes et al., 2011). In terms of the measures of locomotion in this model, only the expression of the human mutant M337V, produced a phenotype in the flies at the young stages, earlier than that seen with the wild type proteins, which may be influenced by the abnormal transport of vesicles recorded. This would also suggest that neurons might have a greater ability to cope with the effects of an excessive amount of the wild type protein. However, age related and progressive decline in motor functioning was a result seen for the wild type overexpression in addition to the mutant. Therefore it is suggested that the vesicle transport defect may be a factor here within the aging paradigm, which negatively impacts the neurons abilities to cope.

6.3 FUS

Axonal transport dysfunction is also a phenotype resulting from loss of Caz. However, unlike the loss of TBPH, both mitochondrial and vesicle transport is affected. Caz therefore appears to have a non-selective role in the functioning of axonal transport and its loss results in a broad-scale defect to this process. Such dysfunction is specifically attributable to the loss of Caz as the re-expression of this protein can rescue these phenotypes. Interestingly, in terms of mitochondria, this can only be achieved at 29°. Thus, it is clear that levels of Caz are vitally important for the correct functioning of mitochondrial axonal transport. In regards to transport vesicles, the re-expression of Caz is fully able to restore the stationary fraction to control level but in conjunction with a partially restored anterograde fraction. This is attributable to a slight increase in the retrograde fraction. This pattern of rescue is also mirrored by expression of the human protein, FUS. However, the mitochondrial rescue was achieved at the standard temperature of 25°C unlike with Caz. Given the fact these transgenes were subject to identical site directed integration and known to be expressing at comparable levels (Wang et al., 2011), a difference in expression does not seem likely as an explanation here, although this was not explicitly examined. Rather, this likely stems from a difference in functionality between the two proteins, possibly owing to differences in structure. The results of rescue with the fly and human homologues of the ALS linked mutation P525L were intriguing, A full rescue of the mitochondrial phenotype was achieved but the vesicle rescue only partially so. A comparative difference is thus apparent in the capability of this mutation to mediate vesicle transport, which may have implications for ALS patients.

As with TDP-43, this study has not attempted to elucidate the exact molecular mechanisms but is considered to occur through the effects of RNA dysregulation. To this end, FUS has been reported to bind to multiple

Kinesin motor proteins including KIF5C, KIF1B and KIF3A, which are involved in the axonal transport of mitochondria and vesicles (Hoell et al., 2011; Colombrita et al., 2012) (see Table 6.1).

The axonal transport phenotypes attributable to the loss of Caz bears a correlational relationship to severe reductions in viability and multiple measures of neuromuscular functioning. This suggests that there may be both mitochondrial related and vesicle related deficiencies at the neuromuscular junction that could be contributing to the dysfunction of these motor activities. In this regard, it was interesting to note the increase in the number of mitochondria at the NMJ in the *caz*^{1} mutant, especially in light of the similar phenotype seen in the loss of TBPH. Examining the functional state of these mitochondria would therefore also be of interest.

The behavioural phenotype rescue results further enhanced understanding of the relationship between axonal transport dysfunction and neuromuscular capacity. Behavioural phenotype rescue was conducted with expression driven in motor neurons only or in all neurons given the incomplete rescue results for some measures in preliminary experiments using only *D42-GAL4*. Rescue of all behavioural phenotypes was achieved by both wild-type Caz and the mutant protein when expressed in either motor neurons only or in all neurons. All of which were undertaken at the standard temperature of 25°C. However, the mitochondrial transport defect could only be rescued at 29°C. It seems unlikely then that there is any weight to be given to a contributory factor of mitochondrial transport dysfunction on neuromuscular functioning. Vesicle transport is however rescued at 25°C, which could be having an impact on behavioural phenotypes, although it is noted there is only a partial rescue with the mutant protein. Thus, the flies have a capacity to cope with this transport defect at this early time point. It may have been useful to age these rescue flies for a determination of whether such

motor activity suffers an age related decline that may be influenced by this transport defect.

There were some small differences in the human proteins abilities to rescue behavioural phenotypes. Compared to the fly homologs, the human proteins were not as capable at rescuing larval locomotion in either motor neurons or in all neurons. This suggests the human homolog may not be as functionally efficient within the fly, and also that extra-neuronal expression of FUS is important for neuromuscular function in agreement with the assessment made by Wang et al., (2011). Further FUS^{P525L} was significantly worse than FUS^{WT}, which was also the case in the attempted rescue of adult climbing. Thus these data suggest there is a loss of function caused by the P525L mutation on neuromuscular functioning, These results bear a correlational relationship to the rescue of axonal transport dysfunction with the lack of complete FUS^{P525L} locomotor rescue possibly at least partly attributable to the partial rescue of vesicle transport.

The overexpression of Caz variants caused severe mitochondrial and vesicle transport defects. Thus, loss and gain of Caz exerts the same effect on transport, possibly through a similar manner to what is postulated for TBPH in terms of ribonucleoprotein complex stoichiometry affecting RNA regulation. Furthermore, though the outcome is comparable, this does not preclude the concept that this may be achieved via different mechanisms. Elucidating the precise mechanisms would be a priority for further work. The result showing that the number of mitochondria at the NMJ is unaffected in these overexpression lines in contrast to the increase seen in the knockout condition further adds weight to the concept that there may be different mechanisms at play. It must also be noted that Caz^{P398L} was found to be nuclear/cytoplasmic (Wang et al., 2011) whereas the others were nuclear, at least as was determined in those experiments, which suggests cytoplasmic localisation

is not necessary to cause these defects, which again suggests a situation centred on ribonucleoprotein complex component levels.

It was surprising to note that whilst overexpression of either human homolog led to a comparable vesicle transport defect, mitochondrial transport was unaffected. This differential effect of the overexpression of fly and human homologs on transport is unclear. Though these proteins are homologs, the human protein may act differently within the fly system in relation to the fly protein, which may be related to structural differences between them.

However, the flies have a good capacity to tolerate these transport defects insofar as maintaining locomotor ability. The overexpression of none of the Caz or FUS variants produced any phenotypes in young animals. Intriguingly, this capacity declines in a progressive age-related manner in each condition with the exception of FUS^{WT}, which nevertheless was trending downwards and may have reached significance at a later time point. To this end it may be useful to extend the assay for this purpose. It is interesting that Caz overexpressing flies were affected at an earlier time point than those expressing the human equivalents, especially given the fact the Caz variants exerted an effect on mitochondrial transport and FUS did not, which it is suggested may be a factor in the milder phenotype seen with overexpression of FUS. Overall these ageing data demonstrate that in this overexpression model there is a progressive age-related decrease in neuromuscular functioning that may be influenced by declining ability to cope with continual axonal transport abnormalities. These results differ slightly from those reported by other groups, who saw phenotypes at earlier stages upon overexpression in *Drosophila* (Xia et al., 2012; Chen et al., 2011; Machamer et al., 2014) but agree with those of Wang et al., (2011). It is not known why this would be the case but may be a result of different lines or conditions used.

In addition to the separate studies of TBPH and Caz, given the similarities and functional interactions between them, a consideration on their relationship in regards to axonal transport was undertaken. It seems that at least in terms of mitochondria, the loss of either TBPH or Caz results in defective transport. This raised the question of whether they are acting in a genetic pathway to mediate this function, as has been discovered in terms of viability and locomotor behaviours through cross-rescue experiments using these transgenes (Wang et al., 2011). This was corroborated in this study in terms of the behavioural assays, however the fact the mitochondrial transport phenotype could not be rescued raises the concept that they are unlikely to interact within a pathway to mediate their role in this transport.

Table 6.1: TDP-43 and FUS RNA targets associated with axonal transport.

Axonal Transport Machinery	Name	ALS model	Vesicles / Mitochondria	Function	Reference
Microtubules	Futsch (MAP1B)	TDP-43, FUS	Both	Stability of microtuble tracks	Godena et al., (2011), Hoell et al., (2011)
Motor proteins	KIF13	TDP-43	Vesicles	Movement of cargo	Colombrita et al., (2012)
	KIF1B	TDP-43, FUS	Mitochondria		Tollervey et al., (2011), Colombrita et al., (2012)
	KIF5A	TDP-43	Mitochondria		Polymenidou et al., (2011)
	KIF5C	FUS	Mitochondria		Hoell et al., (2011), Colombrita et al., (2012)
	KIF3A	FUS	Vesicles		Hoell et al., (2011)
	KIF3B	FUS	Vesicles		Hoell et al., (2011)
	KIF13B	FUS	Vesicles		Hoell et al., (2011)
	DCTN4	FUS	Both		Hoell et al., (2011)
	DCTN5	FUS	Both		Hoell et al., (2011)
	DCTN6	FUS	Both		Hoell et al., (2011)
	DYNC1H1	FUS	Both		Hoell et al., (2011)
	DYNC1I1	FUS	Both		Hoell et al., (2011)
	DYNC1LI1	FUS	Both		Hoell et al., (2011)
	DYNC2LI1	FUS	Both		Hoell et al., (2011)
	DYNC2H1	FUS	Both		Hoell et al., (2011)
Adaptor proteins	KLC1	TDP-43,FUS	Vesicles	Binding of vesicles to Kinesin	Xiao et al., (2011), Hoell et al., (2011)
	TRAK1	TDP-43	Mitochondria	Binding of mitochondria to Kinesin	Colombrita et al., (2012)

6.4: C9orf72

The survey of axonal transport within the C9orf72 models also identified a disruption. The expression of the expanded pure repeats construct clearly caused a disruption of mitochondrial transport. However the effect of such expansion on the transport of vesicles is more complicated being that it was affected by the 3 repeat construct as well, which argues that this may be explained as a consequence of the construct insertion within the fly or that the 3 repeat result is the consequence of this insert causing RNA-mediated targeting of specifically vesicle transport

machinery mRNAs. However, results of the RNA only and PR-only conditions implicate toxicity related to the expansion. Overall it can be concluded that axonal transport is disrupted in this model and represents a novel phenotype of *C9orf72* expansion.

Among the three potential mechanisms of *C9orf72* pathogenesis, haploinsufficiency is generally disfavoured, as multiple animal models have returned results illustrating the lack of overt symptoms upon C9orf72 knockdown/knockout (Lagier-Tourenne et al., 2013; Koppers et al., 2015). A considerable amount of evidence has been gathered in favour of a gain of toxic function of the expanded RNA. These develop into RNA foci that are present in affected brain regions and serve to trap multiple species of RNA binding proteins and trigger a dysfunctional RNA metabolism (Stepto et al., 2014).

However, in this model, axonal transport dysfunction at least regarding mitochondria and transport vesicles is not attributable to a toxic gain of function of the expanded RNA itself. This is consistent with the lack of phenotypes reported in the RNA-only flies in the original study by Mizielinska and colleagues and further by the locomotor results of this study.

However, evidence is mounting for a pathogenic role of the dipeptide repeat proteins that are produced from the expanded RNA transcript through RAN translation. The results from this study further suggest a toxicity of the DPR proteins. Expression of one of these, proline-arginine (PR) results in severe mitochondrial and vesicle transport dysfunction. DPR proteins are highly aggregate prone and form into protein inclusions. It is conceivable that these may be affecting the availability of components of the transport apparatus, making it more likely that cargo will be stationary at any given time. Alternatively, and especially given both cargo were affected, these protein aggregates could be acting as physical

blockades within the axon. It may be of interest in future studies to conduct dual marker experiments for both aggregates and fluorescent transport cargo to elucidate whether this is the case.

Interestingly, it has been shown in cultured astrocytes that the PR species of DPRs is able to enter the nucleus and aberrantly bind to nucleoli causing widespread RNA dysfunction, which ultimately led to cell death (Kwon et al., 2014). This raises the concept of a specific RNA dysfunction arising from the effect of the PR DPR species that may impact axonal transport function. This is further intriguing in light of the recent work suggesting the PR dipeptide may block the nuclear pores and prevent nucleocytoplasmic shuttling (Jovičić et al., 2015). A study utilising a *Drosophila* screen also saw nucleocytoplasmic transport dysfunction particularly of protein import with expression of pathogenic length G4C2 repeats, including of nuclear import of TBPH. However the authors attributed this to RNA toxicity, specifically, the binding of important nucleocytoplasmic transport protein RanGAP to the expanded RNA and failed to detect the presence of DPRs, although they concluded their existence and potential effect could not be ruled out (Zhang et al., 2015). Another study undertook a screen using a *Drosophila* model expressing a $(G4C2)_{58}$ repeats construct which led to nuclear and cytoplasmic inclusions and returned results indicating dysfunction in nucleocytoplasmic transport. Interestingly, they found a significant defect in the process of RNA export, which resulted in the retention of RNA within the nuclear compartment and which was corroborated in HeLa cells and iPSC derived patient neurons (Freibaum et al., 2015). Through the use of the $(G4C2)_{58}$ construct this study identified potential toxicity from both RNA and DPRs and so this dysfunction cannot be concluded as a specific product of DPR toxicity, although they did report toxicity in another fly model exclusively associated with the GR arginine-containing DPR. This is an exciting new area that needs more clarifying studies but there is evidence, particularly from the studies by Kwon et al., (2014) and

Jovičić et al., (2015) to suggest, in common with that of TDP-43 and other aggregate prone proteins (Woerner et al. 2016), a functional mechanism for PR toxicity through which axonal transport (and other cellular processes) could be disturbed if key components are decreased in availability due to the breakdown in the nuclear pore traffic flow.

This study focused on a species of DPR protein that contains arginine as such DPRs were identified in the study by Mizielinska et al., (2014) from whom the fly lines originated, to be the toxic DPR species. No effects on any of the measures of neurodegeneration were seen with the non-arginine containing GA or PA species. This study did not assess these other DPRs in isolation thus, whether axonal transport dysfunction can be attributed specifically to arginine containing species cannot be concluded. However given the previous results it is hypothesised that this would be the case. Though it is noted that the non-arginine DPR proteins do have some evidence to suggest they are toxic (Zu et al., 2013; May et al., 2014). Thus, it would be interesting to examine expression of other DPR proteins to see whether axonal transport dysfunction arises.

The result of the mitochondrial count analysis at the NMJ was difficult to interpret and seems inconsistent with the mitochondrial transport phenotypes. Here, there appeared to be fewer mitochondria, however the difference is small and may simply be an experimental artefact. Furthermore, neither is significantly different from the 3 repeats conditions, which itself, being in the non-pathogenic range, could arguably be used as an additional comparator.

The evidence regarding neuromuscular functioning suggests that these flies are reasonably able to tolerate the axonal transport dysfunction at least at larval and young adult stages. Due to time constraints, viability as measured by level of eclosion was not quantified. However on an observational basis, this was unaffected at 25°C consistent with previous

findings (Mizielinska et al., 2014). At this temperature, larval locomotion was reduced in the DPR only condition and mildly in the pure 36 repeats condition, which is consistent with the axonal transport results. The relative difference in severity between these conditions may be as a result of an increased abundance of a toxic DPR species in the former. The effect of ageing on the locomotor capacity of these flies was not undertaken due to time constraints but would be useful to see whether age related decline in neuromuscular functioning is present in this model. Although previous work by Mizielinska and colleagues has showed that expanded repeats severely reduce the survival time of the flies and that this was not attributable to expanded RNA only toxicity. It is suggested that axonal transport dysfunction may be a factor in this model perhaps by contributing to a vulnerable neuronal environment that may lead to neuronal death and reduced lifespan.

Although the relationship between repeat length and phenotype is not clear, the previous study showed the level of toxicity of expanded *C9orf72* repeats increased with repeat length and thus it may be useful to examine this relationship in regard to axonal transport, such a finding would add further weight to a pathogenic role for axonal transport dysfunction in this model. It is also recognised that these results should not be taken to suggest RNA specific toxicity is not a factor in human disease as many lines of evidence indicate that it is. In this context it may be useful to examine other, perhaps longer repeat RNA-only flies for axonal transport and neurodegenerative behavioural phenotypes.

It must also be noted that this study ectopically expressed these PR only constructs within lower motor neurons in a fly model. However, whether this is clinically relevant is debatable given that within *C9orf72* expansion positive patients DPR inclusions have been described as a limited pathology within these neurons (Gomez-Deza et al., 2015). Nevertheless, they are present in some patients and the possible effect of axonal

transport dysfunction cannot be ruled out. In addition, an examination of axonal transport within other brain neuronal populations may be of interest as it is clearly a phenotype that arises from the expression of at least one DPR protein.

6.5: Conclusions and General Future Directions

The survey of axonal transport within these three models has shown dysfunction in this system is a common finding in models of ALS that may be contributing to the observed neuromuscular dysfunction. The study is limited insofar as it is correlational and descriptive; nevertheless it highlights this pervasive dysfunction in axonal transport and serves as a base for future exploration. One aspect that could be explored further is additional measures of transport such as velocity, and number and length of pauses, which may be a useful expansion to this analysis of transport. Additionally, NMJ morphology was not examined and so it is not possible from this study to comment directly on the contribution of these transport defects to the dying-back process. Although other models of TDP-43, FUS show that NMJ morphology is affected in some models (Feiguin et al., 2009; Estes et al., 2011; Li et al., 2010; Xia et al., 2012; Chen et al., 2011). Furthermore, these axonal transport defects join synaptic transmission dysfunction as early phenotypes recorded in TDP-43 and FUS models (Diaper et al., 2013; Machamer et al., 2014) and raises the idea that they may be a factor in the development of this synaptic dysfunction, which would be interesting to explore. However, it may be that axonal transport disruption is a consequence and not a cause of degeneration, a distinction cannot be concluded here but the early time point of axonal transport defects is an interesting indicator that fits into the concept that transport dysfunction precedes symptom onset in patients.

However, in the SOD1 models of ALS, the relationship between mitochondrial transport dysfunction and degeneration is not clear.

Several studies suggest evidence to support such a relationship, however the inability to rescue this when the mammalian protein, Syntaphilin, a key protein involved in anchoring mitochondria and inhibiting their transport is reduced argued against this (Marinković et al., 2012).Although there is no fly homologue of Syntaphilin, it would perhaps be interesting as an additional justification to assess the effect of reducing the stationary pool within models of TDP-43, FUS and C9orf72 linked ALS. In flies this could potentially be achieved by overexpressing the mitochondrial adaptor protein Milton, which using the mammalian equivalents, significantly increases the motile fraction in mice (Chen and Sheng, 2013). In this manner it could be elucidated whether such a rescue of mitochondrial motility is in fact able to positively impact neuromuscular functioning.

The transport of other cargo, such as several types of vesicles has also been studied in the context of SOD1 models and one such cargo is reported here to be defective in further models of ALS. Thus, it is worth examining other types of cargo beyond mitochondria within such transport studies to gain a more complete picture of the state of axonal transport in ALS.

As described above, this study of axonal transport in these three ALS associated genes found mitochondria and vesicles are affected in some manner for each, further building on the knowledge of axonal transport in ALS gathered from non-*Drosophila* studies of TDP-43 and SOD1, which leads to the conclusion mitochondrial and vesicle transport disruption is a common phenotype in ALS models. However, this axonal transport dysfunction is not a specific pathology to ALS; it is also seen extensively in other neurodegenerative disease models such as Huntington's, Parkinson's and Alzheimer's diseases.

However, the mechanisms underpinning the dysfunction differ between models demonstrating the vast manner in which axonal transport

dysfunction can arise. Within ALS, dysfunction related to TDP-43, FUS and *C9orf72 expansion* are likely to act through dysregulation/disruption of transport-related RNA targets as described above, whereas mutant SOD1 pathologically associates with mitochondria and causes p38 activation which prevents the function of Kinesin (De Vos et al., 2008; Morfini et al., 2013). In non-ALS models, PolyQ Huntingtin creates aggregates which are postulated to cause axonal blockade that disrupts vesicle transport and very probably other cargo in a *Drosophila* model (Sinadinos et al., 2009), prevents the interaction of an adaptor protein with the motors (Morfini et al., 2009) and promotes deacetylation of Tubulin (Dompierre et al., 2007). LRRK2 Roc-COR domain mutants also cause the latter, by binding to deacetylated microtubules, which has a measured severe effect on mitochondrial transport and likely, given the critical nature of stable microtubules as tracks for axonal transport, many other cargoes as well (Godena et al., 2014). In Alzheimer's, mutations in Amyloid precursor protein (APP) and Presenilin 1 (PS1) both cause axonal transport dysfunction, with the former affecting vesicle transport (Salehi et al., 2006) and the latter, motor-cargo binding, inhibiting vesicle and mitochondrial transport (Pigino et al., 2003). Thus, ALS joins the list of neurodegenerative disorders within which multiple genetic models share the common phenotype of axonal transport dysfunction as well as being one of many more disorders with axonal transport dysfunction as a phenotype, which again highlights the importance of axonal transport in neuronal function and its dysfunction in disease.

Overall, this study has shown there exists a commonality of axonal transport dysfunction in multiple models of ALS, which therefore may represent a unifying pathology in this disease, which is suggested to contribute to the development of motor dysfunction and to eventual neuronal loss. In light of this, an expansion of the survey to include other cargo and other time-points should perhaps be considered. Future studies are also needed to elucidate the exact mechanisms underpinning

this dysfunction to further understand the role perturbations to this system play in this devastating disease.

References

Ackerley, S., Grierson, A.J., Brownlees, J., Thornhill, P., Anderton, B.H., Leigh, P.N., Shaw, C.E., and Miller, C.C.J. (2000). Glutamate slows axonal transport of neurofilaments in transfected neurons. *J.Cell Biol.,* 150, 165-175.

Ajroud-Driss, S., and Siddique, T. (2015). Sporadic and hereditary amyotrophic lateral sclerosis (ALS). *Biochim. Biophys Acta.,* 1852, 679-684.

Al-Sarraj, S., King, A., Troakes, C., Smith, B., Maekawa, S., Bodi, I., Rogelj, B., Al-Chalabi, A., Hortobagyi, T., and Shaw, C.E. (2011). p62 positive, TDP-43 negative, neuronal cytoplasmic and intranuclear inclusions in the cerebellum and hippocampus define the pathology of C9orf72-linked FTLD and MND/ALS. *Acta Neuropathol.,* 122, 691-702.

Alami, N.H., Smith, R.B., Carrasco, M.A., Williams, L.A., Winborn, C.S., Han, S.S.W., Kiskinis, E., Winborn, B., Freibaum, B.D., Kanagaraj, A. Clare, A.J., Badders, N.M., Bilican, B., Chaum, E., Chandran, S., Shaw, C.E., Eggan, K.C., Maniatis, T., and Taylor JP. (2014). Axonal Transport of TDP-43 mRNA Granules Is Impaired by ALS-Causing Mutations. *Neuron.,* 81, 536-543.

Alexander, C., Votruba, M., Pesch, U.E.A., Thiselton, D.L., Mayer, S., Moore, A., Rodriguez, M., Kellner, U., Leo-Kottler, B., Auburger, G. Bhattacharya, S.S., and Wissinger, B. (2000). OPA1, encoding a dynamin-related GTPase, is mutated in autosomal dominant optic atrophy linked to chromosome 3q28. *Nat Genet.,* 26, 211-215.

Alfahad, T., and Nath, A. (2013). Retroviruses and amyotrophic lateral sclerosis. *Antiviral Res.,* 99, 180-187.

Andersen, P.M., Nilsson, P., Alahurula, V., Keranen, M.L., Tarvainen, I., Haltia, T., Nilsson, L., Binzer, M., Forsgren, L., and Marklund, S.L. (1995). Amyotrophic Lateral Sclerosis associated with homozygosity for an Asp90Ala Mutation in Cuzn-Superoxide Dismutase. *Nat Genet.,* 10, 61-66.

Anderson, P., and Kedersha, N. (2008). Stress granules: The Tao of RNA triage. *Trends Biochem Sci.,* 33, 141-150.

Andersson, M.K., Stahlberg, A., Arvidsson, Y., Olofsson, A., Semb, H., Stenman, G., Nilsson, O., and Aman, P. (2008). The multifunctional FUS, EWS and TAF15 proto-oncoproteins show cell type-specific expression patterns and involvement in cell spreading and stress response. *BMC Cell Biol.,* 9.

Arai, T., Hasegawa, M., Akiyama, H., Ikeda, K., Nonaka, T., Mori, H., Mann, D., Tsuchiya, K., Yoshida, M., Hashizume, Y., and Oda, T. (2006). TDP-43 is a component of ubiquitin-positive tau-negative inclusions in frontotemporal lobar degeneration and amyotrophic lateral sclerosis. *Biochem Biophys Res Comm.,* 351, 602-611.

Arnold, E.S., Ling, S.-C., Huelga, S.C., Lagier-Tourenne, C., Polymenidou, M., Ditsworth, D., Kordasiewicz, H.B., McAlonis-Downes, M., Platoshyn, O., and Parone, P.A. Da Cruz, S., Clutario, K.M., Swing, D., Tessarollo, L., Marsala, M., Shaw, C.E., Yeo, GW., and Cleveland, D.W. (2013). ALS-linked TDP-43 mutations produce aberrant RNA splicing and adult-onset motor neuron disease without aggregation or loss of nuclear TDP-43. *Proc Natl Acad Sci U S A.,* 110, E736-E745.

Ash, P.E.A., Bieniek, K.F., Gendron, T.F., Caulfield, T., Lin, W.-L., DeJesus-Hernandez, M., van Blitterswijk, M.M., Jansen-West, K., Paul, J.W., III, and Rademakers, R. Boylan, K.B., Dickson, D.W., and Petrucelli, L. (2013). Unconventional Translation of C9ORF72 GGGGCC Expansion Generates Insoluble Polypeptides Specific to c9FTD/ALS. *Neuron.,* 77, 639-646.

Ayala, Y.M., De Conti, L., Avendano-Vazquez, S.E., Dhir, A., Romano, M., D'Ambrogio, A., Tollervey, J., Ule, J., Baralle, M., Buratti, E., and Baralle, F.E. (2011). TDP-43 regulates its mRNA levels through a negative feedback loop. *Embo J.,* 30, 277-288.

Ayala, Y.M., Pantano, S., D'Ambrogio, A., Buratti, E., Brindisi, A., Marchetti, C., Romano, M., and Baralle, F.E. (2005). Human, Drosophila, and C-elegans TDP43: Nucleic acid binding properties and splicing regulatory function. *J Mol Biol.,* 348, 575-588.

Ayala, Y.M., Zago, P., D'Ambrogio, A., Xu., Y.F., Petrucelli, L., Buratti, E., and Baralle, F.E. (2008). Structural determinants of the cellular localisation and shuttling of TDP-43. *J Cell Sci*., 121, 3778-3785.

Barmada, S.J., Serio, A., Arjun, A., Bilican, B., Daub, A., Ando, D.M., Tsvetkov, A., Pleiss, M., Li, X., Peisach, D., Shaw, C., Chandran, S., and Finkbeiner, S. (2014). Autophagy induction enhances TDP43 turnover and survival in neuronal ALS models. *Nat Chem Biol.,* 10, 677-U119.

Barmada, S.J., Skibinski, G., Korb, E., Rao, E.J., Wu, J.Y., and Finkbeiner, S. (2010). Cytoplasmic Mislocalization of TDP-43 Is Toxic to Neurons and Enhanced by a Mutation Associated with Familial Amyotrophic Lateral Sclerosis. *J Neurosci.,* 30, 639-649.

Beck, J., Poulter, M., Hensman, D., Rohrer, J.D., Mahoney, C.J., Adamson, G., Campbell, T., Uphill, J., Borg, A., Fratta, P.,. Orrell, R.W., Malaspina, A., Rowe, J., Brown, J., Hodges, J., Sidle, K., Polke, J.M., Houlden, H., Schott, J.M., Fox, N.C., Rossor, M.N., Tabrizi, S.J., Isaacs, A.M., Hardy, J., Warren, J.D., Collinge, J., and Mead S. (2013). Large C9orf72 Hexanucleotide Repeat Expansions Are Seen in Multiple Neurodegenerative Syndromes and Are More Frequent Than Expected in the UK Population. *Am J Hum Genet*., 92, 345-353.

Beckman, G., Lundgren, E., and Tarnvik, A. (1973). Superoxide-Dismutase isoenzymes in different human tissues, their genetic control and intracellular localisation. *Hum Hered*., 23, 338-345.

Belzil, V.V., Bauer, P.O., Prudencio, M., Gendron, T.F., Stetler, C.T., Yan, I.K., Pregent, L., Daughrity, L., Baker, M.C., Rademakers, R., Boylan, K., Patel, T.C., Dickson, D.W., and Petrucelli L. (2013). Reduced C9orf72 gene expression in c9FTD/ALS is caused by histone trimethylation, an epigenetic event detectable in blood. *Acta Neuropathol*., 126, 895-905.

Bennion Callister, J., and Pickering-Brown, S.M. (2014). Pathogenesis/genetics of frontotemporal dementia and how it relates to ALS. *Exp neurol*., 262 Pt B, 84-90.

Benny, R., and Shetty, K. (2012). The split hand sign. *Ann Indian Acad Neurol*., 15, 175-176.

Bentmann, E., Neumann, M., Tahirovic, S., Rodde, R., Dormann, D., and Haass, C. (2012). Requirements for Stress Granule Recruitment of Fused in Sarcoma (FUS) and TAR DNA-binding Protein of 43 kDa (TDP-43). *J Biol Chem*., 287, 23079-23094.

Bilsland, L.G., Sahai, E., Kelly, G., Golding, M., Greensmith, L., and Schiavo, G. (2010). Deficits in axonal transport precede ALS symptoms in vivo. *Proc Natl Acad Sci USA*., 107, 20523-20528.

Bosco, D.A., Lemay, N., Ko, H.K., Zhou, H., Burke, C., Kwiatkowski, T.J., Jr., Sapp, P., McKenna-Yasek, D., Brown, R.H., Jr., and Hayward, L.J. (2010). Mutant FUS proteins that cause amyotrophic lateral sclerosis incorporate into stress granules. *Hum Mol Genet* 19., 4160-4175.

Bradley, W.G., Borenstein, A.R., Nelson, L.M., Codd, G.A., Rosen, B.H., Stommel, E.W., and Cox, P.A. (2013). Is exposure to cyanobacteria an environmental risk factor for amyotrophic lateral sclerosis and other neurodegenerative diseases? *Amyotroph Lateral Scler Frontotemporal Degener*.,14, 325-333.

Brand, A.H., and Perrimon, N. (1993). Targeted gene expression as a means of altering cell fates and generating dominant phenotypes. *Development*., 118, 401-415.

Brettschneider, J., Van Deerlin, V.M., Robinson, J.L., Kwong, L., Lee, E.B., Ali, Y.O., Safren, N., Monteiro, M.J., Toledo, J.B., Elman, L., McCluskey, L., Irwin, D.J., Grossman, M., Molina-Porcel, L., Lee, V.M., and Trojanowski JQ. (2012). Pattern of ubiquilin pathology in ALS and FTLD indicates presence of C9ORF72 hexanucleotide expansion. *Acta Neuropathol*., 123, 825-839.

Brooks, B.R. (1994). El-Escorial world federation of neurology criteria for the diagnosis of Amyotrophic Lateral Sclerosis. *J Neurol Sci*., 124, 96-107.

Brown, A. (2003). Axonal transport of membranous. and nonmembranous cargoes: a unified perspective. *J Cell Biol*., 160, 817-821.

Buratti, E., and Baralle, F.E. (2001). Characterization and functional implications of the RNA binding properties of nuclear factor TDP-43, a novel splicing regulator of CFTR exon 9. *J Biol Chem*., 276, 36337-36343.

Buratti, E., Brindisi, A., Giombi, M., Tisminetzky, S., Ayala, Y.M., and Baralle, F.E. (2005). TDP-43 binds heterogeneous nuclear ribonucleoprotein A/B through its C-terminal tail - An important region for the inhibition of cystic fibrosis transmembrane conductance regulator exon 9 splicing. *J Biol Chem*., 280, 37572-37584.

Burke, R.E., Levine, D.N., Tsairis, P., and Zajac, F.E. (1973). Physiological types and histochemical profiles in motor units of cat gastrocnemius. *J Physiol*., 234, 723.

Carpenter, S. (1968). Proximal axonal enlargement in motor neuron disease. *Neurology*., 18, 841.

Carvalho, M.D., and Swash, M. (2009). Awaji diagnostic algorithm increases sensitivity of El Escorial criteria for ALS diagnosis. Amyotrophic lateral sclerosis : official publication of the World Federation of Neurology Research Group on Motor Neuron Diseases 10, 53-57.

Chang, C.-R., Manlandro, C.M., Arnoult, D., Stadler, J., Posey, A.E., Hill, R.B., and Blackstone, C. (2010). A Lethal de Novo Mutation in the Middle Domain of the Dynamin-related GTPase Drp1 Impairs Higher Order Assembly and Mitochondrial Division. *J Biol Chem*., 285, 32494-32503.

Chen, Y., and Sheng, Z.-H. (2013). Kinesin-1-syntaphilin coupling mediates activity-dependent regulation of axonal mitochondrial transport. *J Cell Biol*., 202, 351-364.

Chen, Y., Yang, M., Deng, J., Chen, X., Ye, Y., Zhu, L., Liu, J., Ye, H., Shen, Y., Li, Y., Rao, E.J., Fushimi, K., Zhou, X., Bigio, E.H., Mesulam, M., Xu, Q., and Wu, J.Y. (2011). Expression of human FUS protein in Drosophila leads to progressive neurodegeneration. *Protein Cell*., 2, 477-486.

Cheroni, C., Marino, M., Tortarolo, M., Veglianese, P., De Biasi, S., Fontana, E., Zuccarello, L.V., Maynard, C.J., Dantuma, N.P., and Bendotti, C. (2009). Functional alterations of the ubiquitin-proteasome system in motor neurons of a mouse model of familial amyotrophic lateral sclerosis dagger. *Hum Mol Genet*., 18, 82-96.

Chia, R., Tattum, M.H., Jones, S., Collinge, J., Fisher, E.M.C., and Jackson, G.S. (2010). Superoxide Dismutase 1 and tgSOD1(G93A) Mouse Spinal Cord Seed Fibrils, Suggesting a Propagative Cell Death Mechanism in Amyotrophic Lateral Sclerosis. *Plos One*., 5.

Chio, A., Benzi, G., Dossena, M., Mutani, R., and Mora, G. (2005). Severely increased risk of amyotrophic lateral sclerosis among Italian professional football players. *Brain*., 128, 472-476.

Chio, A., Calvo, A., Dossena, M., Ghiglione, P., Mutani, R., and Mora, G. (2009). ALS in Italian professional soccer players: The risk is still present and could be soccer-specific. *Amyotroph Lateral Scler*., 10, 205-209.

Chio, A., Calvo, A., Moglia, C., Mazzini, L., Mora, G., and Grp, P.S. (2011). Phenotypic heterogeneity of amyotrophic lateral sclerosis: a population based study. *J Neurol Neurosurg Psychiatry*., 82, 740-746.

Chio, A., Traynor, B.J., Lombardo, F., Fimognari, M., Calvo, A., Ghiglione, P., Mutani, R., and Restagno, G. (2008). Prevalence of SOD1 mutations in the Italian ALS population. *Neurology*., 70, 533-537.

Chiu, A.Y., Zhai, P., Dalcanto, M.C., Peters, T.M., Kwon, Y.W., Prattis, S.M., and Gurney, M.E. (1995). Age dependent penetrance of disease in a transgenic mouse model of familial Amyotrophic Lateral Sclerosis. *Mol Cell Neurosci*., 6, 349-362.

Coleman., M. (2005). Axon degeneration mechanisms: commonality amid diversity. *Nat Revs Neurosci*., 6, 889-898.

Colombrita, C., Onesto, E., Megiorni, F., Pizzuti, A., Baralle, F.E., Buratti, E., Silani, V., and Ratti, A. (2012). TDP-43 and FUS RNA-binding Proteins Bind Distinct Sets of Cytoplasmic Messenger RNAs and Differently Regulate Their Post-transcriptional Fate in Motoneuron-like Cells. *J Biol Chem*., 287, 15635-15647.

Colombrita, C., Zennaro, E., Fallini, C., Weber, M., Sommacal, A., Buratti, E., Silani, V., and Ratti, A. (2009). TDP-43 is recruited to stress granules in conditions of oxidative insult. *J Neurochem*., 111, 1051-1061.

Conde, C., and Caceres, A. (2009). Microtubule assembly, organization and dynamics in axons and dendrites. *Nat Rev Neurosci.*,10, 319-332.

Cooper-Knock, J., Walsh, M.J., Higginbottom, A., Highley, J.R., Dickman, M.J., Edbauer, D., Ince, P.G., Wharton, S.B., Wilson, S.A., Kirby, J., Hautbergue, G.M., and Shaw, P.J. (2014). Sequestration of multiple RNA recognition motif-containing proteins by C9orf72 repeat expansions. *Brain*., 137, 2040-2051.

Cronmiller, C., and Cummings, C.A. (1993). The daughterless genes product in Drosophila is a nuclear protein that is broadly expressed throughout the organism during development. *Mech Dev*., 42, 159-169.

Crozat, A., Aman, P., Mandahl, N., and Ron, D. (1993). Fusion of Chop to a novel RNA bindinf protein in human Myxiod Liposarcoma. *Nature*., 363, 640-644.

Cuervo, A.M. (2008). Autophagy and aging: keeping that old broom working. *Trends Genet*., 24, 604-612.

D, P., GJ, A., and D, F. (2001). The Primary Motor Cortex: Upper Motor Neurons That Initiate Complex Voluntary Movements. In Neuroscience, 1st eds. (Sunderland (MA): Sinauer Associates).

Dadon-Nachum, M., Melamed, E., and Offen, D. (2011). The Dying-back phenomenon of motor neurons in ALS. *J Mol Neurosci*., 43, 470-477.

D'Ambrogio, A., Buratti, E., Stuani, C., Guarnaccia, C., Romano, M., Ayala, Y.M., and Baralle, F.E. (2009). Functional mapping of the interaction between TDP-43 and hnRNP A2 in vivo. *Nucleic Acids Res.*, 37, 4116-4126.

D'Amico, E., Pasmantier, M., Lee, Y.-W., Weimer, L., and Mitsumoto, H. (2013). Clinical evolution of pure upper motor neuron disease/dysfunction (PUMMD). *Muscle Nerve.*, 47, 28-32.

de Boer, A.S., Koszka, K., Kiskinis, E., Suzuki, N., Davis-Dusenbery, B.N., and Eggan, K. (2014). Genetic validation of a therapeutic target in a mouse model of ALS. *Sci Transl Med.*, 6. 248.

de Munck., E., Munoz-sAEZ., E., Miguel., B.G., Solas., M.T., Ojeda., M.T., Martinez., A., Gil., C., and Arahuetes., R.M. (2013). β -N methylamino-l-alanine causes neurological and pathological phenotypes mimicking Amyotrophic Lateral Sclerosis(ALS): The first step towards a sporadic model for ALS. *Enivron Toxicol Pharmacol.*, 2, 243-255.

De Vos, K.J., Chapman, A.L., Tennant, M.E., Manser, C., Tudor, E.L., Lau, K.-F., Brownlees, J., Ackerley, S., Shaw, P.J., McLoughlin, D.M., Shaw, C.E., Leigh, P.N., Miller, C.C., and Grierson, A.J. (2007). Familial amyotrophic lateral sclerosis-linked SOD1 mutants perturb fast axonal transport to reduce axonal mitochondria content. *Hum Mol Genet.*, 16, 2720-2728.

De Vos, K.J., Grierson, A.J., Ackerley, S., and Miller, C.C.J. (2008). Role of axonal transport in neurodegenerative diseases. *Ann Rev Neurosci.*, 31, 151-173.

Deapen, D.M., and Henderson, B.E. (1986). A case-control study of Amyotrophic Lateral Sclerosis. *Am J Epidemiol.*, 123, 790-799.

Deinhardt, K., Salinas, S., Verastegui, C., Watson, R., Worth, D., Hanrahan, S., Bucci, C., and Schiavo, G. (2006). Rab5 and Rab7 control endocytic sorting along the axonal retrograde transport pathway. *Neuron.*, 52, 293-305.

DeJesus-Hernandez, M., Mackenzie, I.R., Boeve, B.F., Boxer, A.L., Baker, M., Rutherford, N.J., Nicholson, A.M., Finch, N.A., Flynn, H., Adamson, J., Kouri, N., Wojtas, A., Sengdy, P., Hsiung, G.Y., Karydas, A., Seeley, W.W., Josephs, K.A., Coppola, G., Geschwind, D.H., Wszolek, Z.K., Feldman, H., Knopman, D.S., Petersen, R.C., Miller, B.L., Dickson, D.W., Boylan, K.B., Graff-Radford, N.R, and Rademakers, R. (2011). Expanded GGGGCC Hexanucleotide Repeat in Noncoding Region of C9ORF72 Causes Chromosome 9p-Linked FTD and ALS. *Neuron.*, 72, 245-256.

Delettre, C., Lenaers, G., Griffoin, J.M., Gigarel, N., Lorenzo, C., Belenguer, P., Pelloquin, L., Grosgeorge, J., Turc-Carel, C., Perret, E., Astarie-Dequeker, C., Lasquellec, L., Arnaud, B., Ducommun, B., Kaplan, J., and Hamel, C.P. (2000). Nuclear gene OPA1, encoding a mitochondrial dynamin-related protein, is mutated in dominant optic atrophy. *Nat Genet.*, 26, 207-210.

Deng, H., Gao, K., and Jankovic, J. (2014). The role of FUS gene variants in neurodegenerative diseases. *Nat Rev Neurol.*, 10, 337-348.

Desai, J., and Swash, M. (1999). Extrapyramidal involvement in amyotrophic lateral sclerosis: backward falls and retropulsion. *J Neurol Neurosurg Psychiatry*., 67, 214-216.

Detmer, S.A., Velde, C.V., Cleveland, D.W., and Chan, D.C. (2008). Hindlimb gait defects due to motor axon loss and reduced distal muscles in a transgenic mouse model of Charcot-Marie-Tooth type 2A. *Hum Mol Genet*., 17, 367-375.

Dewey, C.M., Cenik, B., Sephton, C.F., Dries, D.R., Mayer, P., III, Good, S.K., Johnson, B.A., Herz, J., and Yu, G. (2011). TDP-43 Is Directed to Stress Granules by Sorbitol, a Novel Physiological Osmotic and Oxidative Stressor. *J Bacteriol*., 193, 1098-U1108.

Di Giorgio, F.P., Carrasco, M.A., Siao, M.C., Maniatis, T., and Eggan, K. (2007). Non-cell autonomous effect of glia on motor neurons in an embryonic stem cell-based ALS model. *Nat Neurosci*., 10, 608-614.

Diaper, D.C., Adachi, Y., Sutcliffe, B., Humphrey, D.M., Elliott, C.J.H., Stepto, A., Ludlow, Z.N., Vanden Broeck, L., Callaerts, P., Dermaut, B., Al-Chalabi, A., Shaw, C.E., Robinson, I.M., and Hirth, F. (2013). Loss and gain of Drosophila TDP-43 impair synaptic efficacy and motor control leading to age-related neurodegeneration by loss-of-function phenotypes. *Hum Mol Genet*., 22, 1539-1557.

Doi, H., Okamura, K., Bauer, P.O., Furukawa, Y., Shimizu, H., Kurosawa, M., Machida, Y., Miyazaki, H., Mitsui, K., Kuroiwa, Y., and Nukina, N. (2008). RNA-binding protein TLS is a major nuclear aggregate-interacting protein in huntingtin exon 1 with expanded polyglutamine-expressing cells. *J Biol Chem*., 283, 6489-6500.

Dompierre, J.P., Godin, J.D., Charrin, B.C., Cordelieres, F.P., King, S.J., Humbert, S., and Saudou, F. (2007). Histone deacetylase 6 inhibition compensates for the transport deficits in Huntington's disease by increasing tubulin acetylation. *Neurobiol Dis*., 27, 3571-3583.

Dormann, D., Madl, T., Valori, C.F., Bentmann, E., Tahirovic, S., Abou-Ajram, C., Kremmer, E., Ansorge, O., Mackenzie, I.R.A., Neumann, M., and Haass, C. (2012). Arginine methylation next to the PY-NLS modulates Transportin binding and nuclear import of FUS. *Embo J*., 31, 4258-4275.

Suh, E., Lee, E.B., Neal, D., Wood, E.M., Toledo, J.B., Rennert, L., Irwin, D.J., McMillan, C.T., Krock, B., Elman, L.B., McCluskey, L.F., Grossman, M., Xie, S.X., Trojanowski, J.Q., and Van Deerlin, V.M. (2015). Semi-automated quantification of C9orf72 expansion size reveals inverse correlation between hexanucleotide repeat number and disease duration in frontotemporal degeneration. *Acta Neuropathol*. 130, 363-372.

Estes, P.S., Boehringer, A., Zwick, R., Tang, J.E., Grigsby, B., and Zarnescu, D.C. (2011). Wild-type and A315T mutant TDP-43 exert differential neurotoxicity in a Drosophila model of ALS. *Hum Mol Genet*., 20, 2308-2321.

Ewer, J., and Truman, J.W. (1996). Increases in cyclic 3',5'-guanosine monophosphate (cGMP) occur at ecdysis in an evolutionarily conserved crustacean cardioactive peptide-immunoreactive insect neuronal network. *J Comp Neurol*., 370, 330-341.

Ezzi, S.A., Urushitani, M., and Julien, J.-P. (2007). Wild-type superoxide dismutase acquires binding and toxic properties of ALS-linked mutant forms through oxidation. *J Neurochem*., 102, 170-178.

Fallini, C., Bassell, G.J., and Rossoll, W. (2012). The ALS disease protein TDP-43 is actively transported in motor neuron axons and regulates axon outgrowth. *Hum Mol Genet*., 21, 3703-3718.

Feiguin, F., Godena, V.K., Romano, G., D'Ambrogio, A., Klima, R., and Baralle, F.E. (2009). Depletion of TDP-43 affects Drosophila motoneurons terminal synapsis and locomotive behavior. *Febs Lett*., 583, 1586-1592.

Ferreirinha, F., Quattrini, A., Pirozzi, M., Valsecchi, V., Dina, G., Broccoli, V., Auricchio, A., Piemonte, F., Tozzi, G., Gaeta, L., Casari, G., Ballabio, A., and Rugarli, EI. (2004). Axonal degeneration in paraplegin-deficient mice is associated with abnormal mitochondria and impairment of axonal transport. *J Clin Invest*., 113, 231-242.

Ferri, A., Cozzolino, M., Crosio, C., Nencini, M., Casciati, A., Gralla, E.B., Rotilio, G., Valentine, J.S., and Carri, M.T. (2006). Familial ALS-superoxide dismutases associate with mitochondria and shift their redox potentials. *Proc Natl Acad Sci USA*., 103, 13860-13865.

Fiesel, F.C., Schurr, C., Weber, S.S., and Kahle, P.J. (2011). TDP-43 knockdown impairs neurite outgrowth dependent on its target histone deacetylase 6. *Mol Neurodegener*., 6.

Finsterer., J. (2006). Familial Amyotrophic Lateral Sclerosis. In Amyotrophic Lateral Sclerosis: New Research, C.A. Murray., ed. (Nova Science), 1-47.

Fischer, L.R., Culver, D.G., Tennant, P., Davis, A.A., Wang, M.S., Castellano-Sanchez, A., Khan, J., Polak, M.A., and Glass, J.D. (2004). Amyotrophic lateral sclerosis is a distal axonopathy: evidence in mice and man. *Exp Neurol*., 185, 232-240.

Forman, H.J., and Fridovich, I. (1973). Stability of bovine superoxide dismutase effects of metals. *J Biol Chem*., 248, 2645-2649.

Forman, M.S., Trojanowski, J.Q., and Lee, V.M.Y. (2007). TDP-43: a novel neurodegenerative proteinopathy. *Curr Opin Neurobiol*., 17, 548-555.

Fratta, P., Mizielinska, S., Nicoll, A.J., Zloh, M., Fisher, E.M.C., Parkinson, G., and Isaacs, A.M. (2012). C9orf72 hexanucleotide repeat associated with amyotrophic lateral sclerosis and frontotemporal dementia forms RNA G-quadruplexes. *Sci Rep*., 2, 1016.

Fratta, P., Polke, J.M., Newcombe, J., Mizielinska, S., Lashley, T., Poulter, M., Beck, J., Preza, E., Devoy, A., Sidle, K., Howard, R., Malaspina, A., Orrell, R.W., Clarke, J., Lu, C.H., Mok, K., Collins, T., Shoaii, M., Nanji, T., Wray, S., Adamson, G., Pittman, A., Renton, A.E., Traynor, B.J., Sweeney, M.G., Revesz, T., Houlden, H., Mead, S., Isaacs, A.M., and Fisher, E.M. (2015). Screening a UK amyotrophic lateral sclerosis cohort provides evidence of multiple origins of the C9orf72 expansion. *Neurobiol Aging*., 36, 546.

Freibaum, B.D., Chitta, R.K., High, A.A., and Taylor, J.P. (2010). Global Analysis of TDP-43 Interacting Proteins Reveals Strong Association with RNA Splicing and Translation Machinery. *J Proteome Res*., 9, 1104-1120.

Freibaum, B.D., Lu, Y., Lopez-Gonzalez, R., Kim, N.C., Almeida, S., Lee, K.-H., Badders, N., Valentine, M., Miller, B.L., Wong, P.C., Petrucelli, L., Kim, H.J., Gao, F.B., and Taylor, J.P. (2015). GGGGCC repeat expansion in C9orf72 compromises nucleocytoplasmic transport. *Nature*., 525, 129-133.

Frey, D., Schneider, C., Xu, L., Borg, J., Spooren, W., and Caroni, P. (2000). Early and selective loss of neuromuscular synapse subtypes with low sprouting competence in motoneuron diseases. *J Neurosci*., 20, 2534-2542.

Fridovich, I. (1995). Superoxide radical and superoxide dismutases. *Ann Rev Biochem*., 64, 97-112.

Fuentealba, R.A., Udan, M., Bell, S., Wegorzewska, I., Shao, J., Diamond, M.I., Weihl, C.C., and Baloh, R.H. (2010). Interaction with Polyglutamine Aggregates Reveals a Q/N-rich Domain in TDP-43. *J Biol Chem*., 285, 26304-26314.

Fujii, R., and Takumi, T. (2005). TLS facilitates transport of mRNA encoding an actin-stabilizing protein to dendritic spines. *J Cell Sci*., 118, 5755-5765.

Gallo, V., Bueno-de-Mesquita, H.B., Vermeulen, R., Andersen, P.M., Kyrozis, A., Linseisen, J., Kaaks, R., Allen, N.E., Roddam, A.W., Boshuizen, H.C., Peeters, P.H., Palli, D., Mattiello, A., Sieri, S., Tumino, R., Jiménez-Martín, J.M., Díaz, M.J., Suarez, L.R., Trichopoulou, A., Agudo, A., Arriola, L., Barricante-Gurrea, A., Bingham, S., Khaw, K.T., Manjer, J., Lindkvist, B., Overvad, K., Bach, F.W., Tjønneland, A., Olsen, A., Bergmann, M.M., Boeing, H., Clavel-Chapelon, F., Lund, E., Hallmans, G., Middleton, L., Vineis, P., and Riboli, E. (2009). Smoking and Risk for Amyotrophic Lateral Sclerosis: Analysis of the EPIC Cohort. *Ann Neurol*., 65, 378-385.

Gendron, T.F., Bieniek, K.F., Zhang, Y.-J., Jansen-West, K., Ash, P.E.A., Caulfield, T., Daughrity, L., Dunmore, J.H., Castanedes-Casey, M., Chew, J., Cosio, D.M., van Blitterswijk, M., Lee, W.C., Rademakers, R., Boylan, K.B., Dickson, D.W., and Petrucelli, L. (2013). Antisense transcripts of the expanded C9ORF72 hexanucleotide repeat form nuclear RNA foci and undergo repeat-associated non-ATG translation in c9FTD/ALS. *Acta Neuropathol*., 126, 829-844.

Gitcho, M.A., Baloh, R.H., Chakraverty, S., Mayo, K., Norton, J.B., Levitch, D., Hatanpaa, K.J., White, C.L., III, Bigio, E.H., Caselli, R., Baker, M., Al-Lozi, M.T., Morris, J.C., Pestronk, A., Rademakers, R., Goate, A.M., and Cairns, N.J. (2008). TDP-43 A315T mutation in familial motor neuron disease. *Ann Neurol.*, 63, 535-538.

Glater, E.E., Megeath, L.J., Stowers, R.S., and Schwarz, T.L. (2006). Axonal transport of mitochondria requires milton to recruit kinesin heavy chain and is light chain independent. *J Cell Biol.*, 173, 545-557.

Godena, V.K., Brookes-Hocking, N., Moller, A., Shaw, G., Oswald, M., Sancho, R.M., Miller, C.C.J., Whitworth, A.J., and De Vos, K.J. (2014). Increasing microtubule acetylation rescues axonal transport and locomotor deficits caused by LRRK2 Roc-COR domain mutations. *Nature Commun.*, 5, 5245.

Gomez-Deza, J., Lee, Y.-B., Troakes, C., Nolan, M., Al-Sarraj, S., Gallo, J.-M., and Shaw, C.E. (2015). Dipeptide repeat protein inclusions are rare in the spinal cord and almost absent from motor neurons in C9ORF72 mutant amyotrophic lateral sclerosis and are unlikely to cause their degeneration. *Acta Neuropathol Commun.*, 3, 38-38.

Gordon, P.H. (2013). Amyotrophic Lateral Sclerosis: An update for 2013 Clinical Features, Pathophysiology, Management and Therapeutic Trials. *Aging Dis.*, 4, 295-310.

Gouveia, L.O., and de Carvalho, M. (2007). Young-onset sporadic amyotrophic lateral sclerosis: A distinct nosological entity? *Amyotroph Lateral Scler.*, 8, 323-327.

Gregory, R.I., Yan, K.P., Amuthan, G., Chendrimada, T., Doratotaj, B., Cooch, N., and Shiekhattar, R. (2004). The Microprocessor complex mediates the genesis of microRNAs. *Nature.*, 432, 235-240.

Grossman, M., Elman, L., McCluskey, L., McMillan, C.T., Boller, A., Powers, J., Rascovsky, K., Hu, W., Shaw, L., Irwin, D.J., Lee, V.M., and Trojanowski, J.Q. (2014). Phosphorylated Tau as a Candidate Biomarker for Amyotrophic Lateral Sclerosis. *JAMA Neurol.*, 71, 442-448.

Guo, W., Chen, Y., Zhou, X., Kar, A., Ray, P., Chen, X., Rao, E.J., Yang, M., Ye, H., Zhu, L., Liu, J., Xu, M., Yang, Y., Wang, C., Zhang, D., Bigio, E.H., Mesulam, M., Shen, Y., Xu, Q., Fushimi, K., and Wu, J.Y. (2011). An ALS-associated mutation affecting TDP-43 enhances protein aggregation, fibril formation and neurotoxicity. *Nat Struct Mol Biol.*, 18, 822-830.

Gurney, M.E., Pu, H.F., Chiu, A.Y., Dalcanto, M.C., Polchow, C.Y., Alexander, D.D., Caliendo, J., Hentati, A., Kwon, Y.W., and Deng, H.X. (1994). Motor neuron degeneration in mice that expresses a human Cu,Zn superoxide dismutase mutation. *Science.*, 264, 1772-1775.

Hafezparast, M., Klocke, R., Ruhrberg, C., Marquardt, A., Ahmad-Annuar, A., Bowen, S., Lalli, G., Witherden, A.S., Hummerich, H., Nicholson, S., Morgan, P.J., Oozageer, R., Priestley, J.V., Averill, S., King, V.R., Ball, S., Peters, J., Toda, T., Yamamoto, A., Hiraoka, Y., Augustin, M., Korthaus, D., Wattler, S., Wabnitz, P., Dickneite, C., Lampel, S., Boehme, F.,, Peraus, G., Popp, A., Rudelius, M., Schlegel, J., Fuchs, H., Hrabe de Angelis, M., Schiavo, G., Shima, D.T,, Russ, P., Stumm, G., Martin, J.E., and Fisher, E.M. (2003). Mutations in dynein link motor neuron degeneration to defects in retrograde transport. *Science*., 300, 808-812.

Hanson, K.A., Kim, S.H., Wassarman, D.A., and Tibbetts, R.S. (2010). Ubiquilin Modifies TDP-43 Toxicity in a Drosophila Model of Amyotrophic Lateral Sclerosis (ALS). *J Biol Chem*., 285, 11068-11072.

Hasegawa, M., Ara, T., Nonaka, T., Kametani, F., Yoshida, M., Hashizume, Y., Beach, T.G., Buratti, E., Baralle, F., Morita, M., Nakano, I., Oda, T., Tsuchiya, K., and Akiyama, H. (2008). Phosphorylated TDP-43 in frontotemporal lobar degeneration and amyotrophic lateral sclerosis. *Ann Neurol*., 64, 60-70.

Haverkamp., L.J., Appel., V., and Appel., S.H. (1995). Natural history of amyotrophic lateral sclerosis in a database population. *Brain*., 118, 707-719.

Heckman., C.J., and Enoka., R.M. (2004). Physiology of the motor neuron and the motor unit. In Clinical neurophysiology of motor neuron diseases, A. Eisen., ed. (B.V: Elsevier), pp. 119-147.

Hegedus, J., Putman, C.T., and Gordon, T. (2007). Time course of preferential motor unit loss in the SODIG93A mouse model of amyotrophic lateral sclerosis. *Neurobiol Dis*., 28, 154-164.

Hegedus, J., Putman, C.T., Tyreman, N., and Gordon, T. (2008). Preferential motor unit loss in the SOD1(G93A) transgenic mouse model of amyotrophic lateral sclerosis. *J Physiol*., 586, 3337-3351.

Henneman, E. (1957). Relation between size of neurons and susceptibility to discharge. *Science*., 126, 1345-1347.

Hicks, G.G., Singh, N., Nashabi, A., Mai, S., Bozek, G., Klewes, L., Arapovic, D., White, E.K., Koury, M.J., Oltz, E.M., Van Kaer, L., and Ruley, H.E. (2000). Fus deficiency in mice results in defective B-lymphocyte development and activation, high levels of chromosomal instability and perinatal death. *Nat Genet*., 24, 175-179.

Hoell, J.I., Larsson, E., Runge, S., Nusbaum, J.D., Duggimpudi, S., Farazi, T.A., Hafner, M., Borkhardt, A., Sander, C., and Tuschl, T. (2011). RNA targets of wild-type and mutant FET family proteins. *Nat Struct Mol Biol*., 18, 1428-1431.

Honda, D., Ishigaki, S., Iguchi, Y., Fujioka, Y., Udagawa, T., Masuda, A., Ohno, K., Katsuno, M., and Sobue, G. (2014). The ALS/FTLD-related RNA-binding proteins TDP-43 and FUS have common downstream RNA targets in cortical neurons. *Febs Open Bio*., 4, 1030-1030.

Hudson, A.J. (1981). Amyotrophic Lateral Sclerosis and its association with dementia, parkinsonism and other neurological disorders- a review. *Brain*., 104, 217-247.

Hwa, J.J., Hiller, M.A., Fuller, M.T., and Santel, A. (2002). Differential expression of the Drosophila mitofusin genes fuzzy onions (fzo) and dmfn. *Mech Dev*., 116, 213-216.

Igaz, L.M., Kwong, L.K., Xu, Y., Truax, A.C., Uryu, K., Neumann, M., Clark, C.M., Elman, L.B., Miller, B.L., Grossman, M., McCluskey, L.F., Trojanowski, J.Q., and Lee, V.M. (2008). Enrichment of C-terminal fragments in TAR DNA-binding protein-43 cytoplasmic inclusions in brain but not in spinal cord of frontotemporal lobar degeneration and amyotrophic lateral sclerosis. *Am J Pathol*., 173, 182-194.

Iguchi, Y., Katsuno, M., Niwa, J.-i., Takagi, S., Ishigaki, S., Ikenaka, K., Kawai, K., Watanabe, H., Yamanaka, K., Takahashi, R., Misawa, H., Sasaki, S., Tanaka, F., and Sobue, G. (2013). Loss of TDP-43 causes age-dependent progressive motor neuron degeneration. *Brain*., 136, 1371-1382.

Iko, Y., Kodama, T.S., Kasai, N., Oyama, T., Morita, E.H., Muto, T., Okumura, M., Fujii, R., Takumi, T., Tate, S., and Morikawa, K. (2004). Domain Architectures and characterization of an RNA-binding protein, TLS. J Biol Chem., 279, 44834-44840.

Ingre, C., Roos, P.M., Piehl, F., Kamel, F., and Fang, F. (2015). Risk factors for amyotrophic lateral sclerosis. *Clin Epidemiol*., 7, 181-193.

Ishigaki, S., Masuda, A., Fujioka, Y., Iguchi, Y., Katsuno, M., Shibata, A., Urano, F., Sobue, G., and Ohno, K. (2012). Position-dependent FUS-RNA interactions regulate alternative splicing events and transcriptions. *Sci Rep*., 2, 529.

Janssens, J., and Van Broeckhoven, C. (2013). Pathological mechanisms underlying TDP-43 driven neurodegeneration in FTLDALS spectrum disorders. *Hum Mol Genet*., 22, 77-87.

Jehle, T., Bauer, J., Blauth, E., Hummel, A., Darstein, M., Freiman, T.M., and Feuerstein, T.J. (2000). Effects of riluzole on electrically evoked neurotransmitter release. *Br J Pharmacol*., 130, 1227-1234.

Johnson, B.S., Snead, D., Lee, J.J., McCaffery, J.M., Shorter, J., and Gitler, A.D. (2009). TDP-43 Is Intrinsically Aggregation-prone, and Amyotrophic Lateral Sclerosis-linked Mutations Accelerate Aggregation and Increase Toxicity. *J Biol Chem*., 284, 20329-20339.

Jordan, H., Fagliano, J., Rechtman, L., Lefkowitz, D., and Kaye, W. (2015). Effects of Demographic Factors on Survival Time after a Diagnosis of Amyotrophic Lateral Sclerosis. *Neuroepidemiol*., 44, 114-120.

Jovicic, A., Mertens, J., Boeynaems, S., Bogaert, E., Chai, N., Yamada, S.B., Paul, J.W., III, Sun, S., Herdy, J.R., Bieri, G., Kramer, N.J., Gage, F.H., Van Den Bosch, L., Robberecht, W., and Gitler, A.D. (2015). Modifiers of C9orf72 dipeptide repeat toxicity connect nucleocytoplasmic transport defects to FTD/ALS. *Nat Neurosci*., 18, 1226.

Juneja, T., PericakVance, M.A., Laing, N.G., Dave, S., and Siddique, T. (1997). Prognosis in familial amyotrophic lateral sclerosis: Progression and survival in patients with glu100gly and ala4val mutations in Cu,Zn superoxide dismutase. *Neurology*., 48, 55-57.

Kabashi, E., Valdmanis, P.N., Dion, P., Spiegelman, D., McConkey, B.J., Velde, C.V., Bouchard, J.-P., Lacomblez, L., Pochigaeva, K., Salachas, F., Pradat, P.F., Camu, W., Meininger, V., Dupre, N., and Rouleau, G.A. (2008). TARDBP mutations in individuals with sporadic and familial amyotrophic lateral sclerosis. *Nat Genet*., 40, 572-574.

Kametani, F., Nonaka, T., Suzuki, T., Arai, T., Dohmae, N., Akiyama, H., and Hasegawa, M. (2009). Identification of casein kinase-1 phosphorylation sites on TDP-43. *Biochem Biophys Res Commun*., 382, 405-409.

Karsai, G., Pollak, E., Wacker, M., Vomel, M., Selcho, M., Berta, G., Nachman, R.J., Isaac, R.E., Molnar, L., and Wegener, C. (2013). Diverse in- and output polarities and high complexity of local synaptic and non-synaptic signaling within a chemically defined class of peptidergic Drosophila neurons. *Front Neural Circuits*., 7, 127-127.

Kawahara, Y., and Mieda-Sato, A. (2012). TDP-43 promotes microRNA biogenesis as a component of the Drosha and Dicer complexes. *Proc Natl Acad Sci USA*.,109, 3347-3352.

Keifer, O.P., Jr., O'Connor, D.M., and Boulis, N.M. (2014). Gene and protein therapies utilizing VEGF for ALS. *Pharmacol Ther*., 141, 261-271.

Kikuchi, H., Almer, G., Yamashita, S., Guegan, C., Nagai, M., Xu, Z.S., Sosunov, A.A., McKhann, G.M., and Przedborski, S. (2006). Spinal cord endoplasmic reticulum stress associated with a microsomal accumulation of mutant superoxide dismutase-1 in an ALS model. *Proc Natl Acad Sci USA*., 103, 6025-6030.

Kim, S.H., Shanware, N.P., Bowler, M.J., and Tibbetts, R.S. (2010). Amyotrophic Lateral Sclerosis-associated Proteins TDP-43 and FUS/TLS Function in a Common Biochemical Complex to Co-regulate HDAC6 mRNA. *J Biol Chem*., 285, 34097-34105.

Koppers, M., Blokhuis, A.M., Westeneng, H.-J., Terpstra, M.L., Zundel, C.A.C., de Sa, R.V., Schellevis, R.D., Waite, A.J., Blake, D.J., Veldink, J.H., van den Berg, L.H., and Pasterkamp, R.J. (2015). C9orf72 ablation in mice does not cause motor neuron degeneration or motor deficits. *Ann Neurol*., 78, 426-438.

Kraemer, B.C., Schuck, T., Wheeler, J.M., Robinson, L.C., Trojanowski, J.Q., Lee, V.M.Y., and Schellenberg, G.D. (2010). Loss of murine TDP-43 disrupts motor function and plays an essential role in embryogenesis. *Acta Neuropathol.*, 119, 409-419.

Krakora, D., Macrander, C., and Suzuki, M. (2012). Neuromuscular junction protection for the potential treatment of amyotrophic lateral sclerosis. *Neurol Res Int.*, 2012, 379657-379657.

Krieger, C., Hu, J.H., and Pelech, S. (2003). Aberrant protein kinases and phosphoproteins in amyotrophic lateral sclerosis. *Trends Pharmacol Sci.*, 24, 535-541.

Kumar, D.R., Aslinia, F., Yale, S.H., and Mazza, J.J. (2011). Jean-Martin Charcot: the father of neurology. *Clinical Med Res.*, 9, 46-49.

Kuo, P.-H., Doudeva, L.G., Wang, Y.-T., Shen, C.-K.J., and Yuan, H.S. (2009). Structural insights into TDP-43 in nucleic-acid binding and domain interactions. Nucleic Acids Research 37, 1799-1808.

Kuroda, M., Sok, J., Webb, L., Baechtold, H., Urano, F., Yin, Y., Chung, P., de Rooij, D.G., Akhmedov, A., Ashley, T., and Ron, D. (2000). Male sterility and enhanced radiation sensitivity in TLS-/- mice. *EMBO J.*, 19, 453-462.

Kuwabara, S., Sonoo, M., Komori, T., Shimizu, T., Hirashima, F., Inaba, A., Misawa, S., Hatanaka, Y., and Tokyo Metropolitan Neuromuscular, E. (2008). Dissociated small hand muscle atrophy in amyotrophic lateral sclerosis: Frequency, extent, and specificity. *Muscle Nerve.*, 37, 426-430.

Kuznicki, M.L., and Gunawardena, S. (2010). In vivo visualization of synaptic vesicles within Drosophila larval segmental axons. *J Vis Exp.*, 44, 2451.

Kwiatkowski, T.J., Jr., Bosco, D.A., LeClerc, A.L., Tamrazian, E., Vanderburg, C.R., Russ, C., Davis, A., Gilchrist, J., Kasarskis, E.J., Munsat, T., Valdmanis, P., Rouleau, G.A., Hosler, B.A., Cortelli, P., de Jong, P.J., Yoshinaga, Y., Haines, J.L., Pericak-Vance, M.A., Yan, J., Ticozzi, N., Siddique, T., McKenna-Yasek, D., Sapp, P.C., Horvitz, H.R., Landers, J.E, and Brown, R.H Jr. (2009). Mutations in the FUS/TLS Gene on Chromosome 16 Cause Familial Amyotrophic Lateral Sclerosis. *Science.*, 323, 1205-1208.

Kwon, I., Xiang, S., Kato, M., Wu, L., Theodoropoulos, P., Wang, T., Kim, J., Yun, J., Xie, Y., and McKnight, S.L. (2014). Poly-dipeptides encoded by the C9orf72 repeats bind nucleoli impede RNA biogenesis and kill cells. *Science.*, 345, 1139-1145.

Lagier-Tourenne, C., Baughn, M., Rigo, F., Sun, S., Liu, P., Li, H.-R., Jiang, J., Watt, A.T., Chun, S., Katz, M., Qiu, J., Sun, Y., Ling, S.C., Zhu., Q., Polymenidou, M., Drenner, K., Artates, J.W., McAlonis-Downes, M., Markmiller, S., Hutt, K.R., Pizzo, D.P., Cady, J., Harms, M.B., Baloh, R.H., Vandenberg, S.R., Yeo, G.W., Fu, X.D., Bennett, C.F., Cleveland D,W., and Ravits J. (2013). Targeted degradation of sense and antisense C9orf72 RNA foci as therapy for ALS and frontotemporal degeneration. *Proc Natl Acad Sci USA*.,110, 4530-4539.

Lagier-Tourenne, C., Polymenidou, M., and Cleveland, D.W. (2010). TDP-43 and FUS/TLS: emerging roles in RNA processing and neurodegeneration. *Hum Mol Genet*., 19, 46-64.

Lagier-Tourenne, C., Polymenidou, M., Hutt, K.R., Vu, A.Q., Baughn, M., Huelga, S.C., Clutario, K.M., Ling, S.-C., Liang, T.Y., Mazur, C., Wancewicz, E., Kim, A.S., Watt, A., Freier, S., Hicks, G.G., Donohue, J.P., Shiue, L., Bennett, C.F., Ravits, J., Cleveland, D.W., and Yeo, G.W. (2012). Divergent roles of ALS-linked proteins FUS/TLS and TDP-43 intersect in processing long pre-mRNAs. *Nat Neurosci*., 15, 1488-1497.

Lalmansingh, A.S., Urekar, C.J., and Reddi, P.P. (2011). TDP-43 Is a Transcriptional Repressor of the testis specific factor mouse acrv1 gene is a TDP-43 target in vivo. *J Biol Chem*., 286, 10970-10982.

LaMonte, B.H., Wallace, K.E., Holloway, B.A., Shelly, S.S., Ascano, J., Tokito, M., Van Winkle, T., Howland, D.S., and Holzbaur, E.L.F. (2002). Disruption of dynein/dynactin inhibits axonal transport in motor neurons causing late-onset progressive degeneration. *Neuron*., 34, 715-727.

Lanson, N.A., Jr., Maltare, A., King, H., Smith, R., Kim, J.H., Taylor, J.P., Lloyd, T.E., and Pandey, U.B. (2011). A Drosophila model of FUS-related neurodegeneration reveals genetic interaction between FUS and TDP-43. *Hum Mol Genet*., 20, 2510-2523.

Lee, Y.-B., Chen, H.-J., Peres, J.N., Gomez-Deza, J., Attig, J., Stalekar, M., Troakes, C., Nishimura, A.L., Scotter, E.L., Vance, C., Adachi, Y., Sardone, V., Miller, J.W., Smith, B.N., Gallo, J.M., Ule, J., Hirth, F., Rogelj, B., Houart, C., and Shaw, C.E. (2013). Hexanucleotide Repeats in ALS/FTD Form Length-Dependent RNA Foci, Sequester RNA Binding Proteins, and Are Neurotoxic. *Cell Rep*., 5, 1178-1186.

Lerga, A., Hallier, M., Delva, L., Orvain, C., Gallais, I., Marie, J., and Moreau-Gachelin, F. (2001). Identification of an RNA binding specificity for the potential splicing factor TLS. J Biol Chem., 276, 6807-6816.

Levine, T.P., Daniels, R.D., Gatta, A.T., Wong, L.H., and Hayes, M.J. (2013). The product of C9orf72, a gene strongly implicated in neurodegeneration, is structurally related to DENN Rab-GEFs. *Bioinformatics*., 29, 499-503.

Li, Q., Yokoshi, M., Okada, H., and Kawahara, Y. (2015). The cleavage pattern of TDP-43 determines its rate of clearance and cytotoxicity. *Nat Commun*., 6. 6183.

Li, Y., Ray, P., Rao, E.J., Shi, C., Guo, W.R., Chen, X.P., Woodruff, E.A., Fushimi, K., and Wu, J.Y. (2010). A Drosophila model for TDP-43 proteinopathy. *Proc Natl Acad Sci USA*., 107, 3169-3174.

Limousin, N., Blasco, H., Corcia, P., Gordon, P.H., De Toffol, B., Andres, C., and Praline, J. (2010). Malnutrition at the time of diagnosis is associated with a shorter disease duration in ALS. *J Neurol Sci*., 297, 36-39.

Lin, D.M. and Goodman, C.S., (1994). Ectopic and increased expression of fasciclin II alters motorneuron growth cone guidance. *Neuron*. 13, 507-523.

Lin, M.-J., Cheng, C.-W., and Shen, C.K.J. (2011). Neuronal Function and Dysfunction of Drosophila dTDP. *PLoS One*., 6, 20371.

Lindquist, S. (1981).Regulation of protein synthesis during heat shock. *Nature*., 293, 311-314.

Ling, S.-C., Albuquerque, C.P., Han, J.S., Lagier-Tourenne, C., Tokunaga, S., Zhou, H., and Cleveland, D.W. (2010). ALS-associated mutations in TDP-43 increase its stability and promote TDP-43 complexes with FUS/TLS. *Proc Natl Acad Sci USA*., 107, 13318-13323.

Ling, S-C., Polymenidou, M., and Cleveland, D.W. (2013). Converging mechanisms in ALS and FTD: Disrupted RNA and protein homeostasis. *Neuron*. 79, 416-438.

Liu, E.Y., Russ, J., Wu, K., Neal, D., Suh, E., McNally, A.G., Irwin, D.J., Van Deerlin, V.M., and Lee, E.B. (2014). C9orf72 hypermethylation protects against repeat expansion-associated pathology in ALS/FTD. *Acta Neuropathol*., 128, 525-541.

Liu-Yesucevitz, L., Bilgutay, A., Zhang, Y.-J., Vanderwyde, T., Citro, A., Mehta, T., Zaarur, N., McKee, A., Bowser, R., Sherman, M., Petrucelli, L., and Wolozin, B. (2010). Tar DNA Binding Protein-43 (TDP-43) Associates with Stress Granules: Analysis of Cultured Cells and Pathological Brain Tissue. *PLoS One*., 5, 13250.

Logroscino, G., Traynor, B.J., Hardiman, O., Chio, A., Mitchell, D., Swingler, R.J., Millul, A., Benn, E., Beghi, E., and Eurals (2010). Incidence of amyotrophic lateral sclerosis in Europe. *J Neurol Neurosurg Psychiatry*., 81, 385-390.

Machamer, J.B., Collins, S.E., and Lloyd, T.E. (2014). The ALS gene FUS regulates synaptic transmission at the Drosophila neuromuscular junction. *Hum Mol Genet*., 23, 3810-3822.

Mackenzie, I.R., Arzberger, T., Kremmer, E., Troost, D., Lorenzl, S., Mori, K., Weng, S.-M., Haass, C., Kretzschmar, H.A., Edbauer, D., and Neumann, M. (2013). Dipeptide repeat protein pathology in C9ORF72 mutation cases: clinico-pathological correlations. *Acta Neuropathol*., 126, 859-879.

Mackenzie, I.R.A., Foti, D., Woulfe, J., and Hurwitz, T.A. (2008). Atypical frontotemporal lobar degeneration with ubiquitin-positive, TDP-43-negative neuronal inclusions. *Brain*., 131, 1282-1293.

Mackenzie, I.R.A., Munoz, D.G., Kusaka, H., Yokota, O., Ishihara, K., Roeber, S., Kretzschmar, H.A., Cairns, N.J., and Neumann, M. (2011). Distinct pathological subtypes of FTLD-FUS. *Acta Neuropathol.*, 121, 207-218.

Mackenzie, I.R.A., Neumann, M., Bigio, E.H., Cairns, N.J., Alafuzoff, I., Kril, J., Kovacs, G.G., Ghetti, B., Halliday, G., Holm, I.E., Ince, P.G., Kamphorst, W., Revesz, T., Rozemuller, A.J., Kumar-Singh, S., Akiyama, H., Baborie, A., Spina, S., Dickson, D.W,, Trojanowski, J.Q., and Mann, D.M. (2010). Nomenclature and nosology for neuropathologic subtypes of frontotemporal lobar degeneration: an update. *Acta Neuropathol.*, 119, 1-4.

Magnus, T., Beck, M., Giess, R., Puls, I., Naumann, M., and Toyka, K.V. (2002). Disease progression in amyotrophic lateral sclerosis: Predictors of survival. *Muscle Nerve.*, 25, 709-714.

Magrane, J., Cortez, C., Gan, W.-B., and Manfredi, G. (2014). Abnormal mitochondrial transport and morphology are common pathological denominators in SOD1 and TDP43 ALS mouse models. *Hum Mol Genet.*, 23, 1413-1424.

Malek, A.M., Barchowsky, A., Bowser, R., Heiman-Patterson, T., Lacomis, D., Rana, S., Youk, A., Stickler, D., Lackland, D.T., and Talbott, E.O. (2014). Environmental and Occupational Risk Factors for Amyotrophic Lateral Sclerosis: A Case-Control Study. *Neurodegener Dis.*, 14, 31-38.

Maniecka, Z., and Polymenidou, M. (2015). From nucleation to widespread propagation: A prion-like concept for ALS. *Virus Res.*, 207, 94-105.

Maraldi, T., Riccio, M., Zambonin, L., Vinceti, M., De Pol, A., and Hakim, G. (2011). Low levels of selenium compounds are selectively toxic for a human neuron cell line through ROS/RNS increase and apoptotic process activation. *Neurotoxicol.*, 32, 180-187.

Marangi, G., and Traynor, B.J. (2015). Genetic causes of amyotrophic lateral sclerosis: New genetic analysis methodologies entailing new opportunities and challenges. *Brain Res.*, 1607, 75-93.

Marinkovic, P., Reuter, M.S., Brill, M.S., Godinho, L., Kerschensteiner, M., and Misgeld, T. (2012). Axonal transport deficits and degeneration can evolve independently in mouse models of amyotrophic lateral sclerosis. *Proc Natl Acad Sci USA.*, 109, 4296-4301.

Maris, C., Dominguez, C., and Allain, F.H.T. (2005). The RNA recognition motif, a plastic RNA-binding platform to regulate post-transcriptional gene expression. *Febs J.*, 272, 2118-2131.

May, S., Hornburg, D., Schludi, M.H., Arzberger, T., Rentzsch, K., Schwenk, B.M., Graesser, F.A., Mori, K., Kremmer, E., Banzhaf-Strathmann, J., Mann, M., Meissner, F., and Edbauer, D. (2014). C9orf72 FTLD/ALS-associated Gly-Ala dipeptide repeat proteins cause neuronal toxicity and Unc119 sequestration. *Acta Neuropathol.*, 128, 485-503.

McCombe, P.A., and Henderson, R.D. (2010). Effects of Gender in Amyotrophic Lateral Sclerosis. *Gend Med*., 7, 557-570.

McCord, J.M., and Fridovich, I. (1969). Superoxide dismutase and enzymatic function for erythrocuprein (hemocuprein). *J Biol Chem*., 244, 6049.

McDonald, K.K., Aulas, A., Destroismaisons, L., Pickles, S., Beleac, E., Camu, W., Rouleau, G.A., and Velde, C.V. (2011). TAR DNA-binding protein 43 (TDP-43) regulates stress granule dynamics via differential regulation of G3BP and TIA-1. *Hum Mol Genet*., 20, 1400-1410.

McGuire, S.E., Le, P.T., Osborn, A.J., Matsumoto, K., and Davis, R.L. (2003). Spatiotemporal rescue of memory dysfunction in Drosophila. *Science*., 302, 1765-1768.

Mehta, P., Antao, V., Kaye, W., Sanchez, M., Williamson, D., Bryan, L., Muravov, O., and Horton, K. (2014). Prevalence of Amyotrophic Lateral Sclerosis - United States, 2010-2011. *MMWR Surveill Summ*., 63, 1-13.

Meissner, M., Lopato, S., Gotzmann, J., Sauermann, G., and Barta, A. (2003). Proto-oncoprotein TLS/FUS is associated to the nuclear matrix and complexed with splicing factors PTB, SRm160, and SR proteins. *Exp Cell Res*., 283, 184-195.

Miguel, L., Frebourg, T., Campion, D., and Lecourtois, M. (2011). Both cytoplasmic and nuclear accumulations of the protein are neurotoxic in Drosophila models of TDP-43 proteinopathies. *Neurobiol Dis*., 41, 398-406.

Millecamps, S., and Julien, J.-P. (2013). Axonal transport deficits and neurodegenerative diseases. *Nat Rev Neurosci*., 14, 161-176.

Miller, K.E., DeProto, J., Kaufmann, N., Patel, B.N., Duckworth, A., and Van Vactor, D. (2005). Direct observation demonstrates that liprin-alpha is required for trafficking of synaptic vesicles. *Curr Biol*., 15, 684-689.

Miller, K.E., and Sheetz, M.P. (2004). Axonal mitochondrial transport and potential are correlated. *J Cell Sci*., 117, 2791-2804.

Miller, R.G., Mitchell, J.D., and Moore, D.H. (2012). Riluzole for amyotrophic lateral sclerosis (ALS)/motor neuron disease (MND). *Cochrane Database Syst Rev*., 14, 3.

Miller, R.G., Munsat, T.L., Swash, M., and Brooks, B.R. (1999). Consensus guidelines far the design and implementation of clinical trials in ALS. *J Neurol Sci*., 169, 2-12.

Mizielinska, S., Groenke, S., Niccoli, T., Ridler, C.E., Clayton, E.L., Devoy, A., Moens, T., Norona, F.E., Woollacott, I.O.C., Pietrzyk, J., Cleverley, K., Nicoll, A.J., Pickering-Brown, S., Dols, J., Cabecinha, M., Hendrich, O., Fratta, P., Fisher, E.M., Partridge, L., and Isaacs, A.M. (2014). C9orf72 repeat expansions cause neurodegeneration in Drosophila through arginine-rich proteins. *Science*., 345, 1192-1194.

Moloney, E.B., de Winter, F., and Verhaagen, J. (2014). ALS as a distal axonopathy: molecular mechanisms affecting neuromuscular junction stability in the presymptomatic stages of the disease. *Front Neurosci*., 8, 252.

Mondola, P., Ruggiero, G., Seru, R., Damiano, S., Grimaldi, S., Garbi, C., Monda, M., Greco, D., and Santillo, M. (2003). The Cu,Zn superoxide dismutase in neuroblastoma SK-N-BE cells is exported by a microvesicles dependent pathway. *Mol Brain Res*., 110, 45-51.

Morfini, G.A., Bosco, D.A., Brown, H., Gatto, R., Kaminska, A., Song, Y., Molla, L., Baker, L., Marangoni, M.N., Berth, S., Tavassoli, E., Bagnato, C., Tiwari, A., Hayward, L.J., Pigino, G.F., Watterson, D.M., Huang, C.F., Banker, G., Brown, R.H. Jr., and Brady ST. (2013). Inhibition of Fast Axonal Transport by Pathogenic SOD1 Involves Activation of p38 MAP Kinase. *PLoS One*., 8, 65235.

Morfini, G.A., You, Y-M., Pollema, S.L., Kaminska, A., Liu, K., Yoshioka, K., Bjorkblom, B., Coffey, E.T., Bagnato, C., Han, C., Huang, C-F., Banker, G., Pignino, G., and Brady, S.T. (2009). Pathogenic huntingtin inhibits fast axonal transport by activating JNK3 and phosphorylating kinesin. *Nat Neurosci*., 12, 864-871.

Mori, K., Lammich, S., Mackenzie, I.R.A., Forne, I., Zilow, S., Kretzschmar, H., Edbauer, D., Janssens, J., Kleinberger, G., Cruts, M., Herms, J., Neumann, M., Van Broeckhoven, C., Arzberger, T., and Haass, C. (2013a). hnRNP A3 binds to GGGGCC repeats and is a constituent of p62-positive/TDP43-negative inclusions in the hippocampus of patients with C9orf72 mutations. *Acta Neuropathol*., 125, 413-423.

Mori, K., Weng, S.-M., Arzberger, T., May, S., Rentzsch, K., Kremmer, E., Schmid, B., Kretzschmar, H.A., Cruts, M., Van Broeckhoven, C., Haass, C., and Edbauer, D. (2013b). The C9orf72 GGGGCC Repeat Is Translated into Aggregating Dipeptide-Repeat Proteins in FTLD/ALS. *Science*., 339, 1335-1338.

Morlando, M., Modigliani, S.D., Torrelli, G., Rosa, A., Di Carlo, V., Caffarelli, E., and Bozzoni, I. (2012). FUS stimulates microRNA biogenesis by facilitating co-transcriptional Drosha recruitment. *EMBO J*., 31, 4502-4510.

Mudher, A., Shepherd, D., Newman, T.A., Mildren, P., Jukes, J.P., Squire, A., Mears, A., Drummond, J.A., Berg, S., MacKay, D., Asuni, A.A., Bhat, R., and Lovestone, S. (2004). GSK-3 beta inhibition reverses axonal transport defects and behavioural phenotypes in Drosophila. *Mol Psychiatry*., 9, 812-812.

Nagai, M., Re, D.B., Nagata, T., Chalazonitis, A., Jessell, T.M., Wichterle, H., and Przedborski, S. (2007). Astrocytes expressing ALS-linked mutated SOD1 release factors selectively toxic to motor neurons. *Nat Neurosci*., 10, 615-622.

Nakata, M., Kuwabara, S., Kanai, K., Misawa, S., Tamura, N., Sawai, S., Hattori, T., and Bostock, H. (2006). Distal excitability changes in motor axons in amyotrophic lateral sclerosis. *Clin Neurophysiol*., 117, 1444-1448.

Neumann, M., Rademakers, R., Roeber, S., Baker, M., Kretzschmar, H.A., and Mackenzie, I.R.A. (2009). A new subtype of frontotemporal lobar degeneration with FUS pathology. *Brain*., 132, 2922-2931.

Neumann, M., Sampathu, D.M., Kwong, L.K., Truax, A.C., Micsenyi, M.C., Chou, T.T., Bruce, J., Schuck, T., Grossman, M., Clark, C.M., McCluskey, L.F., Miller, B.L., Masliah, E., Mackenzie, I.R., Feldman, H., Feiden, W., Kretzschmar, H.A., Trojanowski, J.Q., and Lee, V.M. (2006). Ubiquitinated TDP-43 in frontotemporal lobar degeneration and amyotrophic lateral sclerosis. *Science*., 314, 130-133.

Nichols, R., Kaminski, S., Walling, E., and Zornik, E. (1999). Regulating the activity of a cardioacceleratory peptide. *Peptides*., 20, 1153-1158.

Nzwalo, H., de Abreu, D., Swash, M., Pinto, S., and de Carvalho, M. (2014). Delayed diagnosis in ALS: The problem continues. *J Neurol Sci*., 343, 173-175.

Okamoto, K., Hirai, S., Shoji, M., Senoh, Y., and Yamazaki, T. (1990). Axonal swellings in the cortiospinal tracts in Amyotrophic Lateral Sclerosis. *Acta Neuropathol*., 80, 222-226.

Okamoto, K., Mizuno, Y., and Fujita, Y. (2008). Bunina bodies in amyotrophic lateral sclerosis. *Neuropathol*., 28, 109-115.

Onyike, C.U., and Diehl-Schmid, J. (2013). The epidemiology of frontotemporal dementia. *Int Rev Psychiatry*., 25, 130-137.

Ou, S.H.I., Wu, F., Harrich, D., Garcia-Martinez, L.F., and Gaynor, R.G. (1995). Cloning and characterization of a novel cellular protein, TDP-43, that binds to human immunodeficiency virus type 1 TAR DNA sequence motifs. *J Virol*., 69, 3584-3596.

Park, J.H., Schroeder, A.J., Helfrich-Forster, C., Jackson, F.R., and Ewer, J. (2003). Targeted ablation of CCAP neuropeptide-containing neurons of Drosophila causes specific defects in execution and circadian timing of ecdysis behavior. *Development*., 130, 2645-2656.

Parker, S.J., Meyerowitz, J., James, J.L., Liddell, J.R., Crouch, P.J., Kanninen, K.M., and White, A.R. (2012). Endogenous TDP-43 localized to stress granules can subsequently form protein aggregates. *Neurochem Int*., 60, 415-424.

Pasinelli, P., and Brown, R.H. (2006). Molecular biology of amyotrophic lateral sclerosis: insights from genetics. *Nat Rev Neurosci*., 7, 710-723.

Pesiridis, G.S., Lee, V.M.Y., and Trojanowski, J.Q. (2009). Mutations in TDP-43 link glycine-rich domain functions to amyotrophic lateral sclerosis. *Hum Mol Genet*., 18, R156-R162.

Pigino, G., Morfini, G., Pelsman, A., Mattson, M.P., Brady, S.T., and Buscigilo, J. (2003). Alzheimer's presenilin 1 mutations impair kinesin-based axonal transport. J Neurosci., 11, 4499-4508.

Pilling, A.D., Horiuchi, D., Lively, C.M., and Saxton, W.M. (2006). Kinesin-1 and dynein are the primary motors for fast transport of mitochondria in Drosophila motor axons. *Mol Biol Cell*., 17, 2057-2068.

Polymenidou, M., and Cleveland, D.W. (2011). The Seeds of Neurodegeneration: Prion-like Spreading in ALS. *Cell*., 147, 498-508.

Polymenidou, M., Lagier-Tourenne, C., Hutt, K.R., Huelga, S.C., Moran, J., Liang, T.Y., Ling, S.-C., Sun, E., Wancewicz, E., Mazur, C., Kordasiewicz, H., Sedaghat, Y., Donohue, J.P., Shiue, L., Bennett, C.F., Yeo, G.W., and Cleveland, D.W. (2011). Long pre-mRNA depletion and RNA missplicing contribute to neuronal vulnerability from loss of TDP-43. *Nat Neurosci*., 14, 459-U492.

Pun, S., Santos, A.F., Saxena, S., Xu, L., and Caroni, P. (2006). Selective vulnerability and pruning of phasic motoneuron axons in motoneuron disease alleviated by CNTF. *Nat Neurosci*., 9, 408-419.

Rabbitts, T.H., Forster, A., Larson, R., and Nathan, P. (1993). Fusion of the dominant negative transcription regulator CHOP with a novel gene FUS translocation T(12-16) in malignant liposarcoma. *Nat Genet*., 4, 175-180.

Reaume, A.G., Elliott, J.L., Hoffman, E.K., Kowall, N.W., Ferrante, R.J., Siwek, D.F., Wilcox, H.M., Flood, D.G., Beal, M.F., Brown, R.H., Scott, R.W., and Snider, W.D. (1996). Motor neurons in Cu/Zn superoxide dismutase-deficient mice develop normally but exhibit enhanced cell death after axonal injury. *Nat Genet*., 13, 43-47.

Reid, E., Kloos, M., Ashley-Koch, A., Hughes, L., Bevan, S., Svenson, I.K., Graham, F.L., Gaskell, P.C., Dearlove, A., Pericak-Vance, M.A., Rubinsztein, D.C., and Marchuk, D.A. (2002). A kinesin heavy chain (KIF5A) mutation in hereditary spastic paraplegia (SPG10). *Am J Hum Genet*., 71, 1189-1194.

Renton, A.E., Chio, A., and Traynor, B.J. (2014). State of play in amyotrophic lateral sclerosis genetics. *Nat Neurosci*., 17, 17-23.

Renton, A.E., Majounie, E., Waite, A., Simon-Sanchez, J., Rollinson, S., Gibbs, J.R., Schymick, J.C., Laaksovirta, H., van Swieten, J.C., Myllykangas, L., Kalimo, H., Paetau, A., Abramzon, Y., Remes, A.M., Kaganovich, A., Scholz, S.W., Duckworth, J., Ding, J., Harmer, D.W., Hernandez, D.G., Johnson, J.O., Mok, K., Ryten, M., Trabzuni, D., Guerreiro, R.J., Orrell, R.W., Neal, J., Murray, A., Pearson, J., Jansen, I.E., Sondervan, D., Seelaar, H., Blake, D., Young, K., Halliwell, N., Callister, J.B., Toulson, G., Richardson, A., Gerhard, A., Snowden, J., Mann, D., Neary, D., Nalls, M.A., Peuralinna, T., Jansson, L., Isoviita, V.M., Kaivorinne, A.L., Hölttä-Vuori, M., Ikonen, E., Sulkava, R., Benatar, M., Wuu, J., Chiò, A., Restagno, G., Borghero, G., Sabatelli, M. ; ITALSGEN Consortium, Heckerman, D., Rogaeva, E., Zinman, L., Rothstein, J.D., Sendtner, M., Drepper, C., Eichler, E.E., Alkan, C., Abdullaev, Z., Pack, S.D., Dutra, A., Pak, E., Hardy, J., Singleton, A., Williams, N.M., Heutink, P., Pickering-Brown, S., Morris, H.R., Tienari, P.J., and Traynor BJ. (2011). A Hexanucleotide Repeat Expansion in C9ORF72 Is the Cause of Chromosome 9p21-Linked ALS-FTD. *Neuron*., 72, 257-268.

Riku, Y., Atsuta, N., Yoshida, M., Tatsumi, S., Iwasaki, Y., Mimuro, M., Watanabe, H., Ito, M., Senda, J., Nakamura, R., Koike, H., and Sobue, G. (2014). Differential motor neuron involvement in progressive muscular atrophy: a comparative study with amyotrophic lateral sclerosis. *BMJ Open*., 4, 5213.

Ritson, G.P., Custer, S.K., Freibaum, B.D., Guinto, J.B., Geffel, D., Moore, J., Tang, W.X., Winton, M.J., Neumann, M., Trojanowski, J.Q., Lee, V.M., Forman, M.S., and Taylor, J.P. (2010). TDP-43 Mediates Degeneration in a Novel Drosophila Model of Disease Caused by Mutations in VCP/p97. *J Neurosci*., 30, 7729-7739.

Rizzuto, R., Brini, M., Pizzo, P., Murgia, M., and Pozzan, T. (1995). Chimeric green fluorescent protein as a tool for visualising subcellular organelles in living cells. *Curr Biol*., 5, 635-642.

Robberecht, W., Aguirre, T., VandenBosch, L., Tilkin, P., Cassiman, J.J., and Matthijs, G. (1996). D90A heterozygosity in the SOD1 gene is associated with familial and apparently sporadic amyotrophic lateral sclerosis. *Neurology*., 47, 1336-1339.

Robberecht, W., and Philips, T. (2013). The changing scene of amyotrophic lateral sclerosis. *Nat Rev Neurosci*., 14, 248-264.

Rogelj, B., Easton, L.E., Bogu, G.K., Stanton, L.W., Rot, G., Curk, T., Zupan, B., Sugimoto, Y., Modic, M., Haberman, N., Tollervey, J., Fujii, R., Takumi, T., Shaw, C.E., and Ule, J. (2012). Widespread binding of FUS along nascent RNA regulates alternative splicing in the brain. *Sci Rep*., 2, 603.

Rohrer, J.D., Isaacs, A.M., Mizlienska, S., Mead, S., Lashley, T., Wray, S., Sidle, K., Fratta, P., Orrell, R.W., Hardy, J., Holton, J., Revesz, T., Rossor, M.N., and Warren, J.D. (2015). C9orf72 expansions in frontotemporal dementia and amyotrophic lateral sclerosis. *Lancet Neurol*., 14, 291-301.

Romano, M., Buratti, E., Romano, G., Klima, R., Belluz, L.D.B., Stuani, C., Baralle, F., and Feiguin, F. (2014). Evolutionarily Conserved Heterogeneous Nuclear Ribonucleoprotein (hnRNP) A/B Proteins Functionally Interact with Human and Drosophila TAR DNA-binding Protein 43 (TDP-43). *J Biol Chem*., 289, 7121-7130.

Romano, M., Feiguin, F., and Buratti, E. (2012). Drosophila Answers to TDP-43 Proteinopathies. *J Amino Acids*., 2012, 356081-356081.

Rosen, D.R., Siddique, T., Patterson, D., Figlewicz, D.A., Sapp, P., Hentati, A., Donaldson, D., Goto, J., Oregan, J.P., Deng, H.X., Rahmani, Z., Krizus, A., McKenna-Yasek, D., Cayabyb, A., Gaston, S.M., Berger, R., Tanzi, R.E., Halperin, J.J., Herzfeldt, B., Van Den Bergh, R., Hung, W-Y., Bird, T., Deng, G., Mulder, D.W., Smyth, C., Laing, N.G., Soriano, E., Pericak-Vance, M.A., Haines, J., Rouleau, G.A., Gusella, J.S., Horvitz, H.R., and Brown Jr, R.H. (1993). Mutations in Cu/Zn superoxide-dismutase gene are associated with familial Amyotrophic Lateral Sclerosis. *Nature*., 362, 59-62.

Rothstein, J.D., DykesHoberg, M., Pardo, C.A., Bristol, L.A., Jin, L., Kuncl, R.W., Kanai, Y., Hediger, M.A., Wang, Y.F., Schielke, J.P., and Welty, D.F. (1996). Knockout of glutamate transporters reveals a major role for astroglial transport in excitotoxicity and clearance of glutamate. *Neuron*., 16, 675-686.

Rotunno, M.S., and Bosco, D.A. (2013). An emerging role for misfolded wild-type SOD1 in sporadic ALS pathogenesis. *Front Cell Neurosci*., 7, 253.

Rulten, S.L., Rotheray, A., Green, R.L., Grundy, G.J., Moore, D.A.Q., Gomez-Herreros, F., Hafezparast, M., and Caldecott, K.W. (2014). PARP-1 dependent recruitment of the amyotrophic lateral sclerosis-associated protein FUS/TLS to sites of oxidative DNA damage. *Nucleic Acids Res*., 42, 307-314.

Sabatelli, M., Madia, F., Conte, A., Luigetti, M., Zollino, M., Mancuso, I., Lo Monaco, M., Lippi, G., and Tonali, P. (2008). Natural history of young-adult amyotrophic lateral sclerosis. *Neurology*., 71, 876-881.

Saeed, M., Yang, Y., Deng, H.X., Hung, W.Y., Siddique, N., Dellefave, L., Gellera, C., Andersen, P.M., and Siddique, T. (2009). Age and founder effect of SOD1 A4V mutation causing ALS. *Neurology*., 72, 1634-1639.

Salehi, A., Delcroix, J-D., Belichenko, P.V., Zhan, K., Wu, C., Valletta, J.S., Takimoto-Kimura, R., Kleschevnikov, A.M., Sambamurti, K., Chung, P.P., Xia, W., Villar, A., Campbell, W.A., Kulnane, L.S., Nixon, R.A., Lamb, B.T., Epstein, C.J., Stokin, G.B., Goldstein, L.S.B., and Mobley, W.C. (2006). Increased App expression in a mouse model of Down's syndrome disrupts NGF transport and causes cholingeric neuron degeneration. *Neuron*., 51, 29-42.

Sandoval, H., Yao, C-K., Chen, K., Jaiswal, M., Donti, T., Lin, Y-Q., Bayat, V., Xiong, B., Zhang, K., David, G., Charng, W-L., Shinya, Y., Duraine, L., Graham, B-H. and Bellen, H-J. (2014). Mitochondrial fusion but not fission regulates larval growth and synaptic development through steroid hormone production. *eLife*. 3.

Santos, J.G., Voemel, M., Struck, R., Homberg, U., Nassel, D.R., and Wegener, C. (2007). Neuroarchitecture of Peptidergic Systems in the Larval Ventral Ganglion of Drosophila melanogaster. *PLoS One*., 2, 695.

Sareen, D., O'Rourke, J.G., Meera, P., Muhammad, A.K.M.G., Grant, S., Simpkinson, M., Bell, S., Carmona, S., Ornelas, L., Sahabian, A., Gendron, T., Petrucelli, L., Baughn, M., Ravits, J., Harms, M.B., Rigo, F., Bennett, C.F., Otis, T.S., Svendsen, C.N., and Baloh, R.H. (2013). Targeting RNA Foci in iPSC-Derived Motor Neurons from ALS Patients with a C9ORF72 Repeat Expansion. *Sci Transl Med*., 5, 208.

Sasaki, S., Maruyama, S., Yamane, K., Sakuma, H., and Takeishi, M. (1990). Ultrastructure of swollen proximal axons of anterior horn neurons of motor neuron disease. *J Neurol Sci*., 97, 233-240.

Sasayama, H., Shimamura, M., Tokuda, T., Azuma, Y., Yoshida, T., Mizuno, T., Nakagawa, M., Fujikake, N., Nagai, Y., and Yamaguchi, M. (2012). Knockdown of the Drosophila Fused in Sarcoma (FUS) Homologue Causes Deficient Locomotive Behavior and Shortening of Motoneuron Terminal Branches. *PLoS One*., 7. 39483.

Schwarz, T.L. (2013). Mitochondrial trafficking in neurons. *Cold Spring Harbor Perspect Biol*., 5.

Scotter, E.L., Chen, H.-J., and Shaw, C.E. (2015). TDP-43 Proteinopathy and ALS: Insights into Disease Mechanisms and Therapeutic Targets. *Neurotherapeutics*., 12, 352-363.

Scotter, E.L., Vance, C., Nishimura, A.L., Lee, Y.-B., Chen, H.-J., Urwin, H., Sardone, V., Mitchell, J.C., Rogelj, B., Rubinsztein, D.C., and Shaw, C.E. (2014). Differential roles of the ubiquitin proteasome system and autophagy in the clearance of soluble and aggregated TDP-43 species. *J Cell Sci*., 127, 1263-1278.

Sephton, C.F., Cenik, C., Kucukural, A., Dammer, E.B., Cenik, B., Han, Y., Dewey, C.M., Roth, F.P., Herz, J., Peng, J., Moore, M.J., and Yu, G. (2011). Identification of Neuronal RNA Targets of TDP-43-containing Ribonucleoprotein Complexes. *J Biol Chem*., 286, 1204-1215.

Sephton, C.F., Good, S.K., Atkin, S., Dewey, C.M., Mayer, P., III, Herz, J., and Yu, G. (2010). TDP-43 is a developmentally regulated protein essential for early embryonic development. *J Biol Chem.,* 285, 38740-38740.

Shahidullah, M., Le Marchand, S.J., Fei, H., Zhang, J., Pandey, U.B., Dalva, M.B., Pasinelli, P., and Levitan, I.B. (2013). Defects in synapse structure and function precede motor neuron degeneration in Drosophila models of FUS-related. *J Neurosci*., 33.

Shoesmith, C.L., Findlater, K., Rowe, A., and Strong, M.J. (2007). Prognosis of amyotrophic lateral sclerosis with respiratory onset. *J Neurol Neurosurg Psychiatry*., 78, 629-631.

Shringarpure, R., and Davies, K.J.A. (2002). Protein turnover by the proteasome in aging and disease. *Free Radic Biol Med*., 32, 1084-1089.

Siddique, T., Figlewicz, D.A., Pericakvance, M.A., Haines, J.L., Rouleau, G., Jeffers, A.J., Sapp, P., Hung, W.Y., Bebout, J., McKennayasek, D., Deng, G., Horvitz, H.R., Gusella, J.F., Brown Jr., R.H., and Roses, A.D. (1991). Linkage of a gene causing familial Amyotrophic Lateral Sclerosis to chromosome 21 and evidence of genetic locus heterogeneity. *N Eng J Med*., 324, 1381-1384.

Siddique, T., Pericakvance, M.A., Brooks, B.R., Roos, R.P., Hung, W.Y., Antel, J.P., Munsat, T.L., Phillips, K., Warner, K., and Speer, M. (1989). Linkage analysis of familial Amyotrophic Lateral Sclerosis. *Neurology*., 39, 919-925.

Sinadinos, C., Burbidge-King, T., Soh, D., Thompson, T.M., Marsh, J.L., Wytttenbach, A., and Mudher, A.K. (2009). Live axonal transport disruption by mutant huntingtin fragments in Drosophila motor neuron axons. *Neurobiol Dis*., 34, 389-395.

Smirnova, E., Griparic, L., Shurland, D.L., and van der Bliek, A.M. (2001). Dynamin-related protein Drp1 is required for mitochondrial division in mammalian cells. *Mol Biol Cell*., 12, 2245-2256.

Snowden, J.S., Hu, Q., Rollinson, S., Halliwell, N., Robinson, A., Davidson, Y.S., Momeni, P., Baborie, A., Griffiths, T.D., Jaros, E., Perry, R.H., Richardson, A., Pickering-Brown, S.M., Neary, D., and Mann DM. (2011). The most common type of FTLD-FUS (aFTLD-U) is associated with a distinct clinical form of frontotemporal dementia but is not related to mutations in the FUS gene. *Acta Neuropathol*., 122, 99-110.

Spradling, A.C., Stern, D., Beaton, A., Rhem, E.J., Laverty, T., Mozden, N., Misra, S., and Rubin, G.M.(1999). The Berkeley Drosophila Genome Project gene disruption project: Single P-element insertions mutating 25% of vital Drosophila genes. *Genetics*. 153, 135-177.

Sproviero, W., La Bella, V., Mazzei, R., Valentino, P., Rodolico, C., Simone, I.L., Logroscino, G., Ungaro, C., Magariello, A., Patitucci, A., Tedeschi, G., Spataro, R., Condino, F., Bono, F., Citrigno, L., Monsurrò, M.R., Muglia, M., Gambardella, A., Quattrone, A., and Conforti FL. (2012). FUS mutations in sporadic amyotrophic lateral sclerosis: Clinical and genetic analysis. *Neurobiol Aging*., 33.

Sreedharan, J., Blair, I.P., Tripathi, V.B., Hu, X., Vance, C., Rogelj, B., Ackerley, S., Durnall, J.C., Williams, K.L., Buratti, E., Baralle, F., de Belleroche, J., Mitchell, J.D., Leigh, P.N., Al-Chalabi, A., Miller, C.C., Nicholson, G., and Shaw, C.E. (2008). TDP-43 mutations in familial and sporadic amyotrophic lateral sclerosis. *Science*., 319, 1668-1672.

St Johnston, D. (2002). The art and design of genetic screens: Drosophila melanogaster. *Nat Rev Genet*., 3, 176-188.

Stepto, A., Gallo, J.-M., Shaw, C.E., and Hirth, F. (2014). Modelling C9ORF72 hexanucleotide repeat expansion in amyotrophic lateral sclerosis and frontotemporal dementia. *Acta Neuropathol*., 127, 377-389.

Stolow, D.T., and Haynes, S.R. (1995). Cabeza, a Drosophila gene encoding a novel RNA binding protein, shares homology with EWS and TLS, 2 genes involved in human sarcoma formation. *Nucleic Acids Res*., 23, 835-843.

Sun, Z., Diaz, Z., Fang, X., Hart, M.P., Chesi, A., Shorter, J., and Gitler, A.D. (2011). Molecular Determinants and Genetic Modifiers of Aggregation and Toxicity for the ALS Disease Protein FUS/TLS. *PLoS Biol*., 9.

Swarup, V., Phaneuf, D., Bareil, C., Robertson, J., Rouleau, G.A., Kriz, J., and Julien, J.-P. (2011). Pathological hallmarks of amyotrophic lateral sclerosis/frontotemporal lobar degeneration in transgenic mice produced with TDP-43 genomic fragments. *Brain*., 134, 2610-2626.

Swinnen, B., and Robberecht, W. (2014). The phenotypic variability of amyotrophic lateral sclerosis. *Nat Rev Neurol*., 10, 661-670.

Tarrade, A., Fassier, C., Courageot, S., Charvin, D., Vitte, J., Peris, L., Thorel, A., Mouisel, E., Fonknechten, N., Roblot, N., Seilhean, D., Diérich, A., Hauw, J.J., and Melki, J. (2006). A mutation of spastin is responsible for swellings and impairment of transport in a region of axon characterized by changes in microtubule composition. *Hum Mol Genet*., 15, 3544-3558.

Thomas, M., Alegre-Abarrategui, J., and Wade-Martins, R. (2013). RNA dysfunction and aggrephagy at the centre of an amyotrophic lateral sclerosis/frontotemporal dementia disease continuum. *Brain*., 136, 1345-1360.

Tollervey, J.R., Curk, T., Rogelj, B., Briese, M., Cereda, M., Kayikci, M., Koenig, J., Hortobagyi, T., Nishimura, A.L., Zupunski, V., Patani, R., Chandran, S., Rot, G., Zupan, B., Shaw, C.E., and Ule J. (2011). Characterizing the RNA targets and position-dependent splicing regulation by TDP-43. *Nat Neurosci*., 14, 452-U180.

Traxinger., K., Kelly., C., Johnson., B.A., Lyles., R.H., and Glass., J.D. (2013). Prognosis and epidemiology of amyotrophic lateral sclerosis. In Neurology Clinical Practice, pp. 313-320.

Troakes, C., Hortobagyi, T., Vance, C., Al-Sarraj, S., Rogelj, B., and Shaw, C.E. (2013). Transportin 1 colocalization with Fused in Sarcoma (FUS) inclusions is not characteristic for amyotrophic lateral sclerosis-FUS confirming disrupted nuclear import of mutant FUS and distinguishing it from frontotemporal lobar degeneration with FUS inclusions. *Neuropathol Appl Neurobiol*., 39, 553-561.

Trojsi, F., Monsurro, M.R., and Tedeschi, G. (2013). Exposure to Environmental Toxicants and Pathogenesis of Amyotrophic Lateral Sclerosis: State of the Art and Research Perspectives. *Int J Mol Sci*., 14, 15286-15311.

Turner, M.R., Scaber, J., Goodfellow, J.A., Lord, M.E., Marsden, R., and Talbot, K. (2010). The diagnostic pathway and prognosis in bulbar-onset amyotrophic lateral sclerosis. *J Neurol Sci*., 294, 81-85.

Urushitani, M., Kurisu, J., Tsukita, K., and Takahashi, R. (2002). Proteasomal inhibition by misfolded mutant superoxide dismutase 1 induces selective motor neuron death in familial amyotrophic lateral sclerosis. *J Neurochem*., 83, 1030-1042.

Van Blitterswijk, M., Mullen, B., Heckman, M.G., Baker, M.C., DeJesus-Hernandez, M., Brown, P.H., Murray, M.E., Hsiung, G.-Y.R., Stewart, H., Karydas, A.M., Finger, E., Kertesz, A., Bigio, E.H., Weintraub, S., Mesulam, M., Hatanpaa, K.J., White, C.L., Neumann, M., Strong, M.J., Beach, T.G., Wszolek, Z.K., Lippa, C., Caselli, R., Petrucelli, L., Josephs, K.A., Parisi, J.E., Knopman, D.S., Petersen, R.C., Mackenzie, I.R., Seeley, W.W., Grinberg, L.T., Miller, B.L., Boylan, K.B., Graff-Radford, N.R., Boeve, B.F., Dickson, D.W., and Rademakers R. (2014). Ataxin-2 as potential disease modifier in C9ORF72 expansion carriers. *Neurobiol Aging*., 35.

Van den Bosch, L., Van Damme, P., Bogaert, E., and Robberecht, W. (2006). The role of excitotoxicity in the pathogenesis of amyotrophic lateral sclerosis. *Biochim Biophys Acta*., 1762, 1068-1082.

van der Bliek, A.M., Shen, Q., and Kawajiri, S. (2013). Mechanisms of Mitochondrial Fission and Fusion. *Cold Spring Harbor Perspect Biol*., 5.

Vance, C., Rogelj, B., Hortobagyi, T., De Vos, K.J., Nishimura, A.L., Sreedharan, J., Hu, X., Smith, B., Ruddy, D., Wright, P., Ganesalingam, J., Williams, K.L., Tripathi, V., Al-Saraj, S., Al-Chalabi, A., Leigh, P.N., Blair, I.P., Nicholson, G., de Belleroche, J., Gallo, J.M., Miller, C.C., and Shaw, C.E. (2009). Mutations in FUS, an RNA Processing Protein, Cause Familial Amyotrophic Lateral Sclerosis Type 6. *Science*., 323, 1208-1211.

Vance, C., Scotter, E.L., Nishimura, A.L., Troakes, C., Mitchell, J.C., Kathe, C., Urwin, H., Manser, C., Miller, C.C., Hortobagyi, T., Dragunow, M., Rogelj, B., and Shaw, C.E. (2013). ALS mutant FUS disrupts nuclear localization and sequesters wild-type FUS within cytoplasmic stress granules. *Hum Mol Genet*., 22, 2676-2688.

Van Gijn, J. (1995). THE Babinski reflex. *Postgrad Med J*., 71, 645-648.

Verburg, J., and Hollenbeck, P.J. (2008). Mitochondrial membrane potential in axons increases with local nerve growth factor or semaphorin signaling. *J Neurosci*., 28, 8306-8315.

Vinceti, M., Bonvicini, F., Rothman, K.J., Vescovi, L., and Wang, F. (2010). The relation between amyotrophic lateral sclerosis and inorganic selenium in drinking water: a population-based case-control study. *Environ Health*., 9.

Vinceti, M., Bottecchi, I., Fan, A., Finkelstein, Y., and Mandrioli, J. (2012). Are environmental exposures to selenium, heavy metals, and pesticides risk factors for amyotrophic lateral sclerosis? Reviews on *Environ Health*., 27, 19-41.

Vinceti, M., Guidetti, D., Pinotti, M., Rovesti, S., Merlin, M., Vescovi, L., Bergomi, M., and Vivoli, G. (1996). Amyotrophic lateral sclerosis after long-term exposure to drinking water with high selenium content. *Epidemiology*., 7, 529-532.

Voigt, A., Herholz, D., Fiesel, F.C., Kaur, K., Mueller, D., Karsten, P., Weber, S.S., Kahle, P.J., Marquardt, T., and Schulz, J.B. (2010). TDP-43-Mediated Neuron Loss In Vivo Requires RNA-Binding Activity. *PLoS One*., 5.

Wang, I.F., Wu, L.-S., Chang, H.-Y., and Shen, C.K.J. (2008a). TDP-43, the signature protein of FTLD-U, is a neuronal activity-responsive factor. *J Neurochem*., 105, 797-806.

Wang, J.W., Brent, J.R., Tomlinson, A., Shneider, N.A., and McCabe, B.D. (2011). The ALS-associated proteins FUS and TDP-43 function together to affect Drosophila locomotion and life span. *J Clin Invest*., 121, 4118-4126.

Wang, W., Li, L., Lin, W.-L., Dickson, D.W., Petrucelli, L., Zhang, T., and Wang, X. (2013a). The ALS disease-associated mutant TDP-43 impairs mitochondrial dynamics and function in motor neurons. *Hum Mol Genet*., 22, 4706-4719.

Wang, W.-Y., Pan, L., Su, S.C., Quinn, E.J., Sasaki, M., Jimenez, J.C., Mackenzie, I.R.A., Huang, E.J., and Tsai, L.-H. (2013b). Interaction of FUS and HDAC1 regulates DNA damage response and repair in neurons. *Nat Neurosci*., 16, 1383.

Wang, X., Arai, S., Song, X., Reichart, D., Du, K., Pascual, G., Tempst, P., Rosenfeld, M.G., Glass, C.K., and Kurokawa, R. (2008b). Induced ncRNAs allosterically modify RNA-binding proteins in cis to inhibit transcription. *Nature*., 454, 126-U111.

Wang, X., and Schwarz, T.L. (2009a). Imaging axonal transport of mitochondria. *Methods Enzymol*., 457, 319-333.

Wang, X., and Schwarz, T.L. (2009b). The Mechanism of Ca2+-Dependent Regulation of Kinesin-Mediated Mitochondrial Motility. *Cell*., 136, 163-174.

Weedon, M.N., Hastings, R., Caswell, R., Xie, W., Paszkiewicz, K., Antoniadi, T., Williams, M., King, C., Greenhalgh, L., Newbury-Ecob, R., and Ellard, S. (2011). Exome Sequencing Identifies a DYNC1H1 Mutation in a Large Pedigree with Dominant Axonal Charcot-Marie-Tooth Disease. *Am J Hum Genet*., 89, 308-312.

Weisiger, R.A., and Fridovich, I. (1973). Mitochondrial superoxide dismutase site of synthesis and intramitochondrial localisation. *J Biol Chem*., 248, 4793-4796.

Wijesekera, L.C., Mathers, S., Talman, P., Galtrey, C., Parkinson, M.H., Ganesalingam, J., Willey, E., Ampong, M.A., Ellis, C.M., Shaw, C.E., Al-Chalabi, A., and Leigh, P.N. (2009). Natural history and clinical features of the flail arm and flail leg ALS variants. *Neurol*., 72, 1087-1094.

Williamson, T.L., and Cleveland, D.W. (1999). Slowing of axonal transport is a very early event in the toxicity of ALS-linked SOD1 mutants to motor neurons. *Nature Neurosci*., 2, 50-56.

Wils, H., Kleinberger, G., Janssens, J., Pereson, S., Joris, G., Cuijt, I., Smits, V., Ceuterick-de Groote, C., Van Broeckhoven, C., and Kumar-Singh, S. (2010). TDP-43 transgenic mice develop spastic paralysis and neuronal inclusions characteristic of ALS and frontotemporal lobar degeneration. *Proc Natl Acad Sci USA*., 107, 3858-3863.

Winton, M.J., Igaz, L.M., Wong, M.M., Kwong, L.K., Trojanowski, J.Q., and Lee, V.M.Y. (2008). Disturbance of nuclear and cytoplasmic TAR DNA-binding protein (TDP-43) induces disease-like redistribution, sequestration, and aggregate formation. *J of Biol Chem*., 283, 13302-13309.

Wodarz, A., Hinz, U., Engelbert, M. and Knust, E. (1995). Expression of crumbs confers apical character on plasma membrane domains of ectodermal epithelia of Drosophila. *Cell*. 14, 67-76.

Woerner, A.C., Frottin, F., Hornburg, D., Feng, L.R., Meissner, F., Patra, M., Tatzelt, J., Mann, M., Winkhofer, K.F., Hartl, F.U., Hipp, M.S. (2016). Cytoplasmic protein aggregates interfere with nucleocytoplasmic transport of protein and RNA. *Science*, 351, 173-176.

Wu, L.-S., Cheng, W.-C., Hou, S.-C., Yan, Y.-T., Jiang, S.-T., and Shen, C.K.J. (2010). TDP-43, a Neuro-Pathosignature Factor, is Essential for Early Mouse Embryogenesis. *Genesis*., 48, 56-62.

Xi, Z., Zinman, L., Moreno, D., Schymick, J., Liang, Y., Sato, C., Zheng, Y., Ghani, M., Dib, S., Keith, J., Robertson, J., and Rogaeva, E. (2013). Hypermethylation of the CpG Island Near the G(4)C(2) Repeat in ALS with a C9orf72 Expansion. *Am J Hum Genet*., 92, 981-989.

Xia, R., Liu, Y., Yang, L., Gal, J., Zhu, H., and Jia, J. (2012). Motor neuron apoptosis and neuromuscular junction perturbation are prominent features in a Drosophila model of Fus-mediated ALS. *Mol Neurodegener*., 7.

Xiao, S., Sanelli, T., Dib, S., Sheps, D., Findlater, J., Bilbao, J., Keith, J., Zinman, L., Rogaeva, E., and Robertson, J. (2011). RNA targets of TDP-43 identified by UV-CLIP are deregulated in ALS. *Mol Cell Neurosci*., 47, 167-180.

Xu, Z., Poidevin, M., Li, X., Li, Y., Shu, L., Nelson, D.L., Li, H., Hales, C.M., Gearing, M., Wingo, T.S., and Jin, P. (2013). Expanded GGGGCC repeat RNA associated with amyotrophic lateral sclerosis and frontotemporal dementia causes neurodegeneration. *Proc Natl Acad Sci USA*., 110, 7778-7783.

Yeh, E., Gustafson, K., and Boulianne, G.L. (1995). Green fluorescent protein as a vital marker and reporter of gene expressionin Drosophila. *Proc Natl Acad Sci USA*., 92, 7036-7040.

Yokoseki, A., Shiga, A., Tan, C.F., Tagawa, A., Kaneko, H., Koyama, A., Eguchi, H., Tsujino, A., Ikeuchi, T., Kakita, A., Okamoto, K., Nishizawa, M., Takahashi, H., and Onodera, O. (2008). TDP-43 mutation in familial amyotrophic lateral sclerosis. *Neurosci Res*., 61, S267-S267.

Yu, Y., Su, F.-C., Callaghan, B.C., Goutman, S.A., Batterman, S.A., and Feldman, E.L. (2014). Environmental Risk Factors and Amyotrophic Lateral Sclerosis (ALS): A Case-Control Study of ALS in Michigan. *PLoS One*., 9.

Zhai, J., Lin, H., Julien, J.-P., and Schlaepfer, W.W. (2007). Disruption of neurofilament network with aggregation of light neurofilament protein: a common pathway leading to motor neuron degeneration due to Charcot-Marie-Tooth disease-linked mutations in NFL and HSPB1. *Hum Mol Genet*., 16, 3103-3116.

Zhang, B., Tu, P.H., Abtahian, F., Trojanowski, J.Q., and Lee, V.M.Y. (1997). Neurofilaments and orthograde transport are reduced in ventral root axons of transgenic mice that express human SOD1 with a G93A mutation. *J Cell Biol*., 139, 1307-1315.

Zhang, K., Donnelly, C.J., Haeusler, A.R., Grima, J.C., Machamer, J.B., Steinwald, P., Daley, E.L., Miller, S.J., Cunningham, K.M., Vidensky, S., Gupta, S., Thomas, M.A., Hong, I., Chiu, S.L., Huganir, R.L., Ostrow, L.W., Matunis, M.J., Wang, J., Sattler, R., Lloyd, T.E., and Rothstein, J.D. (2015). The C9orf72 repeat expansion disrupts nucleocytoplasmic transport. *Nature*., 525, 56-61.

Zhou, H., Chen, G., Chen, C., Yu, Y., and Xu, Z. (2012). Association between Extremely Low-Frequency Electromagnetic Fields Occupations and Amyotrophic Lateral Sclerosis: A Meta-Analysis. *PLoS One*., 7.

Zhou, Y., Liu, S., Liu, G., Oeztuerk, A., and Hicks, G.G. (2013). ALS-Associated FUS Mutations Result in Compromised FUS Alternative Splicing and Autoregulation. *PLoS Genet*., 9.

Zhu, Y.-B., and Sheng, Z.-H. (2011). Increased Axonal Mitochondrial Mobility Does Not Slow Amyotrophic Lateral Sclerosis (ALS)-like Disease in Mutant SOD1 Mice. *J Biol Chem*., 286, 23432-23440.

Zinszner, H., Sok, J., Immanuel, D., Yin, Y., and Ron, D. (1997). TLS (FUS) binds RNA in vivo and engages in nucleo-cytoplasmic shuttling. *J Cell Sci*., 110, 1741-1750.

Zu, T., Gibbens, B., Doty, N.S., Gomes-Pereira, M., Huguet, A., Stone, M.D., Margolis, J., Peterson, M., Markowski, T.W., Ingram, M.A.C., Nan, Z., Forster, C., Low, W.C., Schoser, B., Somia, N.V., Clark, H.B., Schmechel, S., Bitterman, P.B., Gourdon, G., Swanson, M.S., Moseley, M., and Ranum LP. (2011). Non-ATG-initiated translation directed by microsatellite expansions. *Proc Natl Acad Sci USA*., 108, 260-265.

Zu, T., Liu, Y., Baez-Coronel, M., Reid, T., Pletnikova, O., Lewis, J., Miller, T.M., Harms, M.B., Falchook, A.E., Subramony, S.H., Ostrow, L.W., Rothstein, J.D., Troncoso, J.C., and Ranum LP. (2013). RAN proteins and RNA foci from antisense transcripts in C9ORF72 ALS and frontotemporal dementia. *Proc Natl Acad Sci USA*., 110, E4968-E4977.

Zuchner, S., Mersiyanova, I.V., Muglia, M., Bissar-Tadmouri, N., Rochelle, J., Dadali, E.L., Zappia, M., Nelis, E., Patitucci, A., Senderek, J., Parman, Y., Evgrafov, O., Jonghe, P.D.,Takahashi, Y., Tsuji, S., Pericak-Vance, M.A., Quattrone, A., Battaloglu, E., Polyakov, A.V., Timmerman, V., Schröder, J.M., and Vance JM. (2004). Mutations in the mitochondrial GTPase mitofusin 2 cause Charcot-Marie-Tooth neuropathy type 2A. *Nat Genet*., 36, 660-660.